

**AUDITORY BIOMARKERS IN AUTISM SPECTRUM DISORDER;
MULTIMODAL TRANSLATIONAL INVESTIGATIONS**

Russell G. Port

A DISSERTATION

in

Neuroscience

Presented to the Faculties of the University of Pennsylvania

in

Partial Fulfillment of the Requirements for the

Degree of Doctor of Philosophy

2016

Timothy P.L. Roberts, PhD - Professor of Radiology
Supervisor of Dissertation

Joshua I. Gold, PhD - Professor of Neuroscience
Graduate Group Chairperson

Dissertation Committee

Steven J. Siegel, MD, PhD - Professor of Psychiatry

Robert T. Schultz, PhD - R.A.C. Endowed Professor of Psychology

Diego Contreras, MD, PhD - Professor of Neuroscience

Donald C. Rojas – Professor of Cognitive Neuroscience, Colorado State University

Gregory C. Carlson, PhD - Professor of Psychiatry

AUDITORY BIOMARKERS IN AUTISM SPECTRUM DISORDER; MULTIMODAL
TRANSLATIONAL INVESTIGATIONS

COPYRIGHT

2016

Russell Graham Port

This work is licensed under the
Creative Commons Attribution-
NonCommercial-ShareAlike 3.0
License

To view a copy of this license, visit

<http://creativecommons.org/licenses/by-nc-sa/2.0/>

Dedication

For Allison, for all the help, love and support you have provided me.

ACKNOWLEDGMENT

I would first like to acknowledge my wife Allison, with out who I would have died in a ditch long ago. In addition, her saintly patience to put up with me is a marvel to see. Thanks are also due to my family and friends for their support, constant up lifting of my mood, and listening to me complain about what ever took my fancy at the time (usually life or my hypochondria). I would like to thank my thesis committee for their insights and contributions to this work, especially Steve who went above and beyond. Without Steve this body of work would not be the same, not just in terms of experiments, but also understanding. Additionally I would like to thank Greg for his efforts towards my development into a neuroscientist. Lastly I would especially like to thank Tim, who kindly mentored me in the face of my ignorance and complaints about not having remote connection and such like (there's a trend here I'm sure). Lastly, the brave soul in the future that reads this should probably also be acknowledged for their efforts of deciphering this.

ABSTRACT

Auditory Biomarkers in ASD; Multimodal Translational Investigations of the Underlying
Neurobiological Mechanisms

Russell G. Port

Timothy P.L. Roberts, Ph.D.

Autism Spectrum Disorder (ASD) is an invasive neurodevelopmental disorder characterized by impaired social/communication functioning and restricted and repetitive behaviors. Prevalence estimates report that 1 in 45 children have been diagnosed with ASD. Investigations into the etiology of ASD have observed many, often apparently disparate, neurobiological alterations. In response “biomarkers” (biologically based markers that correlate to ASD-related behavioral phenotypes) have been proposed to aid with research, diagnoses, stratification and future interventions. Indeed, as a result of their association with behavioral phenotypes, biomarkers are somewhat capable of predicting diagnostic status. In addition, such biomarkers allow for the direct study of analogous constructs across species. Auditory M100 latency delays and electrophysiological gamma-band activity (GAMMA) alterations are exemplar biomarkers for ASD.

While studies have begun to uncover the biological bases of these biomarkers, several unresolved questions prevent their full implementation. While both biomarkers

have been repeatedly observed, the developmental trajectories are unresolved. Furthermore, while recent studies have observed correlations in healthy adults between cortical GAMMA and relative GABA levels in several systems, the analogous relationship within the auditory system has not been demonstrated. Additionally, if such a correlation does indeed occur, its relation in ASD remains unresolved.

This work characterizes M100 delays and GAMMA as ASD-related biomarkers through five projects. First, a longitudinal **MEG** study examined the persistence of electrophysiological biomarker in ASD. Secondly a multimodal study resolved the relationship of GAMMA and GABA concentrations in the auditory system in both typically developing individuals (TD) and ASD. Furthermore, exploiting the translational potential of GAMMA (**Murine EEG**) the analogous relationship was investigated preclinically. Additionally, a mouse model that demonstrates *increased* sociability was investigated for electrophysiological alterations as a crucial positive control for the use of GAMMA as a biomarker for *decreased* sociability in ASD. Lastly, this hypersocial mouse model's *in-vitro* electrophysiological functioning was characterized utilizing **voltage sensitive dye imaging**.

This dissertation demonstrates that electrophysiological activity alterations are persistent biomarkers in ASD, and moreover correlate to neurochemistry in TD. Such coupling is less clearly resolved in ASD. Moreover, such a differential coupling phenomenon is recapitulated preclinically. Lastly, hypersocial mice exhibit commensurate alterations to GAMMA.

TABLE OF CONTENTS

DEDICATION	III
ACKNOWLEDGMENT	IV
ABSTRACT	V
TABLE OF CONTENTS	VII
LIST OF TABLES	XII
LIST OF ILLUSTRATIONS	XIII
CHAPTER 1.....	1
INTRODUCTION	1
Figure Legends:.....	24
Figures:.....	28
CHAPTER 2.....	31
MATURATION OF AUDITORY NEURAL PROCESSES IN AUTISM SPECTRUM DISORDER – A LONGITUDINAL MEG STUDY	31
Abstract:.....	32
1. Introduction:.....	34
2. Materials and Methods:.....	39
2.1 Participants	39
2.2 Recruitment and Inclusion/Exclusion Criteria.....	40
2.3 Electrophysiological Data Collection	43
2.4 Stimuli.....	43
2.5 Data preprocessing	44
2.6 M100 Data Analysis.....	44

2.7 Gamma-band Data Analysis	46
2.8 Correlations with behavioral metrics	48
3. Results:	49
3.1 M100 latency	49
3.2 Gamma-band activity.....	51
3.3 Correlation of MEG Auditory Biomarkers and Behavioral Metrics	52
3.4 Preliminary results for “had ASD”	53
4. Discussion:	55
Tables Legends:	60
Figure Legends:	64
Tables:	69
Figures:	74
CHAPTER 3.....	79
DECREASED AUDITORY SYSTEM GABA CONCENTRATION, GAMMA-BAND COHERENCE AND COUPLING BETWEEN THEM IN ASD	79
Abstract:	80
1. Introduction:	82
2. Materials and Methods:	86
2.1 Participants	86
2.2 Child and Adolescent Recruitment and Inclusion/Exclusion Criteria.....	87
2.3 Adult Recruitment and Inclusion/Exclusion Criteria	89
2.4 Electrophysiological Data Collection	92
2.5 Stimuli.....	92
2.6 Structural MRI and MRS methods	93
2.7 MRS analysis and quantification	94
2.8 Tissue Segmentation and Quantification.....	94
2.9 Gamma-band Data Analysis	95
2.10 Statistical analyses	97
3. Results:	98
3.1 Demographics	98
3.2 ASD participants demonstrate reduced phase-locked activity.....	98
3.3 ASD participants demonstrate decreased GABA+	99
3.4 The relation of relative cortical GABA to phase-locked gamma-band activity is less apparent in ASD	99
4. Discussion:	101

Table Legends:	110
Figure Legends:	113
Tables:	118
Figures:	123
 CHAPTER 4	 128
 IN-VIVO ELECTROPHYSIOLOGICAL AND EX-VIVO NEUROCHEMICAL CHARACTERIZATION OF <i>PCDH10</i>^{+/-} MICE	 128
Abstract:	129
 1. Introduction:	 131
2.1 Animals	136
2.2 Surgery for EEG recordings.....	136
2.3 Recording of EEG activity.....	137
2.4 EEG data analysis.....	138
2.5 Statistical analysis of in-vivo electrophysiological response metrics.....	143
2.6 Tissue Collection and HPLC analysis of amino acids.....	143
 3. Results:	 145
3.1 <i>Pcdh10</i> ^{+/-} mice demonstrate unaltered ERPs	145
3.2 <i>Pcdh10</i> ^{+/-} mice demonstrate select gamma-band activity alterations in response to a white noise click	145
3.3 Male <i>Pcdh10</i> ^{+/-} demonstrate selective increases to high frequency resting-state power	146
3.4 Male <i>Pcdh10</i> ^{+/-} exhibit reduced signal to noise in the high-gamma band.....	147
3.5 Male <i>Pcdh10</i> ^{+/-} exhibit subtle deficits in theta-high gamma CFC.....	147
3.6 Male <i>Pcdh10</i> ^{+/-} show decreased gamma-band, but not lower frequency, ASSRs.....	148
3.7 <i>Pcdh10</i> ^{+/-} mice demonstrate selective neurometabolite alterations and possible reduced coupling between GABA and gamma-band activity	150
 4. Discussion:	 155
 Figure Legends:	 163
Figures:	170
 CHAPTER 5	 177
 ALTERATIONS TO NEUROPHYSIOLOGICAL FUNCTIONING IN <i>OPRM1</i> A112G SNP MICE MIRRORS BEHAVIORAL PHENOTYPES	 177
Abstract:	178

1. Introduction:	179
2. Materials and Methods:	182
2.1 Animals	182
2.2 Surgery for electroencephalogram (EEG) recordings	183
2.3 Recording of EEG activity.....	183
2.4 EEG data analysis.....	184
3. Results:	188
3.1 Evoked potentials demonstrate sex and genotype differences.....	188
3.2 Genotype and Sex differences in spectral activity.....	189
3.3 Genotype differences at baseline (Saline condition).....	190
3.4 Morphine decreases relative responses in all time frequency ROIs, which is recovered by naloxone.....	191
3.5 Morphine acts in a genotype dependent manner for low, but not high, frequency total power gamma-band responses	192
4. Discussion:	194
4.1 Perturbations to ERPs and Gamma-band activity at baseline	194
4.2 Morphine-induced alterations to ERP and oscillatory markers: intermediate phenotypes allowing for understanding of the neurobiological basis of genotypic effects.....	196
4.3 Sex differences and sex X genotype interactions are frequently observed in morphine responses.....	198
4.4 The A112G Oprm1 substitution allows for both the study of morphine-related neurophysiological phenotypes and broader neuropsychiatric disorders related to GABAergic disruption	199
Table Legends:	201
Figure Legends:	202
Tables:	209
Figures:	211
CHAPTER 6.....	216
MOUSE MODEL OF OPRM1 (A118G) POLYMORPHISM HAS ALTERED HIPPOCAMPAL FUNCTION	216
Abstract:	217
1. Introduction:	218
2 Materials and Methods:	221
2.1 Animals	221
2.2 Voltage-sensitive dye imaging (VSDi).....	221
2.3 VSDi data analyses	223
2.4 Surgery for electroencephalogram (EEG) recordings	224

2.5 Recording of EEG activity.....	225
2.6 EEG data analysis.....	226
3 Results:.....	227
3.1 Quantification of baseline responses.....	227
3.2 Analysis of DAMGO-mediated response-changes.....	228
3.3 EEG.....	230
4. Discussion:.....	232
4.1 <i>Ex Vivo</i> VSDi Recordings Demonstrate that the MOPR A112G SNP Results in a Loss of MOPR Functionality and Altered Hippocampal Circuitry Evoked Responses.....	233
4.2 <i>In Vivo</i> EEG Electrophysiological Recordings Also Demonstrate that the MOPR A112G SNP Results in Altered Hippocampal Responses.....	235
4.3 Conclusions.....	237
Figure Legends:.....	240
Figures:.....	246
CHAPTER 7.....	252
SUMMARY & CONCLUSION	252
1. Summary	252
2. Conclusion and future directions.....	255
Table Legend:.....	261
Figure Legend:.....	262
Tables:	263
Figures:.....	264
BIBLIOGRAPHY	265

LIST OF TABLES

Table 2. 1	69
Table 2. 2	70
Supplemental Table 2. 1	71
Supplemental Table 2. 2	73
Table 3. 1	118
Table 3. 2	119
Supplemental Table 3. 1	122
Supplemental Table 5. 1	209
Table 7. 1	263

LIST OF ILLUSTRATIONS

Figure 1. 1	28
Figure 1. 2	29
Figure 1. 3	30
Figure 2. 1	74
Figure 2. 2	75
Figure 2. 3	76
Figure 2. 4	77
Figure 2. 5	78
Figure 3. 1	123
Figure 3. 2	124
Figure 3. 3	125
Figure 3. 4	126
Figure 3. 5	127
Figure 4. 1	170
Figure 4. 2	171
Figure 4. 3	172
Figure 4. 4	173
Figure 4. 5	174
Figure 4. 6	175
Figure 4. 7	176
Figure 5. 1	211
Figure 5. 2	212
Figure 5. 3	213
Figure 5. 4	214
Supplemental Figure 5. 1	215
Figure 6. 1	246
Figure 6. 2	247
Figure 6. 3	248
Figure 6. 4	249
Figure 6. 5	250
Figure 6. 6	251

Figure 7. 1 264

CHAPTER 1

Introduction

Autism spectrum disorder (ASD) is an array of neurodevelopmental syndromes characterized by restricted/stereotyped behaviors and social communication impairments (American Psychiatric Association 2013). Recent estimates suggest a prevalence of 1 in 68 children, potentially reaching as high as 1 in 42 males (Developmental Disabilities Monitoring Network Surveillance Year 2010 Principal Investigators & Centers for Disease Control and Prevention (CDC) 2014). This estimate though is based on the previous version of Diagnostic and Statistical Manual of Mental Disorders (DSM IV-TR); the effect of the reclassification of ASD by the DSM 5 on the prevalence rate has not been resolved. ASD not only affects the individuals themselves as well as direct caregivers and family members of individuals with ASD, but also society in general: estimates suggest that the United States of American spends at least \$61 billion per year on caring for children with ASD (not including the cost of adult individuals with ASD) (Buescher et al. 2014).

The pathogenic underpinning of ASD, except in rare monogenic syndromic forms, is largely unknown and perhaps consequently, a fully effective treatment for ASD has yet to be uncovered. While there are several weak or rare genetic or environmental insults associated with ASD, these are often non-specific for ASD, and have yet to lead to a common neurobiological pathogenic mechanism. Based on concurrent studies

suggesting ASD was a polygenetic interaction of three genes, just under two decades ago Piven and colleagues hypothesized that a linkage analysis of 60 sibling pairs affected by ASD would reveal the genetic basis this disorder (Piven, Palmer, Landa, et al. 1997). Recently, a complex interplay of genetics (with over 200 susceptibility genes), pre/peri/post –natal environmental insults, and epigenetic interactions have been suggested for pathogenic mechanisms of ASD (Tordjman et al. 2014), demonstrating how the suspected range of etiologies of ASD has ballooned since 1997. Furthermore, several leading hypotheses for the neurobiological bases for ASD have been presented, ranging from imbalances of excitation and inhibition (E/I imbalance) within key neural systems (Rubenstein & Merzenich 2003), to divergent connectivity profiles for short and long range brain connectivity (Belmonte et al. 2004). Indeed, the range of neurobiological alterations in individuals with ASD includes oxidative stress, molecular pathways of cortical organization, neurotransmitter/neuromodulator system, cortical architecture and even whole brain connectivity (Santangelo & Tsatsanis 2005). As such, the variety of possible targets for intervention appears dauntingly broad dampening optimism for research to make immediate therapeutic advances. This may be largely due to ASD being *defined* completely *by* characteristic *behaviors*, for which the underlying neural bases are still unknown.

The use of several “biomarkers”, biologically based markers, for ASD has been suggested to improve the likelihood of success in uncovering such etiologies of, and common pathways in, ASD (Port et al. 2015). A biomarker is signal of normal, pathogenic or interventional biological processes, which can be both objectively

measured and evaluated (Biomarkers Definitions Working Group, 2001). For ASD such a biomarker would be a biologically based measure that correlates to an ASD-related behavioral phenotype, and as a result is capable of making diagnostic predictions at the subject level. Ideally such a biomarker would be both diagnostic and prognostic, scale with the disease/disorder severity, be able to stratify a heterogeneous study population based on underlying biology (e.g. for clinical trial enrichment), and signal early signs of the efficacy of an intervention (Biomarkers Definitions Working Group, 2001). In addition, biomarkers should be minimally invasive, easy to implement, robust and ideally, biomarkers should have a direct, or at least plausible, biological underpinning (e.g. M100 latency and thalamocortical white matter integrity) suggesting both mechanistic relevance and, in principle, offering a therapeutic target. Cost minimization, although desirable, is embroiled in a discussion of “value” *viz-a-viz* the \$61B national annual care costs, and lies beyond the scope of this thesis. Biomarkers do not just hold promise for clinical studies; translational preclinical studies benefit from biomarkers by allowing the measurement of analogous constructs across species/modalities. Indeed the recapitulation of a clinically observed biomarker in an animal model might well be construed as providing evidentiary support for the relevance of (and thus validity of) that particular construct. This is especially important for disorders such as ASD, where diagnoses are *completely behaviorally defined*. While there has been success modeling some of the social and behavioral perturbations of ASD (Silverman et al. 2010), no model fully captures the complex behavioral aspects of ASD. Furthermore how to validate (and the degree to which such validation should be expected) such models remain unknown

(Crawley 2007). This is not to imply that biomarkers are universally considered a core goal or “gold standard” of ASD-related research. Recently concerns have been raised about the relative effectiveness (and value) of these biomarkers versus standard behavioral testing, and furthermore the generalizability of said biomarkers to the population at large (e.g. studies take place in adult subjects with an equal split between individuals with ASD and typically developing controls) (Yerys & Pennington 2011). Yerys and Pennington do admit though that biomarkers *will* be especially useful when A) its biological basis is elucidated and subsequently B) when biomarkers can stratify those with ASD into biologically based sub-groups. As such, while biomarkers are currently still under developmental/validation, in future years (when the concerns raised by Yerys & Pennington are resolved) biomarkers may provide substantial and critical utility for the study and treatment of ASD.

Currently there exist many candidate biomarkers for ASD, ranging from blood-based arrays (Anderson et al. 1990), developmental patterns of eye tracking (Rice et al. 2012), medical imaging including MRI and PET (Lange et al. 2010; C. Ecker et al. 2010; Christine Ecker et al. 2010; Chugani et al. 1999), and electrophysiological methodologies such EEG and MEG (Wilson et al. 2007; Gandal et al. 2010; Roberts et al. 2010; Maxwell, Villalobos, et al. 2013; Rojas & Wilson 2014),

Of these techniques magnetoencephalography (MEG) offers a unique position. MEG’s spatial resolution is in the range of millimeters for cortical activity, similar to that of functional magnetic resonance imaging (fMRI) (Leahy et al. 1998). Contrary to fMRI’s measurement of the hemodynamic response through (presumed) neurovascular

coupling (i.e. on the time scale of seconds), MEG allows greater resolution in the temporal dimension (milliseconds) as well as *direct* access to the neuronal *electrical* activity of interest rather than an indirect proxy. Furthermore, secondary to its high temporal sampling rate, MEG can accommodate spectral decomposition, such that activity within different frequency bands (e.g. alpha 8-12Hz, or gamma 30-100Hz) can be interrogated (either separately or in combination). As such, MEG allows for the investigation and characterization of the distribution, timing, synchrony, content and connectivity of actual neural activity directly.

Such temporal precision is not unique to MEG though, its electrical counterpart electroencephalography (EEG) also demonstrates such sensitivity to the temporal dimension. In addition, EEG is considerably less expensive to utilize, both in terms of the equipment, and secondary expenses (e.g. magnetically shielded rooms, helium). EEG though, does not have the precise spatial localization of MEG (though there is debate, see Barkley & Baumgartner 2003), due in part to the differences in electrical conductivity (whereas not magnetic permeability) of different tissue compartments (grey matter/white matter/CSF/calvarium/scalp), which leads to spatial smearing in EEG, but not MEG (Hämäläinen et al. 1993). In addition, the rate of decay with distance of electric potentials versus magnetic fields, often allows less confounding interference from other neural generators using MEG. This can be overcome in EEG, through the use of high density electrode configurations, exact subject specific models of tissue compartments, Laplacian transforms (similar to taking the second derivative of the electrical current), and advanced source modeling (Gevins et al. 1995); though the manipulation of data with such analyses

provides many opportunities for errors to occur, and are sometimes nonetheless limited by the spatial orientation of the underlying generators (this may also be true for MEG which exhibits a different, arguably complementary, orientation preference to EEG). MEG by comparison can tolerate simplistic spherical (single compartment) head models, and basic localization techniques (e.g. equivalent current dipoles) and still have excellent accuracy (~3mm) (Yamamoto et al. 1988). Lastly as alluded to above, and of specific relevance for studies of primary auditory cortex – the focus of this thesis, MEG has sensitivity to sources primarily tangential orientated to the cortex (as compared to radial sources), which is consistent with the orientation of primary and secondary neurons in auditory cortex, and so allows for the direct and independent study of left and right hemisphere auditory cortices.

MEG is also less cumbersome than EEG, with no need to touch the participant's head repeatedly or apply gel when placing the recording electrodes. This is especially relevant in studies of ASD, due to the high sensitivity of individuals with ASD to direct touching (Dawson et al. 2000). For MEG machines, the magnetometers are housed in a dewar, with participants seated under or supine with their head's contained ensuring adequate head coverage. See Figure 1.1.

Moreover, the non-invasive nature of MEG, combined with short passive paradigms and the recording of early obligate responses, defends against attention, performance and movement confounds, issues especially relevant in this traditionally non-compliant study population (individuals with ASD).

Several MEG-derived biomarkers have been suggested for ASD and the specific functional domains associated with impairment in ASD, (auditory M50/M100 latency prolongation, mismatch field/negativity latency delay, gamma-band activity [30-100Hz] deficits), measures which are robustly derived, sensitive to ASD, and tend to scale with at least aspects of symptomatology (Port et al. 2015). Where these biomarkers may differ is their specificity to ASD, responsiveness to treatment, predictiveness and their link to a biological basis.

Auditory magnetic middle latency responses (M50/M100) are characteristic neuroelectrophysiological event related field (ERF) components that can be detected by MEG sensors over auditory cortex ~ 50 and 100 milliseconds (respectively) after the presentation of a sound. These are the magnetic “cousins” to the familiar P50 and N100 commonly encountered in auditory event related potentials (ERP) studies. Such middle latency responses are not stationary across individuals and paradigms, and are modulated by stimulus properties such as intensity (Stufflebeam et al. 1998), frequency (Roberts & Poeppel 1996) and other physical and perceptual features (Roberts et al. 2000). Right hemisphere middle latency response (M50/100) delay has been repeatedly shown in ASD (Port et al. 2015). In ASD, both the right hemisphere M100 latency response to simple sinusoidal tones is delayed (Gage, Siegel & Roberts 2003), and also the developmental trajectory of such responses are also perturbed (Gage, Siegel, Callen, et al. 2003). Of potential note, while the developmental trajectory of M100 latency maturation may be perturbed in ASD, studies with larger populations suggest a similar *slope*, though differential *intercept* to the linear regression of middle latency responses and age for

ASD as compared to typically developing controls (Roberts et al. 2013). As such, a persistent delay or prolongation of latency exists in ASD, which despite similar rate of maturation, results in an atypical developmental trajectory versus typically developing controls (Port et al. 2015). In addition to delayed M100 latencies and altered developmental trajectories of these latencies, further abnormalities exist. As stated above, M100 latencies are sensitive to stimulus properties including frequency (high frequency tones have shorter latencies). The frequency encoding of different tones as signaled by the M100 may also be perturbed in ASD with a reduced dynamic range of the latencies (Gage, Siegel, Callen, et al. 2003).

Auditory M100 alterations were not without controversy though, concurrent studies demonstrated no M100 delays (Tecchio et al. 2003). As suggested in (Port et al. 2015), the discordant results may be due to the choice of stimuli, as well as the methodology for selecting the M100 latency. In short, Tecchio and colleagues defined the M100 as the “first power maximum following the 50-msec latency”, which due to the age (Oram Cardy et al. 2004) and/or ASD diagnostic status (Roberts et al. 2013) of a subject may actually be a prolonged M50 response. Fortunately topographic representations of surface magnetic fields can aid in the separation of the two responses (Oram Cardy et al. 2004). Another potential confound to studies of M100 latency delays in ASD is that M100 latencies are observed more often in typically developing children than children with ASD at a young age (6–10 years old) (Edgar et al. 2014).

Findings of M100 latency prolongation in ASD have since been observed in larger studies (Roberts et al. 2010; Edgar et al. 2014). In addition, these larger studies

have allowed for the determination that while M100 latencies are not related to general cognitive ability, though have not resolved its association with language ability (Oram Cardy et al. 2008; Edgar et al. 2014; Roberts et al. 2010). While M100 latencies may or may not relate to language ability, it appears M100 latency delays are specific to ASD as opposed to general language impairments (Roberts et al. 2012). Further studies of the specificity of M100 latency delays with respect to other diagnoses are underway. Furthermore, partial support for the use of ERP/Fs as specific biomarkers for ASD also comes from a recent clinical study where behavioral interventions led to behavioral improvements and a concurrent normalization of the latency of visual ERPs (Dawson et al. 2012). This effect of behavioral interventions on ERP timings has also been demonstrate for auditory middle latency responses (Russo et al. 2010), though care should be taken due to the small sample of these studies.

In addition, larger studies have also allowed for the detection of bilateral M50 deficits in ASD (Edgar et al. 2014; Roberts et al. 2013). It may be that larger cohorts are required to detect such an effect in this earlier component, because both M100 (Roberts et al. 2010) and M50 latency (Roberts et al. 2013) delays in ASD are approximately 10% of typically developing control latencies (i.e. ~10ms vs. ~5ms, respectively), and thus given similar measurement precision, M50 delays require more statistical power to be resolved (Port et al. 2015).

Middle latency response delays may have plausible biological bases that form working mechanistic hypotheses, and that may in fact be sole or combined explanatory factors (leading to a form of biologically-based stratification). Either poor signal

transduction (i.e. synaptic dysfunction) (Harada et al. 2011; Rojas et al. 2014; Gaetz et al. 2014; Banerjee et al. 2013; C T Engineer et al. 2014) or perturbed signal conduction (Stufflebeam et al. 2008; Roberts et al. 2009; Dockstader et al. 2012; Roberts et al. 2013) or their combination could cause altered ERPs and ERFs. As a specific example of the value of multimodal imaging approaches, the use of diffusion tensor imaging (DTI) has allowed insights to these hypotheses. DTI is a variant of magnetic resonance imaging (MRI) scan that shows sensitivity to the organization and directional preference of tissue water diffusion (Basser et al. 1994; Mori & Barker 1999), and *by common inference* to qualities of the microstructure of white matter in the brain. Typically developing children demonstrate a linear relationship between fractional anisotropy (FA; a quantitative metric of properties of the white matter microstructure) and both age and M100 latency (Roberts et al. 2009). As age or FA increases, M100 latency shortens. An analogous relationship exists between M50, age and FA in typically developing children, whereas the FA to M50 latency coupling appears absent in ASD (Roberts et al. 2013). Additionally in support of white matter alterations causing M100 latency delays, recent studies have shown both M100 latency alterations (Jenkins et al. 2014) and white matter perturbations (Owen et al. 2014) in individuals with 16p11.2 deletions, a genetic anomaly that may exist with or without typical ASD phenotypic signs.

The use of M100 latency prolongation as a biomarker of ASD also holds promise in preclinical rodent models that recapitulate key aspects of ASD. Mice exposed prenatally to valproic acid (VPA) exhibited a delayed N40 (the 40ms EEG-derived rodent analog of the MEG-derived human M100) (Gandal et al. 2010). Similar murine N40

delays in other animal models that are relevant to ASD have since been shown to scale with sociability (Saunders et al. 2013; Billingslea et al. 2014). Since the initial murine description of delay middle response latency, cortical (i.e. middle latency) evoked response delays have been demonstrated for rat-based models that recapitulate key aspects of ASD including prenatal VPA insults (Engineer et al. 2014) and a genetic model of Rett syndrome (Engineer et al. 2015). Of potential note, the rat-based VPA model exhibits shortening of the delay cortical evoked responses with behavioral training (Engineer et al. 2014), similar to the aforementioned clinical trials. One of the advantages of the utilization of such preclinical models, in general, is that more precise anatomic delineation is available; indeed in Engineer et al., delayed N1 generator contributors were specifically localized to auditory association cortex (AAC) areas and not primary auditory cortex (AI), a resolution currently unachievable in humans.

Recent work has suggested another biomarker for the study of ASD, neural gamma-band oscillatory activity (Grice et al. 2001). Gamma-band activity (sometimes, “GBA”) is thought to play critical roles in sensory integration (Başar-Eroglu et al. 1996) and many higher level cognitive processes (for review see Herrmann et al. 2010; Tallon-Baudry & Bertrand 1999). Indeed, at the local cortical circuit level, gamma-band activity has been linked to both increasing signal to noise (Sohal et al. 2009), and gating the amplitude (Cardin et al. 2009) of the evoked responses. While gamma-band alterations with regards to ASD were originally identified in response to a face inversion task (Grice et al. 2001), alterations have since been identified in other visual tasks (Sun et al. 2012), for other sensory systems (Wilson et al. 2007), and at rest (Orekhova et al. 2007; Cornew

et al. 2012). In general, as with all oscillations, deficits may be manifest in three categories: alterations in frequency (Gaetz et al. 2012), phase (Rojas et al. 2008) or amplitude (Wilson et al. 2007). While not specific to ASD (Maharajh et al. 2007; Brenner et al. 2009), gamma-band deficits may relate to core domains of functioning (e.g. as proposed by the Research Domain Criteria [RDoCs] recently presented by the NIMH), for which the exact domain affected is dependent on the time of critical dysfunction or anatomic region involved (Port et al. 2014). Supporting the notion of particular gamma-band metrics being distinct in ASD though, a recent study found that gamma-band perturbed resting-state hemispheric laterality is related to severity of social impairment (Maxwell, Villalobos, et al. 2013). In addition, recovery of normal gamma-band hemispheric asymmetry is related to the behavioral improvements (reduced SRS scores) produced by a behavioral intervention (Van Hecke et al. 2013), suggesting a role for quantitative gamma-band activity as an objective marker of response to targeted therapy.

Within the auditory system, phase-locked gamma-band oscillatory responses to both simple tones (Gandal et al. 2010; Edgar et al. 2015) and gamma-band auditory steady state response (ASSRs) (Wilson et al. 2007; Rojas et al. 2008) have been repeatedly shown to be decreased. For transient gamma-band responses, the decreased phase-locked activity was concurrent to increased non-phase-locked (induced power) activity (Rojas et al. 2008), though this has not been consistently replicated (Gandal et al.

2010). Similar to increases observed in resting state gamma-band activity¹ (Orekhova et al. 2007; Cornew et al. 2012), a recent study demonstrated increased pre-stimulus power for an simple tone based auditory task in children with ASD (Edgar et al. 2015), though the exact interpretation of such findings are unclear due the nature of pre-stimulus activity (rest versus refractory period versus resonant activity versus distracted activity) being unmeasured. Such increases in pre-stimulus gamma-band activity are associated with language abilities (Edgar et al. 2015) according to the CELF-4 core language index, with increased pre-stimulus power (perhaps interpreted as background “noise” in the brain) being associated with lower core language index scores (weaker performance). Some have referred to this concept as the “noisy brain” hypothesis (Pérez Velázquez & Galán 2013).

Interestingly auditory gamma-band activity may be an endophenotype for ASD². First degree relatives of individuals with ASD have been consistently shown to have altered auditory gamma-band activity (Rojas et al. 2008; Rojas et al. 2011; McFadden et al. 2012). Separately such relatives have been shown to exhibit higher rates of the broad autism phenotype (BAP), a subclinical expression of ASD behaviors (Piven, Palmer,

¹ Though such findings of increased resting-state gamma-band activity are disputed (Sheikhani et al. 2012; Maxwell, Villalobos, et al. 2013), and may be related to behavioral, equipment or analysis differences between the studies (Rojas & Wilson 2014).

² An interesting definition property of an endophenotype as opposed to a biomarker in general is that an endophenotype must also exhibit the property of *heritability*, often untested in biomarker research.

Jacobi, et al. 1997). Additionally there is an association between the severity of the BAP in relatives of individuals with ASD and the ASD symptom severity exhibited by the proband (Maxwell, Parish-Morris, et al. 2013). Such social impairments seen in relatives of individuals with ASD are also correlated to the relative's gamma-band activity observed in responses to an auditory gamma-band steady-state tone (Rojas et al. 2011). Therefore current clinical diagnostic resolution may have less resolution/sensitivity than auditory gamma-band alterations to detecting ASD-related phenotypes. Along that line, several recent studies have demonstrated the ability to distinguish between low and high risk for ASD using gamma-band metrics (Tierney et al. 2012; Elsabbagh et al. 2009). This may not be specific for ASD, as other studies have observed the ability of gamma-band activity to relate to current (Benasich et al. 2008) and predict future (Gou et al. 2011) cognitive and language abilities. An alternative view of the first-degree relative data could be that despite gamma-band deficits similar to their affected siblings, their relative lack of behavioral impairment might be associated with some compensatory mechanism (either spontaneous or secondary to environmental differences). As such further study of the un-, or less-affected siblings might shed light on some effective pathways for symptom amelioration or even remediation.

Gamma-band oscillatory activity also has a plausible biological basis, and may be a convergence point (common pathway/mechanism) of several of the described neurobiological alterations seen in ASD (Port et al. 2014). While dependent on several core constituents (e.g. membrane time constants of pyramidal cells), gamma-band activity is hypothesized to arise from *local circuit interactions* (frequently modeled

through simple interneuron–interneuron or pyramidal–interneuron models, also known as interneuron gamma (ING) and pyramidal-interneuron gamma (PING) mechanisms respectively; Figure 1.2), with key roles for excitation and inhibition kinetics (Buzsáki & Wang 2012).

Indeed, a repeated finding is that γ -aminobutyric acid (GABA) receptor activity is necessary for $\sim 40\text{Hz}$ activity (Whittington et al. 2000). In both of the aforementioned models for gamma-band activity generation, inhibitory feedback onto specific cells causes a temporary cessation in population firing, with the GABA_A receptor time constant (25ms) playing a driving role in frequency determination (Traub et al. 1996). Moreover, specifically parvalbumin (PV) positive fast spiking basket cells are thought to be critically involved due to their perisomatically targeted synapses, due to their nature of forming interconnected networks and the observation of narrow spikes due to KV3.1/3.2 channels, among other evidence (Buzsáki & Wang 2012).

The role of GABAergic cells in the generation of gamma band activity was confirmed by expressing the photoactivated Cl^- pump halorhodopsin in parvalbumin (PV) fast spiking cells in-vivo and then effectively temporally removing them local circuit functioning. When this inhibition of PV fast spiking cells occurred, gamma-band activity was suppressed (Sohal et al. 2009). In addition, optogenetically driving PV fast spiking neurons in a naturalistic manner (Sohal et al. 2009), or even with randomly patterned light (Cardin et al. 2009), subsequently increases gamma-band activity in local field potentials (LFPs). Such is not true for analogous stimulation of pyramidal cells by light (Cardin et al. 2009). As such, it appears that resonant circuit properties generate

gamma-band activity in LFPs, not simply the firing rate of PV fast spiking cells. In support of this, the frequency of enhancement in the LFPs is not modulated by the stimulus intensity used, instead the amplitude of the LFP enhancement is (Cardin et al. 2009). Support for this link between GABAergic processes and gamma-band activity has been observed in the human and animal literature, where either *in-vivo* relative cortical GABA concentrations (in humans) (Balz et al. 2015; Muthukumaraswamy et al. 2009; Gaetz et al. 2011) or PV immunodensity (mice) (Nakamura et al. 2015) is related to stimulus evoked gamma-gamma metrics. Furthermore, recently it was also demonstrated that primary visual cortex GABA_A receptor density correlates with gamma-band activity during a visually based response task (non-target stimuli during a N-Back memory task) (Kujala et al. 2015). This is not to imply that only GABA is associated with gamma-band activity, any alterations to inhibitory or excitatory drive will alter gamma-band activity (Lally et al. 2014; Yamawaki et al. 2008; Mann & Mody 2010; Traub et al. 1996; Thomases et al. 2013; Carlén et al. 2012).

Alterations to the balance of excitation and inhibitory have been repeatedly shown in ASD, the majority of which can be related to gamma-band activity dysfunction (Port et al. 2014). Proteins responsible for the synthesis (GAD65/GAD67) of both GABA itself and GABA (GABA_A/GABA_B) receptors are decreased in post-mortem samples of ASD neuronal tissue (Fatemi et al. 2002; Fatemi et al. 2014; Fatemi et al. 2009). While the exact meaning of this is unclear due to possible homeostatic changes (i.e. excessive concentrations of GABA may lead to receptor density decreases) or changes resulting from death, concurrent *in-vivo* studies have demonstrated regionally specific decreased

cortical relative GABA concentrations in ASD (Harada et al. 2011; Rojas et al. 2014; Gaetz et al. 2014). In addition, genetic alterations to the 15q11-13 locus, which encodes many GABA related proteins, is found in as many as 3% of the idiopathic ASD (Meguro-Horike et al. 2011). This locus includes the *Gabrb3* gene, for which polymorphisms have been associated with ASD (Buxbaum et al. 2002). Further supporting this hypothesis of GABAergic dysfunction, post mortem analyses of the hippocampus of individuals with ASD (compared to typically developing age-matched controls) demonstrates interneuron sub-type specific alterations (Lawrence et al. 2010). In both humans and mouse models that recapitulate key aspects of ASD, reductions in cortical density of PV interneurons have been demonstrated (Zikopoulos & Barbas 2013; Gogolla et al. 2009; Nakamura et al. 2015), with reductions in PV (via genetic deletion) leading to ASD-like behavioral phenotypes in mice (Wöhr et al. 2015).

Separately, excitatory drive in ASD has been shown to be perturbed. Glutamate based neurotransmission related messenger RNAs (mRNAs) and proteins have been shown to be altered in post mortem brains of individuals with ASD (Purcell et al. 2001), along with enzymes that regulate glutamate production (as part of the tricarboxylic acid (TCA) cycle) (Shimmura et al. 2013). Again, the exact interpretation of these alterations are unclear, with in-vivo measurements of Glx (a proxy for glutamate; glutamate and glutamine combined) demonstrating both increased and decreased concentrations in the brain of individuals with ASD, with a possible age dependence for the exact finding (Rojas et al. 2015). Interestingly a recent study that examined glutamate by itself using MRS, found increased cortical concentrations in individuals with ASD (Brown et al.

2013). It should be noted that the volume of tissue examined by typical in-vivo MRS studies (>1cc and up to 27cc in humans) renders interpretations of at the tissue, or cellular level, challenging. Separately, the kainate receptor subunit, GluR6 is strongly linked to ASD (Jamain et al. 2002; Shuang et al. 2004; Strutz-Seebohm et al. 2006). Blood-based genotyping studies also have linked ASD to specific metabotropic glutamate receptor 7; again supporting the hypothesis of glutamate's involvement in ASD (Yang & Pan 2013). When combined, with the aforementioned decreases in GABAergic inhibition, this finding of altered glutamatergic tone may explain the concurrent findings of high co-morbidity of seizures in ASD (with a prevalence of co-morbid epilepsy as high as 38%) (Danielsson et al. 2005).

Based on the observations of glutamate and GABA and, especially, the prevalence of comorbid seizure disorders in ASD (attributed to excess glutamate), Rubenstein and Merzenich in 2003 put forward a hypothesis suggesting that the biological basis of ASD might lie in an imbalance of excitatory and inhibitory activity. Much of the above two paragraphs lends support to this theory, specifically in the abundance of key excitatory and inhibitory neurotransmitters and their receptors. It seems that with the above interpretation of gamma-band activity, this hypothesis is open to in-vivo testing with MEG to stratify patients across the autism continuum, to evaluate impact of regional variation in neurotransmitters, and to assess specificity for ASD by comparison with other clinical control groups.

It is not only neurotransmitters that are dysregulated in ASD, neuromodulatory systems have been known to be perturbed for over 15 years (Boullin et al. 1970; Modahl

et al. 1998). Not only do these neuromodulator affect current neurotransmission, they may also play key roles in the development of neuronal tissue (Whitaker-Azmitia 2001). Indeed, rodents prenatally treated with a serotonin receptor agonist demonstrate alterations to key brain regions involved in social activity, as well as a ASD-like behavioral phenotype (McNamara et al. 2008). In addition to prenatal roles for serotonin, serotonin synthesis demonstrates an altered developmental trajectory in children with ASD (Chugani et al. 1999), and depletions of its precursor can exacerbate symptoms in individuals with ASD (McDougle et al. 1996). Conversely serotonin system modulating pharmaceutical interventions are often prescribed in ASD.

Dopamine has also been implicated in ASD, with its role in mediating repetitive and stereotyped behaviors shown in both humans (Staal 2014) and mice (Chartoff et al. 2001). Separately multiple dopamine related genes have been related to ASD (Nguyen et al. 2014), and several studies have observed dopamine increase in cortex of individuals with ASD (Chugani 2012). Dopamine's link to repetitive and stereotyped behaviors is not unique; Acetylcholine has also been link to such behaviors (Karvat & Kimchi 2014), and shown to be dysregulated in ASD (Deutsch et al. 2010).

Neuropeptides may also be involved in ASD, with oxytocin decreased in the blood plasma of patients with ASD (Modahl et al. 1998). Both differences in processing of oxytocin (Green et al. 2001) and an association with the gene encoding the oxytocin receptor has been reported (Wu et al. 2005) in ASD, though the later may depend on the exact study population (Tansey et al. 2010). Furthermore oxytocin has a known role in social behavior and bonding (Lieberwirth & Wang 2014), including that the murine

oxytocin receptor is expressed in regions known to be involved in social behaviors (Ferguson et al. 2000). In further support of this hypothesis, interventions involving oxytocin are effective in both humans and mice models that recapitulate key aspects of ASD at recovering social-related neural functioning (Gordon et al. 2013; Tyzio et al. 2014 respectively). While oxytocin's role is not immediately apparent in excitatory and inhibitory balance, recent work has shown the role of oxytocin in reducing baseline noise (i.e. spontaneous firing), and increase the stimulus-related fidelity of firing (Owen et al. 2013). As such these alterations to neuromodulatory and neuropeptide systems can act both synaptically or on the firing properties of a cell (e.g. kinetics and firing probability of cells).

While serotonin, dopamine and oxytocin represent classes of neurochemical with hypothetical involvement in ASD, the present work *focuses* on the most prevalent E/I imbalance hypothesis, drawing together tools that are sensitive to neurotransmitters (e.g. MRS estimates of GABA) and to the consequence of local circuitry function (MEG measures of gamma band activity).

Architectural alterations have also been seen in ASD that relate to E/I balance. In support of the hypothesis of differentially altered long versus short range connectivity (Belmonte et al. 2004), magnetic resonance imaging suggests that short range connectivity is increased in ASD (Herbert et al. 2004), along with long range connectivity decreases (Jou et al. 2011). As mentioned above, gamma-band activity is thought to be related to local circuit function (Sohal et al. 2009; Cardin et al. 2009), and so possible increases in local connectivity may result in increased local activity at rest (as

observed in ASD; see above). Recent reports though suggest that this sort range hyper-connectivity, may not exist functionally (Khan et al. 2013). Additional architectural alterations have been observed at the local circuit level in individuals with ASD with cortical minicolumns are containing less peripheral neuropil space (thought to be important in inhibitory signaling), while minicolumns concurrently are more densely packed (Casanova et al. 2002).

As such, the repeated findings of gamma-band activity alterations in ASD, its potential role as an endophenotype, and the known biological basis of gamma-band activity (for which relevant disruptions have been found in ASD) suggest gamma-band activity being a potential biomarker for ASD. Furthermore, decreased auditory related gamma-band activity are a conserved phenotype in several animal models of ASD regardless of the nature of the insult utilized (Gandal et al. 2010; Gandal, Sisti, et al. 2012; Gandal, Anderson, et al. 2012; Saunders, Gandal, Roberts, et al. 2012; Tatar-Leitman et al. 2014). Such decreases in phase-locked post-stimulus gamma-band responses have since been independently replicated (Nakamura et al. 2015). Additionally, as in clinical ASD, increased pre-stimulus and baseline activity have been observed in murine models relevant to ASD (Saunders, Gandal & Siegel 2012; Gandal, Sisti, et al. 2012; Tatar-Leitman et al. 2014; Billingslea et al. 2014), though several of these studies are focused on animal models that recreate key suspected genetic etiologies of schizophrenia. However, these mice demonstrate social impairments akin to ASD (Tatar-Leitman et al. 2014; Billingslea et al. 2014), and at least one has been also presented as a model of ASD (Saunders et al. 2013). Furthermore, there is considerable

overlap of symptomatology, comorbid schizophrenia/psychosis and suggestions that neurobiological underpinnings are related (de Lacy & King 2013). Of potential note, baseline power increases in animal models that recapitulate key aspects of ASD have also been observed by independent laboratories (Zhong et al. 2009). Furthermore, a treatment that recovers proper social functioning also recovers baseline gamma-band activity (Tyzio et al. 2014) in animal models that recapitulate key aspects of ASD.

These gamma-band alterations seen in murine models that recapitulate key aspects of ASD have been shown to be associated with several behavioral/biological metrics. Pre-stimulus/baseline gamma-band activity has been shown to correlated to sociability (Gandal, Sisti, et al. 2012) and working memory (Gandal, Sisti, et al. 2012; Billingslea et al. 2014). Moreover, directly increasing baseline excitatory drive in medial prefrontal cortex (via optogenetics) reduces sociability in mice, which can be recovered by supplemental increases to inhibitory drive (Yizhar et al. 2011). These works have since directly spawned analogous analyses in human-based studies, where pre-stimulus gamma-band power predicts language functioning in children (Edgar et al. 2015). Importantly, pre-clinical work has also demonstrate that while related baseline gamma-power and gamma-band evoked power responses are related, they are not redundant measures; only about 27% of variance is explained when directly comparing these metrics (Billingslea et al. 2014). Correlates of gamma-band activity are not restricted to only behavioral or electrophysiological phenotypes in animal models relevant to ASD, stimulus evoked gamma-band responses have been shown to correlate to underlying

synaptic protein levels (Gandal et al. 2010), and PV positive cell density (Nakamura et al. 2015).

Gamma-band alterations have also been investigated in mouse models of monogenetic syndromes that have considerable overlap with ASD. For instance Rett syndrome, a genetic syndrome, results from mutations in the MeCP2 gene (Amir et al. 1999), is marked by ASD-like behavioral alterations, among other perturbations (Chahrour & Zoghbi 2007). Mice with alterations to their *MeCP2* genetic load (i.e. either heterozygous females or site-specific alteration of amino acids) demonstrate altered gamma-band activity both at rest (Goffin et al. 2012), during exploratory activity (Lang et al. 2014) and in response to auditory stimuli (Goffin et al. 2012; Liao et al. 2012). The exact nature of the auditory stimulus produced gamma-band alterations is unclear as studies have found opposing effects (Goffin et al. 2012; Liao et al. 2012), possibly due to the differing genetic insults used.

Though much is known about ASD, E/I balance and MEG-derived auditory biomarkers, there are still several unresolved questions. For instance the developmental trajectories of these biomarkers are still unresolved, and so *it is unknown if the auditory MEG biomarkers for ASD are persistent*, or resolve with time. Furthermore, while there is mounting evidence that gamma-band activity is reliant on, and furthermore coupled to, underlying GABAergic tone (see above) in healthy adults for both motor and visual systems, whether *this coupling holds true for the auditory system remains unknown*. Moreover, *the effect of ASD with regards to such coupling is also undetermined*. Lastly, while gamma-band activity alterations are hypothesized to represent a biomarker for

ASD (Rojas & Wilson 2014), *the relation of gamma-band activity to increased sociability remains unknown.*

To resolve such questions, this dissertation undertakes the following experiments:

1) The first longitudinal characterization of auditory MEG biomarkers from childhood into adolescence 2) A multimodal study examining the coupling between gamma-band activity (utilizing MEG) and relative cortical GABA levels (utilizing MRS) in the auditory system for both typically developing controls as well as individuals with ASD 3) The characterization of the in-vivo electrophysiological activity and ex-vivo amino acid concentrations, in a murine model recapitulating a key genetic insult in familial ASD 4) An *in-vivo* investigation of spectral activity in a mouse model that demonstrate *increased* (rather than decreased) sociability due to a mutation in the μ -opioid receptor 5) An *in-vitro* investigation of the functional consequence of the aforementioned μ -opioid receptor mutation. For the organizational flow of this dissertation, and the feedback of each chapter with regards to previous chapter see Figure 1.3.

Figure Legends:

Figure 1.1 *A participant in a MEG machine, and a subset of potential subsequent analyses.* A child seated in an MEG machine, with their head positioned under the dewar (left top). Note the screen in front of the child is at a comfortable viewing distance for both presentations of stimuli and movies (to minimize fatigue). Analyses can follow two major routes, sensor-space (top) or source-space (bottom). For sensor-space analyses, evoked responses to stimuli (such as auditory tones) can be averaged

over trials to produce event related fields (ERFs) for all channels separately (middle top). Within these multicomponent ERFs, specific responses can be observed such as the M100 (dashed vertical line), with additional use of topographic plots (right top) to verify correct magnetic field orientation. For source-space analyses (bottom), head models (either standard or subject-specific) can be generated for source localization (left bottom). Source-space locations (such as Heschl's Gyrus; 2nd left bottom) can be interrogated within the head model via the use of source localization techniques (e.g. equivalent current dipoles and beamformers). Virtual sensor time courses can then be produced for said location, and source space ERFs produced (3rd left bottom). Such ERFs, derived from either source or sensor space, can be further decomposed into their spectral sub-components to examine otherwise obscured frequency specific alterations (right bottom).

Figure 1.2 *Hypothesized mechanisms of gamma-band activity generation in both interneuron-interneuron & pyramidal cell-interneuron networks.* (A) Interneuron-Interneuron (I-I) networks (also known as interneuron gamma (ING) mechanism) involves two reciprocally connected perisomatically synapsing parvalbumin positive (PV) basket cell interneurons (green) releasing GABA (pink circles) to rhythmically inhibit one another. After an external drive is applied to the network, the interneurons fire in phase with one another at gamma-band frequency. After cell 1 fires an action potential (first vertical dashed line), it releases GABA onto both itself and other interneurons (represented here by cell 2). With the activation of GABA_A receptors, chloride channels open causing an inhibitory post-synaptic current (IPSC). This current hyperpolarizes (via an inhibitory post-synaptic potential (IPSP)) cells 1 and 2 to prevent additional action potentials (purple = membrane potential; blue = intracellular current). After the chloride channels close (~25ms), both cell 1 and 2 are permitted to fire once more in response to the continued external drive (second vertical dashed line). If either cell 1 or 2 does not fire within the timeframe between chloride channels closing and its counterpart's GABA release, the cell's action potential will be postponed (due to the chloride mediated IPSC) until the chloride channels close (cell 2 third/fourth vertical dashed line). External excitatory cells in this model (cell 3; blue cells) also fire action potentials when the chloride conductance is at a minimum. While a single excitatory cell may not have complete firing fidelity to the gamma-band oscillation (cell 3, vertical line 4), fidelity is kept across the population of excitatory cells (cell 3 dashed resting potential/intracellular current).

The recorded local field potential (LFP; green) will be sensitive to the post-synaptic potentials of the excitatory cells, but not the interneurons, due to the cellular morphology of each class of cell. (B) Excitatory-Inhibitory (E-I) (also known as pyramidal-interneuron gamma (PING) mechanism) networks for gamma generation involves reciprocally connected excitatory pyramidal cells (cell 1; blue), and perisomatically synapsing PV basket cell interneurons (cell 2; green). External drive causes the excitatory cell to fire an action potential and release glutamate (red circle). This in turn excites the inhibitory cell to fire an action potential and release GABA back onto the excitatory cell (feedback inhibition). Similar to the I-I network, the excitatory cell is now prevented from firing due to increased chloride conductance. After ~ 25 ms the chloride channels close and cell 1 becomes depolarized due to external excitatory drive and fires an action potential, repeating the cycle. Note in both models the prominent role for perisomatically targeting PV interneurons, GABA release, and the $GABA_A$ receptor time constant. In addition, in both models, the $GABA_A$ receptor time constant leads to firing at 40Hz (i.e. $1/25$ ms; gamma-band activity). Figure based on (Whittington et al. 2000; Tiesinga & Sejnowski 2009; Gonzalez-Burgos & Lewis 2008).

Figure 1.3 *Organizational flow of dissertation with the feedback of later chapters on original questions.* Circles = major question; Arrow/Square = Chapters with specific findings with respect to the previous question; Dashed line = Feedback between chapters

Figures:

Figure 1. 1

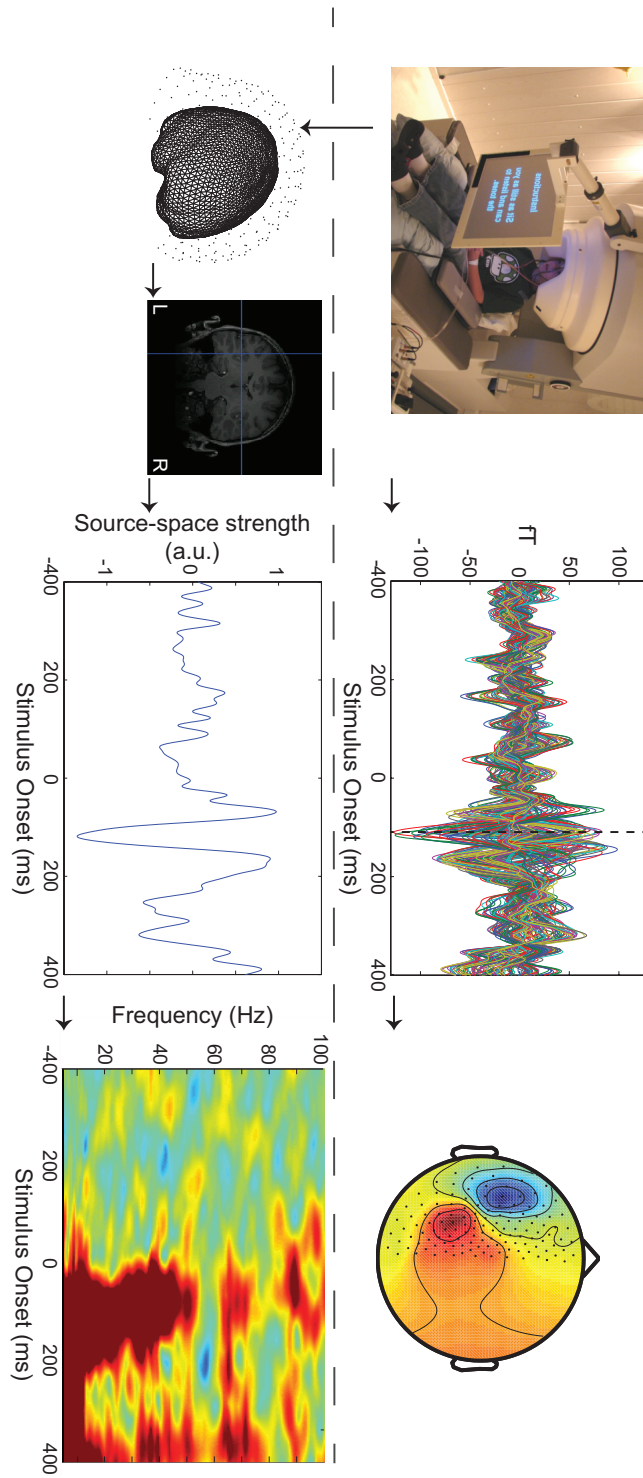


Figure 1. 2

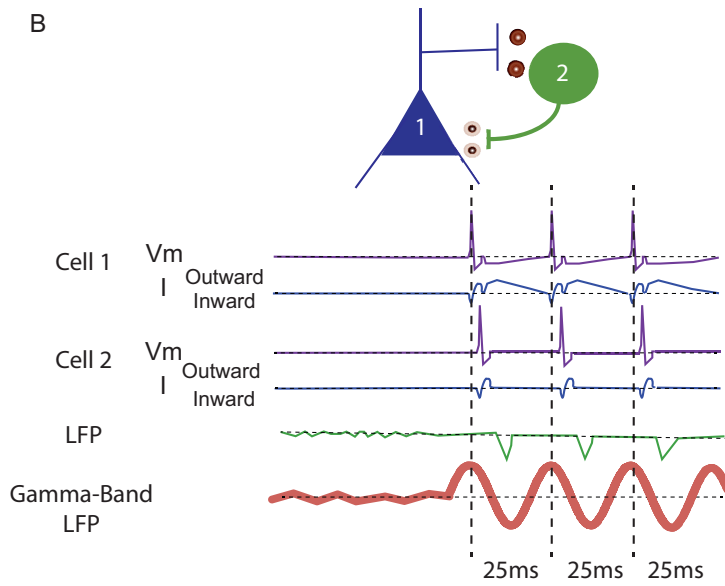
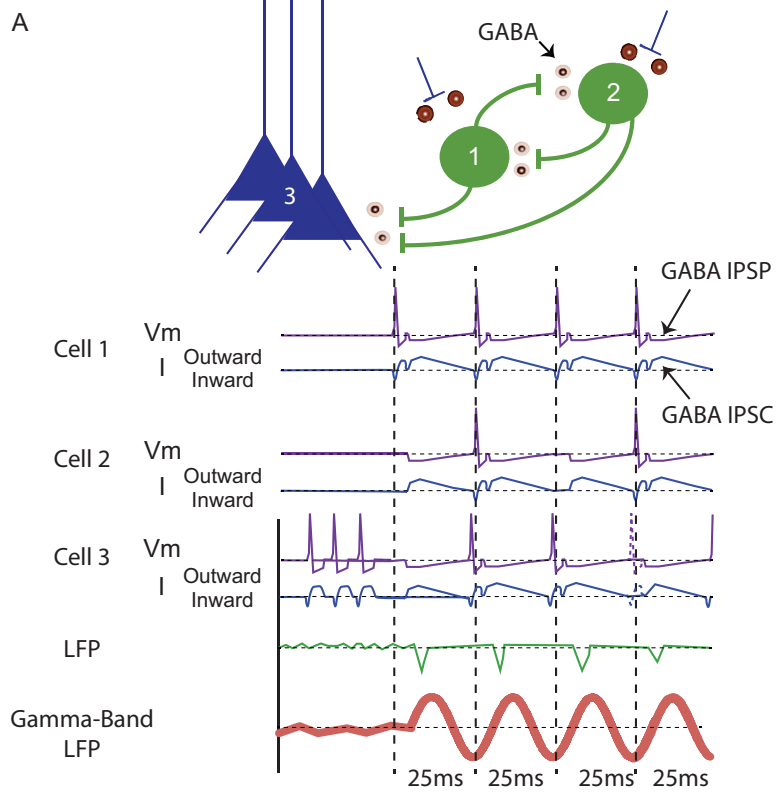
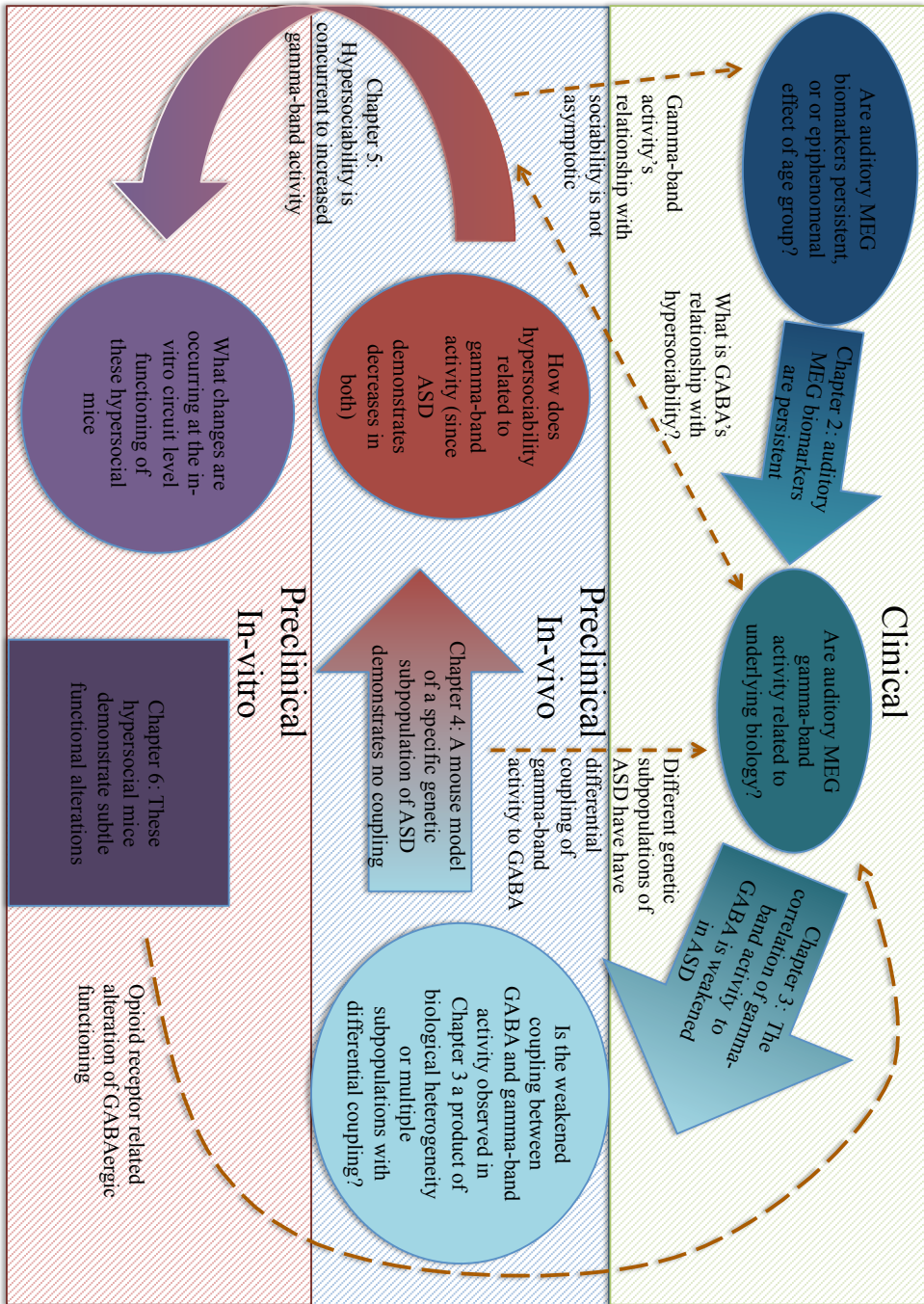


Figure 1. 3



CHAPTER 2

Maturation of auditory neural processes in autism spectrum disorder – a longitudinal MEG study

Russell G Port¹, J Christopher Edgar¹, Matthew Ku¹, Luke Bloy¹, Rebecca Murray¹, Lisa
Blaskey¹, Susan E Levy², Timothy PL Roberts¹

¹Lurie Family Foundations MEG Imaging Center, Department of Radiology, Children's
Hospital of Philadelphia, Philadelphia, PA, USA

²Department of Pediatrics, Children's Hospital of Philadelphia, Philadelphia, PA, USA

Presented here as submitted to NeuroImage: Clinical (under review)

Abstract:

Background:

Individuals with autism spectrum disorder (ASD) show atypical brain activity, perhaps due to delayed maturation. Previous studies examining the maturation of auditory electrophysiological activity have been limited due to the use of a cross-sectional design. The present study took a first step in examining magnetoencephalography (MEG) evidence of abnormal auditory response maturation in ASD via the use of a longitudinal design.

Methods:

Initially recruited for a previous study, 27 children with ASD and nine typically developing (TD) children, aged 6- to 11-years-old, were re-recruited two to five years later. At both timepoints, MEG data were obtained while participants passively listened to sinusoidal pure-tones. Bilateral primary/secondary auditory cortex time domain (100ms evoked response latency (M100)) and spectrotemporal measures (gamma-band power and inter-trial coherence (ITC)) were examined.

Results:

M100 latencies were delayed in ASD versus TD at the initial exam (~19 ms) and at follow-up (~18 ms). At both exams, M100 latencies were associated with clinical ASD

severity. In addition, gamma-band evoked power and ITC were reduced in ASD versus TD. M100 and gamma-band maturation rates did not differ between ASD and TD. MEG measures were also qualitatively examined for five children who exhibited “optimal outcome”, initially on spectrum, but no longer meeting diagnostic criteria at follow-up. These data, presented to motivate future studies, showed M100 latency and gamma-band mean values in this cohort in-between TD and ASD at both time points.

Conclusions

Children with ASD showed perturbed auditory cortex neural activity, as evidenced by M100 latency delays as well as reduced transient gamma-band activity. Despite evidence for maturation of these responses in ASD, the neural abnormalities in ASD persisted across time. Of note, five children initially diagnosed on spectrum and no longer meeting ASD diagnostic criteria at follow-up qualitatively showed more ‘normal’ brain auditory responses. Further investigation with larger cohorts is needed to determine if the above auditory response phenotypes have prognostic utility, predictive of clinical outcome.

1. Introduction:

Autism spectrum disorder (ASD) describes a group of disorders characterized by social/communication impairments and restricted/repetitive behaviors (American Psychiatric Association 2013). Recent prevalence estimates report that 1 in 68 children have ASD (Developmental Disabilities Monitoring Network Surveillance Year 2010 Principal Investigators & Centers for Disease Control and Prevention (CDC) 2014). Given that interventions for ASD show variable success (Erickson et al. 2014; Van Hecke et al. 2013; Dawson et al. 2010), and given that treatment outcome is difficult to predict at treatment onset, there is a need for early response indicators. Pre-clinical (animal) studies of novel treatments are also hampered by the lack of directly translatable metrics. “Biomarkers” offer a biological target for therapeutics, a bridge between preclinical and clinical studies, and may also serve as early response indicators of treatment success/failure (Port et al. 2015; Port et al. 2014).

Two prospective brain biomarkers, Superior Temporal Gyrus (STG) M100 auditory latency (Gage, Siegel & Roberts 2003; Roberts et al. 2010; Edgar, Lanza, et al. 2014) and STG post-stimulus auditory gamma-band activity (Wilson et al. 2007; Gandal et al. 2010; J Christopher Edgar et al. 2015; Edgar et al. 2016), have been identified as abnormal in ASD as well as in animal models that recapitulate key aspects of ASD (Gandal et al. 2010; C T Engineer et al. 2014). Auditory M100 responses, and their electrical counterpart the N1, are characteristic electrophysiological responses seen in the auditory event related fields/potentials (ERF/P) (Hari et al. 1980). M100 responses become stronger and are observed at earlier latencies as a function of typical

development (Paetau et al. 1995; Edgar, Lanza, et al. 2014) First described by Gage and colleagues in our group (Gage, Siegel, Callen, et al. 2003), right-hemisphere auditory M100 latencies were observed to be prolonged by ~10% in children with ASD versus age-matched typically developing controls (TD). This ~10 ms right hemisphere M100 latency prolongation in children with ASD was observed in later studies, with group differences in M100 latency remaining even after co-varying cognitive and language ability (Roberts et al. 2010; J Christopher Edgar et al. 2015; Edgar, Lanza, et al. 2014). These later studies, with moderately large samples (also including (Edgar, Lanza, et al. 2014)), also allowed for the observation that M100 group differences existed even in the presence of a seemingly normal M100 latency maturation rate in ASD, suggesting that the persistent delay in auditory M100 latencies in children as well as adolescents with ASD was due to an early initial M100 latency ‘offset’.

In addition to M100 latency, STG auditory post-stimulus *gamma-band* (typically > 30Hz) activity has received considerable attention as a biomarker for ASD. Though not specific to ASD (Maharajh et al. 2007; Krishnan et al. 2009; Edgar, Chen, et al. 2014), altered post-stimulus gamma-band activity has been repeatedly demonstrated in ASD in different sensory systems, stimulus complexity, and in children and adults with ASD (Grice et al. 2001; Wilson et al. 2007; Rojas et al. 2008; Gandal et al. 2010; Sun et al. 2012). Within the auditory system, post-stimulus phase-locked gamma-band measures (evoked power as well as inter-trial coherence) have been found to be reduced in ASD (Wilson et al. 2007; Rojas et al. 2008; Gandal et al. 2010; J Christopher Edgar et al. 2015; Edgar et al. 2016). Auditory gamma-band alterations may represent

endophenotypes, observed in first degree relatives of individuals with ASD (Rojas et al. 2008; Rojas et al. 2011; McFadden et al. 2012), with some evidence that gamma-band activity in relatives is associated with their social functioning (Rojas et al. 2011). Although the existence of post-stimulus gamma-band alterations in first-degree relatives may call into question the appropriateness of this measure as a diagnostic or response biomarker, subclinical expression of social impairment (Broad Autism Phenotype) is thought to exist in the relatives of individuals with ASD (Piven, Palmer, Landa, et al. 1997). As such, gamma-band biomarkers may support a basis for a clinical discrimination (Port et al. 2015). Along this line, several recent studies have demonstrated the ability to distinguish between infants at low and high risk for ASD (typically the risk being conferred by the presence of an older sibling with ASD) via gamma-band metrics (Tierney et al. 2012; Elsabbagh et al. 2009). Such findings, however, may not be specific to ASD, as other studies have shown that gamma-band activity relates to *current* (Benasich et al. 2008) as well as *future* (Gou et al. 2011) cognitive and language abilities.

The aforementioned cross-sectional studies of M100 latency prolongation and post-stimulus gamma-band alterations in ASD, although informative, have limitations. In addition to the limits inherent to cross-sectional studies (e.g., inter-subject “biological” variability), cross-sectional designs do not allow for developmental changes over time, a particular limitation as some children initially diagnosed with ASD may show significant improvement over time (known as “optimal outcome”) (Zappella 2002; Mukaddes et al. 2014; Helt et al. 2008; Granpeesheh et al. 2009). Though much remains to be known about “optimal outcome”, research suggests a small cohort of individuals originally

diagnosed with ASD no longer meet diagnostic criteria at later follow-up. Indeed domain specific measures suggest they may later function well within normal ranges with respect to cognitive and social abilities (Helt et al. 2008). The role, impact, and specificity of interventions associated with “optimal outcome” are currently unknown. Although it has been suggested that such individuals demonstrate better social skills and higher intelligence, certain clinical measures (i.e., higher IQ) are not strongly predictive of “optimal outcome”. In addition, initial autism severity is not associated with “optimal outcome” (Helt et al. 2008). Of note, individuals showing “optimal outcome” do demonstrate subtle residual impairments even after “losing” their ASD diagnosis (Kelley et al. 2006). With regard to the above, an objective *prognostic biomarker* and/or real-time monitor of intervention efficacy would be of use.

In an attempt to address the aforementioned limitations of cross-sectional studies (inter-subject variability and the insensitivity to developmental improvement), the present study utilized a *longitudinal* design to examine auditory M100 latencies, auditory gamma-band responses, and their maturation in TD children and children with ASD. The present study tested the hypotheses that children with ASD would demonstrate prolonged auditory M100 latencies as well as reduced post stimulus phase-locked gamma-band metrics. Furthermore, cross-sectional analyses allowed direct assessment of whether M100 latencies in ASD show evidence of abnormal maturation. Given longitudinal findings showing similar rates of M100 latency maturation in TD and ASD, it was hypothesized that the children with ASD would demonstrate a persistent prolongation in M100 latency delay given a similar *rate* of maturation in TD and ASD (i.e., maturation

rates not faster than TD and thus the M100 latency in older individuals with ASD does not ‘catch up’ with older TD M100 latencies). In addition, the use of a *longitudinal* design allowed for examination of associations between MEG measures and both *current* and *future* clinical/behavioral status. It was hypothesized that M100 latencies would be associated with *current* autism severity, but not language ability (Roberts et al. 2010), and that gamma-band metrics would be associated with *follow-up* language ability, but not autism severity (Gou et al. 2011).

2. Materials and Methods:

2.1 Participants

Initial time point 1 data were obtained from previous magnetoencephalography (MEG) studies (10;20). A subsample of participants (TD = 9, ASD = 27) were re-recruited two to five years later (mean age = 12.1 years). The longitudinal cohort was smaller than our previously published studies because of a restricted intake age-range (to allow for subsequent follow-up during the adolescent period) as well as difficulties re-contacting and re-recruiting participants over a long time interval, and additional exclusion criteria that arose (such as dental work in the intervening period, or contra-indicating medication use).

Of note, a subset of the re-recruited children with ASD (N = 5) showed considerable improvement at follow-up (i.e., sub-threshold for a diagnosis of ASD). These individuals are referred to here as “had ASD”. All 36 participants (9 TD [3 males], 22 ASD [22 males], 5 “had ASD” [4 males]) had evaluable M100 data. Table 2.1 reports diagnostic scores and demographics for the three groups (TD, ASD, “had ASD”). Due to gamma-band activity analyses (which relied on individual MRI) being more sensitive to artifacts (e.g. motion) than M100 latency measures, measures that are also extracted from raw sensor data, eight children (1 TD, 7 ASD) were excluded from gamma-band activity analyses. This left 28 participants (8 TD [3 male], 15 ASD [15 male], 5 “had ASD” [4 male]) for the gamma-band activity analyses. Table 2.2 reports population diagnostic scores and demographics for the three groups (TD, ASD, “had ASD”) included in gamma-band activity analyses. Due to the requirements of parametric statistics (i.e. linear

mixed effect model (LMM) due to missing responses) and the small sample size of the “had ASD” group, the cohort of “had ASD” individuals were not included in the statistical analyses and the data from this group were instead only descriptively reported.

2.2 Recruitment and Inclusion/Exclusion Criteria

Akin to procedures described in Edgar et al. 2015, subjects with ASD were originally recruited from the Regional Autism Center of The Children’s Hospital of Philadelphia (CHOP), the Neuropsychiatry program of the Department of Psychiatry of the University of Pennsylvania School of Medicine, and from local and regional parent support groups such as ASCEND (Asperger Syndrome Information Alliance for Southeastern Pennsylvania) and local chapters of Autism Speaks. All children screened for inclusion in the ASD sample had a prior ASD diagnosis made by an expert clinician, typically a developmental pediatrician in the Regional Autism Center at the Children’s Hospital of Philadelphia. The original diagnosis was made after an extensive clinical interview, documentation of DSM-IV criteria for ASD, and use of various ASD diagnostic tools, such as the Childhood Autism Rating Scale and, in many cases, the ADOS. Subjects with typical development (TD) were recruited through local newspaper advertisements and from pediatric practices of the CHOP primary care network.

Research participants made two visits to CHOP. During the first visit (2–3 weeks prior to the MEG exam), clinical and diagnostic testing was performed to confirm the referral ASD diagnosis, to administer neuropsychological tests, and to ensure that the TD

children met study inclusion/exclusion criteria. Assessments were performed by licensed child psychologists with expertise in autism (L.B., E.S.K.). Given the extensive clinical evaluations upon which original ASD diagnosis was made, an abbreviated diagnostic battery was used to confirm the original diagnosis. Specifically, the ASD diagnosis was confirmed with standard diagnostic tools, including direct observation with the Autism Diagnostic Observation Schedule (ADOS; Lord et al. 2000) and parent report on the Social Communication Questionnaire (SCQ; Rutter et al. 2003). Dimensional symptom severity ratings were also obtained by parent report on the Social Responsiveness Scale (SRS; Constantino & Gruber 2012). The Autism Diagnostic Interview-Revised (ADI-R), a parent interview about current and prior ASD symptoms, was utilized to resolve diagnostic discordances between the ADOS and parent rating scales in the rare instances in which such discordances occurred. At the time of their original study visit, children were required to exceed established cut-offs on both the ADOS and SCQ, or, in the event of a discordance between those measures, on both the ADOS and ADI-R. Children 1 point below ADOS cut-offs were included if they also exceeded cut-offs on at least two parent questionnaires or on the ADI-R. For children for whom original diagnosis was not made by an expert clinician according to DSM criteria (e.g., diagnoses made by a school), more rigorous standards were applied, and the child was required to exceed cut-offs on both the ADOS and ADI-R for inclusion in the ASD group. For final inclusion in the ASD group, children had to meet the above criteria at the time of their original study participation and also had to exceed diagnostic cut-offs on the ADOS at their two to five - year follow-up (parent rating scale corroboration was not required at follow-up). To rule

out global cognitive delay, all subjects were required to score at or above the 2nd percentile ($SS > 70$) on the Perceptual Reasoning Index (PRI) of the Wechsler Intelligence Scale for Children-IV (WISC-IV; Wechsler 2003). In all subjects, the WISC-IV Verbal Comprehension Index (VCI) was also obtained.

Inclusion criteria for the TD children included scoring below the cut-off for ASD on all domains of the ADOS as well as parent questionnaires, and performance above the 16th percentile on the Clinical Evaluation of Language Fundamentals—4th edition (CELF-4; Semel & Wiig 2003). In addition to the above inclusion/exclusion criteria, all subjects and families were native English speakers and had no known genetic syndromes or neurological (e.g., cerebral palsy, epilepsy), or sensory (hearing, visual) impairments. The study was approved by the CHOP Institutional Review Board and all participants' families gave written informed consent. As indicated by institutional policy, where competent to do so, children over the age of seven additionally gave verbal assent.

TD children were free of medications at both exams, except for one participant who was prescribed Naltrexone at follow-up. In the children with ASD, 12 were prescribed medications/took dietary supplements at the first scan. At follow-up, 14 took medications/supplements. The “had ASD” cohort did not report taking medications at the initial exam. At follow-up 3 “had ASD” participants were taking medication. Supplemental Table 1 provides medication information.

2.3 Electrophysiological Data Collection

MEG data were obtained using a whole-cortex 275-channel system (VSM MedTech Inc., Coquitlam, BC) in a magnetically shielded room. Prior to data acquisition, three head-position indicator coils were attached to the participant's scalp at the nasion and left- and right-preauricular points. These head coils provided continuous specification of head position and orientation in relation to the MEG sensors. To minimize fatigue, during the task, participants viewed (but did not listen to) a movie projected onto a screen positioned at a comfortable viewing distance. Electrodes were attached to the left and right clavicles for electrocardiogram recordings (ECG) and to the bipolar oblique (upper and lower left sites) for electrooculogram recordings (EOG). A band-pass filter (0.03–300 Hz) was applied to the EOG, ECG, and MEG signals, with signals digitized at 1200 Hz, and with third-order gradiometer environmental noise reduction of the MEG data.

After the MEG session, structural magnetic resonance imaging (sMRI) provided T1-weighted, 3D MP-RAGE anatomical images for source localization acquired on a 3T Siemens Verio™ scanner (Siemens Healthcare, Erlangen, Germany) with voxel size 0.8 x 0.8 x 0.9 mm³.

2.4 Stimuli

Stimuli consisted of sinusoidal tones presented using Eprime v1.1. Tones were presented via a sound pressure transducer and sound conduction tubing to the

participant's peripheral auditory canal via ear-tip inserts (ER3A, Etymotic Research, IL). Prior to data acquisition, 1000Hz tones (300 ms duration, 10 ms rise time) were presented binaurally and loudness incrementally decreased until reaching auditory threshold for each ear. Stimulus tones were then presented at 45dB sensation level above threshold. During the task participants passively listened to binaurally presented interleaved 200, 300, 500 and 1000 Hz sinusoidal tones (tones 300 ms duration; 10 ms ramps) with a 1000 ms (± 100) inter-trial interval. Participants heard a total of 130 tones/frequency.

2.5 Data preprocessing

MEG responses were analyzed using the MatLab (Mathworks, Natick, MA) open-source toolbox Fieldtrip (Oostenveld et al. 2011). Using the continuous data and the procedures outlined in Fieldtrip (FieldtripWiki, 2015), ICA identified heartbeat and eye artifacts (blinks and saccades), and then these artifact components were removed from the epoched data (± 500 ms around trigger). Trials with jump and muscle artifact were also rejected (using Fieldtrip's Z-score based artifact rejection). Lastly, to account for differences in head motion during the MEG scan, if any fiducial moved more than 10 mm from the average head position during a trial that trial was rejected.

2.6 M100 Data Analysis

For each group, over 92% of trials remained after motion and artifact rejection (TD = $95.3 \pm 1.29\%$, ASD = $92.7 \pm 0.82\%$). A LMM (random intercept and random slope

of Timepoint) showed a trend towards a main effect of Diagnosis ($F(1,29.02)=3.02, p < 0.10$), and a marginally significant main effect of Timepoint ($F(1,28.9) = 4.01$ initial = 95.3 ± 0.98 , follow-up = $92.7 \pm 1.00, p = 0.052$). The interaction of Diagnosis X Timepoint was not significant, nor was any term involving stimulus frequency. Although a group difference in number of evaluable trials was suggested, rejection rates across groups were considered low, and given generally similar mean trial values between the groups, this difference was deemed unlikely to affect any group difference M100 latency finding.

Determination of the latency of M100 sources in the left and right Heschl's Gyrus was accomplished using the data from the above analyses pipeline. In addition, a 3 – 40 Hz band-pass filter was applied to the multi-channel (all ipsilateral channels) waveforms. In each participant, the left and right M100 peaks were then identified as the largest point in the M100 scoring window (90–190 ms) using the sensor butterfly plot of the band-passed ERF. To confirm that the M100 was accurately identified, magnetic field topographic plots over all ipsilateral sensors at the selected latency were examined to ensure a topography reflecting a M100 dipolar source.

Given a M100 latency dependence on stimulus frequency (Roberts & Poeppel 1996), and given that M100 responses are occasionally missing/unidentifiable for individual stimulus tone frequencies, M100 analyses were performed using LMM (with both random intercepts and a random slope for timepoint), with pairwise comparisons on the marginal means for Diagnosis, Timepoint, Hemisphere, Condition, as well as the Diagnosis X Hemisphere and Diagnosis X Timepoint, and Diagnosis X Timepoint X Hemisphere interactions. To investigate M100 latency maturation, LMMs were used to

create a tone-frequency independent “effective” M100 latency for each hemisphere. The effective M100 latencies were then used to compute a rate of maturation: (follow-up M100 effective latency – initial M100 effective latency)/change in years. A LMM (with random intercept) investigated statistical differences in rate of maturation, with pairwise comparison for Diagnosis, Hemisphere and Diagnosis X Hemisphere.

2.7 Gamma-band Data Analysis

For each group, over 93% of trials remained (TD = $95.2 \pm 0.83\%$, ASD = $93.1 \pm 0.61\%$). A LMM (analogous to used for testing of group differences in M100 trials remaining) showed a marginally significant main effect of Diagnosis ($p = 0.052$), and a main effect of Timepoint ($F(1,21)=5.28$; initial = 95.0 ± 0.62 , follow-up = 93.3 ± 0.64 , $p < 0.05$). The interaction of Diagnosis X Timepoint was not significant, although ASD but not TD demonstrated a change (gain) in the amount of remaining trials between initial and follow-up. Although group differences in the number of evaluable trials were suggested, rejection rates across groups were considered low, and given generally similar mean trial values between the groups, this difference was deemed unlikely to affect any group difference gamma-band finding.

Subject-specific single-shell head models were created from each participant’s MP-RAGE MRI. To coregister MEG and sMRI data, three anatomical landmarks (nasion and right and left preauriculars points) as well as an additional 200+ points on the scalp and face were digitized for each participant using the Probe Position Identification (PPI)

System (Polhemus, Colchester, VT), and a transformation matrix that involved rotation/translation between the MEG and sMRI coordinate systems was obtained via a least-squares match of the PPI points to the surface of the scalp and face. This head model was then fitted to the mean head position (in MEG coordinate space) as determined by the fiducials (Figure 2.1A). Separately, the participant's MRI was normalized to an age-matched average brain template (Fonov et al. 2011) using non-linear warping. A left and right Heschl's Gyrus location was identified and then reverse transformed to subject space. A linearly-constrained minimum variance (LCMV) beamformer was computed for each participant's left and right Heschl's Gyrus, discarding the contralateral hemisphere's sensors to reduce inter-hemispheric signal cancelation due to correlated activity (Herdman et al. 2003). Heschl's Gyrus virtual electrodes (VE) were then computed using a dipole orientation optimized for post-stimulus gamma-band activity (i.e. orientation determined via principal component analysis on the 0-270 ms post-stimulus window filtered 30-58 Hz).

Broadband resultant VE time courses were time-frequency transformed (Hilbert transform) using in-house MatLab scripts. For each participant, evoked power, total power (evoked and induced power) and inter-trial coherence (ITC) were calculated. Mean power/coherence was then derived for the spectrotemporal regions containing a gamma-band response. To avoid erroneously quantifying gamma-band activity by either a) not correctly accounted for gamma-band response maturation, or b) including low-level non-stimulus related signal (noise), gamma-band responses were quantified based on a time-frequency region containing both TD and ASD group-level activity (initial scan – evoked

power: 10-180 ms, 30-100 Hz, ITC: 10-170 ms 30-65 Hz, total power: 20-180 ms, 30-58 Hz; follow-up scan – evoked power: 10-170 ms, 30-100 Hz, ITC: 10-150 ms, 30-75 Hz, total power: 20-160 ms, 30-57 Hz). Gamma-band activity analyses were performed using LMMs, with pairwise comparisons on Diagnosis, Hemisphere, Timepoint, Diagnosis X Hemisphere, Diagnosis X Timepoint, and Diagnosis X Timepoint X Hemisphere. To test maturation group differences, a gamma-band activity maturation measure was computed: (follow-up gamma-band activity metric – initial gamma-band activity metric)/change in years.

2.8 Correlations with behavioral metrics

To test hypotheses regarding clinical measures as well as to examine the specificity of such associations, LMM (random intercept) analyses examined associations between MEG measures and scores on the Social Responsiveness Scale (SRS; a measure of ASD symptom severity, (Constantino et al. 2003)), CELF-4 core language index (CLI; a measure of language functioning), WISC-IV GAI (a measure of global cognitive function), and WISC-IV VCI (a measure of verbal comprehension). Each LMM had fixed effects of Timepoint, Age and behavioral metric, and were co-varied for Age and behavioral metric. Hierarchical regressions tested the hypothesis that *initial* gamma-band activity explained *additional* variance in the *follow-up* behavioral metrics (SRS, CELF-4 CLI, WISC-IV GAI & VCI) beyond the variance accounted for by initial behavioral measure and age (Dependent Variable = Behavioral Metric at follow-up; block 1 = Age and Behavioral Metric at initial exam, Block 2 = MEG measure).

3. Results:

As shown in Table 2.1, TD versus ASD did not differ on age at initial exam or at follow-up. As expected, children with ASD had higher SRS and ADOS Calibrated Severity Scores (CSS) (Gotham et al. 2009; Hus & Lord 2014) than TD at both exams. No group differences were observed in global functioning (WISC-IV GAI) at either time point. Group differences in verbal functioning (WISC-IV VCI) were present at the initial exam but not at follow-up. Children with ASD scored significantly lower on the CELF-4 Core Language Index than TD at both exams. The population included in gamma-band activity analyses exhibited a similar demographic profile: ASD exhibited higher scores on autism metrics (SRS and ADOS CSS), and decreased CELF-4 Core Language Indices at both exams. At the initial exam, ASD demonstrated significantly lower WISC-IV VCI than TD, though not so at follow-up. Lastly, in the gamma-band activity analyses participants, group differences in age or general functioning (WISC-IV GAI) were not observed.

3.1 M100 latency

A main effect of Condition (stimulus tone), $F(3,114.62) = 17.53$ $p < 0.001$, showed the expected earlier M100 latencies to higher versus lower frequency tones (Roberts & Poeppel 1996); a main effect of Hemisphere, $F(1,154.53) = 111.76$, $p < 0.001$, showed the expected earlier right than left M100 latencies (Roberts et al. 2000); and a main effect of Timepoint, $F(1,21.77) = 8.52$, $p < 0.01$, showed the expected maturational change with earlier latencies at follow-up versus initial exam. The main

effect of Diagnosis (ASD versus TD) was significant, $F(1,23.27) = 7.43, p < 0.05$, confirming the *a priori* hypothesis of delayed M100 latencies in ASD versus TD (TD = 122 ± 6.0 ms; ASD = 141 ± 4.0 ms). Simple effect analyses of a significant Diagnosis X Hemisphere X Timepoint interaction, $F(2,152.94) = 3.30, p < 0.05$, showed significantly earlier M100 latencies at follow-up versus the initial exam in both groups and both hemispheres except for no significant right-hemisphere changes in TD. This interaction though is potentially confounded due to inter-subject (despite no group difference) differences in follow-up interval. None of the other interaction terms involving Diagnosis were significant. M100 latency values for all groups at both exams (marginal means after collapsing across condition) are shown in Figure 2.2.

Additional analyses examined group differences in the M100 latency maturation rate measure (i.e., (follow-up M100 effective latency – initial M100 effective latency)/change in years). Both TD and ASD demonstrated the characteristic ~3-5 ms/year M100 latency maturation, with no significant differences for Diagnosis, Hemisphere or their interaction ($p > 0.05$). Thus both TD and ASD showed maturational shortening in M100 latency with no resolvable difference in maturation *rate* between groups, despite the above persistent and significant absolute latency difference between groups.

3.2 Gamma-band activity

To increase signal-to noise, responses were averaged across condition (shown effective in (Gandal et al. 2010)). As shown in Figure 2.3, at both exams, gamma-band activity was visible in the grand average time-frequency response for each group.

An LMM (with subject as a random effect) tested for group differences in total power. Gamma-band total power did not differ between TD and ASD at either exam (data not shown). For evoked power (tested via LMM with random intercepts), a main effect of Diagnosis, $F(1,41.6) = 8.68$, $p < 0.01$, confirmed the *a priori* hypotheses of reduced gamma-band evoked activity in ASD ($38.4 \pm 4.7\%$ change from baseline) versus TD ($61.5 \pm 6.4\%$ change from baseline; Figure 2.4A). The main effect of Timepoint was also significant, $F(1,43.07) = 8.04$, $p < 0.01$, demonstrating *maturation* of evoked response power over time (initial = $41.1 \pm 3.1\%$ change from baseline, follow-up = $58.8 \pm 6.4\%$ change from baseline). Of note, although Figure 2.4A suggests greater gamma-band evoked group differences at follow-up ($33.1 \pm 12.8\%$ change difference between TD and ASD; $p = 0.013$) versus initial exam ($13.2 \pm 6.2\%$ change difference between TD and ASD; $p = 0.046$), the interaction term was not significant. Finally, analyses examined group differences in evoked gamma-band maturation rates (LMM with random intercepts). Although showing a four-fold faster maturation rate, the rate of change in evoked gamma-band activity for TD ($7.7 \pm 3.0\%$ change from baseline /year) was not significantly different from ASD ($2.1 \pm 2.2\%$ change from baseline /year; Figure 2.4).

For gamma-band ITC (tested via LMM with random intercept and Timepoint as a random slope), a main effect of Diagnosis, $F(1,22.24) = 6.30, p < 0.05$, indicated greater ITC in TD versus ASD (ASD = 0.040 ± 0.003 ITC, TD = 0.053 ± 0.004 ITC). Although the interaction was not significant, ASD exhibited only a qualitative decrease in ITC versus TD at initial exam (ASD = 0.040 ± 0.003 , TD = 0.050 ± 0.005 , TD-ASD = $0.010 \pm 0.007, p = 0.116$), which became significant at follow-up exam (TD-ASD = $0.016 \pm 0.006, p < 0.05$). As shown in Figure 2.4, analyses examining ITC maturation (LMM with random intercept) showed no significant group differences.

3.3 Correlation of MEG Auditory Biomarkers and Behavioral Metrics

Data from all participants (including “had ASD”) were included in the correlational analyses. To ensure specificity of any associations and to provide negative controls, all comparisons between behavioral metrics and MEG-derived measures (excluding rates of maturation) were examined. Of note, the behavioral measures (SRS, CELF-4 CLI, WISC-IV GAI, WISC-IV VCI) shared considerable variance, especially the CELF-4 CLI, WISC-IV GAI and WISC-IV VCI, with up to 80% variance shared (see Supplemental Table 2.2 for bivariate correlations among behavioral measures).

Examining all participants at both timepoints, both left and right hemisphere M100 latencies were associated with SRS after removing variance associated with Age and Time (LH: SRS $F(1,54.30) = 6.48 p < 0.05$, estimate = 0.2 ms/SRS point, RH: SRS $F(1,62.38) = 15.20 p < 0.001$, estimate = 0.2 ms/SRS point; Figure 2.5). No associations

were observed for CELF-4 Core Language Index or WISC-IV metrics (GAI/VCI) in either hemisphere ($p > 0.1$), or for any gamma-band metric.

Although M100 latency did not correlate with *current* language scores, right-hemisphere *initial* M100 latency predicted *additional* variance in the *follow-up* CELF-4 Core Language Index metric (R^2 change = 0.03, $p < 0.05$). In addition, a trend was observed for an association between *initial* evoked gamma-band power and *follow-up* WISC-IV VCI (R^2 change = 0.033, $p < 0.1$). Furthermore, *initial* gamma-band ITC predicted *additional* variance in follow-up WISC-IV VCI after removing the effect of age and initial WISC-IV VCI score (R^2 change = 0.05, $p < 0.05$). Thus, these MEG measure may offer a prognostic indication of language outcome (perhaps signifying “capacity for improvement”).

3.4 Preliminary results for “had ASD”

As previously mentioned, a third group of participants emerged over the course of the study - the “had ASD” group. Although too small for statistical assessment, data from these participants are included as *descriptive* preliminary findings. These participants showed a diagnostic profile similar to the primary ASD group at the initial exam (Table 2.1 & 2.2, SRS = 75.0, ADOS CSS = 7.8). At follow-up, however, these participants had intermediate SRS and ADOS scores (Table 2.1 & 2.2, SRS = 54.4 ADOS CSS = 2.5). Such “optimal outcome” has been demonstrated before, with such children tending to have initial language/communication scores that predict outcome (Helt et al. 2008). Not

inconsistent with this, these five children scored between TD and ASD on the WISC-IV VCI at both time points (initial = 104.2, follow-up = 109.6).

With regard to M100 latencies, as shown in Figure 2.2A, M100 latencies in the “had ASD” group at the initial exam were either similar to TD (left hemisphere) or in-between TD and ASD (right hemisphere). As shown in 2B and 2C, this profile was also observed at follow-up as well as for the M100 latency maturation rate measure. In addition, “had ASD” showed gamma-band evoked power and ITC values between TD and ASD at the initial and follow-up exams. Follow-up studies are needed to confirm if this represents an electrophysiological signature of “capacity for improvement”.

4. Discussion:

M100 latencies and phase-locked gamma-band evoked power matured from initial to follow-up exam. This finding supports findings from cross-sectional studies (Paetau et al. 1995; Rojas et al. 2006). In addition, similar to previous studies (Gage, Siegel & Roberts 2003; Roberts et al. 2010; Roberts et al. 2013; Wilson et al. 2007; J Christopher Edgar et al. 2015; J. Christopher Edgar et al. 2015; Edgar et al. 2016), delayed right hemisphere M100 latencies and reduced gamma-band evoked power and ITC were observed in ASD versus TD. Of note, different from previous studies, left-hemisphere M100 group differences were also observed in ASD, with bilateral M100 latency findings in the present study perhaps associated with greater power in longitudinal studies. Interestingly, M100 latency delays were greater than those reported in previous studies (Gage, Siegel & Roberts 2003; Roberts et al. 2010; Roberts et al. 2013; J Christopher Edgar et al. 2015), an effect perhaps due to the use of cross-sectional designs in previous studies. In particular, whereas cross-sectional studies likely include some children that later exhibit “optimal outcome”, in the present study such information was available and these ASD subjects (“had ASD”) were excluded from primary analyses. Indeed, reanalysis of the data for timepoint 1 that included the “had ASD” individuals in the ASD group, while still showing significant group differences, decreased the effect size by several milliseconds.

Maturation rates for M100 latency as well as the gamma-band metrics did not differ between TD and ASD, a finding that confirms previous cross-sectional maturation rate estimates (Roberts et al. 2013; Edgar, Lanza, et al. 2014) As such, present findings

support findings from previous studies suggesting a perturbed developmental *trajectory* (despite similar maturation *rate*) of M100 latency in ASD, due to a persistent latency offset.

Analyses examined the relationship of the two auditory biomarkers to current and future behavior. Four separate (though related) behavioral metrics were tested in order to examine the specificity of associations. Right- and left- hemisphere M100 latencies were associated with greater clinical impairment (higher SRS scores). To the authors' knowledge, this is the first time such associations have been demonstrated.

Although analogous relationships were not observed for gamma-band metrics, *initial* gamma-band ITC predicted variance in *follow-up* WISC-IV VCI scores. Gamma-band evoked power exhibited a similar, though non-significant relationship, with WISC-IV VCI scores. Somewhat unexpectedly, right M100 latencies also predicted CELF-4 Core scores. Although in previous studies gamma-band metrics predicted future cognitive and language abilities (Gou et al. 2011), such associations have not been previously reported for M100 latencies. Although the current right-hemisphere M100 associations with CELF-4 Core score may appear contradictory (no association at the current exam, but an association scores at the *later* exam), a potential explanation for such a result may be that language-related issues arising from M100 latency prolongations are *cumulative*. As such, the later the language-related measure taken, the greater the observed language deficit for that subject. Over a population, this would allow for a greater range of language ability, making an association with M100 latencies easier to detect. Thus, it is hypothesized that a M100 latency delay relates to diminished capacity for language

improvement (and as well that an earlier M100 latency predicts the availability of capacity for improvement). Given “capacity” for improvement, the degree of improvement will likely depend on interventions in the follow-up interval, and thus the M100 latency measure is suggested as a prognostic/predictive biomarker for future intervention studies. Previous (cross-sectional) studies examining the association of M100 latencies and general language ability are inconsistent (Oram Cardy et al. 2008; Roberts et al. 2010; Roberts et al. 2013), perhaps due to the prevalence (as well as variety) of language impairments in ASD or the language measure taken concurrently to the M100 measurement. Of note, the M100 latency delay in children appears to be specific to ASD, at least in comparison to children with specific language impairment (SLI) (Roberts et al. 2012).

A few study limitations are of note. First, a potential confound is the gender bias (more females in the control group). In a separate analysis, previously collected and published datasets were investigated for gender effects for M100 latency and gamma-band evoked power and ITC (Roberts et al. 2010; J Christopher Edgar et al. 2015). The main effect of Gender was not significant for any analysis. Gender therefore likely does not confound present findings.

A second limitation is that children were only scanned twice (two to five year inter-scan interval). To determine if the findings here extend to other developmental periods (i.e. before or after the age range sampled here), multiple time points are required. Longer follow-up periods would also provide resolution of statistical tendencies in maturation rates that did not reach significance in the present study. Multiple

timepoints and an extended study age-range would also permit the consideration of non-linear dependencies of observed variables on age.

Finally, given the small sample, statistical analyses could not be performed on the “has ASD” cohort. In these children, M100 latency and gamma-band findings were qualitatively observed to be in-between TD and the remaining ASD group, suggesting that these auditory neural measures may serve as prognostic biomarkers. These findings are only suggestive though, and a larger cohort is needed to confirm and establish the precision/sensitivity of the above observations. As noted in the Introduction, the endogenous, environmental or therapeutic factors that contribute to clinical change are currently generally unknown. The literature on “optimal outcomes”, however, does indicate that in children who exhibit “optimal outcome” subtle impairments are still observed (Orinstein et al. 2015), a finding supported in the present study via the observation in “had ASD” of auditory neural measures at follow-up with values *between* TD and ASD. In future studies with larger samples, quantitative assessments of the intervention/treatments the children with ASD receive are needed to help identify the basis and/or mechanism for improvement.

To conclude, the present study demonstrated altered auditory M100 and gamma-band neural activity in children with ASD. Electrophysiological measures correlated with, and predicted subsequent change in behavioral measures. The children with ASD who showed clinical improvement appeared to have somewhat more normal electrophysiological responses at the first and follow-up exams. As such, present findings

may suggest that the auditory neural measures investigated in this study may serve as prognostic biomarkers, with further study needed to validate such findings.

Tables Legends:

Table 2.1 *Demographics of M100 study population.* No significant differences in age (4th block from left) or Wechsler Intelligence Scale for Children-IV General Ability Index (WISC-IV GAI) (5th block from left) were observed between TD (top), and ASD (middle). Children with ASD exhibited significantly higher Social Responsiveness Scale (SRS) and Autism Diagnostic Observation Schedule Calibrated Severity Scores (ADOS CSS) at both initial and follow-up exams (1st and 2nd block from the right). Wechsler Intelligence Scale for Children-IV Verbal Comprehension Index (WISC-IV VCI) scores were significantly lower in children with ASD (middle right) at initial exam. ASD children also demonstrated significantly lower scores on the Clinical Evaluation of Language Fundamentals – fourth edition (CELF-4 Core Language Index). A subgroup of children who had an initial diagnosis of ASD no longer met diagnosis criteria at the follow-up exam (“had ASD” (bottom)). These children exhibited SRS and ADOS CSS scores similar to children with ASD at the initial exam, and then intermediate corresponding scores at follow-up. These children had similar age and GAI to children with ASD, though intermediate WISC-IV VCI scores. Values are counts or mean (standard deviation).

Table 2.2 *Demographics of gamma-band study population.* Identical to the M100 study population: No significant differences in age (4th block from left) or Wechsler Intelligence Scale for Children-IV General Ability Index (WISC-IV GAI) (5th block from left) were observed between TD (top) , and ASD (middle). Children with ASD exhibited significantly higher Social Responsiveness Scale (SRS) and Autism Diagnostic Observation Schedule Calibrated Severity Scores (ADOS CSS) at both initial and follow-up exams (1st and 2nd block from the right). Wechsler Intelligence Scale for Children-IV Verbal Comprehension Index (WISC-IV VCI) scores were significantly lower in children with ASD (middle right) at initial exam. ASD children also demonstrated significantly lower scores on the Clinical Evaluation of Language Fundamentals – fourth edition (CELF-4) Core Language Index. A subgroup of children who had an initial diagnosis of ASD no longer met diagnosis criteria at the follow-up exam (“had ASD” (bottom)). These children exhibited SRS and ADOS CSS scores similar to children with ASD at the initial exam, and then intermediate corresponding scores at follow-up. These children had similar age and GAI to children with ASD, though intermediate Wechsler Intelligence Scale for Children-IV Verbal Comprehension Index WISC-IV VCI scores. Values are counts or mean (standard deviation).

Supplemental Table 2.1 *Medications and supplements*. Subjects, listed by Diagnosis (Dx) and subject number, and showing medications and supplements at initial exam (2nd column) and follow-up exam (right column). General health medications are in blue, while medications for comorbid psychiatric disorders are in black.

Supplemental Table 2.2 *Correlation between behavioral measures.* Bivariate Pearson's correlations between the four behavioral measures used in this study. Social Responsiveness Scale (SRS); Wechsler Intelligence Scale for Children-IV General Ability Index (WISCV-IV GAI); Clinical Evaluation of Language Fundamentals – fourth edition (CELF-4) Language Core Index; Wechsler Intelligence Scale for Children-IV Verbal Comprehension Index (WISC-IV VCI). * $p < 0.05$, ** $p < 0.01$

Figure Legends:

Figure 2.1 *Gamma-band activity analyses.* (A) Head models were generated from each subject's structural MRIs and centered at the average head position. Trials where any fiducial moved in any direction >10mm from this average position were rejected (B) After normalizing individual MRIs to an age-matched template, Heschl's Gyrus was non-linear reverse source interpolated. (C) A LCMV beamformer (with only ipsilateral sensors included) at subject space Heschl's Gyrus was used to generate virtual electrode time courses (D) Left and right STG time courses were used to obtain time frequency measures (evoked, total power, ITC) using in-house scripts. Arrow points to gamma-band activity response.

Figure 2.2 *M100 latencies predict diagnosis.* (A) T-tests showed that children with ASD versus TD had prolonged left and right-hemisphere M100 latencies at the initial exam. (B) At the follow-up exam, children with ASD again showed prolonged M100 latencies. The “had ASD” exhibited non-significant intermediate M100 latencies at both timepoints. (C) No group differences between TD and ASD were present for maturation rates. Intermediate M100 latency maturation (as compared to TD and ASD) rates are exhibited by the “had ASD” cohort. Although analyses were conducted for only ASD and TD, mean and SE values are also shown for “the had” ASD group. # $p < 0.10$, * $p < 0.05$

Figure 2.3 *Children with ASD exhibit reduced gamma-band evoked power.* (A) Group average evoked power plots for TD children (left) at initial exam (upper, A) and follow-up exam (lower, C) show the auditory gamma-band post-stimulus response. At both time points, children with ASD (right) showed reduced gamma-band responses (initial exam– upper, B; follow-up exam – lower, D). Dashed box show gamma-band ROI used.

Figure 2.4 *Children with ASD exhibit reduced gamma-band evoked power and inter-trial coherence.* Evoked power (top row) responses were reduced in children with ASD at both initial (A) and follow-up exam (B). The “had ASD” group exhibited qualitatively intermediate responses at both timepoints. Maturation of the evoked gamma-band response (upper C) was reduced four-fold in ASD versus TD. ITC (bottom row) demonstrated a similar pattern, though not significant at initial exam. # $p < 0.10$, * $p < 0.05$

Figure 2.5 *M100 latencies and SRS scores.* Effective right-hemisphere M100 latencies (removing effect of condition) were associated with social responsiveness scores across the study population. *** $p < 0.001$

Tables:

Table 2. 1

	N	Male	Age (years)		WISC-IV GAI		WISC-IV VCI		CELF-4 CLI		SRS (Raw)		ADOS CSS	
			Initial	Follow-up	Initial	Follow-up	Initial	Follow-up	Initial	Follow-up	Initial	Follow-up		
Control	9	3	8.4 (1.3)	11.9 (1.5)	116.3 (17.3)	113.8 (20.4)	113.2 (19.0)	110.3 (21.5)	108 (14.6)	105.8 (15.5)	46.3 (7.1)	41.3 (4.4)	1.2 (0.4)	1.3 (0.8)
ASD	22	22	8.4 (1.1)	12.1 (1.3)	104.9 (15.5)	102.2 (15.0)	94.0 (15.8)	97.3 (12.9)	85.3 (17.1)	89.5 (18.0)	75.1 (9.4)	70.5 (12.5)	8.3 (1.8)	7.0 (1.6)
“had ASD”	5	4	8.7 (0.7)	11.8 (0.4)	102.6 (9.0)	105.6 (13.6)	104.2 (10.1)	109.6 (9.7)	90.8 (12.7)	96.4 (9.7)	75.0 (18.7)	54.4 (12.1)	7.8 (2.7)	2.5 (1.0)
<i>p</i> ([TD top] vs. ASD[middle])			0.99	0.77	0.11	0.18	0.02	0.15	<0.001	0.02	<0.001	<0.001	<0.001	<0.001
Cohen's d							1.1		1.43	0.97	-3.46	-3.12	-5.45	-4.51

Table 2. 2

	N	Male	Age (years)		WISC-IV GAI		WISC-IV VCI		CELF-4 CLI		SRS (Raw)		ADOS CSS	
			Initial	Follow-up	Initial	Follow-up	Initial	Follow-up	Initial	Follow-up	Initial	Follow-up		
Control	8	2	8.4 (1.4)	12.1 (1.5)	118.3 (17.5)	116.0 (21.0)	114.4 (20.0)	112.3 (22.4)	110.3 (13.8)	108.9 (13.3)	46.4 (7.6)	40.1 (3.3)	1.2 (0.4)	1.3 (0.8)
ASD	15	15	8.6 (1.1)	12.2 (1.3)	104.9 (13.6)	105.2 (15.0)	95.1 (14.3)	101.0 (12.2)	88.9 (12)	93.2 (11.8)	74.6 (10.5)	71.5 (14.5)	8.1 (1.7)	7.4 (1.6)
"had ASD"	5	4	8.7 (0.7)	11.8 (0.4)	102.6 (9.0)	105.6 (13.6)	104.2 (10.1)	109.6 (9.7)	90.8 (12.7)	96.4 (9.7)	75.0 (18.7)	54.4 (12.1)	7.8 (2.7)	2.5 (1.0)
			μ (TD[top] vs. ASD[middle])	0.80	0.89	0.09	0.25	0.03	0.25	<0.001	0.01	<0.001	<0.001	<0.001
			Cohen's d				1.11		1.65	1.25	-3.08	-2.99	-5.59	-4.82

Supplemental Table 2. 1

Dx #	Medications	
	Original Visit	Follow-up Visit
TD 1	None	Naltrexone
TD 2	None	None
TD 3	None	None
TD 4	None	None
TD 5	None	None
TD 6	None	None
TD 7	None	None
TD 8	None	None
TD 9	None	None
ASD 1	None	None
ASD 2	None	None
ASD 3	Ritalin, Daytrana, Risperidone, Vistaril, Melatonin	Ritalin, Daytrana, Celexa, Catapres, Risperidone,
ASD 4	None	None
ASD 5	None	None
ASD 6	Adderall, Trileptal, Abilify, Paxil CR, Desmopressin	Lamictal, Xanax, Zyprexa
ASD 7	None	None
ASD 8	None	None
ASD 9	None	Abilify
ASD 10	None	Vyvanse
ASD 11	None	None

ASD 12	Vyvanse	Vyvanse
ASD 13	Strattera	Strattera, Zoloft
ASD 14	Metadate, Claritin, Vitamin B12 injections	Metadate, Ritalin, Claritin, Vitamin B12 injections
ASD 15	Vitamins	Melatonin
ASD 16	Intuniv	Metadate, Abilify
ASD 17	Ritalin, Melatonin	Ritalin, Melatonin, Fish Oil, Vitamins
ASD 18	Focalin	Focalin
ASD 19	Vyvanse	Strattera, Fluoxetine
ASD 20	Flovent	Flovent, Albuterol
ASD 21	None	None
ASD 22	Vitamins	Vitamins
“had ASD” 1	None	Fluoxetine
“had ASD” 2	None	Intuniv
“had ASD” 3	None	None
“had ASD” 4	None	Concerta, Nasonex (seasonal)
“had ASD” 5	None	None

Supplemental Table 2. 2

		SRS	WISC-IV GAI	CELF-4 CLI	WISC-IV VCI
SRS	Pearson Correlation	1	-.223	-.300*	-.291*
	Sig. (2-tailed)		.081	.016	.020
	N	64	62	64	64
WISC-IV GAI	Pearson Correlation	-.223	1	.733**	.894**
	Sig. (2-tailed)	.081		.000	.000
	N	62	64	64	64
CELF-4 CLI	Pearson Correlation	-.300*	.733**	1	.304*
	Sig. (2-tailed)	.016	.000		.012
	N	64	64	67	67
WISC-IV VCI	Pearson Correlation	-.291*	.894**	.304*	1
	Sig. (2-tailed)	.020	.000	.012	
	N	64	64	67	67

Figures:

Figure 2. 1

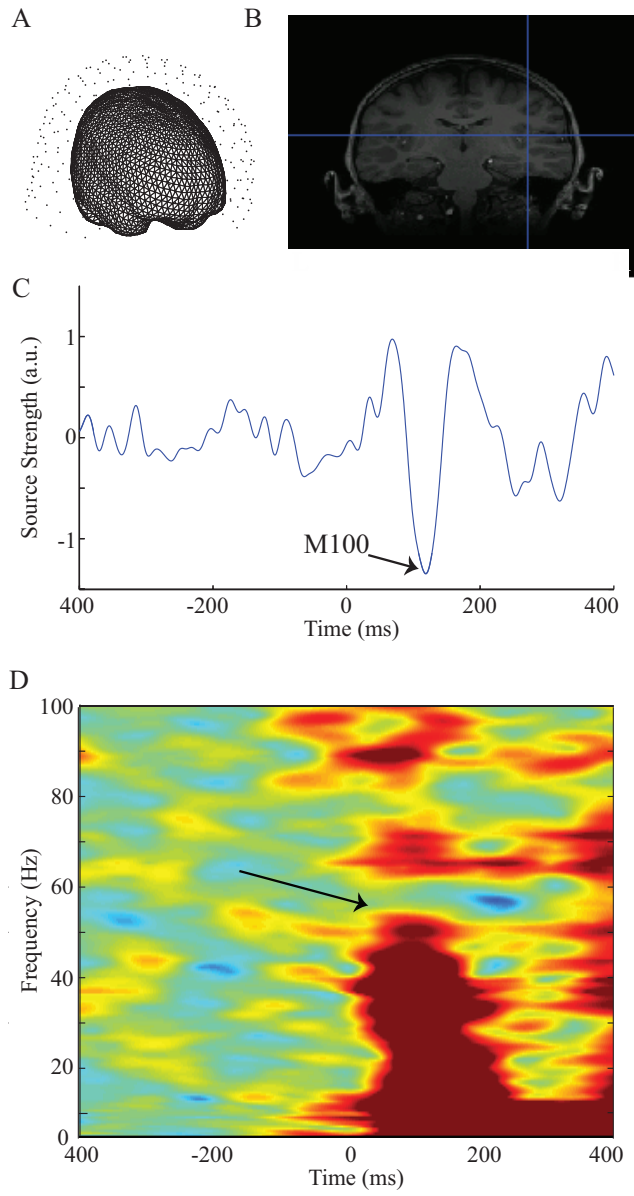
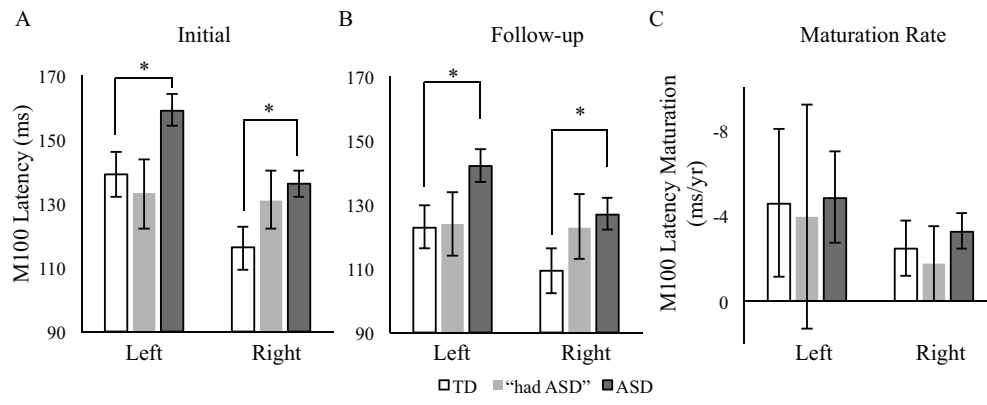


Figure 2. 2



*

Figure 2.3

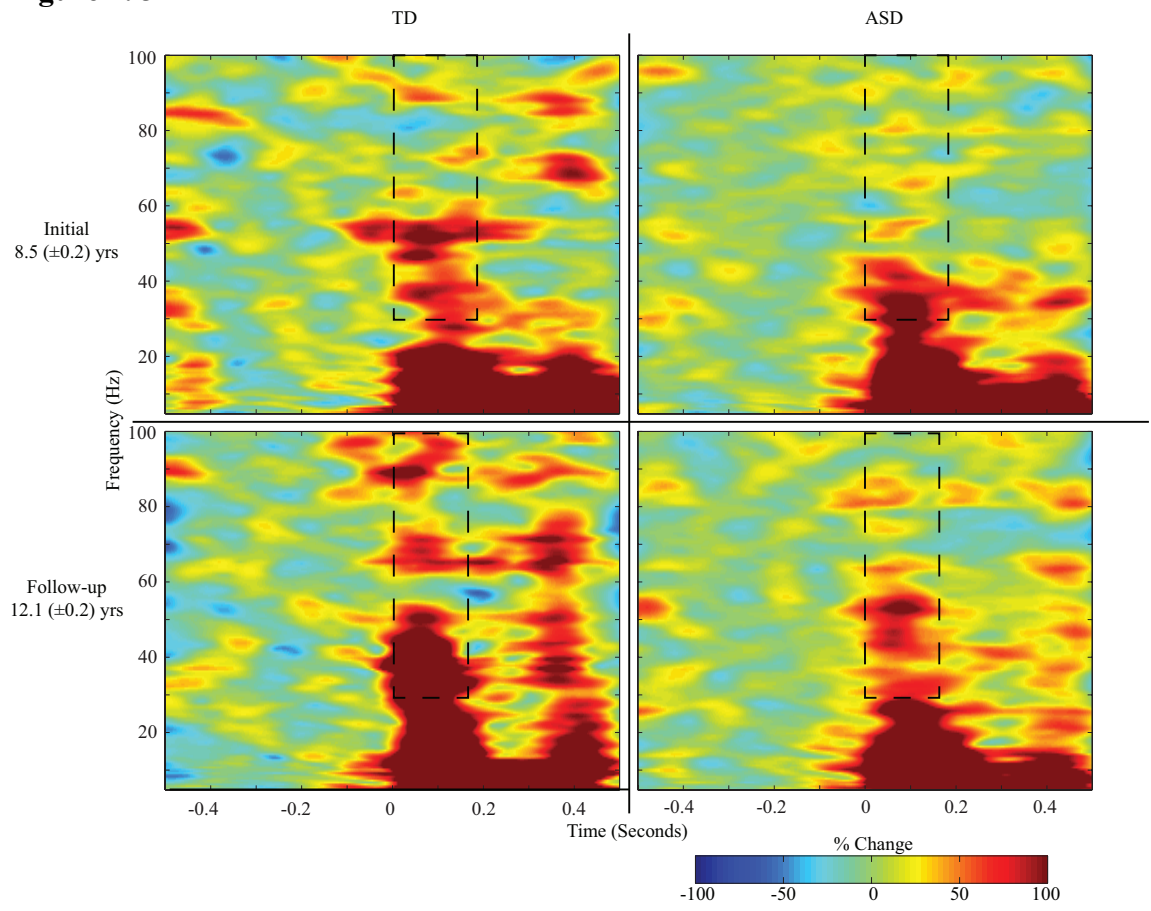


Figure 2. 4

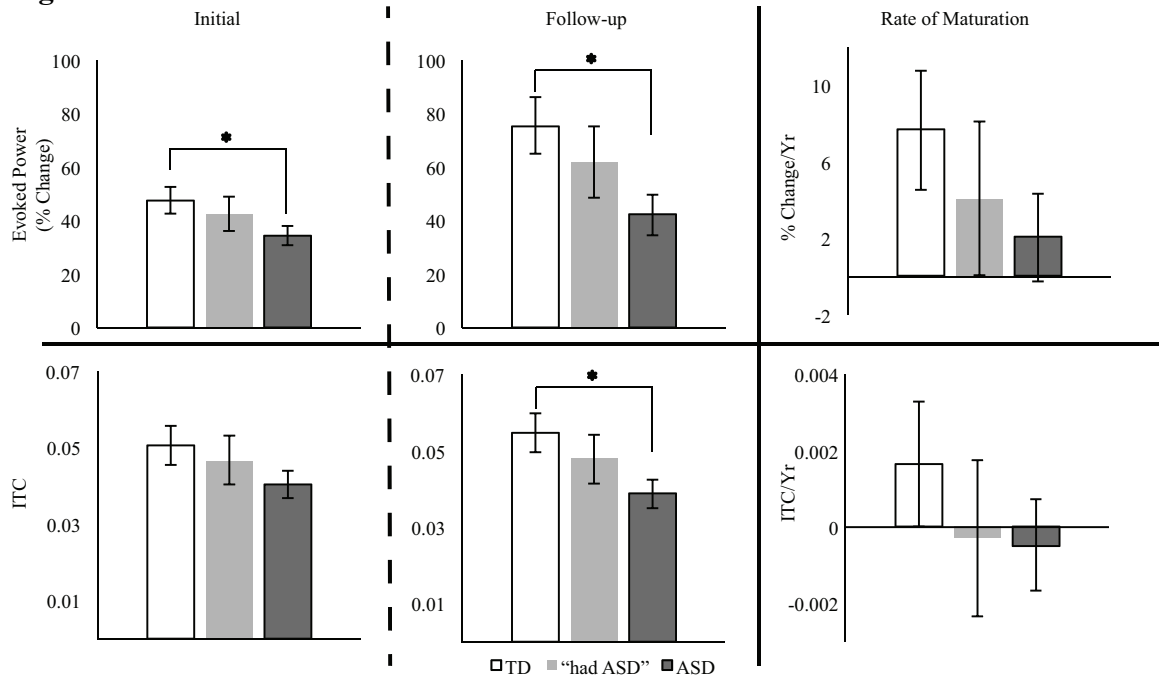
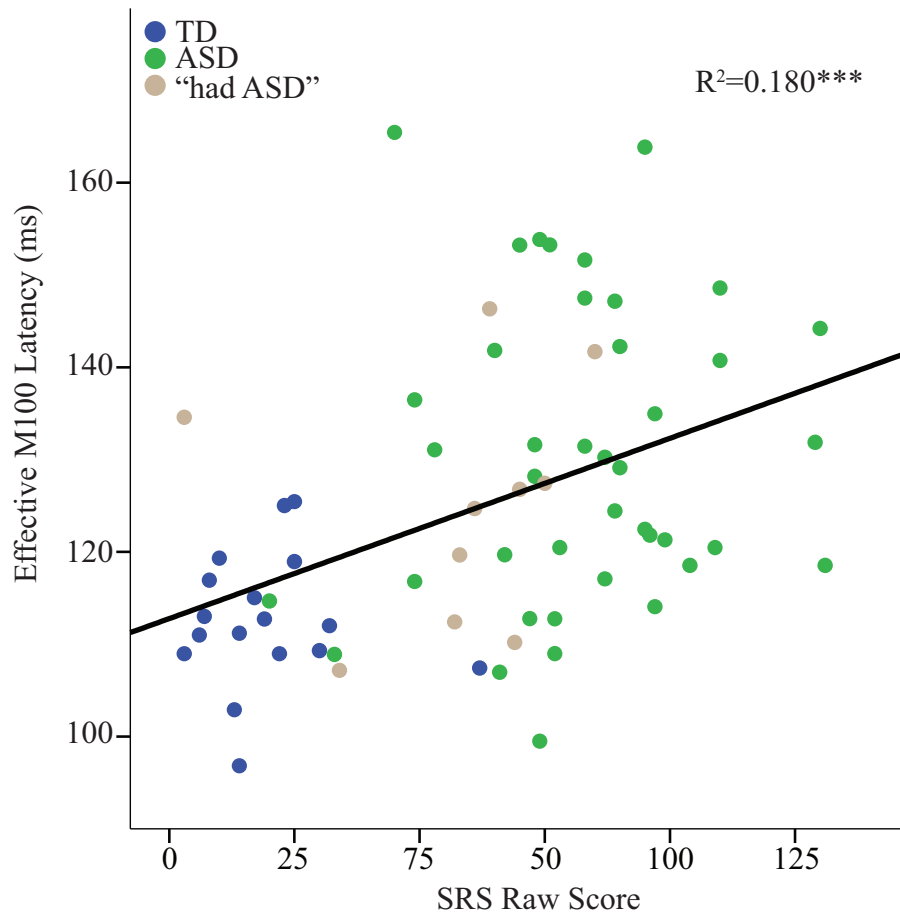


Figure 2.5



CHAPTER 3

Decreased auditory system GABA concentration, gamma-band coherence and coupling between them in ASD

Russell G. Port¹, William Gaetz¹, Dah-Jyuu Wang¹, Luke Bloy¹, Lisa Blaskey¹, Emily S. Kushner¹, Susan E. Levy², Edward S. Brodtkin³, Timothy PL Roberts¹

¹Lurie Family Foundations MEG Imaging Center, Department of Radiology, Children's Hospital of Philadelphia, Philadelphia, PA, USA

²Department of Pediatrics, Children's Hospital of Philadelphia, Philadelphia, PA, USA

³Department of Psychiatry, Perelman School of Medicine at the University of Pennsylvania, Philadelphia, Pennsylvania 19104

Present here as to be submitted to Autism Research

Abstract:

Autism spectrum disorder (ASD) is hypothesized to arise from imbalances between excitatory and inhibitory neurotransmission (E/I imbalance). Recent studies have demonstrated E/I imbalance in both individuals with ASD as well as in corresponding rodent models. One process thought to be reliant on E/I balance is gamma-band activity (Gamma), with support arising from observed correlations between motor, as well as visual, Gamma and underlying GABA concentrations in healthy adults. In accordance with these correlations, perturbed Gamma has also been observed in ASD individuals and in relevant animal models, though the relationship between Gamma and related GABA concentrations in ASD remains unexplored. This study combined magnetoencephalography (MEG) and edited magnetic resonance spectroscopy (MRS) in 17 typically developing individuals (TD) and 31 individuals with ASD. Auditory cortex localized phase-locked Gamma was compared to resting Superior Temporal Gyrus relative cortical GABA concentrations. Replicating previous studies both gamma-band inter-trial coherence (ITC) and GABA⁺/Cr were decreased in ASD versus TD. For all subjects independent of diagnosis, Gamma metrics (coherence/power) were significantly correlated to relative cortical GABA concentrations. For TD ITC and to a lesser extent evoked power were correlated to relative GABA concentrations. Individuals with ASD demonstrated a non-significant trend between gamma-band ITC and relative GABA concentrations, and no correlation between evoked power and GABA concentrations. Additionally, linear regression slopes were not significantly different between groups for ITC-based coupling. This suggests that a “functional to neurochemical coupling” or

“GABA efficiency” metric may provide early indication for treatment stratification with regards to interventions that recover E/I balance.

1. Introduction:

Autism spectrum disorder (ASD) is a neurodevelopmental disorders characterized by pervasive invasive social/communication impairments and restricted/repetitive behaviors (American Psychiatric Association, 2013). Current prevalence estimates suggest that 1 in 68 children is diagnosed with ASD (Developmental Disabilities Monitoring Network Surveillance Year 2010 Principal Investigators & Centers for Disease Control and Prevention (CDC), 2014). For over a decade an imbalance in neural excitation/inhibition (E/I imbalance) has been explored as a pathogenic mechanism of ASD (Rubenstein & Merzenich, 2003), with support coming from both clinical in-vivo imaging (Brown, Singel, Hepburn, & Rojas, 2013; Gaetz et al., 2014; Harada et al., 2011; Rojas, Singel, Steinmetz, Hepburn, & Brown, 2014) and post-mortem (Casanova et al., 2006; Fatemi, Folsom, Reutiman, & Thuras, 2009; Fatemi, Reutiman, Folsom, & Thuras, 2009; Fatemi et al., 2002; Zikopoulos & Barbas, 2013) studies. Furthermore, such E/I imbalance phenotypes have been recapitulated in animal models that recreate key aspects of ASD (Calfa, Li, Rutherford, & Pozzo-Miller, 2015; M J Gandal, Anderson, et al., 2012; Gogolla et al., 2009; Liao, Gandal, Ehrlichman, Siegel, & Carlson, 2012; Lin, Gean, Wang, Chan, & Chen, 2013; Saunders, Gandal, Roberts, & Siegel, 2012).

Recently E/I imbalance has been investigated in ASD via the use of magnetic resonance spectroscopy (MRS), a technique that allows in-vivo measurement of resting neurochemical concentrations. Such experiments have observed alterations to both relative cortical inhibitory (γ -Aminobutyric acid (GABA)) as well as excitatory (glutamate) neurotransmitters in individuals with ASD (for review see (Rojas, Becker, &

Wilson, 2015)). While these studies have found ASD-related alterations to *in vivo* concentrations, these findings should be carefully considered because the direct link by which these group level differences explain phenotypic (i.e., clinical/behavioral) symptoms is far from conclusive.

Excitatory and inhibitory neurotransmitters are thought to form the basis for neural communication in the brain. Numerous studies suggest that the gamma-band response (30-80 Hz) is critically dependent on E/I signaling (Cardin et al., 2009; Sohal, Zhang, Yizhar, & Deisseroth, 2009; Whittington, Traub, Kopell, Ermentrout, & Buhl, 2000; Yizhar et al., 2011), and known to be important for basic sensory (e.g. visual system and auditory system) functions (Başar-Eroglu, Strüber, Schürmann, Stadler, & Başar, 1996; Gray, König, Engel, & Singer, 1989) as well as higher order cognitive processes (Herrmann, Fründ, & Lenz, 2010). The gamma-band response is also clearly perturbed in multiple systems (i.e. visual, auditory and rest) in ASD (Grice et al., 2001; Orekhova et al., 2007; Wilson, Rojas, Reite, Teale, & Rogers, 2007). Furthermore this neurophysiological ASD-related phenotype is conserved in animal models that recreate key aspects of ASD, while not reliant on the nature of the specific insult (i.e. environmental insult versus genetic insult) (M J Gandal, Anderson, et al., 2012; Michael J Gandal et al., 2010; Saunders et al., 2012).

Although *in-vivo* relative cortical GABA has been shown to be decreased in ASD (Gaetz et al., 2014; Harada et al., 2011; Rojas et al., 2014), further replication is warranted. Furthermore, whereas gamma-band neurophysiological correlates of GABA concentrations have been observed in the visual and motor system of healthy adults

(Gaetz, Edgar, Wang, & Roberts, 2011; Muthukumaraswamy, Edden, Jones, Swettenham, & Singh, 2009), there has been some controversy (Cousijn et al., 2014). A recent EEG study in adults showed a positive correlation between GABA level and gamma-band power (Balz et al., 2015). However, no such correlation has been observed in the auditory system for either typically developing (TD) individuals or individuals with ASD.

As such this study tests the following three hypotheses; 1) Replicating previous studies, relative GABA concentrations in Superior Temporal Gyrus (STG) (Gaetz et al., 2014; Rojas et al., 2014), as well as phase-locked gamma-band responses (Edgar et al., 2015; Michael J Gandal et al., 2010; Rojas, Maharajh, Teale, & Rogers, 2008; Wilson et al., 2007) will be decreased in ASD. 2) In line with previous studies involving multimodal sensory integration (Balz et al., 2015) *in-vivo* relative cortical GABA concentrations will positively correlate to phase-locked gamma-band activity in the auditory system for TD individuals. 3) Since previous studies suggest decreases in both relative cortical GABA levels as well as phase-locked gamma-band activity (see above), individuals with ASD will also exhibit a direct linear relationship between relative cortical GABA concentrations and phase-locked gamma-band activity.

These hypothesized relationships between relative cortical GABA levels and gamma-band dysfunction are novel and have yet to be demonstrated explicitly within the same subjects. As such, the following three competing, but not mutually exclusive, outcomes may occur. 1) altered E/I balance and gamma-band dysfunction are *not* correlated in an overall ASD population, or are at least not resolvable due to separate sub-

populations of ASD individuals, some of whom demonstrate GABA⁺/gamma-band activity correlation, and some of whom do not; 2) altered E/I balance (GABA⁺) and gamma-band dysfunction are present in ASD, yet with altered coupling (regression slope) as compared to typically developing individuals, or 3) altered E/I balance and gamma-band dysfunction exist in ASD with the same regression slope as in TD, and though the coupling is similar, both measures are concomitantly decreased.

This study aims to determine the extent to which *in-vivo* relative GABA concentration (via spectrally edited Magnetic Resonance Spectroscopy (MRS)) predicts gamma-band activity (recorded by magnetoencephalography (MEG)) in both typically developing participants and especially in participants with ASD. If the neurochemical-neurophysiological relationship is conserved in ASD, such observations provide key interpretational value for diminished gamma-band activity as a “biomarker” (a biologically based marker) of ASD (Rojas & Wilson, 2014), with anomalous GABA levels providing the etiological basis for this coupling. Moreover this observation would suggest a possible mechanism of treatment: restoring E/I balance may recover neuronal functioning. This is especially relevant because several GABA-related pharmacological interventions have recently been tested for, and are emerging for, treatment of ASD (Berry-Kravis et al., 2012; Erickson et al., 2014; Lemonnier et al., 2012). In addition, these interventions have been shown effective in murine models of ASD to effectively normalize behavioral phenotypes (e.g. enhance sociability) (Silverman et al., 2015; Tyzio et al., 2014) and restore neural functioning (M J Gandal, Sisti, et al., 2012; Tyzio et al., 2014).

2. Materials and Methods:

2.1 Participants

Sixty-two participants (21 TD, 41 ASD), ranging from 6 to 29 years old (mean age = 16.3 ± 6.1 (mean \pm standard deviation)), were recruited into the current study and completed both MEG and MRS scans. While the age range of the recruited population was comparatively large, such a range allowed for the opportunity to detect possible age-specific alterations both within and across diagnostic groups (i.e. developmental trajectories). In addition such a large age range ensured that resultant observations were indeed a persistent phenotype across ages, and not an epiphenomenon of study recruitment criteria. Final study population demographics are summarized in Table 1, and additional sample characteristics are shown in Supplemental Table 1. Of these participants, 24 participants' MEG data had previously been reported for gamma-band alterations, with these studies demonstrating decreased phase-locked gamma-band activity in ASD versus TD (Edgar et al., 2015; Port et al., 2016). These studies examined neither GABA alterations, nor the relation between GABA and gamma-band activity measures. One TD subject was prescribed medication (though non-psychotropic). Fourteen individuals with ASD were prescribed medications/took dietary supplements. Table 2 provides medication information. Tailored recruitment and evaluation strategies were used for children vs. adult participants:

2.2 Child and Adolescent Recruitment and Inclusion/Exclusion Criteria

Following procedures described in Edgar et al. 2015, subjects with ASD were recruited from the Regional Autism Center of The Children's Hospital of Philadelphia (CHOP), from the Neuropsychiatry program of the Department of Psychiatry of the University of Pennsylvania School of Medicine, from local and regional parent support groups such as ASCEND (Asperger Syndrome Information Alliance for Southeastern Pennsylvania) and local chapters of Autism Society of America. All children screened for inclusion in the ASD sample had a prior ASD diagnosis made by an expert clinician, typically a developmental pediatrician in the Regional Autism Center at the Children's Hospital of Philadelphia. The original diagnosis was made after an extensive clinical interview, documentation of DSM-IV criteria for ASD, and use of various ASD diagnostic tools, such as the Childhood Autism Rating Scale and, in many cases, the Autism Diagnostic Observation Schedule (ADOS; Lord et al. 2000). Subjects with typical development (TD) were recruited through local newspaper advertisements and from pediatric practices of the CHOP primary care network.

Research participants made two visits to CHOP. During the first visit (2–3 weeks prior to the MEG exam), clinical and diagnostic testing was performed to confirm the referral ASD diagnosis, to administer neuropsychological tests, and to ensure that the TD children met study inclusion/exclusion criteria. Assessments were performed by licensed child psychologists with expertise in autism (L.B., E.S.K.). Given the extensive clinical evaluations upon which original ASD diagnosis was made, an abbreviated diagnostic battery was used to confirm the original diagnosis. Specifically, the ASD diagnosis was

confirmed with standard diagnostic tools, including direct observation with the ADOS and parent report on the Social Communication Questionnaire (SCQ; Rutter et al. 2003). Dimensional symptom severity ratings were also obtained by parent report on the Social Responsiveness Scale (SRS; Constantino & Gruber 2012). The Autism Diagnostic Interview-Revised (ADI-R), a parent interview about current and prior ASD symptoms, was utilized to resolve diagnostic discordances between the ADOS and parent rating scales in the rare instances in which such discordances occurred. For final inclusion in the ASD group, children were required to exceed established cut-offs on both the ADOS and SCQ, or, in the event of a discordance between those measures, on both the ADOS and ADI-R. Children 1 point below ADOS cut-offs were included if they exceeded cut-offs on at least two parent questionnaires or the ADI-R. For children for whom original diagnosis was not made by an expert clinician according to DSM criteria (e.g., diagnoses made by a school), more rigorous standards were applied, and the child was required to exceed cut-offs on both the ADOS and ADI-R for inclusion in the ASD group. A subset of children included in this sample were part of a three-year longitudinal study. This subset of children met all described inclusion criteria at the time of their original study participation. At three-year follow-up, they continued to be included in the ASD group if they exceeded diagnostic cut-offs on the ADOS; parent rating scale corroboration was not required. Only 1 of these participants provided imaging data at both their initial and longitudinal follow-up visit. To rule out global cognitive delay, all subjects were required to score at or above the 2nd percentile ($SS > 70$) on the Perceptual Reasoning Index (PRI) of the Wechsler Intelligence Scale for Children-IV (WISC-IV; Wechsler

2003). In all subjects, the WISC-IV Verbal Comprehension Index (VCI) was also obtained.

Inclusion criteria for the TD children included scoring below the cut-off for ASD on all domains of the ADOS as well on parent questionnaires, and demonstrating performance above the 16th percentile on the Clinical Evaluation of Language Fundamentals—4th edition (CELF-4; Semel & Wiig 2003). In addition to the above inclusion/exclusion criteria, all subjects and families were native English speakers and had no known genetic syndromes or neurological (e.g., cerebral palsy, epilepsy), or sensory (hearing, visual) impairments. The study was approved by the CHOP Institutional Review Board and all participants' families gave written informed consent. As indicated by institutional policy, where competent to do so, children over the age of seven additionally gave verbal assent.

2.3 Adult Recruitment and Inclusion/Exclusion Criteria

This sample included 23 young adults between the ages of 18 and 29. Adult participants with ASD (N=13; 20.8±2.2 years old (mean age ± standard deviation)) were recruited from the Adult Autism Spectrum Program in the Department of Psychiatry at the Hospital of the University of Pennsylvania, as well as from cohorts of participants participating in prior MEG studies by the current investigators and prior studies at the Center for Autism Research at the Children's Hospital of Philadelphia. TD participants (N=10, 25.0±3.3 years old (mean age ± standard deviation)) were recruited through local

newspaper advertisements and from participation in prior studies. Diagnostic procedures were similar to those described for the child cohort but were modified to meet the constraints of an adult sample. All adults were required to have a prior diagnosis of ASD, made by an expert clinician according to DSM criteria. At the time of study participation, they had to exceed established cut-offs on the ADOS-2 as well as *either* the SCQ (Lifetime) or SRS-2 Adult-Informant Report (Constantino & Gruber, 2012). Individuals for whom informant report was not available were included in the ASD group if they had a documented prior diagnosis of ASD and exceeded established cut-offs on the ADOS-2 as well as on *both* the SRS-2 Adult-Self Report and Broad Autism Phenotype Questionnaire (BAPQ; Hurley et al. 2007). Individuals 1 point below diagnostic cut-offs on the ADOS-2 were included if they exceeded cut-offs on two informant report questionnaires or on the ADI-R. To rule out global cognitive delay, all subjects were required to score at or above the 2nd percentile ($SS > 70$) on the Perceptual Reasoning Index (PRI) of the Wechsler Abbreviated Intelligence Scale-II (WASI-II; Wechsler 2011) For all subjects, the WASI-II Verbal Comprehension Index (VCI) was also obtained.

Inclusion criteria for the TD adults included scoring below the cut-off for ASD on all domains of the ADOS-2 and below cut-offs on informant and self-report questionnaires, along with performance above the 16th percentile on the CELF-4 (if within age-range for this measure (Semel & Wiig, 2003)), WASI-II Verbal Comprehension Index, and average of the Peabody Picture Vocabulary Test-4 (PPVT-4; Dunn & Dunn 2007) and Expressive Vocabulary Test-2 (EVT-2; Williams 2007). TD

adults also had no history of current psychiatric illness, as documented during initial screening and by subsequent self and informant ratings on the Adult Behavior Checklist (ABCL; Achenbach & Rescorla 2003), and they were taking no psychotropic medications. As with the child sample, all adult participants were native English speakers, had no known genetic syndromes or neurological (e.g., cerebral palsy, epilepsy), or sensory (hearing, visual) impairments, and had a negative drug and alcohol screen administered prior to both study visits.

Electrophysiological Data Collection

Magnetoencephalography data were obtained using a 275-channel system (VSM MedTech Inc., Coquitlam, BC) in a magnetically shielded room. Prior to data acquisition, three head-position indicator coils were attached to the subject's scalp at the nasion, left and right-preauricular points, which provided continuous measurement of head position in relation to the MEG sensors. To minimize fatigue, during the task participants viewed (but did not listen to) a movie projected onto a screen positioned at a comfortable viewing distance.

Electrodes were attached to the left and right clavicles for electrocardiogram (ECG) recordings and to the bipolar oblique (upper and lower left sites) for electrooculogram recordings (EOG). A band-pass filter (0.03–300 Hz) was applied to the EOG, ECG, and MEG signals, and signals were digitized at 1200 Hz with third order gradiometer environmental noise reduction applied to the MEG data.

2.4 Electrophysiological Data Collection

Magnetoencephalography data were obtained using a 275-channel system (VSM MedTech Inc., Coquitlam, BC) in a magnetically shielded room. Prior to data acquisition, three head-position indicator coils were attached to the subject's scalp at the nasion, left and right-preauricular points, which provided continuous measurement of head position in relation to the MEG sensors. To minimize fatigue, during the task participants viewed (but did not listen to) a movie projected onto a screen positioned at a comfortable viewing distance.

Electrodes were attached to the left and right clavicles for electrocardiogram (ECG) recordings and to the bipolar oblique (upper and lower left sites) for electrooculogram recordings (EOG). A band-pass filter (0.03–300 Hz) was applied to the EOG, ECG, and MEG signals, and signals were digitized at 1200 Hz with third order gradiometer environmental noise reduction applied to the MEG data.

2.5 Stimuli

Stimuli consisted of 200, 300 500 and 1000 Hz sinusoidal tones presented using Eprime v1.1 (Psychology Software Tools Inc., Pittsburgh, USA). Tones were presented via a sound pressure transducer and sound conduction tubing to the participant's peripheral auditory canal via ear-tip inserts (ER3A, Etymotic Research, IL, USA). Prior to data acquisition, 1000 Hz tones (300 ms duration, 10 ms rise time) were presented

binaurally and incrementally until reaching auditory threshold for each ear. Stimulus tones were presented at 45 dB sensation level above threshold. Each trial consisted of participants passively listened to binaurally presented random 200, 300, 500 & 1000 Hz sinusoidal tones (130 tones/frequency; 300 ms duration; 10 ms ramps) plus a 1000 ms (± 100 ms) inter-trial interval. In total, this experimental protocol took approximately 12 minutes.

2.6 Structural MRI and MRS methods

After MEG, structural MRI and MRS data were acquired on a 3T Siemens Verio™ scanner using a 32-channel receive only head RF coil. First an axial orientated 3D MP-RAGE anatomic scan was obtained for each subject (field of view = $256 \times 256 \times 192$ mm and matrix = $256 \times 256 \times 192$ to yield 1 mm isotropic voxel resolution (TR/TE = 1900/2.87 ms; inversion time = 1100 ms; flip angle = 9°)). Then the MEGA-PRESS spectral editing sequence (Mescher, Merkle, Kirsch, Garwood, & Gruetter, 1998), with TE = 68 ms, TR = 1500 ms and 128 pairs of interleaved spectra (acquisition time ~ 7 minutes) was utilized to obtain single voxel (4 cm x 3 cm x 2 cm) GABA MRS. Pilot observations and recent published studies (Gaetz et al., 2014) indicated that this approach provided a reasonable compromise between SNR vs. exposure to degradation over acquisition time due to motion and potential static field drift. The MRS voxel was first aligned to the left mid-temporal lobe with the long aspect (4 cm) of the cuboid positioned such that the top of the voxel contained the Superior Temporal Gyrus. Medial–lateral adjustments were then made to abut (but not include) the left lateral ventricle.

2.7 MRS analysis and quantification

GABA measurements using the conventional MEGA-PRESS sequence are known to contain some contribution from co-edited macromolecules. Thus, our “GABA plus” macromolecule measurements are reported using the conventional GABA+ notation. A 5 Hz Lorentzian line-broadening filter was applied prior to jMRUI fitting. Then for the un-edited runs, Hankel Lanczos Singular Value Decomposition (HLSVD) was used to quantify creatine (Cr) and N-acetylaspartate (NAA), with the amplitude of each component being recorded. HLSVD fits used up to 15 components to minimize residual signal in the 1-4ppm region. For the subtraction-edited spectra, GABA+ was modeled using an identical technique (up to 15 components, one component modeling the entire GABA+ signal at 3ppm, with no other component overlapping the GABA component region).

2.8 Tissue Segmentation and Quantification

To account for possible confounding effects of tissue composition on any MRS result, all subjects had the tissue composition (i.e. gray matter, white matter, and cerebral spinal fluid) of their MRS voxel calculated, using the subject’s MP-RAGE. The automated tissue segmentation tool, FAST (Zhang et al., 2001) was utilized to yield three partial volume images, each describing the fraction of tissue type present in the imaging voxels. The relative contribution of each tissue fraction to the MRS voxels were then

computed by summing their respective number of imaging voxels located within the prescribed MRS voxel. Tissue composition fraction was included as a covariate, or additional regressor in analyses (see below).

2.9 Gamma-band Data Analysis

Gamma-band responses were analyzed using the MatLab (Mathworks, Natick, MA) open-source toolbox Fieldtrip (Oostenveld, Fries, Maris, & Schoffelen, 2011), using identical procedures as (Port et al., 2016). Using the continuous data and using the procedures outlined in Fieldtrip (FieldtripWiki, 2015a, 2015b), independent component analysis (ICA) identified heartbeat and eye artifacts (blinks and saccades), and then these artifact components were removed from the stimulus-epoch data (+/- 500 ms around trigger). Trials with jump and muscle artifact were then rejected using Fieldtrip's Z-score based artifact rejection method. Lastly, to account for differences in head motion during the MEG scan, if any fiducial moved more than 10mm from the average head position during a trial, the trial was rejected. For each group, over 93% (483 trials) of trials remained (TD = $96 \pm 0.3\%$, ASD = $94 \pm 0.7\%$; $p < 0.01$), far exceeding the required amount of trials to give a stable response. Thus slight group differences were considered mitigated.

Subject-specific single-shell head models were created from individual participant's MP-RAGE MRI scans. To coregister MEG and sMRI data, three anatomical landmarks (nasion and right and left preauricular) as well as an additional 200+ points on

the scalp and face were digitized for each participant using the Probe Position Identification (PPI) System (Polhemus, Colchester, VT), and a transformation matrix that involved rotation/translation between the MEG and sMRI coordinate systems was obtained via a least-squares match of the PPI points to the surface of the scalp and face. This head model was then fitted to the mean head position (in MEG coordinate space) as determined by the fiducials. Separately, the participant's MRI was normalized to an age-matched average brain template (children - (Fonov et al., 2011); adults - ICBM152 average brain) using non-linear warping. A left and right Heschl's Gyrus location was identified and then reverse non-linear transformed to subject space.

A linearly-constrained minimum variance (LCMV) beamformer was computed for each participant's left and right Heschl's Gyrus, discarding the contralateral hemisphere's sensors to reduce inter-hemispheric signal cancelation due to correlated activity (Herdman et al., 2003). Heschl's Gyrus virtual electrodes (VE) were then computed using an orientation optimized for post-stimulus gamma-band activity (i.e. orientation calculated by using principal component analysis on the 0-270ms post-stimulus window with filtering 30-58Hz). Broadband resultant VE time courses were then time-frequency transformed (Morlet Wavelets; 3 – 100 Hz; cycles ranging from 3 (low) to 6 (high); both with 100 linearly spaced bins). For each participant, baseline corrected evoked power (relative change) and inter-trial coherence (ITC) were calculated. Fieldtrip's permutation testing was then utilized to choose a spectrotemporal ROI for which to quantify gamma-band activity (Monte-Carlo permutation test with cluster correction for multiple comparison correction). The post-stimulus region containing the gamma-band response

(0 to 200 ms) was compared to the pre-stimulus (-300 to -100 ms) for all participants, and the regions of statistical difference calculated between the two. This resultant statistical map (Figure 1) was used to mask individual subject's time-frequency plots (with only regions that were both $p < 0.05$ and above 30 Hz included), for which then the average evoked-power and ITC was calculated on a subject-wise basis.

2.10 Statistical analyses

To assess significance for group differences ANOVAs were utilized. For GABA+/Cr analyses, covariates of Gray Matter contribution and Age were applied to GABA+/Cr measures, with the fixed effects of Diagnosis, Age and Gray Matter (co-varied for age). For gamma-band measures (evoked power and ITC), ANOVAs with a fixed effect of Diagnosis were applied.

To determine if gray matter contributed differences to GABA+/Cr difference, a hierarchical linear regression was utilized, with Diagnosis and Age entered into the first block, and then Gray Matter in the second. Linear regression analyses were also performed for each gamma-band metrics and its relation to relative GABA+ concentrations. These relative cortical GABA+ to gamma-band activity regressions were performed for both diagnoses separately, and after collapsing across diagnosis.

3. Results:

3.1 Demographics

Sixty-two participants were recruited into the study and completed both MEG and MRS experiments. Of these, 15 participants were removed due to poor MEG/MRS scan quality (4 - TD, 10 - ASD). As such, forty-eight participants remained in the final data analyses (17 TD, 31 ASD), of whom 6 were females (5 TD, 1 ASD). A Chi-squared test demonstrated that groups did not differ on gender ($p > 0.05$). In addition groups did not significantly differ on age (TD = 19.31 ± 1.82 years old, ASD = 15.57 ± 0.88 years old, mean \pm SEM, $p > 0.05$). Note there is a non-significant tendency for elevated age in the TD group. See Table 1 as well as Supplemental Table 1 for more information. Similar effects are observed if the TD sample is selectively subjected to *a-posteriori* decimation to reduce TD average age (at the expense of sample count).

3.2 ASD participants demonstrate reduced phase-locked activity

Gamma-band responses were visible at the diagnostic group level for both TD and ASD cohorts (Figure 1A & 1B). A significant main effect of Diagnosis, $F(1,46) = 4.25$, $p < 0.05$, demonstrated gamma-band coherence (ITC) was significantly decreased in participants with ASD as compared to TD (TD = 0.071 ± 0.004 ITC, ASD = 0.060 ± 0.003 ITC, mean \pm SEM, Figure 2B). A similar, though non-significant, main effect of Diagnosis ($F(1,46) = 2.53$, $p = 0.119$) demonstrated decreased gamma-band evoked power in ASD versus TD (TD = 2.89 ± 0.58 relative change from baseline, ASD =

1.75±0.43 relative change from baseline, mean ± SEM, Figure 2C). Thus, gamma-band ITC was observed to be more sensitive to group differences than gamma-band evoked power, largely attributable to its lower measurement variance.

3.3 ASD participants demonstrate decreased GABA+

A main effect of Age, $F(1,44) = 4.94, p < 0.05$, revealed a decrease of GABA+/Cr with maturation (standardize beta coefficient from hierarchical regression = -0.32). In addition, a significant main effect of Diagnosis was observed, $F(1,44) = 4.85, p < 0.05$, demonstrating that ASD group exhibited less relative cortical GABA concentrations than the TD group (TD = 0.311±0.011 GABA+/Cr, ASD = 0.280±0.008 GABA+/Cr, mean ± SEM, Figure 2A). Notably, a significant main effect of voxel Gray Matter Fraction was *not* observed, $F(1,44) = 1.14, p > 0.1$) between groups, and furthermore Gray Matter Fraction did not account for significant variance above that accounted for by Age and Diagnosis (R^2 change = 0.021, $p > 0.10$).

3.4 The relation of relative cortical GABA to phase-locked gamma-band activity is less apparent in ASD

Across the study population, gamma-band ITC was significant correlated with relative cortical GABA+ ($R^2 = 0.188, p < 0.01$; Figure 3). This relationship was also significant in the TD group ($R^2 = 0.238, p < 0.05$; Figure 3), though only trended towards significance for the ASD cohort ($R^2 = 0.089, p = 0.110$; Figure 3). An ANCOVA

(dependent variable = gamma-band ITC, fixed effects = Diagnosis, GABA+/Cr and their interaction, covariate = GABA+/Cr), demonstrated no significant differences in the slopes of the regression between TD and ASD (Diagnosis X GABA+/Cr interaction, $p > 0.1$).

The GABA+ coupling to gamma-band evoked power was weaker than for ITC in all groups. Relative cortical GABA significantly correlated to stimulus evoked gamma-band power across the study population ($R^2 = 0.108$, $p < 0.05$, Figure 4). Within diagnostic groups (TD and ASD) though, this relationship was trending towards significance in TD, and not significant in ASD (TD $R^2 = 0.173$, $p < 0.1$; ASD $R^2 = 0.021$ $p > 0.1$; Figure 4). An ANCOVA (same structure as used for ITC) demonstrated no difference in the slope of the regression lines (Diagnosis X GABA+/Cr interaction, $p > 0.1$).

4. Discussion:

The brain is thought to communicate using excitatory and inhibitory neurotransmission, and numerous studies have suggested that in particular the brain's gamma-band response is critically reliant on such E/I balance (Cardin et al., 2009; Sohal et al., 2009; Whittington et al., 2000; Yizhar et al., 2011). This gamma-band activity is thought to be involved with numerous brain functions ranging from basic sensory (e.g. visual system and auditory system) (Başar-Eroglu et al., 1996; Gray et al., 1989) functions to higher order cognitive processes (Herrmann et al., 2010). Of relevance to this study the gamma-band response has been repeatedly observed to be perturbed in ASD (Grice et al., 2001; Orekhova et al., 2007; Wilson et al., 2007). Supporting the notion of gamma-band activity being reliant on E/I balance, several independent studies have demonstrated decreased in-vivo relative cortical GABA in ASD (Gaetz et al., 2014; Harada et al., 2011; Rojas et al., 2014). Moreover, gamma-band neurophysiological activity has been shown to correlate to corresponding GABA concentrations in both the visual and motor system of healthy adults (Gaetz et al., 2011; Muthukumaraswamy et al., 2009), though this is not fully resolved (Cousijn et al., 2014). In addition, Balz and colleagues (2015) recently observed a correlation between gamma-band power and GABA levels for visual-audio sensory integration in the human brain. However, the analogous correlation had yet to be observed for the auditory system for either typically developing (TD) children or individuals with ASD.

This study examined both the gamma-band response to simple auditory tones as well as also the corresponding STG GABA levels in individuals with ASD and age

matched TD controls. The ASD cohort demonstrated both reduced relative GABA+ concentration and gamma-band ITC deficits compared to TD. Across diagnoses, a significant correlation was observed between the concentrations of relative cortical GABA and gamma-band coherence. However, this association only reached statistical significance in the TD group, though trended towards significance in individuals with ASD. In addition, statistical testing of the slopes of the two linear regressions showed no significant effect of diagnostic group.

The lack of a significant correlation of gamma-band activity to GABA+ in ASD could be interpreted in *at least 3* ways: 1) the correlation is not resolvable because it is confounded by inter-subject biological differences in the heterogeneous ASD population, which manifests as increased measurement variance, precluding statistical resolution, 2) the ASD population in fact consists of two (or more) stratified sub-populations, some of whom demonstrate a gamma-band coherence to GABA+/Cr correlation and some of whom do not, 3) the relationship between gamma-band coherence and GABA+/Cr observed in typically developing individuals and interpreted as reflecting intact neuronal local circuitry is simply disrupted in ASD and may reflect an impairment in the function of that local circuitry.

In agreement with previous studies, both gamma-band ITC (Edgar et al., 2015; Michael J Gandal et al., 2010; Rojas et al., 2008) and relative cortical GABA (Gaetz et al., 2014; Rojas et al., 2014) were significantly reduced in ASD, as compared to TD. However, auditory gamma-band evoked *power* deficits in ASD (as compared to TD) failed to reach significance. Of note, this lack of significance does not negate the three

aforementioned hypotheses, as this lack of finding of significance may likely arise from the elevated variance associated with the ASD population. While the differential significance (ITC significant, evoked power not significant) for the group differences in phase-locked gamma-band activity metrics is contrary to previous studies (Edgar et al., 2015; Rojas et al., 2008), non-significant trends in reduced ASD evoked power have also been reported previously (Michael J Gandal et al., 2010). This non-significant decrease in evoked power may be due to the use of a larger age range in the current study or other undetermined population effects. In addition, previous studies have averaged over hemispheres to increase signal to noise (Michael J Gandal et al., 2010; Port et al., 2016), whereas the current study only reported the left hemisphere responses to compare directly with in-vivo left auditory cortex MRS GABA.

While relative cortical GABA is significantly reduced in ASD as compared to TD in support of previous findings (Gaetz et al., 2014; Rojas et al., 2014), the relative consequence of such a specific GABA deficiency is also unknown. Additionally, a limitation of this study (and several previous studies) is the relative inaccessibility of a simultaneous measure of the neurotransmitter glutamate. This arises partly from technical resolution challenges (often leading to a proxy measure of Glx, comprising both glutamate and glutamine (Rojas et al., 2015)) but more importantly from the existence of glutamate in the brain in both a neurotransmission and metabolic role. Glutamate is known to be involved in both synaptic transmission and metabolic processing, shuttling between neurons and astrocytes as part of the Glutamate – Glutamine cycle (for review see Hertz 2013). Of note though, a recent study that specifically examined glutamate

concentrations in ASD (without glutamine) demonstrated that glutamate is increased (Brown et al., 2013), also consistent with increased excitation to inhibition ratio in ASD.

GABA, with its function as the main inhibitory neurotransmitter, also has a role in the TCA cycle. The exact role of GABA is hypothesized to be dependent on the isoform of glutamate decarboxylase (GAD) that produced the molecule (GAD65 = neurotransmission, GAD67 = GABA shunt) (Martin & Rimvall, 1993). This clear separation of GAD65/67 derived GABA in neurotransmission has been called into question though (Soghomonian & Martin, 1998). Nevertheless, current MRS methods are not able to resolve the metabolite versus neurotransmitter pools of either glutamate or GABA, because the voxel size required to achieve adequate signal in reasonable time encompasses all neuronal compartments (e.g. synaptic, white matter & somatic compartments) and in addition glial cells. This concern should temper interpretations. Nonetheless establishing any association between GABA and gamma-band activity would support the hypothesis of gamma-band activity representing a proxy index of the relevant neurotransmitter functioning GABA.

The present data support the hypothesis that decreases in relative cortical GABA+ is of functional consequence. Consistent with previous studies, a significant relationship of relative cortical GABA to gamma-band activity was determined in TD controls (Balz et al., 2015; Gaetz et al., 2011; Muthukumaraswamy et al., 2009). As such, these and previous findings, support the hypothesis that relative cortical GABA concentrations derived from MRS may relate to the E/I balance within TD participants. Furthermore, in a disorder marked by alterations to the neural excitatory and inhibitory systems (see

introduction), this coupling of MRS-derived GABA and MEG-derived gamma-band activity seems to be perturbed. Of note, this is the first study report such an association for the auditory system, and also the first to demonstrate the association between GABA and gamma-band coherence. In addition, this is only the second to observe this relationship for gamma-band power. Lastly, this is also the first study to examine the relationship in individuals with ASD.

Both across the study population, and for TD controls, ITC was significantly related to relative cortical GABA concentration. For individuals with ASD this association was trending towards significance ($p = 0.110$), possibly limited by ASD heterogeneity. The correlation of evoked power (as opposed to ITC) to relative GABA+ was less prominent. Indeed, TD demonstrated only trending significance for the coupling of evoked power to relative GABA+, and ASD demonstrated no relationship. This weaker coupling of relative GABA+ to evoked power may arise from the constituents of the evoked power signal. An oscillation has three core characteristics, phase, frequency and amplitude. Evoked power consists of both phase and amplitude information, whereas ITC is solely based on phase. As such, this stronger coupling for ITC (to GABA) may be a result of small alterations in relative cortical GABA concentrations affecting the synchrony/reliability of oscillatory activity (i.e. exact timing of neuronal firing across trials) more than the amount of neurons firing across trials. If so, then when relative cortical GABA is reduced both ITC and evoked-power would be reduced in turn, though the ITC signal's reduction would be more prominent due to the evoked power signal still having the same amplitude (amount of neurons firing) though reduced phase.

Evoked power responses demonstrated considerable increased variance as compared to ITC in the present study. The sources of such variance cannot be determined as either biologically based or relating to methodological procedures (i.e. less effective measuring of the evoked power signal). It may be that ITC is more reliable since it is only sensitive to phase, as opposed to phase and amplitude. Such a case could occur when the underlying neurons contributing to the responses fire at the same phase (from trial to trial), though the amount (which affects the amplitude of the oscillatory activity) of neurons firing alters between trials.

Interestingly, relative to TD, the ASD group showed uniformly weaker coupling (lower R^2) between gamma-band activity and relative cortical GABA. However, ANCOVAs demonstrated no significant differences ($p > 0.10$) between diagnostic groups for the coupling (i.e. slope of the regression). These ANCOVA findings are difficult to interpret due to the lack of a significant association for evoked power in ASD. As such, further (and ideally with larger populations) studies are needed to determine if this weaker, though similar, coupling is due to the increase variance associated with ASD. Additionally, the coherence to GABA coupling may only occur within a sub-population of ASD. Thus, the current findings may ultimately yield a class of stratification biomarkers markers for ASD treatment. For example, when considering a metric based on relative cortical GABA and gamma-band coherence (Figure 5), an individual ASD score that falls within range of the corresponding TD derived relationship (i.e. within the 95% confidence interval of age-matched controls; Figure 3) may be aided by therapies that increase GABAergic signaling. In such a situation, both the GABA+/Cr and gamma-

band coherence are concomitantly decreased, and so “rescuing” GABAergic activity may recover gamma-band activity. The clinical trials of arbaclofen (Berry-Kravis et al., 2012), and other GABA-related treatments have not been effective in a broad study population, but identifying such a sub-population might allow such clinical trial populations to be enriched. As such, speculation lends support to the hypothesis that GABAergic treatments may be efficacious in a sub-population of those with ASD. What remains unknown is the neuroelectrophysiological characteristics (i.e. gamma-band activity profile) of both responders and non-responders in these clinical trials. While highly speculative, it may be the case that for those who improve clinically in response to GABAergic modulation, gamma-band activity may also be normalized. Such an observation would allow gamma-band activity to be used a treatment marker, reflecting at least drug sensitivity (target engagement). It still remains to be established if diminished gamma-band activity is causal for the behavioral alterations in ASD, or a closely linked proxy for relevant neural bases. Further studies are needed to confirm both the use of these measures as biomarkers appropriate for stratification for treatment, and their causal relationship to behavioral symptomatology.

Alternatively, Figure 5 may also be interpreted as measure of “GABAergic efficiency”. While in a typically developing population GABA has a certain efficiency at creating gamma-band activity, in ASD the efficiency is reduced in most cases. Hence such an interpretation places a key causal link between GABA and gamma-band activity. In cases those with low “GABAergic efficiency” supplementing GABA, or its relative action, might again be expected to aid in the normalization of electrophysiological

activity (e.g. gamma-band activity), although perhaps less efficiently. Although highly related, there are subtle differences between a coupling (“functional to neurochemical coupling”) and efficiency (“GABAergic efficiency”) arguments (e.g. causality, and whether the underlying relationship is intact). Both hypotheses though promote the use of GABA-related interventions in individuals with ASD who demonstrate coupling between gamma-band activity and GABA+/Cr levels.

While a significant relationship between gamma-band coherence and relative cortical GABA was observed when collapsing across diagnostic group, these measures are not redundant. For both gamma-band evoked power and ITC, relative cortical GABA explained around 10-20 % of the variance. As such, there was still significant variance unaccounted for. Previous work has demonstrated the efficacy of combining both functional and structural data when available for creating quantifiable markers of ASD (Ingalhalikar, Parker, Bloy, Roberts, & Verma, 2014). It maybe that a multi-modal biomarker that includes both information from gamma-band activity and relative cortical GABA, as well as other factors (e.g. M100 latency, DTI measures of thalamocortical microstructure) will prove to be optimal.

The current study focused solely on the auditory system, however previous findings have demonstrated relative cortical GABA to be differentially altered depending on which cortical/subcortical structure was examined (Gaetz et al., 2014; Harada et al., 2011). What remains undetermined is if the relationship between underlying neurochemistry and oscillatory activity remains and is of the same magnitude in other brain systems.

To conclude, this study observed correlations between MEG measures of gamma-band oscillatory activity and regionally co-localized estimates of GABA concentrations within the auditory system in TD individuals. However, for individuals with ASD weaker coupling between relative cortical GABA+ and gamma-band coherence was observed. Further work is needed to test the hypothesis that a “functional to neurochemical coupling” metric may be of use for the stratification of the heterogeneous ASD population into treatment/clinical trial enrichment cohorts based on the underlying biological pathology.

Table Legends:

Table 3.1 *Demographics of study population.* No significant difference exists in age between TD and ASD individuals. A chi-squared test revealed no significant effect of gender distribution between groups ($p>0.3$). Values are counts or mean (standard deviation).

Table 3.2 *Medications and supplements taken by participants.* Subjects listed by
Diagnosis (Dx) with corresponding supplements/medications.

Supplemental Table 3.1 *Age characteristics of study population.* TD (top) versus ASD (bottom) counts for age ranges of study participants. Participants younger than 18 are shown in the middle column, and those 18 and over are shown in the right column.

Figure Legends:

Figure 3.1 *Both TD and ASD individuals demonstrated robust and quantifiable results.*

Group average evoked power (A) and ITC (B) in response to auditory stimuli demonstrate quantifiable results for both TD (left) and ASD (right). Individuals with ASD exhibit less phase-locked gamma-band activity in response to the auditory stimuli. Outline is the permutation test derived region of significant post-stimulus gamma-band activity (C) Exemplar MRS spectra for TD (left) and ASD (right) show clear and defined GABA+ peaks (gray bar overlay).

Figure 3.2 *Individuals with ASD exhibit less gamma-band coherence and relative cortical GABA in auditory cortex.* (A) Relative cortical GABA+ in auditory cortex is reduced in ASD (red) as compared to TD (blue). (B) A significant decrease in gamma-band coherence in response to auditory stimuli is observed for ASD compared to TD (C) A similar, though only qualitative decrease is observed for gamma-band evoked power in ASD as compared to TD. * $p < 0.05$.

Figure 3.3 *Auditory gamma-band coherence and relative cortical GABA in auditory cortex are associated across the study population, and within TD (though suggested for ASD as well).* The linear regression of TD (blue) and all individuals pooled (black) together is significant, and positively correlated. Blue boundary lines are the 95% confident interval of the TD mean. ASD (red) trend towards a similar relationship. Slopes of the TD and ASD linear fits are not significantly different ($p > 0.1$). # $p = 0.11$; * $p < 0.05$; ** $p < 0.01$

Figure 3.4 Auditory *gamma-band evoked power and relative cortical GABA in auditory cortex are associated across the study population.* The study population (black) exhibits a positive relationship between relative cortical GABA and gamma-band coherence. A trend towards a similar relationship is seen in TD (blue). ASD (red) demonstrate no coupling. Blue boundary lines are the 95% confident interval of the TD mean. # $p < 0.10$; * $p < 0.05$

Figure 3.5 *Functional to neurochemical coupling may serve as a potential biomarker for ASD sub-population stratification.* TD (blue) and ASD (red) relative functional (evoked power = left; ITC = right) to neurochemical (relative cortical GABA+) coupling may allow for identification of those individuals amenable to GABA-related interventions to increase gamma-band activity. Error bars are the 95% confident interval.

Tables:

Table 3. 1

	N	Female	Age
Control	17	5	19.31 (7.51)
ASD	31	1	15.57 (4.88)

p >0.3 >0.05

Table 3. 2

DX #	Medications
ASD 1	Abilify
ASD 2	Buproion HCL, Concerta ER, Clonidine HCL
ASD 3	Concerta, Metadate, Focalin
ASD 4	Concerta, Doxycycline hyclate
ASD 5	Flovent, Albuterol
ASD 6	Focalin
ASD 7	Focalin, Prozac, Melatonin
ASD 8	Lamictal, Xanax, Zyprexa
ASD 9	Metadate, Abilify
ASD 10	Metadate, Claritin, Vitamin B12 injections, Ritalin
ASD 11	None
ASD 12	None
ASD 13	None
ASD 14	None
ASD 15	None
ASD 16	None
ASD 17	None
ASD 18	None
ASD 19	None
ASD 20	None
ASD 21	None
ASD 22	None

ASD 23	None
ASD 24	Strattera, Fluoxetine
ASD 25	Tenex, Focalin, Strattera, Abilify
ASD 26	Zoloft
ASD 27	None
ASD 28	Intuniv
ASD 29	Concerta, Wellbutrin
ASD 30	None
ASD 31	Zoloft
TD 1	None
TD 2	None
TD 3	None
TD 4	None
TD 5	None
TD 6	None
TD 7	None
TD 8	None
TD 9	None
TD 10	None
TD 11	None
TD 12	None
TD 13	None
TD 14	None
TD 15	None

TD 16	None
TD 17	Omeprazole, Ketoconazole (topical cream)

Supplemental Table 3. 1

	Count	
	>18	18 and over
TD	7	10
ASD	18	13

Figures:

Figure 3. 1

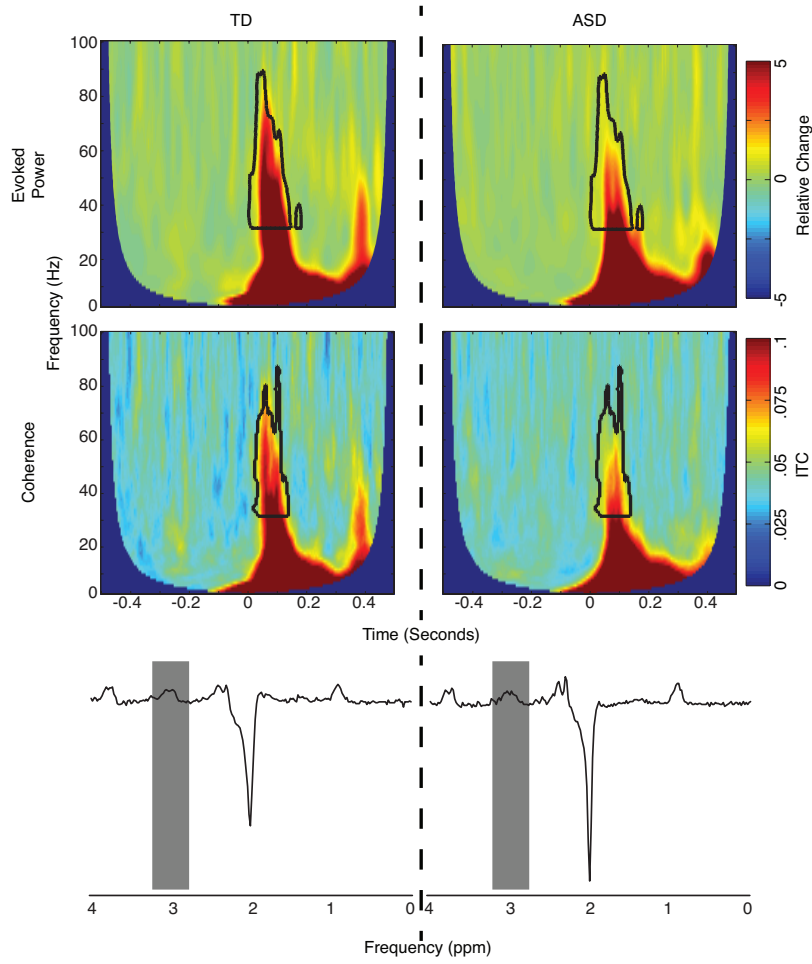


Figure 3. 2

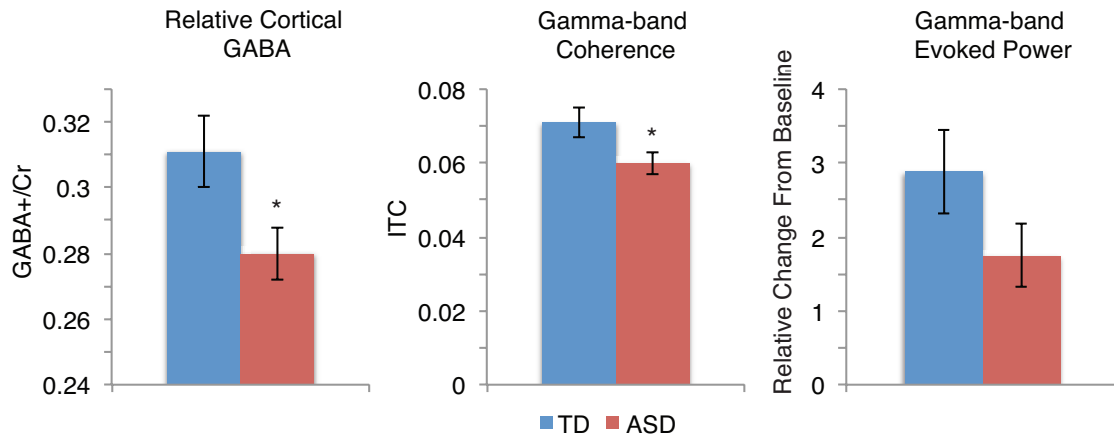


Figure 3. 3

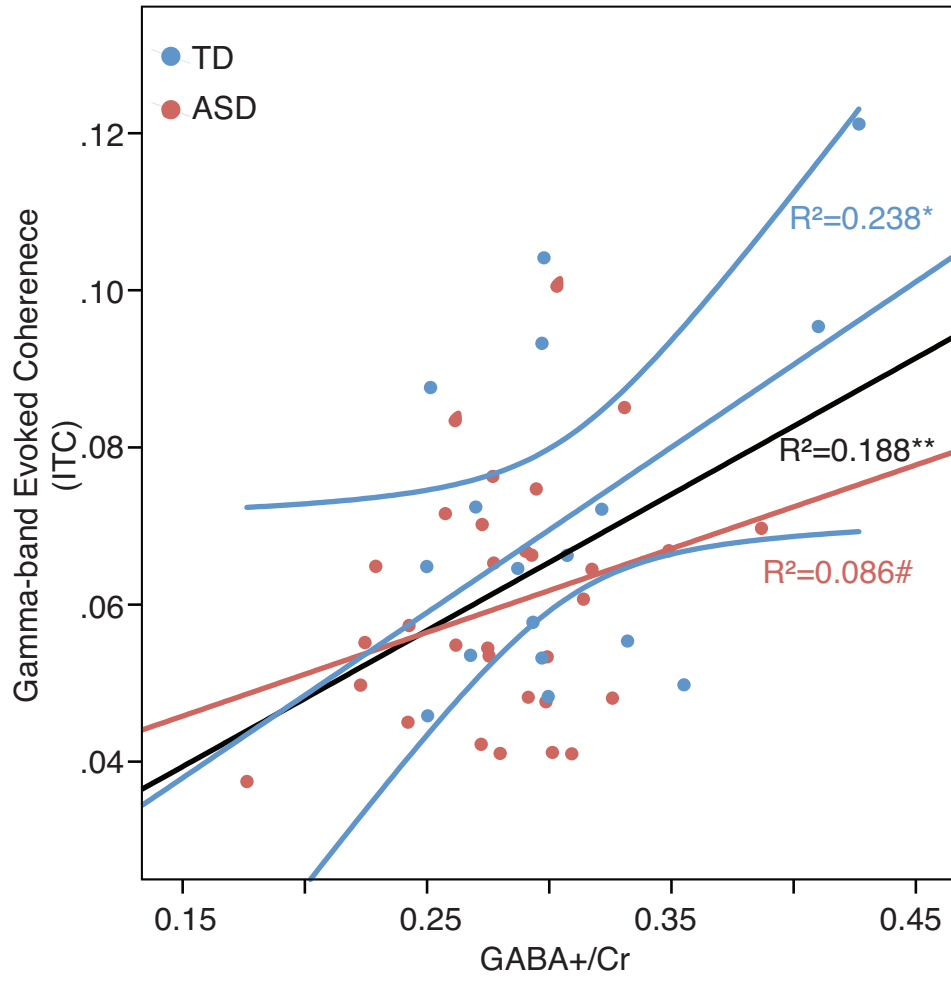


Figure 3. 4

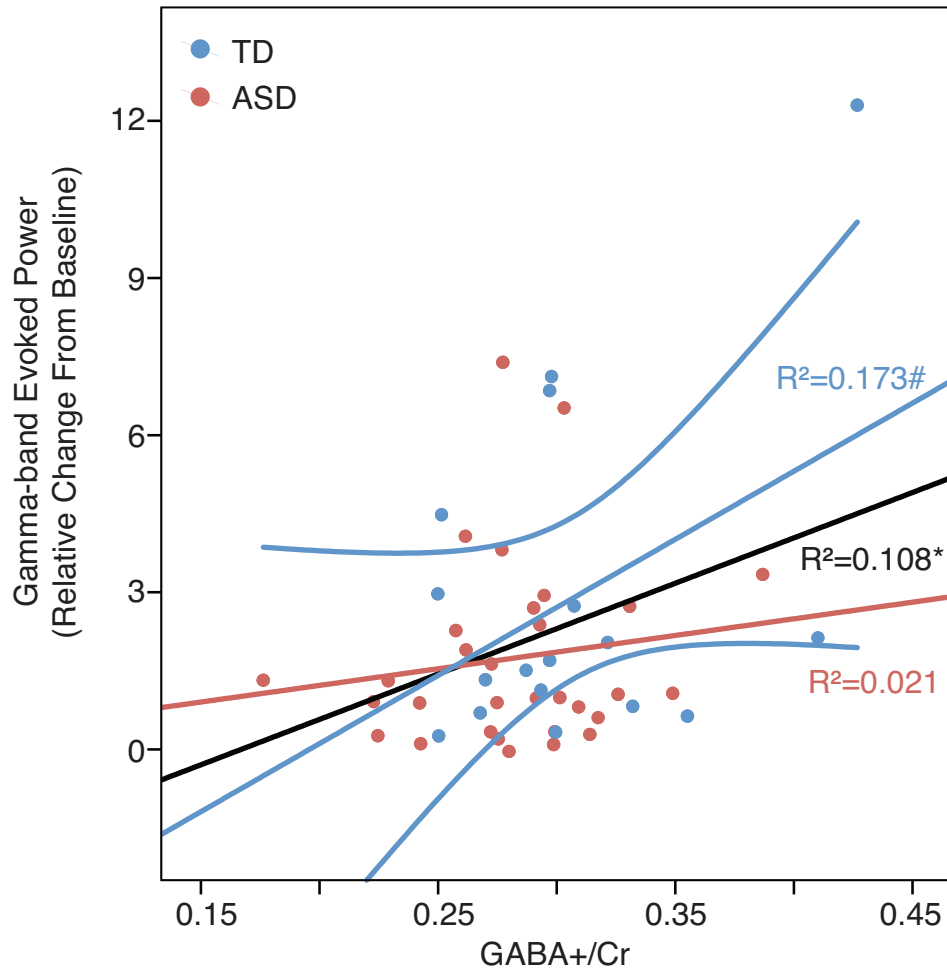
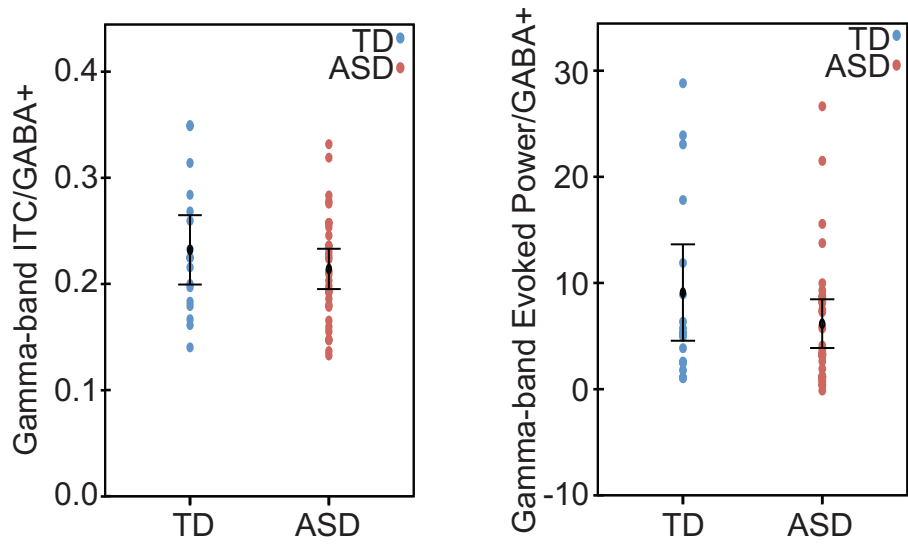


Figure 3. 5

Functional to Neurochemical Coupling



CHAPTER 4

In-vivo electrophysiological and ex-vivo neurochemical characterization of *Pcdh10*^{+/-} mice

Russell G. Port^a, Christopher Gawjewski^a, Elizabeth Krizman^{b,c}, Michael B.
Robinson^{b,c,d}, Gregory C. Carlson^a, Steven J. Siegel^a

^aDepartment of Psychiatry University of Pennsylvania Perelman School of Medicine,
Philadelphia, PA 19104.

^bChildren's Hospital of Philadelphia Research Institute, and ^cDepartments of Pediatrics
and ^dSystems Pharmacology and Experimental Therapeutics, University of Pennsylvania,
Pennsylvania 19104

Abstract:

Autism Spectrum Disorder currently affects 1 in 45 children, causing characteristic social/communication impairments as well as restricted and repetitive behaviors. Recent studies have linked a subset of familial ASD to mutations in the Protocadherin 10 (*Pcdh10*) gene. Subsequently mice heterozygous for *Pcdh10* (*Pcdh10*^{+/-}) have begun to be investigated in an effort to understand the neurobiology of ASD. *Pcdh10*^{+/-} mice demonstrate face validity by exhibiting specific alterations to social behavior, and moreover, such social deficits are sex-specific (affecting only male mice). As such this mouse model recapitulates the gender bias observed in ASD. Furthermore, these male *Pcdh10*^{+/-} mice demonstrate precise alterations to high frequency responses in in-vitro slice preparations. The *in-vivo* ramifications of such decreased high frequency responses observed *in-vitro* are unknown. Therefore, to further characterize the effect of *PCDH10* loss, *Pcdh10*^{+/-} mice and their wild-type littermates underwent in-vivo depth electroencephalography (EEG) as well as ex-vivo amino acid concentration quantification using High Performance Liquid Chromatography (HPLC). Male *Pcdh10*^{+/-} mice demonstrated select reductions to gamma-band (30-100 Hz), but not lower frequency, auditory steady state responses versus their wild-type littermates. In addition, the signal to noise ratio for high gamma-band (60-100 Hz) activity was decreased in male *Pcdh10*^{+/-} mice versus their wild-type counterparts, concurrent to low gamma-band (30-60 Hz) resting-state power increases. *Pcdh10*^{+/-} mice also demonstrated increases in multiple amino acids including GABA. Of note, whilst WT mice demonstrated coupling between underlying GABA concentrations and auditory gamma-band activity, *Pcdh10*^{+/-}

mice did not. As such, this study provides crucial insight into the hypothesis of E/I imbalance in ASD and its functional consequences.

1. Introduction:

Autism Spectrum Disorder (ASD) is characterized by marked impairments to social/communication functioning, and the appearance of restricted/stereotyped behaviors (American Psychiatric Association, 2013). Recent estimates suggest that 1 in 45 children between the ages of 3 and 17 are diagnosed with ASD, with three quarters of these being male (Zablotsky et al., 2015). Many biological alterations have been identified in ASD, including those affecting neuronal synapses (for review see Port et al., 2014). One such set of alterations involves the cell adhesion molecules encoded by the cadherin/Protocadherin superfamily of genes (Kim et al., 2011; Morrow et al., 2008; O’Roak et al., 2012), including Protocadherin 10 (*Pcdh10*) (Bucan et al., 2009; Morrow et al., 2008).

PCDH10 has been linked directly to cell migration (Nakao et al., 2008) and indirectly to spinogenesis (Pilpel and Segal, 2005). As such, the protein seems to have an important role in neuronal circuit formation. Moreover, PCDH10 is involved in synapse elimination through linking ubiquitinated PSD-95 to the proteasome (Tsai et al., 2012). Of note, Tsai and colleagues (2012) also demonstrated that *Pcdh10* translation is suppressed by Fragile X mental retardation protein (FMRP). This is of particular relevance because transcriptional silencing of the *Fmr1* gene that encodes FMRP causes Fragile X Syndrome, a syndromic form of ASD (O’Donnell and Warren, 2002). Recently, male mice heterozygous for *Pcdh10* (*Pcdh10*^{+/-}) were shown to demonstrate perturbed behavioral (reduced sociability) and neuroanatomical (abnormal dendritic spine density and morphology) phenotypes (Schoch et al., 2016). Of particular note, the

reduced sociability was not demonstrated in female *Pcdh10*^{+/-} mice, *perhaps consistent with the gender bias of ASD* (see above). As such, this murine model recapitulates several key aspects of ASD. Furthermore, these male *Pcdh10*^{+/-} mice also demonstrated specific alterations to in-vitro amygdala electrophysiological responses for high-frequency, but not single, stimulation (Schoch et al., 2016). The purpose of such high-frequency stimulation within in-vitro preparations is to induce high-frequency activity, in an effort to mimic the analogous activity seen within in-vivo systems (Contreras and Llinas, 2001). Such higher frequency activity (in particular gamma-band activity) is thought to play key roles in local circuit functions (Cardin et al., 2009; Sohal et al., 2009) and is correlated to many cognitive/behavioral functions (for review see Herrmann et al., 2010).

Deficits in gamma-band (30-100 Hz) electrophysiological activity have been hypothesized as a biomarker for ASD (Rojas and Wilson, 2014). Gamma-band activity alterations have been repeatedly observed in ASD (Grice et al., 2001; Maxwell et al., 2013; Orekhova et al., 2007; Wilson et al., 2007). In addition, gamma-band perturbations in ASD correlate to social functioning (Maxwell et al., 2013) and show normalization with clinically effective behavioral intervention (Van Hecke et al., 2013). Alterations to gamma-band activity are also observed in first degree relatives of individuals with ASD, and as such may constitute an endophenotype (Rojas et al., 2008). Moreover, within these first degree relatives gamma-band activity is associated with sociability (Rojas et al., 2011). Such perturbations to gamma-band activity appear to represent a conserved phenotype in multiple murine models recapitulating key aspects of ASD, regardless of the nature of the specific insult (Gandal et al., 2012a, 2010; Saunders et al., 2012).

Furthermore, the normalization of in-vivo preclinical gamma-band activity is concurrent with behavioral improvements (Gandal et al., 2012b; Yizhar et al., 2011). Of note, gamma-band alterations seen in such murine models are correlated with underlying neurobiology such as specific cell densities (Nakamura et al., 2015) as well as synaptic protein levels (Gandal et al., 2010).

An additional potential clinical biomarker for ASD is auditory M100 latency prolongations (for review see (Port et al., 2015)). Using magnetoencephalography (MEG) Gage and colleagues (Gage et al., 2003) first identified a ~10 ms delay in children with ASD for the neuromagnetic response that occurs ~100 ms post auditory stimuli (M100). Since this initial description, subsequent larger studies have recapitulated this M100 delay and also demonstrated that such findings cannot be accounted for by cognitive or language abilities (Edgar et al., 2015, 2014; Roberts et al., 2010). Analogous delays to middle latency responses (e.g. the electroencephalographic murine counterpart to the M100, the N40) have been observed in preclinical models which recapitulate key aspects of ASD (Billingslea et al., 2014; Engineer et al., 2015, 2014; Gandal et al., 2012a, 2010; Saunders et al., 2013, 2012a). Such latency prolongations are associated with sociability in these murine models (Billingslea et al., 2014; Saunders et al., 2013).

In fulfillment of their biomarker statuses, both gamma-band activity and auditory M100 latencies have plausible biological bases. In both cases perturbed signal transduction (synaptic transmission) may cause the observed alterations in ASD (Port et al., 2015). Moreover, γ -Aminobutyric acid (GABA) may play a crucial role for the two aforementioned biomarkers of ASD, with excitatory/inhibitory (E/I) imbalance being

posited as a potential underlying pathogenic mechanism for ASD (Rubenstein and Merzenich, 2003). GABA-related alterations in individuals with ASD are well documented both in post-mortem (Casanova et al., 2006; Fatemi et al., 2014, 2009a, 2009b, 2002) and in-vivo (Gaetz et al., 2014; Harada et al., 2011; Rojas et al., 2014) clinical studies. Further support for GABAergic dysfunction in ASD comes from preclinical models, where alterations to GABAergic expression (Gandal et al., 2012b; Gogolla et al., 2014, 2009; Zhang et al., 2014) or function (Banerjee et al., 2013; Cellot and Cherubini, 2014; Han et al., 2012) have frequently been observed. Direct measurements of neural GABA concentrations in rodent models recapitulating key aspects of ASD and other related disorders are less consistent, with decreases (Bitanirwe et al., 2010; Groves et al., 2013; Ide et al., 2005), increases (Ali and Elgoly, 2013; Gruss and Braun, 2004, 2001) and no change (Fatemi et al., 2008) in GABA concentrations being observed. Such observations are confounded by concurrent and inconsistent alterations to glutamate (Ali and Elgoly, 2013; Bitanirwe et al., 2010; Gruss and Braun, 2004, 2001; Ide et al., 2005). Alterations to GABA, glutamate and/or their relative concentrations, are further complicated by *sex*, regional and age dependencies (Gruss and Braun, 2004, 2001).

As such, several questions remain unresolved: 1) If *Pcdh10*^{+/-} mice demonstrate altered auditory electrophysiological responses akin to clinical ASD (e.g. delayed N40 latencies and reduced gamma-band activity), 2) If *Pcdh10*^{+/-} mice demonstrate altered underlying E/I balance, 3) how do such electrophysiological and neurochemical profiles relate to one another, and 4) what is the role of *sex* in these aforementioned questions as

only male *Pcdh10*^{+/-} mice display social deficits. As such, *Pcdh10*^{+/-} (heterozygous for *Pcdh10*) mice underwent electrophysiological characterization. To do so, depth electroencephalography (EEG) was recorded in these mice and their wild-type littermates. In addition, High Performance Liquid Chromatography (HPLC) was utilized to quantify *ex-vivo* amino acid concentrations in these WT and *Pcdh10*^{+/-} mice.

2. Materials and methods:

2.1 Animals

Adult (3 - 4 months of age; males and females) *Pcdh10*^{+/-} mice and their wild-type (WT) littermates were used in this study. Originally created by Lexicon Pharmaceuticals Inc. (USA) using a LacZ-neo selection cassette replacement of the first exon of *Pcdh10*; for this study Male *Pcdh10*^{+/-} mice were crossed with female C57BL/6J mice (see Schoch et al., 2016 for additional details). This produced both *Pcdh10*^{+/-} and WT (*Pcdh10*^{+/+}) littermates for subsequent examination. Mice were group-housed (2-4 per cage) with *ad libitum* food and water access and maintained on a 12-hour light/dark cycle. The final sample size for each group (Sex by Genotype) was 11 male WT, 9 female WT, 9 male *Pcdh10*^{+/-}, and 8 female *Pcdh10*^{+/-}. All experiments were conducted in accordance and with approval with the University of Pennsylvania's Institutional Animal Care and Use Committee (IACUC) and the National Institutes of Health guidelines.

2.2 Surgery for EEG recordings

All mice had intracranial electrodes (tri-polar stainless steel electrodes, 200 μ m diameter, Plastics One, Roanoke VA) implanted (AP -2.7 mm, ML +4.0 mm, DV -2.8 mm; targeted to primary auditory cortex) via stereotactic surgery. Mice were anesthetized with isoflurane (with confirmation of sedateness) and their scalps cleaned with betadine. Then the skull was exposed (bregma to lambdoid sutures) and electrodes secured in the aforementioned coordinates with dental cement. These tri-polar electrodes were low

impedance ($<5\text{k}\Omega$, 1000 Hz) (Gandal et al., 2010). Similar electrode configurations (though targeted to hippocampus) demonstrate the ability to detect auditory brain stem responses, as well as later subcortical and cortical responses (P1, N40, P2, P3A) (Connolly et al., 2003; Siegel et al., 2003), analogous to human Cz electrode recordings (Siegel et al., 2003). In addition, such hippocampal targeted configurations have demonstrated face and predictive validity for genetic, developmental and pharmacologic manipulations in mice (Gandal et al., 2012a, 2010; Saunders et al., 2012).

2.3 Recording of EEG activity

All mice received a minimum of one-week recovery following surgery. EEG recordings were collected in home cages, which were placed within a Faraday cage. Modified (heightened) cage tops were used to accommodate stimulus speakers and electrode cables. Electrode cables were connected to a high-impedance differential AC amplifier (A-M Systems, Carlsborg, Washington, USA). Mice were acclimatized to the testing apparatus for 30 minutes before testing to ensure habituation to the environment. Habituation and recordings took place in the presence of 55 dB background white noise. During testing stimuli consisted of either 100 white-noise clicks (10 ms duration, 85 dB, 8 second inter-trial interval) or an amplitude-modulated white-noise stimulus at 20, 40, 50, 60, and 80 Hz frequencies (100 trials per frequency, 1 second train duration, 85 dB, 1 second inter-stimulus interval). In addition, the white-noise click paradigm also included a 60 second stimulus-free period at the beginning of the paradigm to allow for the collection of “resting-state” data. Stimuli were generated by Micro1401 hardware and

Spike 6 software (Cambridge Electronic Design, Cambridge, England) and delivered by speakers atop each cage. Signals were continuously sampled at 1667 Hz and an online bandpass filter (1–500 Hz) was applied to all EEG signals.

2.4 EEG data analysis

White-noise click paradigm analysis

EEG signals were analyzed using the Fieldtrip (Oostenveld et al., 2011) toolbox for MatLab (Mathworks, Natick, USA). Single trials epochs (± 1 second relative to auditory stimulus onset) were extracted from continuous data. Artifact-containing epochs (e.g. movement) were then rejected using Fieldtrip's Z-score based artifact detection routine with experimenter input adjusting the threshold for artifact determination. This produced between 89 and 93 trials remaining on average per sex by genotype group (e.g. male WT). A 2 X 2 ANOVA with the main effects of Sex, Genotype and their interaction demonstrated a significant main effect of Genotype, with the *Pcdh10*^{+/-} group having more trials remaining than their WT littermates (WT trials remaining = 89.6 ± 0.8 ; *Pcdh10*^{+/-} trials remaining = 92.3 ± 0.9 , $p < 0.05$). Even with this difference in remaining trials between genotypes (less than 3%), the number of trials remaining was considered sufficient for all analyses and unlikely to cause group-wise significant differences. Trials were then baseline-corrected (baseline = -400 to -100 ms relative to stimulus onset) and subsequently averaged together to produce event related potentials (ERP). Latency and amplitude changes in the components of such ERPs are associated with psychiatric

disorders (Roberts et al., 2010; Rojas et al., 2007; Turetsky et al., 2007). As such, these components were quantified in all mice. The current electrode configuration targeted at auditory cortex recorded a multicomponent ERP which demonstrated two noticeable negative deflections occurring at ~20 ms and ~40 ms (Figure 4.1A), and are denoted throughout as AN20 (AuditoryN20) and AN40 (AuditoryN40). The amplitudes and latencies for both of these responses were determined by the time of the deflection peak (visual examination by RGP), defined by the negative vertex in the corresponding time window (AN20: 8-25 ms; AN40: 30-45 ms). Thus similar to equivalent electrode configurations targeted to hippocampus, these components have corresponding latencies (though at 40%) to analogous human evoked components (Siegel et al., 2003).

To further characterize the *Pcdh10*^{+/-} mice's auditory electrophysiological responses, recordings were spectrally decomposed (Morlet wavelets; 100 linearly spaced frequency bins between 3 and 100 Hz; wavelet cycles increasing from 3 (at low frequencies) to 6 (at high frequencies)) as previously published (Gandal et al., 2010). Multiple forms of spectral activity can be calculated, each of which has a particular sensitivity profile to the underlying oscillatory activity. Phase locked metrics (evoked power and inter-trial coherence (ITC)) quantify the brain's ability to align oscillatory activity over multiple trials. As such, they are often considered a measure of reliability of the brain's oscillatory activity. Non-phase locked activity, also known as induced power, is oscillatory activity in response to a stimuli which is *not* aligned with respect to phase over trials. The combination of both evoked power (phase locked) and induced power (non-phase locked) produces total power.

Baseline corrected total power (% change from baseline; baseline period = -700 to -150 ms relative to stimulus onset) and ITC were calculated for all epoched trials. Subsequent analyses focused on the ± 500 ms (relative to the stimulus onset) region as previous studies have demonstrated alterations in this region (Gandal et al., 2010; Liao et al., 2012; Saunders et al., 2012). Based on *a-priori* observations (see introduction) the gamma-band frequency range was selected for further analyses. Both early gamma-band total power and ITC responses (as defined by group-average time-frequency plots; Total power: 30-100 Hz, 0-120 ms post stimulus; ITC: 30-100 Hz, 0-40 ms post stimulus) as well as later (150-470 ms post stimulus) gamma-band total power responses were examined. ITC responses were not examined for this later response (150-470 ms post stimulus) due to the time-frequency plots demonstrating no activity above baseline in this region. The later total power responses were separated into high and low gamma-band frequencies (high gamma = 60-100 Hz; low gamma = 30-60 Hz) in accordance with previous observations (Carlson et al., 2011). For these spectrotemporal regions of interest (ROI) the average power and coherence was calculated for each mouse.

As mentioned above, the white-noise click paradigm also included a 60 second stimuli-free period at the beginning of the paradigm to allow for the collection of “resting-state” responses. Data during this period was imported into Fieldtrip and the power spectral density (PSD) calculated using fast Fourier transformations. This PSD data was then divided into specific spectral sub-regions in accordance with previous studies (Gandal et al., 2012b). In addition, examination of the group-level (e.g. male WT) PSD showed a potential ROI (28-45 Hz) where a differential pattern resting-state power

was selectively occurring. Additional analyses focused on this specific frequency range since this ROI was not represented by the *a-priori* regions above.

Resting-state data was also combined with the white-click stimulus produced ITC response (average ITC for 0-40 ms post stimulus onset) to produce signal to noise ratios (SNR) for both high (60-100 Hz) and low (30-60 Hz) frequency regions. In each case the resting-period frequency range utilized for this analysis was consistent to the ITC frequency range.

In addition the data from this “resting-period” was analyzed for phase-amplitude cross-frequency coupling (CFC) using a previously published analysis pipeline (Berman et al., 2015). This CFC analysis pipeline has previously revealed specific alterations to alpha to gamma (alpha-gamma) CFC in children with ASD (Berman et al., 2015). These CFC alterations may have been detected due to the variable bandwidth filtering utilized by this analysis pipeline, which is more sensitive to CFC involving modulation frequencies higher than the theta-band (Berman et al., 2012). In brief, resting-period data was again imported into fieldtrip and CFC was calculated utilizing the methodology first described by Tort and colleagues (Tort et al., 2010). Modulation frequencies ranged from 3 to 15 Hz and observed (carrier) frequencies ranged from 20 to 100 Hz (both ranges using 1 Hz bins) for CFC calculations. Previous literature supports the investigation of two separate ROIs for this analysis. First, as previously mentioned, Berman and colleagues (2015) observed alterations in alpha-gamma coupling in children with ASD. Secondly, theta to high-gamma (theta-high gamma) coupling has been demonstrated in recordings from subdural neocortical electrocorticograms of patients with epilepsy

(Canolty et al., 2006). As such, both alpha-gamma (“phases” = 8 to 11 Hz; “amplitudes” = 35 to 55 Hz) and theta-high gamma (“phases” = 3 to 7 Hz; “amplitudes” = 50 to 100 Hz) were assessed. For each CFC ROI a subject average modulation index (MI) was calculated.

Amplitude-modulated stimuli paradigm analyses

Similar to the white-noise click analyses, single trial epochs (± 1 second relative to onset of the stimuli) were imported into Fieldtrip for each frequency condition. Artifact containing epochs were identified and rejected using identical procedures to the white-noise click paradigm analysis. This artifact rejection resulted in Sex by Genotype groups containing on average between 88 to 94 trials remaining. A series of 2 X 2 ANOVAs tested each frequency condition for the main effects of Sex, Genotype and their interaction on the number of trials remaining. No significant effects of Sex, Genotype or their interaction were observed. Baseline corrected total power (% change from baseline; the same parameters to the white-noise click paradigm) and ITC were calculated using identical Morlet wavelet decomposition as for the white-noise click paradigm. Each mouse’s auditory steady state response (ASSR) was quantified by taking the average value in the post-stimulus steady state response (Stimulus Frequency ± 5 Hz; 200 – 700 ms post stimulus).

2.5 Statistical analysis of in-vivo electrophysiological response metrics

For all in-vivo electrophysiological measures a series of 2 (Sex) X 2 (Genotype) ANOVAs testing the main effects and their interaction as fixed factors were implemented (IBM SPSS, Armonk, New York). Moreover, the specific pairwise comparison of males (WT versus *Pcdh10*^{+/-}) was also examined due to previous observations suggesting that only male *Pcdh10*^{+/-} mice demonstrate altered social interaction (Schoch et al., 2016). Of note, if the ANOVA violated Levene's Test of Equality, then a t-test (assuming unequal variance if appropriate) tested for significant differences between males.

2.6 Tissue Collection and HPLC analysis of amino acids

At least one week after final EEG data collection, mice were humanely euthanized via isoflurane sedation followed by decapitation. Brains were dissected over ice to collect tissue samples for amino acid analyses. Four regions were harvested during the tissue collection - cerebellum, right-hemisphere hippocampus (ipsilateral to the recording site), and bilateral posterior cortex (guided by the placement of the recording electrode and the corresponding area on the contralateral hemisphere). Tissue samples were immediately flash frozen using isopentane and dry ice. All dissections were performed quickly (within ~ 7 minutes of euthanasia). To prepare samples for HPLC analyses, tissue samples were homogenized in 0.8 N perchloric acid buffer (containing 1 mM L-alpha-aminoadipate). HPLC analyses were performed at the Children's Hospital of Philadelphia's Intellectual and Developmental Disabilities Research Center (specifically the Analytical Neurochemistry Core) to measure concentrations of aspartate, glutamate, GABA, and

glutamine as previously published (Kilpatrick et al., 2010). In short, the samples underwent reverse-phase HPLC analysis with o-phthaldialdehyde precolumn derivatization. A Model 717 plus Autosampler (Waters, Millipore, Milford, MA, USA) automatically derivatized samples with o-phthaldialdehyde and injected said processed samples onto a reverse-phase C-18 column. Processed samples were eluted using a sodium acetate buffer (50 mM, pH 6.0) with either 20 or 80% methanol using a stepped linear gradient. Finally a McPherson Model FL-750 fluorescence detector (Acton, MA, USA) with a xenon-mercury lamp set at 316 nm excitation detected concentrations of each amino acid (Kilpatrick et al., 2010). Of important note, all HPLC runs were blinded. For each amino acid the identity was determined by elution time and reported as nmol/mg tissue. Results were tested for group differences using a Linear Mixed Effects Model (LMM) (Random intercept, Fixed factors = Sex X Genotype X Brain region (repeated measure), Repeated Factor = Subject) (IBM SPSS, Armonk, New York) with both main effects and their interactions tested. Additionally statistical differences between male WT and male *Pcdh10*^{+/-} were tested separately using the pairwise comparison for the Sex by Genotype interaction derived from the LMM as the within male comparison was of *a-priori* interest.

3. Results:

3.1 *Pcdh10*^{+/-} mice demonstrate unaltered ERPs

White noise clicks produced stereotypical multicomponent responses as shown in Figure 4.1A. No significant differences were observed for Sex, Genotype or their interaction for AN20 or AN40 response latencies ($p > 0.1$; data not shown). Similarly, the amplitude of the AN20 response demonstrated no significant effect of Sex, Genotype, or their interaction ($p > 0.1$; data not shown). A significant main effect of Sex was observed for the AN40 response amplitude, demonstrating larger responses in females than males ($F(1,24) = 4.29, p < 0.05$; Figure 4.1B). The main effect of Genotype and its interaction with Sex was not significant for AN40 amplitude ($p > 0.1$). Although significant Sex by Genotype interactions were not observed previous findings have suggested that alterations in *Pcdh10*^{+/-} mice are sex specific (Schoch et al., 2016) and so the within male pairwise comparison was also examined. For all ERP-related metrics, this comparison was non-significant ($p > 0.1$; data not shown).

3.2 *Pcdh10*^{+/-} mice demonstrate select gamma-band activity alterations in response to a white noise click

Group-level total power time frequency plots are presented in Figure 4.2A. Early gamma-band activity in response to white-noise clicks for both total power and ITC were not significantly modulated by Sex, Genotype or their interaction ($p > 0.1$; data not shown). Additionally there was no significant effect of Sex, Genotype or their interaction on late

high gamma-band total power ($p > 0.1$; data not shown). A significant main effect of Genotype was observed for late low gamma-band total power ($F(1,33) = 4.52, p < 0.05$; Figure 4.2B), demonstrating reduced power in *Pcdh10*^{+/-} mice versus WT. No significant effect of Sex or its interaction with Genotype was observed for this ROI. The pairwise comparison of male mice was examined to test for *a-priori* specified sex-specific alterations in *Pcdh10*^{+/-} mice. No significant differences between male mice existed at any ROI ($p > 0.1$).

3.3 Male *Pcdh10*^{+/-} demonstrate selective increases to high frequency resting-state power

The group-level PSD are presented in Figure 4.3A. For all *a-priori* ROIs a main effect of Sex was either significant (15-25 Hz - $F(1,33) = 7.63, p < 0.01$, Figure 4.3C; 60-100 Hz - $F(1,33) = 5.32, p < 0.05$, Figure 4.3E) or trending toward significance (4-12 Hz - $F(1,33) = 3.53, p < 0.1$ Figure 4.3A; 30-60 Hz - $F(1,33) = 3.27, p < 0.1$, Figure 4.3D), with female mice demonstrating greater resting power than males. Of note though, Levene's Test of Equality was violated for the 60-100 Hz ROI ($p < 0.01$) so care should be taken in interpretation of significant observations. Examining the *a-posteriori* ROI revealed that Levene's Test of Equality was again violated ($p < 0.05$). Additionally for this *a-posteriori* ROI a significant main effect of Sex was observed ($F(1,33) = 4.34, p < 0.05$, Figure 4.3F) with females demonstrating greater resting power than males. The within male pairwise comparison was investigated for those ROI that did not violate Levene's Test of Equality since the male comparison was of *a-priori* interest. No significant differences existed between males for the *a-priori* ROIs ($p < 0.1$; data not shown). If Levene's Test of

Equality was violated for a ROI a t-test examined the within male comparison (assuming unequal variance if appropriate). No significant difference between males was observed for the 60-100 Hz ROI ($p < 0.1$; data not shown). For the *a-posteriori* ROI (28-45 Hz) a significant increase in resting power for male *Pcdh10*^{+/-} mice versus male WT was observed ($t(18) = -2.12, p < 0.05$).

3.4 Male *Pcdh10*^{+/-} exhibit reduced signal to noise in the high-gamma band

Gamma-band SNR was examined for both high and low gamma-band regions. For both high and low gamma-band SNR no significant main effect (Sex/Genotype) or their interaction was observed ($p > 0.1$; low gamma - data not shown, high gamma – Figure 4.4). *A-priori* hypotheses specified the examination of the within male comparisons. While no significant difference was observed for the within male comparison of low-gamma SNR ($p > 0.1$; data not shown) pairwise comparisons revealed significantly lower SNR in male *Pcdh10*^{+/-} versus male WT mice ($F(1,33) = 4.40, p < 0.05$, Figure 4.4).

3.5 Male *Pcdh10*^{+/-} exhibit subtle deficits in theta-high gamma CFC

Figure 4.5A show group-average comodulograms. Alpha-gamma CFC demonstrated a trend towards significance for the main effect of Sex ($F(1,33) = 3.10, p < 0.1$; data not shown), though again such findings should be treated with caution because Levene's Test of Equality was violated ($p < 0.01$). The main effect of Genotype and its interaction with

Sex was not significant for alpha-gamma CFC. For theta-high gamma CFC Levene's Test of Equality was also violated ($p < 0.01$). Within the theta-high gamma ROI a near significant main effect of Genotype was determined ($(F(1,33) = 2.91, p < 0.10$, Figure 4.5B). No other effects were significant. T-tests were used to examine the within male comparison due to this comparison being of *a-priori* interest as well as to remove the potential issues arising from the violation of Levene's Test of Equality, While alpha-gamma CFC demonstrated no significant group differences ($p > 0.1$; data not shown), male *Pcdh10*^{+/-} mice demonstrated a trend towards significantly decreased theta-high gamma CFC versus male WT mice ($t(10.1) = 1.88, p < 0.1$, Figure 4.5B).

3.6 Male *Pcdh10*^{+/-} show decreased gamma-band, but not lower frequency, ASSRs

Group-level 40 Hz ASSR are shown in Figure 4.6A. No significant effect of Sex, Genotype or their interaction was observed for the 20 Hz total power ASSR ($p > 0.10$, Figure 4.6B). Levine's Test of Equality was violated for 40 Hz total power ASSR ($p < 0.05$). In addition, a significant Sex by Genotype interaction was observed for the total power 40 Hz ASSR ($F(1,33) = 4.55, p < 0.05$, Figure 4.6C), where male *Pcdh10*^{+/-} mice demonstrated significantly reduced ASSR power than male WT mice ($p < 0.05$), and a trends towards significance for male WT exhibiting greater ASSR power than female WT ($F(1,33) = 4.45, p < 0.1$). No significant effect of Sex, Genotype or their interaction was observed for the total power 50 Hz ASSR ($p > 0.1$, Figure 4.6D). Levene's Test of equality was also violated for the 60 Hz ASSR ($p < 0.01$). The total power 60 Hz ASSR demonstrated a significant main effect of Genotype ($F(1,33) 38.2, p < 0.01$, Figure 4.6E)

with *Pcdh10*^{+/-} exhibiting less ASSR power versus WT mice. A significant main effect of Sex was observed for the 80 Hz ASSR total power response ($F(1,33)=4.43, p < 0.05$, Figure 4.6F), demonstrating female mice exhibiting less ASSR power than males. Again, pairwise comparisons (if Levene's Test of Equality was not violated) or t-tests (if Levene's Test of Equality was violated) were utilized since *a-priori* hypotheses specified examination of the within male comparison. Pairwise comparisons of male mice for both the 50 Hz and 80 Hz total power ASSR revealed that male *Pcdh10*^{+/-} demonstrated significantly or marginally significant (respectively) less ASSR power versus male WT (50 Hz ASSR - $F(1,33) = 5.31, p < 0.05$, Figure 4.6D; 80 Hz ASSR - $F(1,33) = 4.02, p = 0.053$, Figure 4.6F). A similar pattern of male *Pcdh10*^{+/-} mice demonstrating significantly less ASSR power than their male WT littermates was also observed for 40 Hz and 60 Hz ASSRs (40 Hz - $t(13.4) = 3.05, p < 0.01$, Figure 4.6C; 60 Hz - $t(11.5) = 11.5, p < 0.05$, Figure 4.6E).

ITC was also calculated for the ASSRs to further characterize the ASSR of *Pcdh10*^{+/-} mice. No significant main effect of Sex or Genotype was found at any frequency stimulation ($p > 0.1$; data not shown). Levene's Test was violated for the 40 Hz ITC ASSR ($p < 0.05$). Additionally the 40 Hz ITC ASSR demonstrated a significant Genotype by Sex interaction was observed ($F(1,33) = 4.29, p < 0.05$, Figure 4.6G). A t-test was performed to test *a-priori* hypotheses about sex specificity and to counteract the violation of Levene's Test of Equality. For the 40 Hz ITC ASSR male *Pcdh10*^{+/-} mice demonstrated significantly less ITC than their male WT littermates ($t(18) = 2.30, p < 0.05$, Figure 4.6G).

3.7 *Pcdh10*^{+/-} mice demonstrate selective neurometabolite alterations and possible reduced coupling between GABA and gamma-band activity

Group-level amino acid concentrations are shown in Figures 4.7A-D. The LMM for aspartate demonstrated a near significant main effect of Genotype, $F(1,95.69) = 3.41$, $p < 0.1$, with *Pcdh10*^{+/-} tissue containing higher aspartate concentrations than their WT littermates (Figure 4.7A). In addition, a main effect of Region was significant, $F(3,72.17) = 10.68$, $p < 0.05$, with several pairwise comparisons reaching significance. Right hemisphere auditory cortex demonstrated significantly lower aspartate concentrations than either left hemisphere auditory cortex or cerebellum (pairwise comparison between auditory cortices – $p < 0.05$; pairwise comparison of right hemisphere to cerebellum – $p < 0.001$). Furthermore, hippocampus contained significantly lower aspartate concentrations than cerebellum (pairwise comparison – $p < 0.05$). No other main effect or interaction was significant ($p > 0.1$).

The LMM for glutamate concentrations demonstrated a significant main effect of Region (Figure 4.7B), $F(3,69) = 5.68$ $p < 0.01$, with again right hemisphere auditory cortex demonstrating lower glutamate concentrations than either left hemisphere auditory cortex or cerebellum (pairwise comparison between auditory cortices – $p < 0.01$; pairwise comparison of right hemisphere to cerebellum – $p < 0.01$). No other main effect or interactions were significant ($p > 0.1$).

The LMM for GABA concentrations (Figure 4.7C) demonstrated a significant interaction of Sex by Region, $F(3,77.56) = 3.19, p < 0.05$, where females exhibited significantly less GABA in left hemisphere auditory cortex as compared to cerebellum and hippocampus (female pairwise comparison for left hemisphere auditory cortex versus cerebellum – $p < 0.01$; female pairwise comparison for left hemisphere auditory cortex versus hippocampus – $p < 0.01$). In contrast to these female specific observations, male mice demonstrated significantly reduced GABA concentrations in both left and right hemisphere auditory cortices versus hippocampus, (male pairwise comparison for left hemisphere auditory cortex versus hippocampus – $p < 0.01$; male pairwise comparison for right hemisphere auditory cortex versus hippocampus – $p < 0.001$), but no significant differences between cerebellum and left or right auditory cortex GABA concentrations ($p > 0.1$). The main effect of Genotype was also significant, $F(1,100.73) = 16.98, p < 0.001$, with *Pcdh10*^{+/-} mice demonstrating significantly higher GABA concentrations than their WT littermates. In addition, a main effect of Region was also significant, $F(3,77.56) = 12.52, p < 0.001$, with both auditory cortices demonstrating significantly reduced GABA concentrations versus hippocampus as well as cerebellum (pairwise comparison for left hemisphere auditory cortex versus hippocampus – $p < 0.001$; pairwise comparison for left hemisphere auditory cortex versus cerebellum – $p < 0.01$; pairwise comparison for right hemisphere auditory cortex versus hippocampus – $p < 0.001$; pairwise comparison for right hemisphere auditory cortex versus cerebellum – $p < 0.05$). There were no significant differences between auditory cortices or between hippocampus and cerebellum ($p > 0.1$).

Lastly, the LMM for glutamine concentrations demonstrated a significant main effect of Genotype, $F(1,107.59) = 4.30, p < 0.05$, demonstrating significantly increased glutamine concentrations in *Pcdh10*^{+/-} mice versus their WT littermates. Additionally, a trend towards a significant main effect of Region was observed, $F(3,72.827) = 2.33, p < 0.1$, where right hemisphere auditory cortex demonstrated a trend towards significance for reduced glutamine (pairwise comparison for right hemisphere auditory cortex versus cerebellum – $p = 0.105$).

The corresponding pairwise comparisons (Sex X Genotype) were investigated since the within male comparison was of *a-priori* interest. GABA was significantly increased for male *Pcdh10*^{+/-} mice versus male WT littermates (pairwise comparison – $p < 0.05$). No other within male pairwise comparison for amino acid concentrations was significant.

Previous clinical studies have demonstrated significant correlations between relative cortical GABA and gamma-band activity in humans (Balz et al., 2015; Gaetz et al., 2011; Muthukumaraswamy et al., 2009). In support of this coupling, a recent preclinical study demonstrated a significant correlation between parvalbumin immunoreactive cell density and corresponding gamma-band ITC (Nakamura et al., 2015). As such, it seems that coupling between relative cortical GABA and gamma-band metrics may exist both clinically and preclinically. Furthermore, Chapter 3 demonstrated that such coupling might be perturbed in ASD. As such, the coupling of underlying GABA concentrations to gamma-band activity metrics were investigated in the current data. Only 3 gamma-band activity metrics were considered to restrict type 1 statistical error. The early gamma-band ITC observed in response to white-noise clicks (30-100 Hz, 0-40 ms; same ROI as used

for above EEG analyses) was investigated to be consistent with Chapter 3. In addition, the 40 Hz ASSR responses (both total power and ITC) were probed for correlations to underlying GABA concentration since activity around 40 Hz is thought to be reliant on GABA for its creation (for review see Whittington et al., 2000). Of note, for subsequent analyses groups were collapsed across sex since the main effect of Genotype, but not Sex, was significant for GABA concentrations, Early ITC in response to white-noise clicks was significantly correlated to auditory cortex GABA in WT ($R^2 = 0.33$, $p = 0.01$), but not *Pcdh10*^{+/-} mice (Figure 4.7E). Additionally a similar, though only trending towards significant, association was determined for auditory cortex GABA concentrations and 40 Hz ASSR ITC for WT mice ($R^2 = 0.18$, $p < 0.10$; Figure 4.7F). Such a coupling was not observed in *Pcdh10*^{+/-} mice ($p > 0.1$). On the other hand, total power 40 Hz ASSRs failed to correlate to right-hemisphere auditory cortex GABA concentrations for either WT or *Pcdh10*^{+/-} mice ($p > 0.1$).

Of note, activity from adjacent brain regions may be superimposed on auditory cortex activity because the electrodes used in this study were low impedance. In the mouse brain the hippocampus lies next to auditory cortex, and volume conduction of the hippocampal responses may contaminate cortical recording (Harvey et al., 2012). Therefore, hippocampal gamma-band activity probably accounts for part of the variance of the recorded electrophysiological signals. As such, white noise click-produced early gamma-band ITC and 40 Hz ASSRs were also compared to hippocampal GABA concentrations. White noise click-produced early gamma-band ITC did not correlate with hippocampal GABA in either WT or *Pcdh10*^{+/-} mice ($p > 0.1$). On the other hand, 40 Hz total power

ASSRs demonstrated near significant coupling to hippocampal GABA ($R^2 = 0.20$, $p = 0.055$) in WT mice, which was in direct contrast their *Pcdh10*^{+/-} counterparts who demonstrated no coupling ($p > 0.1$; Figure 4.7G).

4. Discussion:

The main findings of this study were gamma-band selective alterations to electrophysiological activity and altered GABA concentrations in *Pcdh10*^{+/-} versus WT littermates (Figures 4.2-7). This was in direct comparison to the lack of alterations to either amplitudes or latencies of ERP components (Figure 4.1). Furthermore, WT mice demonstrated a coupling between GABA and the gamma-band activity measure that *Pcdh10*^{+/-} failed to recapitulate (Figure 4.7).

The present study demonstrated significantly reduced late transient low-gamma band activity in *Pcdh10*^{+/-} mice (Figure 4.2). Moreover, male *Pcdh10*^{+/-} mice exhibited significantly reduced power in gamma-band, but not lower frequency, ASSRs (Figure 4.6). Male *Pcdh10*^{+/-} mice additionally demonstrated significantly reduced high gamma-band SNR (Figure 4.4), which was concurrent to a lack of a significant difference in corresponding resting-state power comparison (Figure 4.3). Further examination of resting-state PSD demonstrated a frequency region where male *Pcdh10*^{+/-} mice demonstrated significantly increased high frequency (28-45 Hz) resting-state power as compared to male WT. Such gamma-band observations were in clear distinction to the lack of any significant alterations to any ERP based metric.

While gamma-band activity alterations are frequently observed in ASD (Rojas and Wilson, 2014), such alterations are not unique to ASD as similar alterations are seen in bipolar disorder (Maharajh et al., 2007) and schizophrenia (Leicht et al., 2010). The *reduced late low* gamma-band activity exhibited by *Pcdh10*^{+/-} mice (Figure 4.2) is in direct contrast to the recent observations of *increased late high* gamma-band activity in a

murine model that recreates a key genetic insult of schizophrenia (Carlson et al., 2011). While such a discrepancy may be due to the particular murine model studied and so as such not generalizable, it may be that this differential response profile could separate/classify according to diagnosis (e.g. schizophrenia versus ASD). If so, this would resolve the specificity of gamma-band deficits, and could prompt further investigation of the biological differences between ASD and schizophrenia that produce such differential biomarkers.

High gamma-band SNR was also reduced in male *Pcdh10*^{+/-} mice versus male WT littermates (Figure 4.4). No such difference existed in the low-gamma band range. While previous preclinical studies have demonstrated reduced SNR in ASD and related disorders (Billingslea et al., 2014; Gandal et al., 2012b; Tatard-Leitman et al., 2014), to the Authors' knowledge, this is the first study to localize such an alteration to a subsection of gamma-band frequencies. Of note, the resting-state power for the corresponding high gamma frequency band did not display significant differences for this within male comparison (Figure 4.3). As such, it appears that simple alterations to resting-state power cannot account for the present findings. *A-posteriori* examination of group-level resting-state activity also revealed a frequency band where male *Pcdh10*^{+/-} mice demonstrated significantly *increased* power (28-45 Hz; Figure 4.3). As such, the current observations support the hypothesis of increased baseline activity, or alternatively poor signal to noise, in ASD (Pérez Velázquez and Galán, 2013).

Gamma-band, but not lower frequency, total power ASSRs were reduced in male *Pcdh10*^{+/-} mice versus their WT counterparts (Figure 4.6). Of note, all mice used in this

study were adult mice. An analogous clinical study demonstrated reduced gamma-band ASSR in first-degree adult relatives of individuals with ASD (Rojas et al., 2011). This study also reported frequency-selective reductions in coherence within the gamma-band frequency range of these ASSR of first-degree relatives of ASD (Rojas et al., 2011). Such frequency-selective reductions within the gamma-band range were also observed in the *Pcdh10*^{+/-} male mice, though the exact frequency at which the reduced coherence occurs was not consistent (clinical = 48 Hz, preclinical = 40 Hz), which may be due related to species-specific effects.

The biological bases for gamma-band activity is relatively understood, with key roles for excitatory and inhibitory kinetics (Buzsáki and Wang, 2012). Not only does the GABA_A receptor's time constant play a crucial role in the determination of the frequency of such activity (Traub et al., 1996), but in addition GABA_A receptors have been repeatedly found to be critical for activity around 40 Hz (Whittington et al., 2000). GABA's role in gamma-band activity has further been confirmed by optogenetic-based inhibiting or driving (exciting) of specific (parvalbumin positive [PV]) interneurons leading to decreases (Sohal et al., 2009) or increases (Cardin et al., 2009; Sohal et al., 2009) in locally recorded gamma-band activity. These specific alterations to gamma-band activity are unique to PV interneuron modulation, with analogous driving of regular-spiking neurons causing alterations to low, but not high, frequency activity (Cardin et al., 2009). Further support for this GABA to gamma-band activity coupling comes from clinical studies where in-vivo GABA levels correlate to attributes of gamma-band activity (Balz et al., 2015; Gaetz et al., 2011; Muthukumaraswamy et al., 2009), though these findings

have been challenged (Cousijn et al., 2014).

The lack of significant genotypic differences for ERP-based amplitude and latency metrics (Figure 4.1) suggests that alterations to synapse formation/elimination (here due to the role of *Pcdh10*) are not responsible for M100 latency delays in individuals with ASD. Alternatively this lack of genotypic differences for the AN40 latency may be due to this study only examining adult mice, for whom homeostatic changes have had a longer time to allow for recovery. Several studies have found associations between ERP component latency and white matter microstructure (Dockstader et al., 2012; Roberts et al., 2013, 2009; Stufflebeam et al., 2008). Furthermore, recent studies suggest the relationship of middle latency response timing and white-matter microstructure is perturbed in ASD (Roberts et al., 2013). Alterations to white-matter pathways are not the only plausible cause of ERP-related latency delays. Preclinical studies have also demonstrated that alterations to neurotransmitters receptor density (as opposed to the current synapse formation/elimination targeted alteration) also produce ERP component latency delays (Billingslea et al., 2014; Gandal et al., 2012a). However, these studies have used constitutive knock out of receptors and so developmental homeostasis may account for the noted middle latency response prolongations. Further studies are needed to see if other genetic insults that disrupt synaptic formation and regulation spare ERP latencies and/or amplitudes.

A significant main effect of Sex was observed for the AN40 latency (Figure 4.1). This finding replicates previous studies where sex differences have been reported in N40

latencies (Amann et al., 2008), and so provides a degree of validation to this current study.

Across Sex by Genotype groups the observed amino acid concentrations were consistent with previous studies (Erecińska and Silver, 1990). Noticeably, the main effect of Region was consistently significant across amino acids, suggesting that there is regional specificity in amino acid concentrations. Previous work supports such findings, though additionally observed regional specificity in neurometabolite alterations in a mouse model of Fragile X (Gruss and Braun, 2004, 2001). Such regional specificity was not observed in the current study, possibly due to the LMM being underpowered to detect such significant Genotype or Sex by Region interactions. Additionally, select amino acid alterations were observed in *Pcdh10*^{+/-} mice. GABA, aspartate and glutamine concentrations were either significantly, or trending towards significantly, increased in *Pcdh10*^{+/-} versus WT mice. While the exact meaning of such findings is unclear, one possible interpretation could be that glutamate might be relatively decreased compared to other amino acids in *Pcdh10*^{+/-} mice. Further studies will need to ascertain whether other neurometabolites are increased in *Pcdh10*^{+/-} mice versus their WT counterparts. Such analyses will allow for the determination of whole-scale increases in neurochemical concentrations (except for glutamate) in *Pcdh10*^{+/-} mice. If such global increases in neurometabolites are observed then the cellular density in *Pcdh10*^{+/-} neural tissue should be investigated because such increases may be due to increased cell density.

While the observed increased GABA concentrations contradict observations from clinical studies of individuals with ASD (Gaetz et al., 2014; Rojas et al., 2014), these increases

still point to altered E/I balance (Rubenstein and Merzenich, 2003) since glutamate concentrations were not commensurately altered. A limitation of the current study is that the exact interpretation of increased GABA with regards to neurotransmission is unclear. In addition to its role as the main inhibitory neurotransmitter, GABA can also enter the tricarboxylic acid cycle through the GABA shunt. While initially it was suggested that the exact role of GABA could be determined by which isoform of glutamate decarboxylase (GAD) the GABA molecule was produced by (GAD65 – neurotransmission; GAD67 – GABA shunt) (Martin and Rimvall, 1993) this hypothesis has been called into question (Soghomonian and Martin, 1998). Regardless, the tissue samples taken in during this study contained both neurotransmitter and metabolic GABA pools and there is no method available to separate the functionally different GABA. As such, while there may be an increase in GABA in the *Pcdh10*^{+/-} mice, it is not known how this directly relates to neurotransmission.

An indirect measure of how the observed increased GABA concentrations in *Pcdh10*^{+/-} mice relates to neurotransmission can be identified via the correlation of GABA concentrations to gamma-band activity. The early ITC in response to white-noise clicks was correlated to electrode site (right hemisphere auditory cortex) GABA concentrations in WT, but not *Pcdh10*^{+/-}, mice. Additionally a trend towards a significant correlation was observed between right hemisphere auditory cortex and 40 Hz ASSR ITC in WT, but not *Pcdh10*^{+/-}, mice. Moreover while the hippocampus was not the recording site, hippocampal gamma-band activity likely accounted for the part of the recorded gamma-band signal, due to the combination of volume conduction of the hippocampus responses

(Harvey et al., 2012) and the use of low impedance electrodes. In WT mice hippocampal GABA near significantly correlated to the total power 40 Hz ASSR. This correlation was not observed in *Pcdh10*^{+/-}.

Another possible interpretation of the correlation between hippocampal GABA and the recorded total power gamma-band ASSRs is that a remote pacemaker is driving the total power ASSR activity observed in auditory cortex more than the local GABAergic tone.

As such, a simple explanation could be the hippocampus and its underlying GABAergic concentrations are driving the ASSRs in auditory cortex more than the local GABAergic tone. Similar gamma-band pacemaker functions for auditory cortex have been observed by high frequency stimulation of the thalamic reticular nucleus (Macdonald et al., 1998).

Another possibility is that although there is an external pacemaker for auditory cortex, it is not the hippocampus. As mentioned above, such a pacemaker could be the thalamus. In this scenario, if thalamic GABAergic tone was more strongly correlated to the hippocampus inhibitory tone rather than auditory cortex inhibitory tone, a possible consequence may be the appearance of a cross-site GABA concentrations to gamma-band activity correlation as observed in this study. Indeed, though by no means correlative, results from Gruss and Braun (2001, 2004) demonstrate that group-level GABA concentrations were at least qualitatively more similar between thalamus and hippocampus than between thalamus and caudal cortex. To resolve such questions future studies should A) collect thalamic tissue, B) use high-impedance electrodes in auditory cortex to ensure that only auditory cortex activity is recorded or C) high impedance electrodes should be placed into potential pacemaker structures in addition to the use of

low impedance recording electrodes in auditory cortex,.

When considering the lack of GABA coupling to gamma-band activity in *Pcdh10*^{+/-} mice in conjunction with the increases in GABA concentrations observed in these same mice, two possible hypotheses are readily available. First, previous studies have observed that increasing GABA concentrations via the administration of tiagabine (hypothesized to block synaptic GABA reuptake) results in decreases in gamma-band activity (Nutt et al., 2015) potentially due to extra-synaptic GABA_B receptors being activated. Such GABA_B receptors inhibit both pre- and postsynaptic neurons using long duration inhibitory currents that can modulate fast-oscillatory activity (for review see Kohl and Paulsen, 2010). As such the increased GABA concentrations observed in *Pcdh10*^{+/-} mice ultimately cause less gamma-band activity due to network level inhibition. Second, the relative amount of neurotransmission-related GABA in *Pcdh10*^{+/-} mice is altered with possibly a greater proportion of the measured GABA concentrations relating to metabolic processes (see above).

In conclusion this study has demonstrated select gamma-band activity, but not ERP component, alterations in *Pcdh10*^{+/-} mice as compared to their WT littermates. Moreover, such gamma-band alterations co-existed with alterations to E/I balance in the *Pcdh10*^{+/-} mice. In addition, the typical coupling of GABA concentrations to gamma-band activity seen in WT mice was not exhibited by *Pcdh10*^{+/-} mice. As such, the current study supports the notion of E/I imbalance in ASD leading to gamma-band activity perturbations, though questions previous findings of decreased GABAergic concentrations in ASD.

Figure Legends:

Figure 4.1 *Pcdh10*^{+/-} mice demonstrate unaltered ERPs. (A) Males (blue) and females (pink) demonstrate stereotyped auditory event related potentials (ERPs), with a negative vertex at ~20 ms (AN20) and ~40 ms (AN40). (B) Females demonstrate significantly greater AN40 amplitude than their male counterparts. * $p < 0.05$

Figure 4.2 *Pcdh10*^{+/-} mice demonstrate select gamma-band activity alterations in response to a white noise click. (A) Genotype level total power time frequency plots for WT (left) and *Pcdh10*^{+/-} (right) mice. Black square is region interrogated in B. (B) *Pcdh10*^{+/-} mice demonstrate significantly reduced late low gamma-band activity in response to white-noise clicks. * $p < 0.05$

Figure 4.3 Male *Pcdh10*^{+/-} demonstrate selective increases to high frequency resting-state power. (A) Group level power spectrum density (PSD) plots (male WT – solid black line, female WT – dashed black line, male HET – solid red line, female HET – dashed red line) demonstrate the stereotypical decay of power with increased frequency. Black dashed box is the *a-posterior* ROI. *A-priori* ROIs demonstrated either significantly increased (C, E) or trending towards significantly increased (B, D) resting-state power in female versus male mice. (F) The *a-posteriori* ROI demonstrate significantly higher resting power in female as compared to male mice. In addition the within male comparison demonstrated male *Pcdh10*^{+/-} exhibiting significantly more resting-state power than male WT in this ROI. # $p < 0.10$, * $p < 0.05$, ‡ $p(WT\ male\ versus\ Pcdh10^{+/-}\ male) < 0.05$

Figure 4.4 Male *Pcdh10*^{+/-} exhibit reduced signal to noise in the high-gamma band. WT male mice demonstrate significantly greater SNR than *Pcdh10*^{+/-} in the high-gamma band frequency range. Note, due to high frequency resting-state PSD measures being negative (a product of Log-based normalization; see Figure 3), a linear shift (arbitrarily chosen to be +5) was incorporated for these values to negate potential issue when calculating SNR (SNR = ITC / (Resting PSD + 5)). ‡ $p(\text{WT male versus } Pcdh10^{+/-} \text{ male}) < 0.05$

Figure 4.5 Male *Pcdh10*^{+/-} exhibit subtle deficits in theta-high gamma CFC. (A) Average comodulograms for WT (top) and *Pcdh10*^{+/-} (bottom), additionally split by males (left) and females (right). (B) Following *a-priori* hypotheses the theta-high gamma CFC was examined for *Pcdh10*^{+/-} dependent alterations. A trend towards male *Pcdh10*^{+/-} exhibiting significantly less coupling between theta and high gamma-band activity than male WT mice was observed. † $p(\text{WT male versus } Pcdh10^{+/-} \text{ male}) < 0.10$

Figure 4.6 Male *Pcdh10*^{+/-} demonstrate decreased gamma-band, but not lower frequency, ASSRs. (A) Average ASSR split both by male (left) and female (right), as well as WT (top) and *Pcdh10*^{+/-} (bottom). Gamma-band (C, D, E, F) but not 20 Hz, (B) total power ASSRs demonstrate significantly reduced power for male *Pcdh10*^{+/-} versus male WT mice. (G) 40 Hz ITC ASSR demonstrated significantly reduced coherence in male *Pcdh10*^{+/-} versus male WT mice. * $p < 0.05$, † $p(\text{WT male versus } Pcdh10^{+/-} \text{ male}) < 0.10$, ‡ $p(\text{WT male versus } Pcdh10^{+/-} \text{ male}) < 0.05$

Figure 4.7 *Pcdh10*^{+/-} mice exhibit selective increases to amino acids and altered coupling between GABA and gamma-band activity. *Pcdh10*^{+/-} mice demonstrate significantly increased aspartate (A), GABA (C) and Glutamine (D) compare to WT littermates. No significant genotypic alterations to glutamate were observed (B). ACxR = right hemisphere auditory cortex; ACxL = left hemisphere auditory cortex; HIP = right hemisphere hippocampus; CERE = cerebellum. (E) Early ITC in response to white noise clicks significantly correlated to right hemisphere auditory cortex GABA concentrations in WT (white diamonds; black line = WT linear regression) but not *Pcdh10*^{+/-} mice (grey squares; grey line = *Pcdh10*^{+/-} linear regression). (F) 40 Hz ASSR ITC near significantly correlates to right hemisphere auditory cortex GABA concentrations in WT but not *Pcdh10*^{+/-} mice. (G) The 40 Hz total power ASSR correlates to hippocampal GABA concentrations in WT but not *Pcdh10*^{+/-} mice. # $p < 0.1$, $p < 0.05$

Figures:

Figure 4. 1

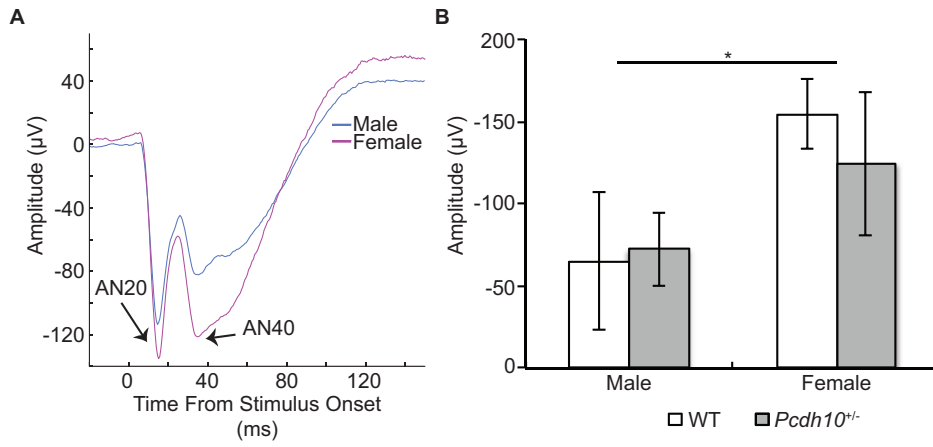


Figure 4. 2

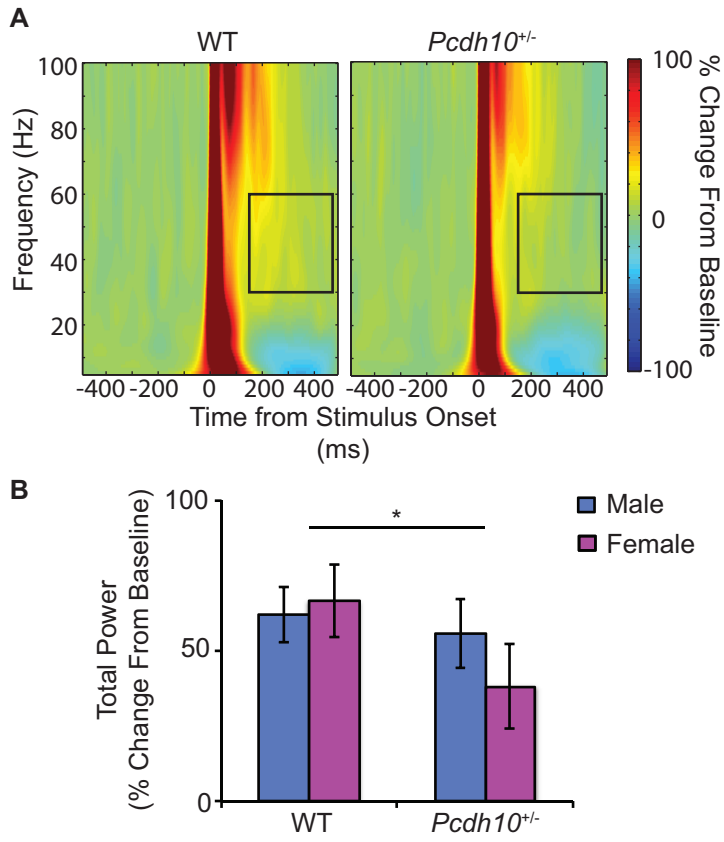


Figure 4.3

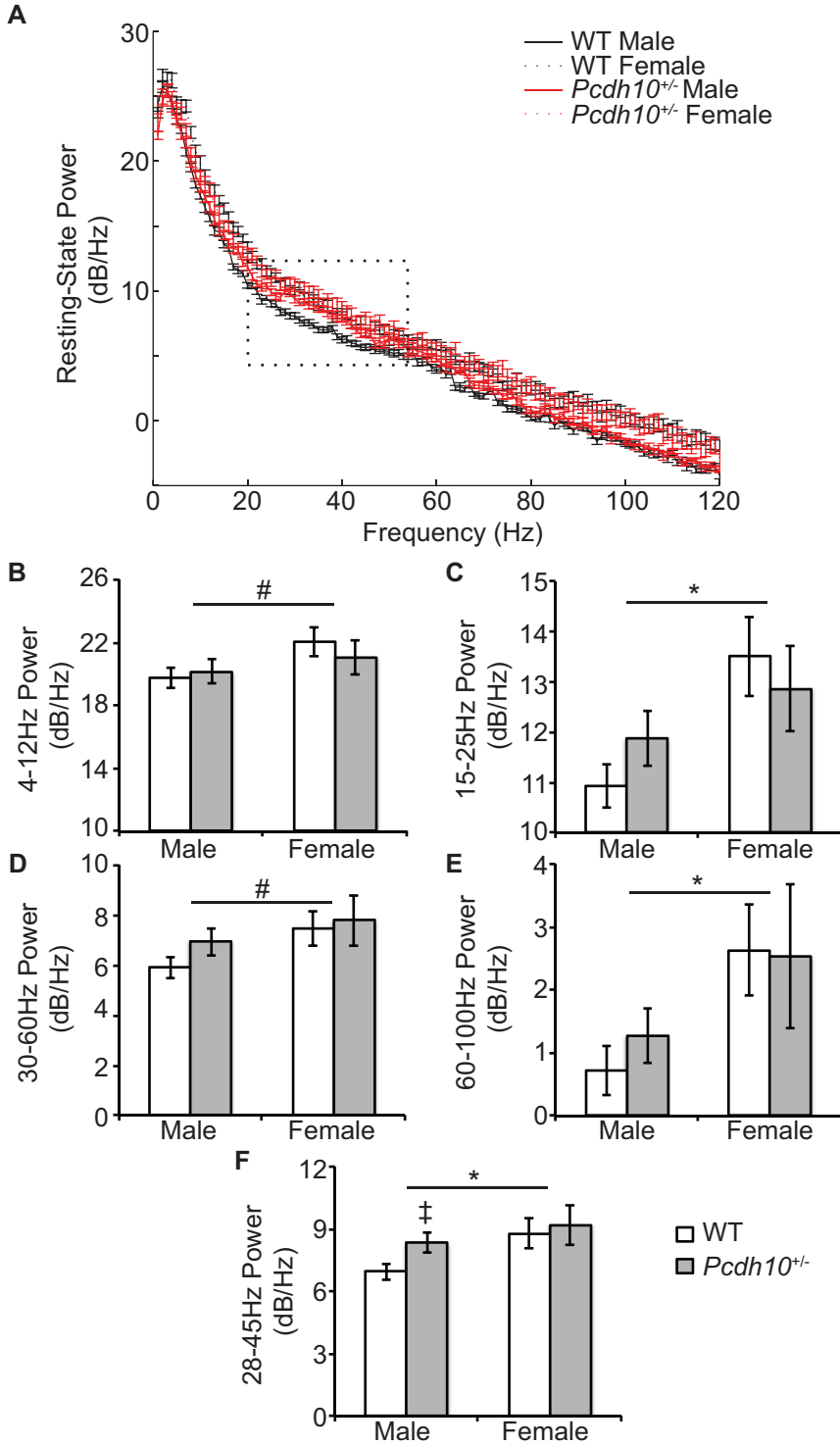


Figure 4. 4

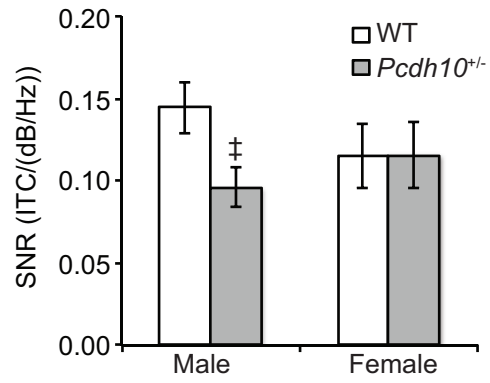
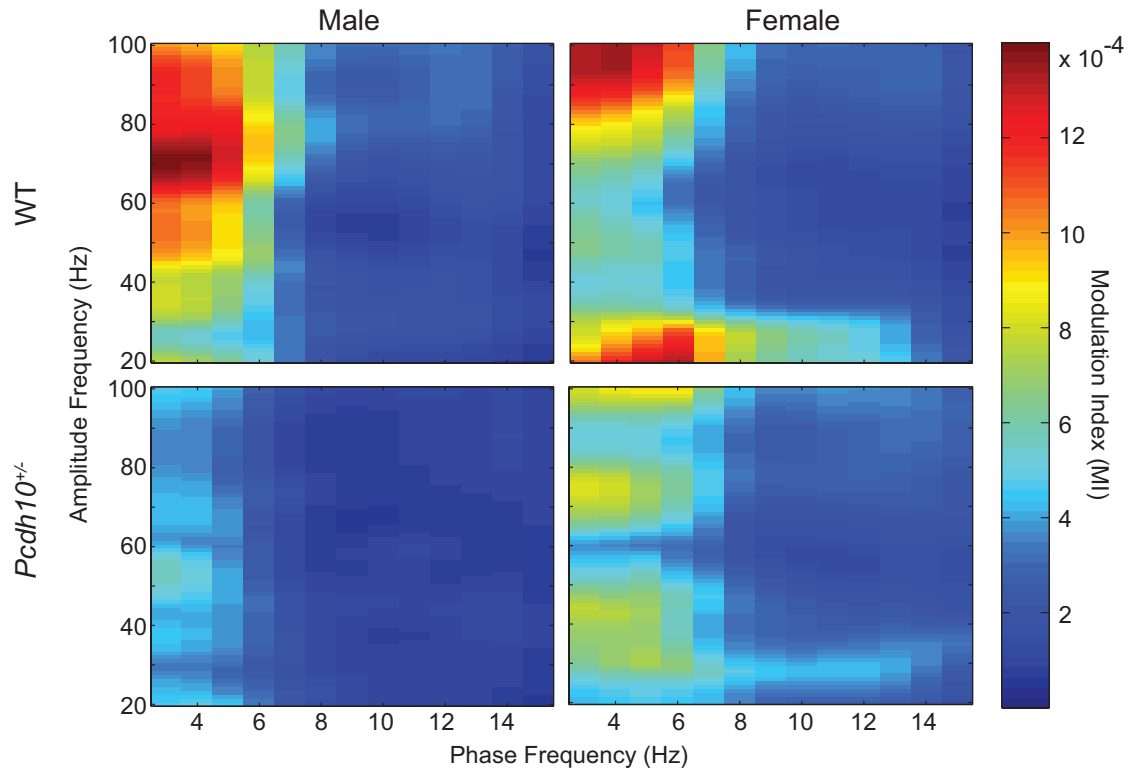


Figure 4.5

A



B

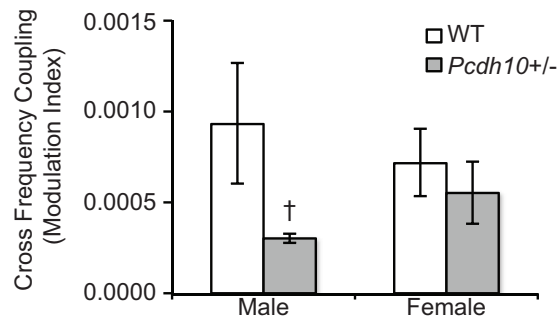


Figure 4. 6

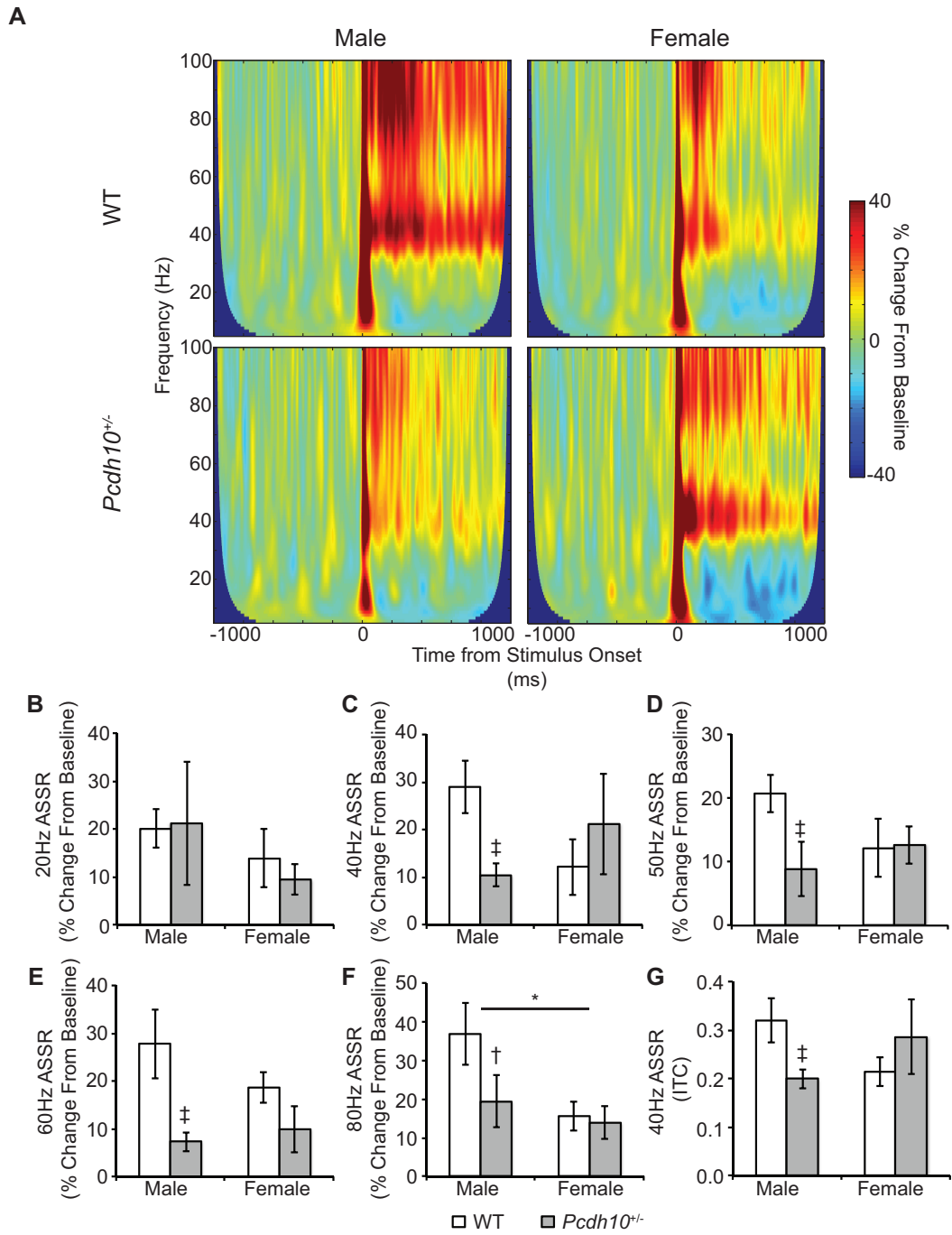
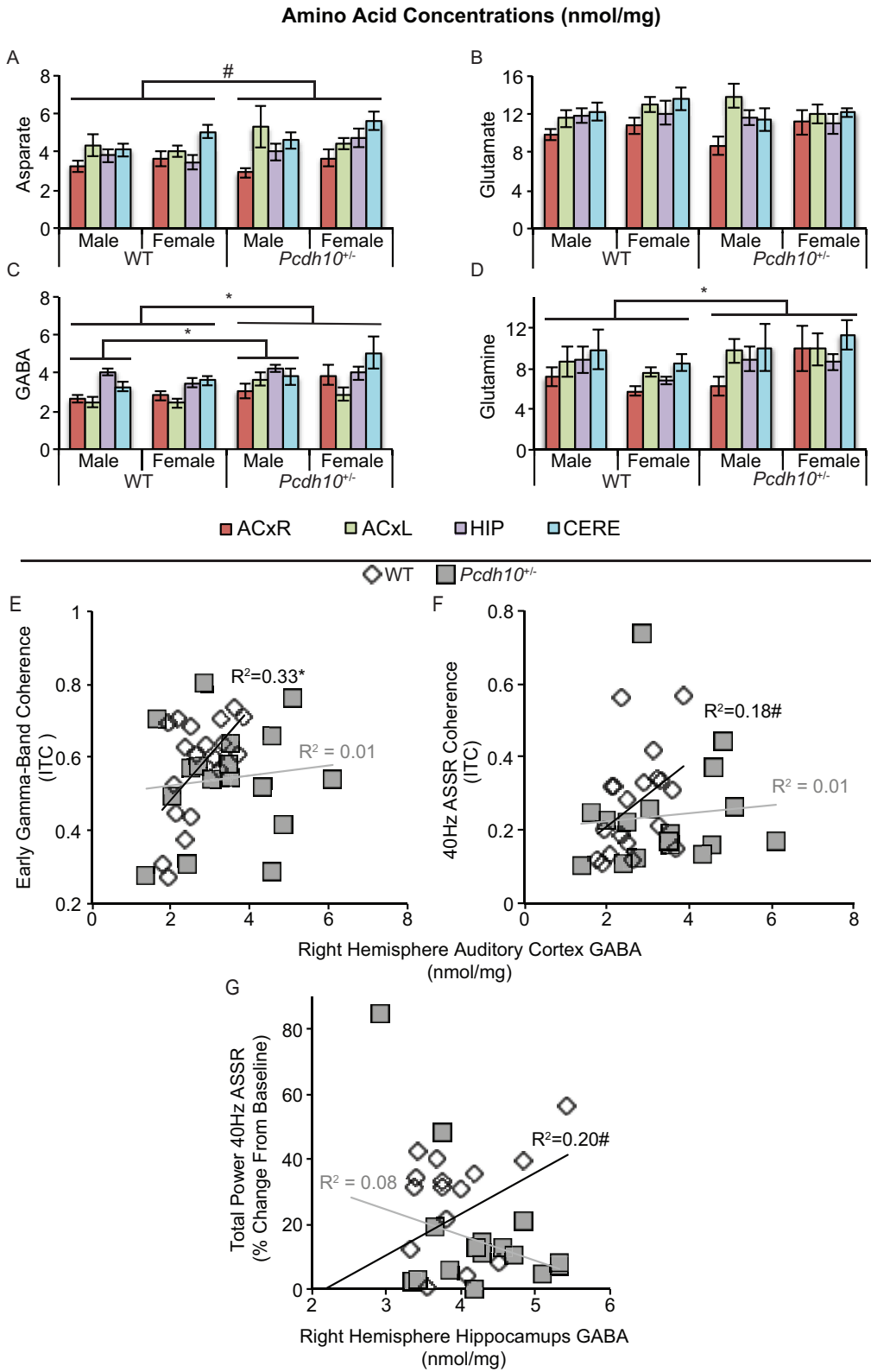


Figure 4. 7



CHAPTER 5

Alterations to neurophysiological functioning in *OPRM1* A112G SNP mice mirrors behavioral phenotypes

Russell G. Port (B.S.)^a, Stephen D. Mague (Ph.D.)^b, Michael E. McMullen (BA)^a, Mary
F. McMullen (BA)^a, Michael J. Gandal (MD/Ph.D.)^d, Jill R. Turner (Ph.D.)^c, Julie A.
Blendy (Ph.D.)^{b,e} Greg C. Carlson (Ph.D.)^a, and Steven J. Siegel (MD/Ph.D.)^a

Department of Psychiatry^a, Pharmacology^b University of Pennsylvania Perelman School
of Medicine, Philadelphia, PA 19104.

^cDepartment of Drug Discovery and Biomedical Sciences, South Carolina College of
Pharmacy, University of South Carolina, Columbia, SC 29036, USA

^dSemel Institute for Neuroscience and Human Behavior, University of California at Los
Angeles, Los Angeles, CA, USA

^eAbramson Cancer Center, University of Pennsylvania School of Medicine, Philadelphia,
PA 19104

Presented here as submitted to Genes, Brain and Behavior (under review)

Abstract:

The human μ -opioid receptor (MOR) gene single nucleotide polymorphism (SNP) *OPRM1* A118G has multiple associations with pain sensitivity, addiction, and social behavior in primates (including humans). The murine analogue (*Oprm1* A112G) causes similar behavioral alterations, and these mice also demonstrate reduced MOR sensitivity at both the cellular and local circuit levels. To link these findings, in-vivo depth EEG was utilized. EEG provides a measure of neuronal function that has been correlated with multiple forms of behavior (including sociability). At baseline G/G mice demonstrated increased stimulus evoked high gamma-band activity. Previous studies have observed that mice with this SNP also demonstrate increased sociability. As such, a juxtaposition exists between the pairings of increased post-stimulus gamma-band activity with increase sociability, as opposed to the decreases in post-stimulus evoked gamma-band activity and sociability seen in several neuropsychiatric disorders. To further probe the effect of G/G substitution a morphine challenge was implemented. G/G mice demonstrated reduced sensitivity to morphine-related suppression of sensory processing (P1-N1 event related potential amplitude) and induced gamma-band responses. These observations mirror recent morphine-related behavioral findings in mice with identical SNPs. Furthermore, sex by genotype interactions were consistently observed in responses, which again parallel previous behavioral findings. Therefore these results may help understand the role of the A118G SNP (and MORs in general) in the link between neurophysiological activity and behavior.

1. Introduction:

The μ -opioid receptor (MOR) single nucleotide polymorphism (SNP) A118G has been repeatedly shown to modulate the analgesic responses to opioids (Chou et al. 2006; Sia et al. 2008) and influence the vulnerability for developing opioid addiction (van den Wildenberg et al. 2007; Ray & Hutchison 2004; Drakenberg et al. 2006). Furthermore, the A118G SNP augments the efficacy of opioid-based alcohol (Anton et al. 2008; Ray & Hutchison 2007) and nicotine addiction (Lerman et al. 2004) therapies. This SNP is also associated with the pleasure gained from social interactions (Troisi et al. 2012), suggesting its role in mediating endogenous opiate responses.

The A118G MOR SNP may have roles beyond mediating reward. A recent study demonstrated an increased risk of schizophrenia with the presence of the G allele (Šerý et al. 2010). This increased susceptibility may be due to the specific localization of MOR to parvalbumin positive (PV+) interneurons. These PV+ interneurons are thought to be critical for proper oscillatory activity (particularly gamma-band activity). Both the parvalbumin positive (PV+) interneurons and gamma-band activity are thought to be disrupted in schizophrenia (Drake & Milner 1999; Drake & Milner 2002). Moreover, gamma-band activity is hypothesized to be involved with basic cortical processing as well as higher cognitive functions (for review see (Ainsworth et al. 2012; Herrmann et al. 2010) respectively). Separately many neuropsychiatric disorders demonstrate altered gamma-band activity both at rest and during tasks (for review see (Herrmann & Demiralp 2005)). Hence, a slight disruption to healthy local circuit function may ultimately predispose individuals for psychiatric disorders. Furthermore, the study of a such

polymorphism may provide neurophysiological insight to a recent hypothesis that multiple separate, yet converging, cellular/circuit alterations can lead to a common a neurophysiological outcome (such as those observed in neuropsychiatric disorders) (Port et al. 2014).

Imbalances of excitatory/inhibitory drive (E/I imbalance) have been postulated for multiple neuropsychiatric disorders (Rubenstein & Merzenich 2003; Gonzalez-Burgos & Lewis 2008). While many rodent models have been used to study E/I imbalance in neurodevelopmental psychiatric disorders, mice with an analogous substitution (MOR A112G SNP) have not. These mice display a decrease in morphine-related behaviors, and decreased MOR expression in several regions (Mague et al. 2009). This study also observed sex-specific deficits within G/G homozygous mice for morphine reward. Only the G/G female mice failed to find morphine rewarding (Mague et al. 2009). Recent work also suggests reduced receptor functionality (Mague et al. 2015) in regions where MOR expression is constant between genotypes (i.e. hippocampus) (Mague et al. 2009; Wang et al. 2012; Wang et al. 2014). This reduced receptor functionality may be due to altered GTP γ S binding to the MOR and subsequent intracellular signaling cascades (Wang et al. 2014). Further linking this murine model to its human analogue, a recent study observed that mice with this substitution are more social and resilient to social stress (Briand et al. 2015).

As such, precise alterations to circuitry may lead to significant behavioral alterations in both human and rodent. To model such a phenomena, we examined the effect of the A112G MOR SNP on auditory event related potentials (ERP) and spectral

neural activity. Moreover, we evaluated if the previously observed interactions between sex and genotype for morphine-related behaviors were recapitulated at the neurophysiological level. Intracranial depth EEG was utilized in these studies, as EEG can be used to assess the same type of neurophysiological activity in both experimental models and clinical disorders. The ultimate goal of the study was to determine if behavioral alterations previously described in these mice (such as alterations to sociability, and morphine related reward behavior) were reflected at the neurophysiological level.

2. Materials and Methods:

2.1 Animals

Adult mice (10-20 weeks of age; 20-35 g, male and female) homozygous for the A112 (wild-type) or G112 (knock-in) allele were used for these experiments. To generate these mice, site-directed mutagenesis of the C57BL/6 mouse *Oprm1* was performed in bacterial artificial chromosomes to create the aspartic acid substitution of asparagine at amino acid position 38 via replacing the adenine at nucleotide position 112 with a guanine. This eliminated the equivalent N-linked glycosylation site of the A118G SNP found in humans (Mague et al. 2009; Huang et al. 2012) Mice were bred using A112G heterozygous to A112G heterozygous pairings, and tested for homozygosity via gel electrophoresis of DNA PCR products (see (Mague et al. 2009) for further details). Mice were group-housed with food and water available *ad libitum* and maintained on a 12-h light/dark cycle in accordance with the University of Pennsylvania Animal Care and Use Committee. Mice were generated using C57Bl/6 ES cells (Chemicon) and the colony was maintained in this background. The final count for each genotype by sex grouping was 11 AA females, 10 AA males, 11 GG females, and 8 GG male. All possible effort was taken to minimize pain and discomfort in experimental subjects throughout the entire study. Furthermore, all protocols were approved by the University of Pennsylvania Institutional Animal Care and Use Committees and were conducted in accordance with National Institutes of Health guidelines.

2.2 Surgery for electroencephalogram (EEG) recordings

Adult A112G mice (4-5 months of age, male/female) had intracranial electrodes implanted (AP -1.82 mm, ML 1.10 mm, DV -1.9 mm) via stereotaxic surgery. All electrodes were tri-polar stainless steel electrodes (200 μ m diameter, Plastics One, Roanoke VA). These tri-polar electrodes were low impedance electrodes, for which similar configurations demonstrate ability to detect auditory brain stem responses, as well as later subcortical and cortical responses (P1, N40, P2, P3A) (Siegel et al. 2003; Connolly et al. 2003). Previous studies have demonstrated that ERP responses from such recordings display a pattern similar to human Cz electrode recordings (Siegel et al. 2003). Mice were anaesthetized with isoflurane. Once fully sedated and their scalps cleaned with betadine, the skull was exposed (bregma to lambdoid sutures) and electrodes secured in the aforementioned coordinates.

2.3 Recording of EEG activity

The low-impedance tri-polar electrode configuration utilized in this study provides EEG responses very similar to the human clinical responses (see above). In addition they have also demonstrated face and predictive validity for genetic, developmental and pharmacologic manipulations in mice (Gandal et al. 2010; Saunders, Gandal, Roberts, et al. 2012; Gandal, Anderson, et al. 2012). All mice had a minimum of two weeks recovery following surgery. Recordings were made following IP injections of saline and 1, 2, 7 and 20 mg/kg morphine. Following the 20 mg/kg morphine injection and recording session, an IP injection of the specific MOR antagonist naloxone (1 mg/kg)

was administered. The purpose of this additional control was to assess if morphine's actions specifically at the MOR was responsible for changes in EEG responses. EEG recordings were collected in home cages (between 10AM and 4PM; light phase), which were placed within a Faraday cage. Special cage tops were used to accommodate stimulus speakers and electrode cables. Electrode cables were connected to a high-impedance differential AC amplifier (A-M Systems, Carlsborg, Washington, USA). Mice were acclimatized to the testing apparatus for 30 min before testing to ensure habituation to the environment. Habituation and recordings took place in the presence of background white noise of 55 dB. Speakers atop each cage delivered stimuli generated by Micro1401 hardware and Spike 6 software (Cambridge Electronic Design). Stimuli consisted of 150 white-noise clicks (10ms duration, 85dB) with a 9 second inter-trial interval. Signals were continuously sampled at 1667 Hz and an online bandpass filter (1–500 Hz) was applied to all EEG signals.

2.4 EEG data analysis

The auditory clicks induced a typical multi-component ERP (Figure 5.1). Latency and amplitude changes in these components are associated with psychiatric disorders. As such, we measured these components across both dosages and genotype. EEG signals were analyzed similar to previously published studies (Gandal et al. 2010), using the EEGLab toolbox in MatLab (Delorme & Makeig 2004). In brief, single trials epochs (± 1000 ms relative to auditory stimuli) were extracted from continuous data. Artifact-containing epochs (e.g. movement) were then rejected via an activity threshold of >2 SD

of the mean. This left between 131 and 140 trials remaining on average per mouse for all conditions. This is well above the generally accepted number of required trials to gain stable responses. Trials were then baseline corrected to the -400 to -100ms period and subsequently averaged together. The amplitudes and latencies for both the P1 and N1 responses were determined from the resultant waveforms (defined by the most positive/negative deflection in the corresponding time window P1: 12.6-27.6ms; N1: 28.2-49.2ms; previously used in (Saunders et al. 2013)). These components have similar morphology (though at 40% of the latency) of analogous human evoked components (Siegel et al. 2003). Components (P1 and N1) were verified by visual examination by RGP. P1 latency was investigated using a mixed model ANOVA (drug (repeated measure) X genotype X sex) (IBM SPSS Statistics, Version 22, IBM Corp, Armonk, NY). The amplitude of the N1 peak (negative) was subtracted from the amplitude of the P1 peak to account for inter-subject variability. An identical mix model ANOVA was used for this relative amplitude change (IBM SPSS Statistics, Version 22, IBM Corp, Armonk, NY).

To further investigate the data, all auditory-evoked response waveforms were spectrally decomposed (Morlet Wavelets; 100 linearly spaced frequency bins between 3.0 and 100 Hz; wavelet cycles increasing from 3 (at low frequencies) to 6 (at high frequencies)). There are several forms of spectral activity available for investigation. Each of these have differing sensitivity to the characteristics of the underlying oscillatory signal. Both evoked power and ITC measure the ability of the brain to align activity over trials in response to stimuli and as such it can be seen as a measure of reliability (Port et

al. 2014). On the other hand, induced power (or non-phase locked power) is activity that occurs after the stimulus but is not aligned (with respects to phase) across trials. Total power is the combination of both evoked and induced power.

Total power (in decibels (dB); baseline period -200 to 0 ms) and inter-trial coherence (ITC) were calculated \pm 500ms around the stimuli as previous studies have found alterations to this region (Gandal et al. 2010; Liao et al. 2012; Saunders, Gandal & Siegel 2012). To choose regions of interest (ROI) within the spectral responses, EEGLAB's in-built permutation test (random trials, 200 repetitions) was applied in a drug (saline, 20mg/kg morphine and 20mg/kg morphine + 1mg/kg naloxone) and genotype/sex (i.e. A/A males, A/A females, G/G males, G/G females) comparison. Such a test allows for an unbiased, data-driven, selection of the ROIs from time frequency plots. In addition, this approach incorporates controls for multiple comparisons. In short, the time-frequency plots were pooled, and then randomly sorted into groups the same size as the original groups. One-way/repeated measures ANOVAs were then calculated between these randomly chosen groups at each time-frequency bin. The resultant maximum F-statistic retained. Repeating this procedure generated a distribution of F-statistics. Then the F-statistics from the experimental grouping were compared to this distribution. To reduce multiple comparisons, only data from -0.1 to 0.2 seconds were included. In addition, all statistical maps resulting from permutation testing were corrected using Holm's multiple comparison correction to ensure that the ROIs identified were not due to multiple comparisons Eight ROIs were chosen from this output based on either the intersection of the statistical maps or the effect of morphine across

genotype/sex. Each region of interest had a binary mask created, and only those time-frequency bins within the mask were averaged to produce metrics of power. Drug condition spectral responses were normalized to the saline trial for each animal (e.g. $(20\text{mg/kg drug trial} - \text{saline trial}) / \text{saline trial}$) when looking at the effect of morphine/naloxone to negate baseline differences. Group differences in power/coherence (either normalized or raw) were statistically assessed by a two-way ANOVA (genotype X sex) at specific drug doses or mixed model ANOVA (genotype X sex X dose (repeated measure)). Select pairwise comparisons for sex, drug condition, genotype, and their interactions were conducted using Sidak corrections for multiple comparisons (IBM SPSS Statistics, Version 22, IBM Corp, Armonk, NY).

3. Results:

3.1 Evoked potentials demonstrate sex and genotype differences

We first measured auditory ERP latencies and amplitudes in responses to escalating dosages of morphine (0 – 20 mg/kg), followed by acute naloxone (1 mg/kg). In a mixed model ANOVA (drug condition (repeated measure) X sex X genotype), a main effect of drug demonstrated that morphine prolonged P1 latencies (Figure 5.1; $F_{(3,525, 126,915)} = 27.742$, Greenhouse-Geisser adjusted, $p < 0.001$). We hypothesized that morphine's activation of opioid receptors led to this increased P1 response latency. If so, these latency prolongations would be recovered by co-administration of naloxone. A-priori pairwise comparisons supported this hypothesis with naloxone reversing the morphine induced P1 latency prolongation (saline to 20mg/kg morphine - $p < 0.001$, saline to naloxone - $p > .1$). We examined the role of the MOR polymorphism within this prominent impact of morphine. A significant genotype X drug condition interactions was present (mixed model ANOVA, $F_{(3,525, 126,915)} = 3.452$, Greenhouse-Geisser adjusted, $p < 0.05$), with differences between A/A and G/G suggested at saline and 1 mg/kg morphine (post-hoc pairwise comparisons: G/G prolonged latency saline $p < 0.1$, one mg/kg Morphine $p < 0.1$). In addition, there was a significant drug condition X genotype X sex interaction (mixed model ANOVA, $F_{(3,525, 126,915)} = 3.712$, Greenhouse-Geisser adjusted, $p < 0.01$).

Morphine also significantly decreased the amplitude of the P1-N1 ERP composite responses, which again was partially recovered by naloxone (Figure 5.1; mixed model ANOVA, main effect of drug $F_{(3,836, 138,107)} = 68.711$, $p < 0.001$, saline to 20 mg/kg

morphine $p < 0.001$, 20mg/kg morphine to naloxone $p < 0.001$). We additionally hypothesized that if the A112G *Oprm1* substitution was reducing the sensitivity of the MOR receptor, then activating MOR receptors may allow for genotypic differences to be seen. Indeed, G/G homozygous mice demonstrating reduced sensitivity to morphine during the 20 mg/kg condition (pairwise comparison: Figure 5.1, $p < 0.05$). Previous studies have observed sex specific responses to morphine. As such, a-priori pairwise comparisons also demonstrated that at 20 mg/kg, males were significantly less sensitive than females to morphine (pairwise comparison: Figure 5.1, $p < 0.05$). Moreover, previous studies of genetically identical mice demonstrate a genotype X sex interaction (females demonstrating greater genotypic differences than male mice). Our results reflected this, with G/G female mice less sensitive to morphine than A/A females (pairwise comparison: Figure 5.1, $p < 0.05$). Thus, this sex X genotype interaction for morphine's effect on ERP amplitude and latency appears to parallel previously reported behavioral and in vitro findings for the A118G *OPRM1* SNP and its murine counterpart.

3.2 Genotype and Sex differences in spectral activity

Recent clinical and translational work in psychiatric disorders has focused on changes in the evoked and baseline spectral responses, particularly with in the gamma-band (for review see Port et al. 2015; Port et al. 2014). Similar to the ERP's, we found a dose dependent decrease of power/coherence by morphine (largest reductions at 20 mg/kg) (Supplemental Figure 5.1). We compared the saline, 20 mg/kg morphine and 20 mg/kg morphine + 1 mg/kg naloxone conditions using permutation testing to assess

genotype/sex alterations in spectral activity. Such permutation testing of time–frequency plots provides an unbiased selection of ROIs. Saline condition responses were utilized to test for genotype and sex differences at baseline. The intersections across each of the genotype X sex (e.g. G/G Male) statistical maps were taken to determine ROIs for morphine-induced alterations to spectral activity. Four ROIs were identified for comparison (Figure 5.2), which correspond to pre-stimulus low frequency, pre-stimulus high frequency, post-stimulus gamma frequency, and post-stimulus high gamma frequency (Figure 5.2).

Permutation testing of the individual subject ITC figures (in an identical manner to total power), demonstrated 4 ROIs (Figure 5.2). Again, these regions were chosen due their intersection of multiple statistical maps. The ROIs represented post stimulus low frequencies, post stimulus high gamma, post stimulus beta, and post stimulus gamma/beta power. In addition the ITC response within the total power post stimulus gamma ROI was calculated to test if phase-locked signals account for the alterations seen in total power.

3.3 Genotype differences at baseline (Saline condition)

Permutation testing of individual time frequency plots revealed significantly altered high-gamma frequency post-stimulus activity when comparing between the separate genotype/sex combinations (A/A male X A/A female X G/G male X G/G female) during the saline condition ($p < 0.05$). G/G mice demonstrated significantly

increased mean total power values for this region (Figure 5.3; mixed model ANOVA, $F_{1, 36}=7.936, p < 0.01$). In addition a trend for a sex X genotype interaction was also present (Figure 5.3; mixed model ANOVA, $F_{1, 36}= 3.101, p=0.087$), with the greatest difference in total power was observed in A/A and G/G females (Figure 5.3; $F_{1, 36}= 11.724, p < .001$).

3.4 Morphine decreases relative responses in all time frequency ROIs, which is recovered by naloxone

Morphine suppressed the responses for all total power ROIs regardless of genotype or sex (Figure 5.3; Mixed ANOVA (genotype X sex X dose (repeated measure)); post-stimulus low gamma effect of drug $F_{2, 72}= 61.865, p < .001$: saline to 20mg/kg morphine $p < 0.001$, post stimulus high gamma effect of drug $F_{2, 72}= 78.807, p < .001$: saline to 20mg/kg morphine $p < 0.001$, pre stimulus high frequencies effect of drug $F_{1, 929, 69, 430}= 19.128, p < .001$: saline to 20mg/kg morphine $p < 0.001$, pre stimulus low effect of drug $F_{1, 948, 70, 118}= 19.128, p < .001$: saline to 20mg/kg morphine $p < 0.001$). This effect which was partially reversed by naloxone (Mixed ANOVA (genotype X sex X dose (repeated measure); 20mg/kg Morphine to naloxone - post stimulus gamma $p = 0.001$, post stimulus high gamma $p = 0.001$, pre stimulus high frequencies $p < 0.01$, pre stimulus low frequencies $p < 0.001$).

A similar pattern was seen for ITC, though in contrast naloxone failed to recover coherence in the post-stimulus low frequency ROI (Figure 5.4; Mixed ANOVA

(genotype X sex X dose (repeated measure); post-stimulus gamma-beta effect of drug $F_{2, 72} = 72.199$ $p < .001$: saline to 20mg/kg morphine $p < 0.001$: 20 mg/kg morphine to naloxone $p < 0.001$, post-stimulus high gamma effect of drug $F_{2, 72} = 61.404$ $p < .001$: saline to 20 mg/kg morphine $p < 0.001$: 20 mg/kg morphine to naloxone $p < 0.001$, post stimulus beta effect of drug $F_{2, 72} = 53.820$ $p < .001$: saline to 20 mg/kg morphine $p < 0.001$: 20 mg/kg morphine to naloxone $p < .891$), post stimulus low frequency effect of drug $F_{2, 72} = 15.120$ $p < .001$: saline to 20 mg/kg morphine $p < 0.001$: 20 mg/kg morphine to naloxone $p < .891$). While these naloxone effects point to morphine primarily working through MOR, these data also allow for minor non-MOR affects.

3.5 Morphine acts in a genotype dependent manner for low, but not high, frequency total power gamma-band responses

G/G mice demonstrated less sensitivity to morphine's ability to suppress lower frequency gamma-band responses as compared to A/A mice (Figure 5.3, mixed model ANOVA, $F_{(1,36)} = 4.933$, $p < .05$). The greatest difference existed again between A/A and G/G females (Figure 5.3, mixed model ANOVA, $F_{(1,36)} = 3.350$, $p = 0.076$). Naloxone abolished any genotypic differences induced by morphine. Interestingly, this genotypic effect may be due to alterations in induced (non-phase locked activity). Supporting this hypothesis was that neither the gamma/beta nor the beta ITC ROIs showed an effect of genotype or sex for morphine suppression of saline-normalized coherence ((20mg/kg coherence – saline trial coherence) / saline trial coherence). To further investigate the role of induced activity in the post-stimulus low gamma ROI, we applied the same post

stimulus low gamma ROI from the total power analyses to ITC data. Morphine-induced suppression of coherence in this ROI was non-genotype specific. This suggests that the induced component of total power had been altered. In comparison, the morphine-induced effect on power and coherence in post-stimulus high gamma frequencies was not significant for either genotype or sex.

Additional findings of interest are presented in Supplementary Table 5.1. These include a trend towards alterations to pre-stimulus power for both high and low frequencies either by sex (males demonstrating more power than females), and a sex by genotype interaction (G/G males demonstrating greater power than G/G females), ($p < 0.10$). In addition there is a trend towards a reduction of morphine-induced suppression of post-stimulus low frequency ITC ($F_{(1,40)} = 3.243, p < 0.10$).

4. Discussion:

4.1 Perturbations to ERPs and Gamma-band activity at baseline

MORs preferentially co-localize to PV+ interneurons in hippocampus (Drake & Milner 1999; Drake & Milner 2002). These MORs mediate fast inhibitory responses and so contribute to fast circuit activity (including high-frequency oscillations). As such, the A112G MOR SNP may be a potential model for observing the effects of a precise cellular alteration on the oscillatory activity of large regions of the brain. This is not to say that MORs are only located to PV+ interneurons, or are not present in other regions of the brain. Instead, this model may demonstrate how a slight molecular alteration that is present in multiple regions alters the large-scale brain function (i.e. the recorded gamma-band activity). Altered gamma-band function has been demonstrated in many neuropsychiatric disorders (e.g. schizophrenia (Sun et al. 2011), ASD (Rojas & Wilson 2014) and even opiate addiction (Wang et al. 2015)). Such alterations have also been seen in pre-clinical models that recapitulate key aspects of neuropsychiatric disorders (Amann et al. 2010; Port et al. 2014). The most common findings in these pre-clinical studies are altered basic sensory processing (ERP component latency/amplitude) and alterations to oscillatory activity. In this study we demonstrate both in the A112G MOR SNP mouse model.

At baseline, there were near significant delays for P1 latency in G/G homozygous mice. This suggests a subtle level of functional alteration in mice with A112G substitutions. Mice homozygous for G/G also demonstrate increased baseline post stimulus high gamma-band activity. A potential confound of such a finding could be

behavioral (e.g. locomotor) differences during the recording sessions. However, previous findings have demonstrated no locomotor differences during baseline/saline treatment in these mice, attenuating this potential confound (Mague et al. 2009). Alterations to gamma-band auditory responses have been repeatedly observed in clinical (Maharajh et al. 2007; Wilson et al. 2007; Kwon et al. 1999) and preclinical studies of neuropsychiatric disorders (Amann et al. 2010; Port et al. 2014). Interestingly, contrary to our current findings of increased post-stimulus gamma in G/G mice, Autism Spectrum Disorders (ASD) demonstrated decreased analogous (post stimulus) gamma-band responses (Gandal et al. 2010). Recent findings shed light on this disparity. Mice with this A112G SNP are actually more social (Briand et al. 2015), as opposed to individuals with ASD. Support for this hypothesis comes from previous animal studies where concurrent expression of decreased sociability and decreased post-stimulus gamma-band activity have been previously demonstrated in mice (Gandal, Anderson, et al. 2012). Moreover, the recovery of gamma-band signal to noise is concurrent to increased sociability mice (Gandal, Sisti, et al. 2012). As such, it appears while decreases in post-stimulus gamma-band responses are associated with decreased sociability (ASD), increases in post-stimulus gamma-band activity may relate to increases in sociability. Moreover, a recent study suggests no increased risk for ASD by being a carrier for a G allele at the A118G SNP. It remains difficult to determine if a protective effect exists for being a carrier for homozygous G alleles because only two subjects in this study were G/G (though both were non ASD) (Cieślińska et al. 2015).

4.2 Morphine-induced alterations to ERP and oscillatory markers: intermediate phenotypes allowing for understanding of the neurobiological basis of genotypic effects

Clinical studies have shown an effect of the MORP A1118G SNP on a range of behaviors and drug responses in humans (for review (Mague & Blendy 2010)). Similar findings have been observed in the mouse homolog MOR A112G SNP (Mague et al. 2009). Morphine challenge masked baseline genotypic differences seen in early sensory processing (P1 latency). Moreover, the G/G homozygous mice demonstrated decreased sensitivity to opioid activation (as seen in P1-N1 peak amplitude) (Figure 5.1). This finding is analogous to recent hippocampal slice findings where G/G homozygous mice demonstrated significantly less sensitivity in response to μ -opioid receptor activation (via DAMGO challenge) (Mague et al. 2015). The use of supplemental naloxone suggested that the effects of morphine on auditory event related potentials were induced by μ opioid activation. Naloxone by itself does not affect these early auditory evoked responses (Arnsten et al. 1984; Ehlers 1989). Furthermore, consistent with previous studies all experiments took place between 10 AM and 4 PM (Gandal et al. 2010; Saunders et al. 2013; Siegel et al. 2003; Billingslea et al. 2014; Gandal, Anderson, et al. 2012), indicating that time of day cannot account for observations in this study. Alternatively, it is possible that there could be an effect of multiple injections. However, the inverted U pattern of activity, suggests this was not the reason for increased amplitude over time as the administration of naloxone yielded an effect which was opposite to that of the previous 4 injections.

Morphine's effects on auditory responses were also tested with regards to sub-spectral regions derived from permutation testing. These windows each have different proposed roles in neuronal activity (e.g. gamma-band activity is involved for local circuit activity (Sohal et al. 2009)). Morphine challenge produced genotypic differences within these spectral sub-components, such as post stimulus low gamma frequency total power and a suggested genotype-dependent low frequency ITC response (see supplement Table 5.1). Interestingly, G/G were less sensitive than A/A to morphine-induced suppression of post stimulus low gamma total power (phase and non phase locked activity) but not ITC (phase locked). This indicates that it is not the phase-locked activity that is the mediator of genotypic differences, but rather non-phase locked activity (also known as induced activity). Moreover, the differences were mainly driven by alterations within females (G/G being less sensitive to morphine than A/A), mimicking previous behavioral data of A112G mice (Mague et al. 2009).

Both the morphine-induced decreased P1-N1 amplitude and the post stimulus gamma-band activity alterations are occurring in the same time frame. A decrease in P1-N1 would likely cause a reduction in activity at all frequencies during that time window. The current finding suggests that these reductions in activity are only significant for the gamma-band activity, mirroring what is found clinically. The repeated finding of altered spectral activity in this study may be explained by the location of μ opioid receptors within specific circuits. As stated above, μ opioid receptors are predominantly located on PV+ basket cells in hippocampus. Again, these PV+ cells are key in the production of gamma-band activity (Sohal et al. 2009; Cardin et al. 2009). Therefore, MOR A112G

substitution may have downstream effects on inhibition that could alter pyramidal cell firing synchrony in local circuits, leading to disruption of high frequency activity and altering hippocampal/cortical function (Faulkner et al. 1998).

Theta frequencies were also marginally affected by genotype in this study (a trend of genotype; $p = 0.08$), suggesting a role for mu opioid receptors in the circuits that generate these frequencies. This also is consistent with the known cellular mechanisms of generating theta rhythms. Theta-generating GABAergic cells are modulated by MOR, (Nagode et al. 2014) cholinergic inputs, and cannabinoids (Nagode et al. 2014). Thus, a genotype-dependent difference in theta response to MOR activation suggests additional complex interactions with other modulatory systems, including nicotinic systems where A118G polymorphism has been implicated in addictive behavior.

4.3 Sex differences and sex X genotype interactions are frequently observed in morphine responses

Multiple morphine-related sex-dependent alterations were also observed during this study, with such alterations attenuated by naloxone (Supplemental Table 5.1). Previously, sex dependent alterations have been observed in response to opioid administration (Craft 2008). In both humans and rodents, females are more likely to administer opioids and show greater response to rewarding properties of opioids (Cicero et al. 2003; Roe et al. 2002). In contrast, males demonstrate greater analgesic response when morphine was infused into the periaqueductal gray (Lloyd et al. 2008).

Within hippocampus, both the availability of MORs (Torres-Reveron et al. 2009) and levels of opioid peptides (Roman et al. 2006; Williams et al. 2011) are influenced by ovarian steroid hormones. Interestingly, the most common comparison to demonstrate/suggest significance was the A/A females to G/G females. G/G female mice demonstrated altered baseline activity and were less sensitive to morphine's effects than the A/A female mice. A comparable lack of response to morphine has been demonstrated behaviorally, with G/G mice demonstrating reduced rewarding effects and blunted negative effects of withdrawal (Mague et al. 2009). These data indicate the need to include female subjects in assessments of genetic factors.

4.4 The A112G Oprm1 substitution allows for both the study of morphine-related neurophysiological phenotypes and broader neuropsychiatric disorders related to GABAergic disruption

The results from this study indicate that there are specific alterations due to sex, A112G genotype and their interaction for both evoked potentials and spectral sub-components activity. Mice with the SNP demonstrate increased baseline high gamma power. In addition, these mice show reduced sensitivity to morphine suppression of early sensory processing and non-phase locked gamma-band activity. Moreover, it was common that significant or near significant differences were due to differences between A/A and G/G females. Interestingly, our in-vivo electrophysiological results mirror that of recent behavioral (both social and morphine-related) results from a cohort of mice with the identical SNP (Briand et al. 2015; Mague et al. 2009). This study has multiple

significant contributions. First, the direct impact of the A112 MOR substitution on behavior at baseline (where increased sociability has been demonstrated) is reflected in alterations to neurophysiological activity in accordance with a-priori hypotheses. Second, using the A112 MOR SNP as a model of specific and selective molecular alterations, the concept of such precise changes leading to gamma-band perturbations in broader *neuropsychiatric disorders* can be investigated. Lastly, a potential biological basis has been determined for the genetic, and sex by genotype, differences observed in behavioral studies of these mice previously. Thus this study highlights translational relevance by providing physiological insight into the behavioral changes seen across rodents, non-human primates and people, providing targets for electrophysiological studies in humans.

Table Legends:

Supplemental Table 5.1 Multiple sex or sex by genotype interactions were observed at significant or near significant levels during this study, often following the same pattern as previously observed with behavioral metrics.

Figure Legends:

Figure 5.1 *Auditory evoked-potentials exhibit genotype-based alterations at baseline as well as morphine-induced sex and genotype-based differences.* A) Grand Average (across genotype and sex) evoked potential and locations of P1 and N1. B) Peak-to-peak measurements between P1 and N1 (P1-N1) exhibit significant alterations in the presence of morphine, which was partially recovered by naloxone. Morphine challenge also produced genotypic and sex based alterations to evoked responses. C) Baseline (saline) P1 latencies suggest a genotypic difference, which are not present after morphine challenge. # = $p < 0.01$

Figure 5.2 *Permutation test-based dissection of sex and genotype time-frequency*

differences. Using permutation testing for both total power and ITC plots, maps of statistical difference regions were computed (for both drug effects within genotype/sex combinations and genotype/sex combination effects across drug conditions). Regions of interested (ROI) where selected via the intersection of statistical maps, or for effects of genotype/sex during the saline condition. A) Total power plots were tested for difference during saline (top row) or across drug conditions for each sex X genotype combination (columns). Total power ROIs were chosen for further study via either an effect during saline or the intersection of the drug effect statistical maps with regions representing post stimulus low gamma (red), post stimulus high gamma (light blue), pre-stimulus high frequencies (yellow), and pre-stimulus low frequencies (orange). B) A similar analysis occurred for ITC plots, again with ROIs chosen by the intersection of drug-related statistical maps (no differences during the saline condition were observed). Regions represented post stimulus gamma/beta (light orange), post stimulus high gamma (pink), post stimulus low frequencies (dark red), and post stimulus beta frequencies (white). For all regions, binary masks were created and were applied to individual subject's respective plots to derive responses.

Figure 5.3 Total power plots reveal sex and genotype and their interaction differences in the multiple ROIs. A) The ROIs chosen from statistical permutation testing of time frequency plots demonstrate effects of sex, genotype and their interaction during the saline condition (left) and 20 mg/kg morphine and naloxone condition (center and right; respectively shown as relative change from saline). The four regions span both pre-stimulus (top 2 rows), and post-stimulus windows (bottom 2 rows). Morphine causes significant relative reductions of power in all ROIs; with naloxone reversing these effects (Mixed ANOVA - (genotype X sex X dose (repeated measure))). Genotypic differences can be observed both during saline (post-stimulus high frequencies), and 20mg/kg morphine (post-stimulus low gamma). A sex X genotype interaction was seen during the saline period for post-stimulus high gamma, with significant differences between A/A and G/G females. Pre-stimulus high frequency power and pre-stimulus low frequency power (trending and significant respectively) exhibited sex dependent changes, with males demonstrating a greater power. Based on *a-priori* hypotheses, examining the sex X genotype interaction showed that G/G homozygous mice, but not A/A, demonstrated differences in pre-stimulus high (trending) and low (significant) power. B) Radar plots of spectral responses relative to saline condition demonstrate specific sex, genotype and sex by genotype interactions. Each genotype by sex (A/A male - bottom quadrant, A/A female - left quadrant, G/G male - top quadrant, G/G female - right quadrant) shows a differing profile of spectral activity in response to saline (blue), 20 mg/kg morphine (red) and supplemental naloxone (green). All data is shown as relative change from saline

(hence saline always equals 0). Again morphine is seen to decrease responses in all time frequency ROIs, which is recovered by naloxone. Interestingly, morphine-induced suppression of power was attenuated in G/G mice for low gamma-band response (left most), with the greatest difference between females. A similar trend was seen for low frequency pre-stimulus power (middle left). No such effects were seen for pre-stimulus high frequencies (middle right) or post-stimulus high gamma. * = $p < 0.05$, Mixed model ANOVA genotype X sex X dose (repeated measure), with Sidak correction for multiple comparisons.

Figure 5.4 *ITC plots reveal sex, genotype and their interaction differences in the multiple ROIs. Morphine significantly reduces relative coherence in all ROIs, with naloxone reversing these effects in all ROIs except low frequency (Mixed ANOVA - (genotype X sex X dose (repeated measure)). A) Unlike total power, ITC was not affected by sex at baseline A genotype by sex interaction occurred at the gamma/beta ROI (second row, left), demonstrating significant pairwise differences between females. This divergence between females was also seen in the beta (top row, left) ROI. B) Radar plots of coherence relative to saline condition. Each genotype by sex combination (A/A male - bottom quadrant, A/A female - left quadrant, G/G male - top quadrant, G/G female - right quadrant) shows a differing profile of coherence in response to saline (blue), 20 mg/kg morphine (red) and supplemental naloxone (green). All data is shown as relative change from saline (hence saline always equals 0). Again, morphine decreased responses in all time frequency ROIs. A/A mice demonstrated near significant increases of this morphine-induced suppression of post stimulus low frequencies coherence as compared to G/G mice. The beta (top left) and the gamma/beta (top middle) ITC ROIs showed no effect of genotype or sex for morphine suppression of coherence. Separately, the low gamma ROI for total power was applied to the plots (third row) to determine if genotypic alterations seen in total power were due to phase-locked signals. Contrary to total power, morphine's suppression of coherence in the total power low gamma ROI was non-genotype specific. Morphine's suppression is recovered by naloxone, except for the low frequency ROI (bottom right). Naloxone's ability to reverse morphine suppression of*

coherence in the beta ROI was genotype specific. In addition, a genotype by sex interaction for naloxone's effect was significant in the total power low gamma ROI (Fig. 5; $F_{(1,36)} = 5.051$, $p < 0.05$) with A/A males and G/G females demonstrating increased coherence. . * = $p < 0.05$, Mixed model ANOVA genotype X sex X dose (repeated measure), with Sidak correction for multiple comparisons.

Supplemental Figure 5.1 *Morphine causes a dose dependent decrease in auditory stimulus related potentials and power.* A. As quantified by the voltage difference between P1 and N1 components, grand averages of responses to single tones are decreased by 20mg morphine. This change is for the most part reversed by the MOR antagonist naloxone (Nal), (*) show significant reductions from saline, (+) points to significant increase of potentials in NAL from 20mg/kg morphine. When the individual evoked responses are wavelet transformed and averaged to generate the time-frequency plots (B) for each dosage of morphine. These plots show a wide-band increase in power (yellow to red) often followed by a strong suppression in the beta-band shown in blue. There is also a reduction in activity with increasing levels of morphine that is reversed by naloxone. Similarly, there is an increase in inter-trial coherence (ITC) (black to yellow).

Tables:

Supplemental Table 5. 1

Condition	Period	Frequency	Power/ITC	Effect	F	p
		Range				
Saline	Pre-stimulus	High Frequency	Total Power	Male>Female	F _(1,36) = 4.128	0.05
Saline	Pre-stimulus	Low Frequency	Total Power	Male>Female	F _(1,36) = 3.147	0.085
Saline	Pre-stimulus	Low Frequency	Total Power	G/G Male>G/G Females		0.07
Naloxone	Post-stimulus	Beta	ITC	GG show less recovery	F _(1,36) = 4.251	<0.05
Naloxone	Post-stimulus	Beta	ITC	A/A females > G/G females recovery	F _(1,36) = 4.892	<0.05
Naloxone	Post-stimulus	Total Power Low Gamma ROI	ITC	A/A males and G/G females have increased coherence	F _(1,36) = 5.051	<0.05
20 mg/kg	Pre-	Low	Total Power	Females >	F _(1,40) =	0.057

Morphine	stimulus	Frequencies		Male	3.874,	
				suppression		
20 mg/kg	Post-	Low	ITC	A/A > G/G	$F_{(1,40)}$	0.080
Morphine	stimulus	frequency		suppression	=3.243	

Figures:

Figure 5. 1

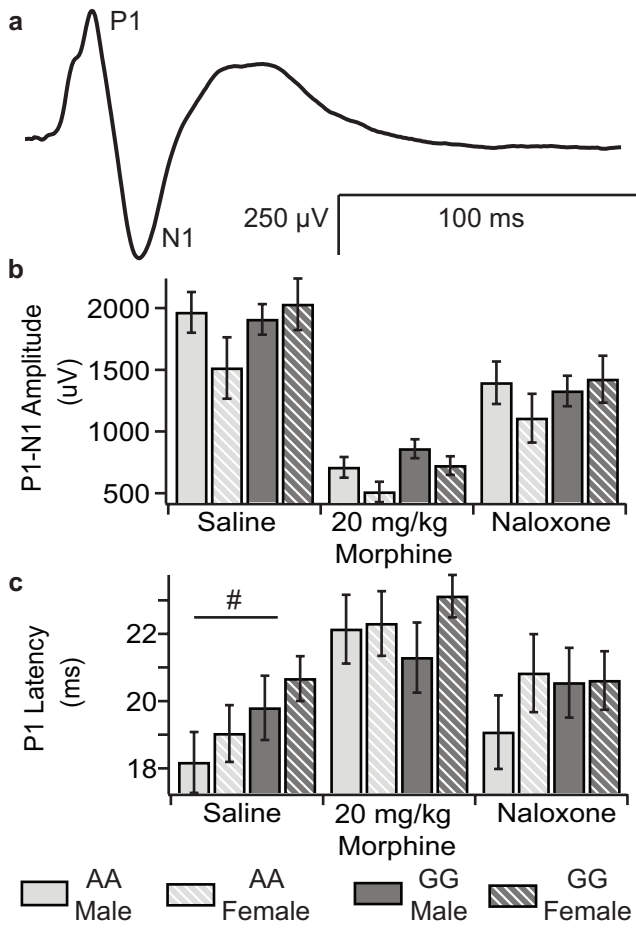


Figure 5. 2

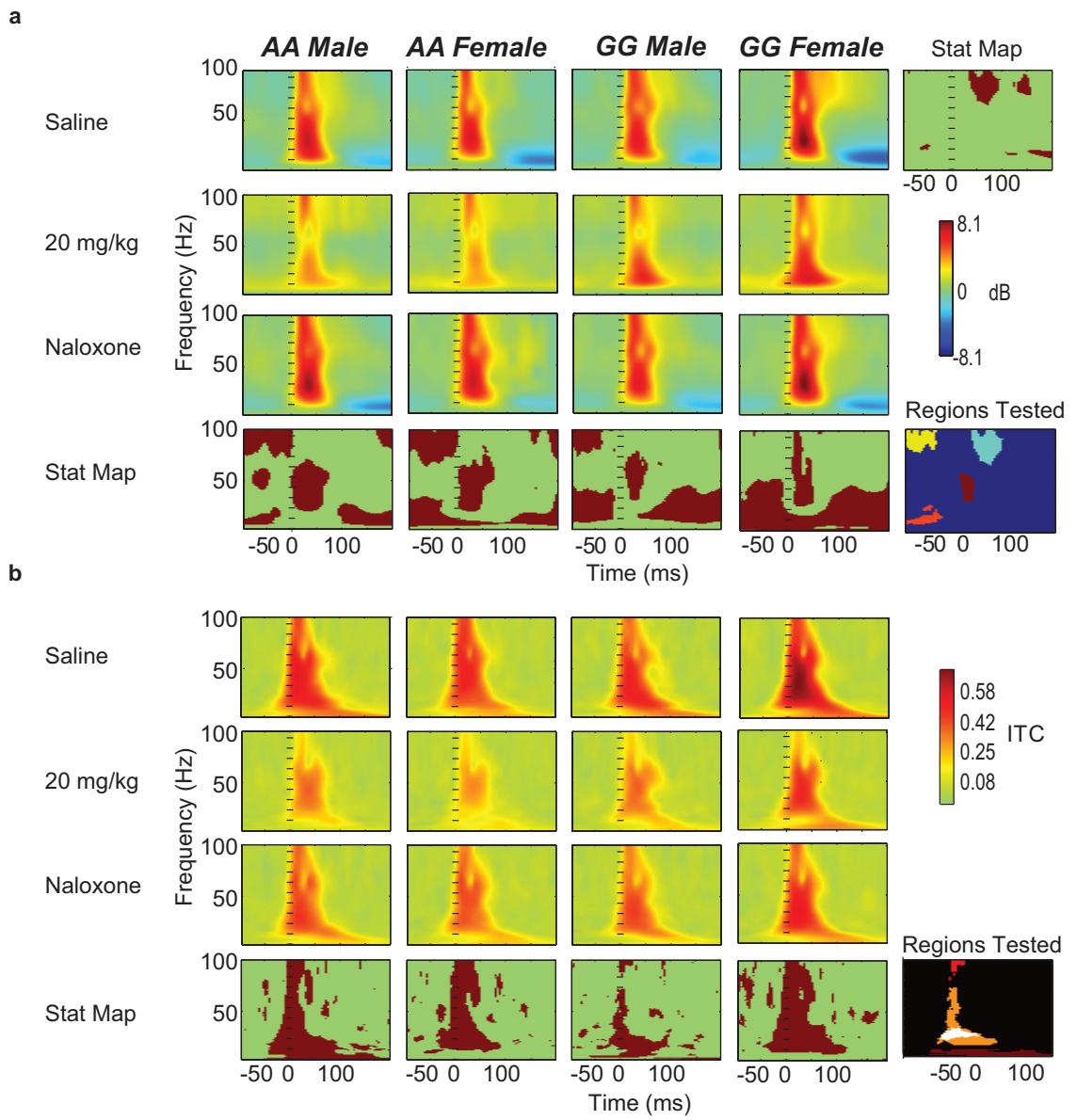


Figure 5.3

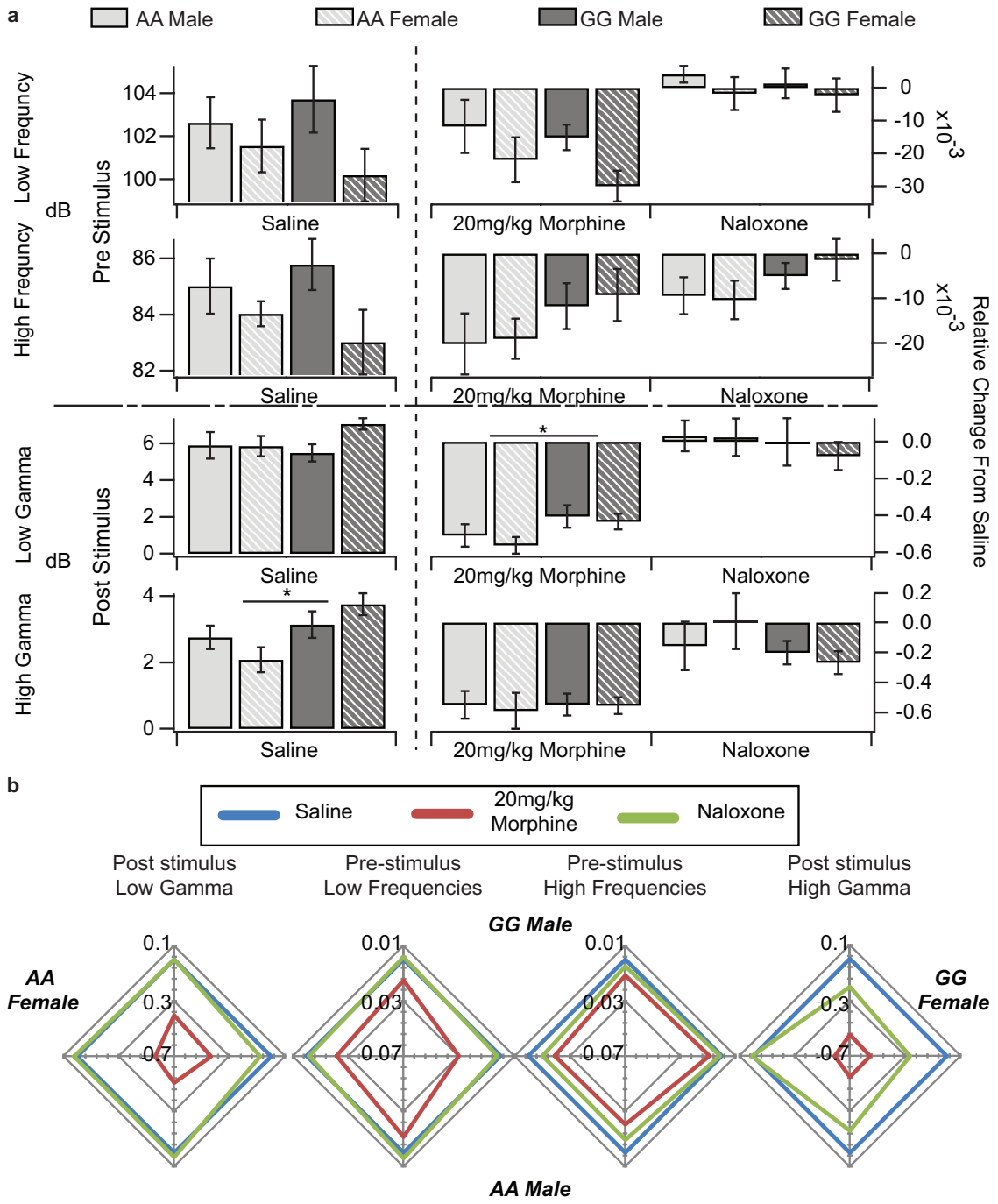
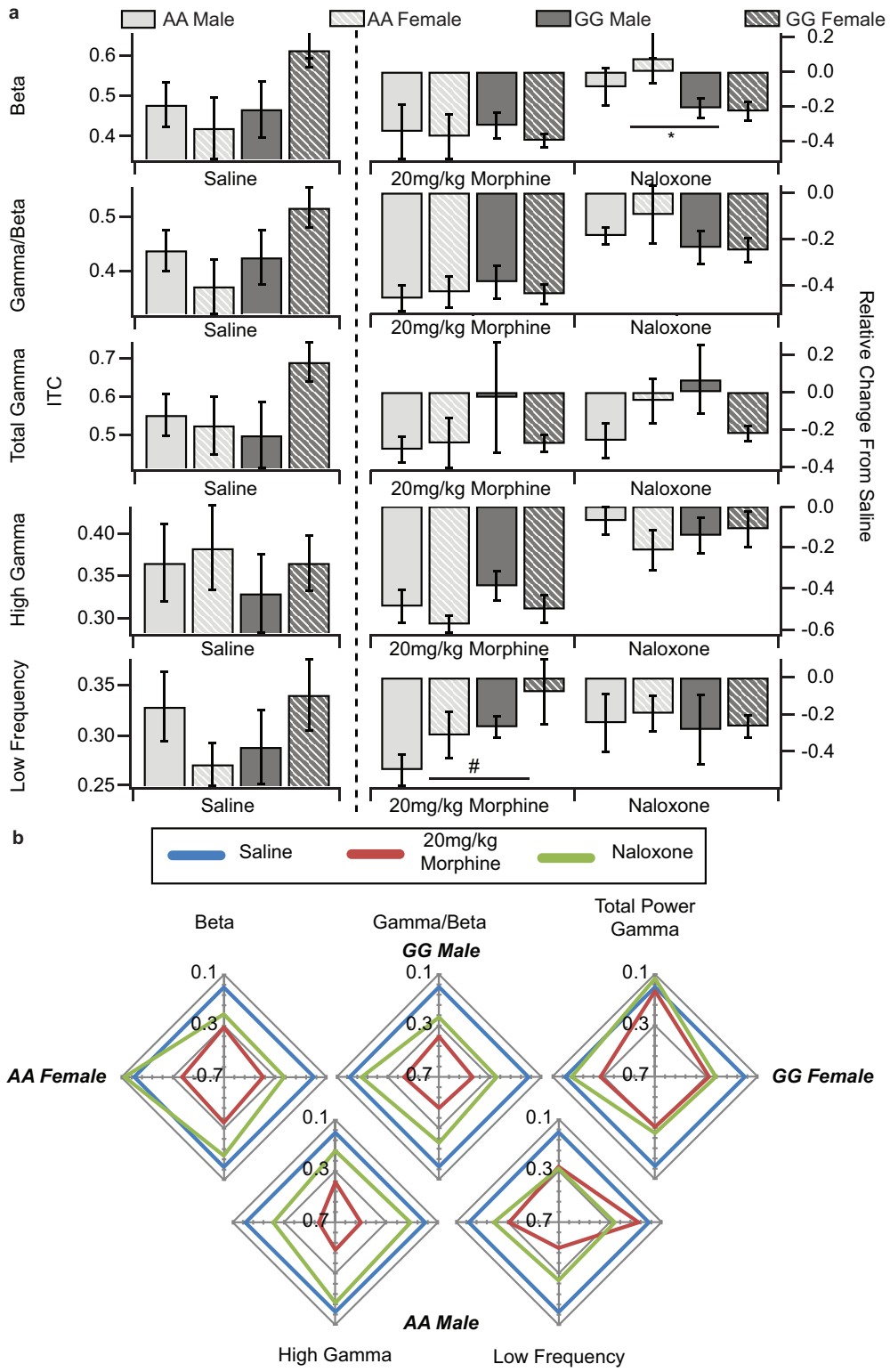
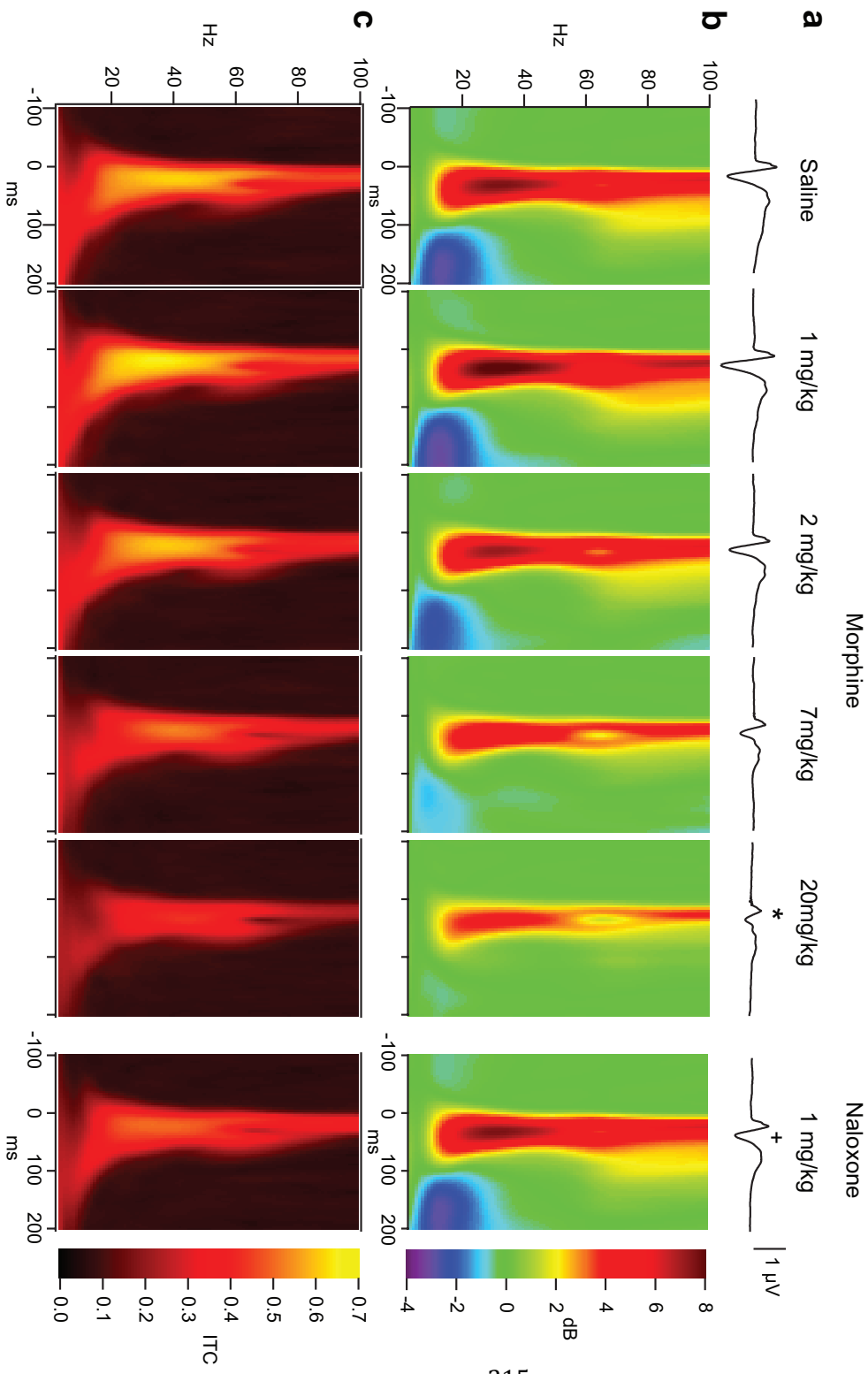


Figure 5. 4



Supplemental Figure 5. 1



Chapter 6

Mouse model of OPRM1 (A118G) polymorphism has Altered hippocampal function

Stephen D. Mague^{1b}, Russell G Port^{1c}, Michael E. McMullen^c,

Greg C. Carlson^c, Jill R. Turner^{a#}

¹ Authors contributed equally

^aDepartment of Drug Discovery and Biomedical Sciences, South Carolina College of Pharmacy, University of South Carolina, Columbia, SC 29036 and Department of Pharmacology^b and Psychiatry^c, University of Pennsylvania School of Medicine, Philadelphia, PA 19104

Originally published as: Mague SD, Port RG, McMullen ME, Carlson GC, Turner JR (2015): Mouse model of OPRM1 (A118G) polymorphism has altered hippocampal function. *Neuropharmacology*. 1: 1–10.

Abstract:

A single nucleotide polymorphism (SNP) in the human μ -opioid receptor gene (*OPRM1* A118G) has been widely studied for its association in a variety of drug addiction and pain sensitivity phenotypes; however, the extent of these adaptations and the mechanisms underlying these associations remain elusive. To clarify the functional mechanisms linking the *OPRM1* A118G SNP to altered phenotypes, we used a mouse model possessing the equivalent nucleotide/amino acid substitution in the *Oprm1* gene. In order to investigate the impact of this SNP on circuit function, we used voltage-sensitive dye imaging in hippocampal slices and *in vivo* electroencephalogram recordings of the hippocampus following MOPR activation. As the hippocampus contains excitatory pyramidal cells whose activity is highly regulated by a dense network of inhibitory neurons, it serves as an ideal structure to evaluate how putative receptor function abnormalities may influence circuit activity. We found that MOPR activation increased excitatory responses in wild-type animals, an effect that was significantly reduced in animals possessing the *Oprm1* SNP. Furthermore, in order to assess the *in vivo* effects of this SNP during MOPR activation, EEG recordings of hippocampal activity following morphine administration corroborated a loss-of-function phenotype. In conclusion, as these mice have been shown to have similar MOPR expression in the hippocampus between genotypes, these data suggest that the MOPR A118G SNP results in a loss of receptor function.

1. Introduction:

Mu-opioid receptors (MOPR) modulate several pathways including pain and pleasure. The A118G single nucleotide polymorphism (SNP) in the μ -opioid receptor gene (*OPRM1*) has been associated with an altered vulnerability to opioid addiction (Drakenberg et al. 2006; Ray & Hutchison 2004; van den Wildenberg et al. 2007), a decreased response to opioid-induced analgesia (Chou et al. 2006; Sia et al. 2008), and an enhanced response to therapies for alcohol (Anton et al. 2008; Ray & Hutchison 2007) and nicotine addiction (Lerman et al. 2004). Mice possessing the equivalent SNP (A112G) have decreased MOPR expression and morphine-evoked behaviors, altered GTP γ S binding to the MOPR and downstream intracellular signaling cascades, and sex-specific deficits in morphine reward (Knapman et al. 2014; Mague et al. 2009; Wang et al. 2014; Wang et al. 2012). Additionally, recent studies in humans possessing the A118G SNP (Troisi et al. 2012; Way et al. 2010; Way et al. 2009) and in this mouse model of the A118G SNP (Briand et al. 2015) have shown in parallel that this SNP may have important ramifications for more complex behaviors, such as stress resiliency, which would also impact relapse behaviors in addiction. However, it has not been determined whether these effects result from decreased receptor availability or altered receptor function. For instance, male and female mice homozygous for the G112 allele (G/G) show equivalent MOPR expression decreases in reward-related brain regions; however, only the females show decreased morphine reward (Mague et al. 2009; Wang et al. 2014; Wang et al. 2012).

In order to address if alterations in receptor function were responsible for these changes, we evaluated circuit function in the hippocampus, a region displaying similar MOPR expression between genotypes and sexes (Mague et al. 2009; Wang et al. 2014; Wang et al. 2012). In CA1, MOPRs are predominantly found on somatodendritic and axonal aspects of fast-spiking, parvalbumin (PV)-containing GABAergic basket cells. Activation of MOPRs hyperpolarizes these cells and decreases GABAergic neurotransmission, thereby disinhibiting glutamatergic neurons and providing net excitatory activity (Glickfeld et al. 2008; Neumaier et al. 1988); for visual, see Figure 6.1. As perisomatic GABAergic inhibition can induce fast changes in neuronal polarity and gate cell firing at high frequencies (Csicsvari et al. 2003; Uhlhaas & Singer 2010), regulation of excitatory output by PV neurons may underlie network synchrony and gamma-band oscillatory activity (Whittington & Traub 2003) and influence memory storage/retrieval (Montgomery & Buzsáki 2007; Montgomery et al. 2009). Indeed, loss of GABAergic modulation induced by MOPR activation has been shown to reduce high-frequency oscillations in the hippocampus (Whittington et al. 1998) and cortex (Sun et al. 2006; Zuo et al. 2007) and mediate conditioned effects of morphine (Rezayof et al. 2007).

In order to better understand the synaptic and circuit-level alterations conferred by the A112G SNP, we employed voltage-sensitive dye imaging (VSDi) techniques in hippocampal slice preparations to evaluate opioid-stimulated responses. CA1 pyramidal cells supply a clear view of inhibition because they do not generate recurrent excitation; accordingly, excitatory postsynaptic potentials (EPSPs) induced by afferents are followed

almost exclusively by locally-induced inhibitory postsynaptic potentials (IPSPs). As a result, CA1 IPSPs form a temporally distinct and measurable VSDi component (Ang et al. 2005; Carlson & Coulter 2008). In these studies, we found that while baseline net circuit activity elicited by a single excitatory stimulus was similar between wild-type A/A and G/G mice, DAMGO-mediated increases in circuit activity were significantly attenuated in G/G mice, suggesting a loss-of-function of the MOPR. Furthermore, *in vivo* hippocampal EEG recordings showed a MOPR loss-of-function in G/G mice following a systemic injection of morphine. These data, which support clinical findings of decreased responses to opioidergic modulation, demonstrate both *ex vivo* and *in vivo* functional receptor deficits resulting from this SNP.

2 Materials and Methods:

2.1 Animals

All experiments utilized adult male and female mice (3–5 months of age; 20–35 g). Estrous cycle for female mice was not determined. Mice used in these experiments were either homozygous for the A112 (wild-type) or G112 (knock-in) allele [for detailed description of generation of *Oprm1*^{tm1Jabl} mice, see (Mague et al. 2009)]. Briefly, an equivalent N-linked glycosylation site to the A118G SNP found in humans was eliminated using site-directed mutagenesis in a bacterial artificial chromosome containing the C57BL/6 mouse *oprm1*. This was accomplished by replacing the adenine at nucleotide position 112 with a guanine, resulting in an aspartic acid substitution of asparagine at amino acid position 38. These mice were maintained on a C57BL/6 background and were bred, group housed, and maintained on a 12 h light/dark cycle with food and water available *ad libitum* in accordance with the University of Pennsylvania Animal Care and Use Committee.

2.2 Voltage-sensitive dye imaging (VSDi)

VSDi experiments were performed according to previous studies [(Ang et al. 2005; Ang et al. 2006); for detailed methodology, see (Carlson & Coulter 2008)]. Briefly, mice were decapitated following isoflurane anesthesia. The brain was removed and horizontal hippocampal slices (350 μ m) were cut using an Integraslice 7550 PSDS vibrating microtome (Campden Instruments, Lafayette, IN) in ice-cold sucrose artificial

cerebrospinal fluid (ACSF), in which NaCl was replaced with an equiosmolar concentration of sucrose. ACSF consisted of 130 mM NaCl, 3 mM KCl, 1.25 mM NaH₂PO₄, 26 mM NaHCO₃, 10 mM glucose, 1 mM MgCl₂, 2 mM CaCl₂ (pH 7.2-7.4 when saturated with 95% O₂/5% CO₂). Slices were then transferred to a static interface chamber (34°C) for 30 min and kept at 22-25°C thereafter. The osmolarity of all solutions was 305-315 mOsm.

Slices were stained for 20 min with 0.125 mg/ml (in ACSF) of the voltage-sensitive dye di-3-ANEPPDHQ (D36801, Invitogen), and imaged in an oxygenated interface chamber using an 80 x 80 CCD camera recording at a 1 kHz frame rate (NeuroCCD: RedShirtImaging, Decatur, GA). Epi-illumination was provided by a custom LED illuminator. Compared to the more commonly used photodiode array, the CCD chip well size (215,000 electrons) requires use of relatively low light-intensities, thereby minimizing photodynamic damage. The structures and regions of the slice were identified thusly: SO – stratum oriens, SR – stratum radiatum, SLM – stratum lacunosum moleculare, CTX – cortex, DG – dentate gyrus. Schaffer collateral stimulation using a single 20- μ A, 200- μ s pulse was administered with the electrode placed in SR near the CA3/CA1 border (Figure 6.2a,b). This stimulation protocol was utilized to highlight influences of PV interneurons, as these cells have been shown to respond with high reliability to initial, but not repeated, afferent input (Pouille & Scanziani 2004; Spruston 2008). A field-recording electrode was also placed in SR to monitor population responses following stimulation; these data, however, were not analyzed or included in this manuscript. After initial electrode-placement and evaluation of population responses, the

slice was allowed to recover for at least 5 min prior to testing. Baseline responses elicited by 12 single-stimulus trials, each separated by 20s, were recorded during bath application of ACSF. Following these recordings, the control ACSF was replaced by ACSF containing the selective MOPR agonist [d-Ala(2),N-Me-Phe(4),Gly(5)-ol]-enkephalin [DAMGO; 1 μ M (Sigma-Aldrich)], which bathed the slice for at least 10 min prior to the presentation of 12 single-stimulus trials of 20- μ A, 200- μ s pulses.

2.3 VSDi data analyses

VSD data was analyzed in IGOR (Wavemetrics, Lake Oswego, OR) on 12-trial-averages as previously described (Ang et al. 2005; Ang et al. 2006). Briefly, fluorescence-changes were calculated as the percent change in fluorescence divided by the resting fluorescence ($\% \Delta F / F_0$). Fitted double exponentials were subtracted from the normalized fluorescence to compensate for photobleaching. Raster Plot Quantification: Raster plots were generated by plotting the fluorescence signals across an imaginary line drawn through the peak of the response from SO to the SLM over the slice image and plotting the fluorescence signal from those pixels that fall under the line for all sampling points in time (Figure 6.2c). To determine net excitatory changes resulting from DAMGO administration, we employed a raster plot subtraction method that compared pixel-changes before and after DAMGO administration. Specifically, we subtracted the DAMGO raster plot (Figure 6.4a_{ii}) from the basal raster plot (Figure 6.4a_i), resulting in a representation of the alteration in inhibitory regulation as a result of MOPR stimulation (Figure 6.4a_{iii}). From 2D traces corresponding to average subtracted pixel-changes for

SO, SR, and SLM, we determined 1) the *peak amplitude* of disinhibition, determined by the greatest change in fluorescence ($\% \Delta F/F_0$), 2) the *duration* of disinhibition, measured as time (ms) that the loss of inhibition remained elevated, and 3) the *area under the curve (AUC)*, which summed the subtracted changes in fluorescence for a 50-ms window following the stimulation (Figure 6.4b_{iii}). Statistical analyses were performed with GraphPad Prism 5.0 software package (GraphPad Software, San Diego, CA). Differences between groups (genotype and sex) were assessed using two-way ANOVAs.

2.4 Surgery for electroencephalogram (EEG) recordings

Male and female A112G mice underwent stereotaxic implantation of bipolar, twisted, stainless steel electrodes into region CA1 of the hippocampus (200 μ m diameter, Plastics One, Roanoke VA). All surgeries used aseptic techniques and were performed with sterile gloves and full gown. The surgical field, table and stereotaxic frame were disinfected prior to surgery. Animals were anaesthetized with isoflurane and then placed in a stereotaxic frame for hippocampal depth electrode placement with continuous isoflurane inhalation by facemask. The scalp was cleaned with betadine and a midline incision was made, exposing the bregma and lambdoid sutures. Hippocampal depth electrodes (stainless steel) were placed using stereotaxic coordinates (AP -1.82 mm, ML 1.10 mm, DV -1.9 mm). The electrodes were cemented in place and the animals were kept under a warming light and carefully observed until fully awake and mobile.

2.5 Recording of EEG activity

Recording of EEG activity was performed between 10AM and 4PM, after a minimum of two weeks recovery from surgery. The mice were tested in their home cages, which were fitted with special tops to accommodate speakers and electrode cables, and placed inside a Faraday cage. The mice were acclimatized to the testing apparatus for 30 min before the first stimulus onset. Following a baseline trial, animals were injected with increasing doses (0, 1, 2, 7, and 20 mg/kg; i.p.) of morphine sulfate (NIDA) dissolved in saline. Subsequently, in order to demonstrate that the effects of morphine were mediated by MOPRs, naloxone (1 mg/kg; i.p.) was co-administered with a second 20 mg/kg injection of morphine. The head stage was connected to a three-channel electrode cable, which was connected to a high-impedance differential AC amplifier (A-M Systems, Carlsborg, Washington, USA). Auditory stimuli were generated by Micro1401 hardware and Spike 6 software (Cambridge Electronic Design) and delivered through speakers attached to the cage top. All experiments were done in the presence of background white noise of 55 dB. For gating experiments, 150 white-noise clicks pairs (S1, S2) were presented with a 500 msec inter-stimulus interval and a 9 second inter-trial interval. EEG signal was bandpass filtered online between 1 and 500 Hz, and grand average waveforms were created from -500 ms to 1000 ms relative to the auditory stimulus. To remove movement artifacts, trials containing activity over 2 SD of the mean were rejected. Initial peak analysis was performed in Microsoft Excel (Redmond, WA) or Igor (Wavemetrics, OR) on the remaining averaged trials. The baseline was corrected at stimulus onset of S1 and S2 independently.

2.6 EEG data analysis

Spectral decomposition of auditory-evoked response waveforms were performed using the EEGLab toolbox in MatLab (Delorme & Makeig 2004), as published previously (Gandal et al. 2010). Single-trial epochs between -0.1 and 0.2 seconds relative to the first stimulus (S1) were extracted from the continuous EEG data sampled at 1667 Hz. For each epoch, total power (i.e., event-related spectral perturbation, ERSP) was calculated using Morlet wavelets in 100 linearly spaced frequency bins between 2.0 and 100 Hz, with wavelet cycles increasing from 3 (at low frequencies) to 6 (at high frequencies). Total power was calculated in decibels (dB) relative to baseline power (-100 to 0 ms) in each frequency band. Data from specific time and frequency windows were extracted as the average power for each window. For comparisons of group level data, only saline, 20mg/kg morphine, and 20mg/kg morphine + Naloxone were considered. Since the differential effect of genotype on morphine's ability to modulate responses was of primary interest and total power at baseline (saline condition) was not different between A/A and G/G mice, results for the 20mg/kg morphine condition and 20mg/kg morphine + Naloxone conditions were normalized to the saline condition. A repeated measures mixed-model (genotype x condition) ANOVA assessed significance of power changes (IBM SPSS Statistics, Version 22, IBM Corp, Armonk, NY); pairwise comparisons were deduced using least squares differences.

3 Results:

3.1 Quantification of baseline responses

To evaluate differences in circuit responses to afferent activity, compound population responses in CA1 were induced with a single 20- μ A, 200- μ s pulse delivered to Schaffer collateral axons passing through SR of CA1. VSDi of area CA1 recorded an evoked fast depolarization followed by a rapid repolarization (Figure 6.2), reflecting responses at the single-cell level (Ang et al. 2005; Ang et al. 2006; Carlson & Coulter 2008). As previously validated, these alterations in fluorescence depict net functional changes in neuronal activity, which have been shown to be comparable to AMPA/NMDA-mediated EPSPs and GABA-mediated IPSPs measured by intracellular electrophysiological techniques (Ang et al. 2005; Ang et al. 2006; Carlson & Coulter 2008). The initial depolarization, which directly activated CA1 dendrites and local interneurons, propagated to distal regions of SR and outwards towards SLM and SO and was followed by a longer hyperpolarization. This can be visualized spatially in snapshots of the averaged peak excitatory (Figure 6.2b_i) or inhibitory (Figure 6.2b_{ii}) responses and temporally as 2D traces of fluorescence changes over time (Figure 6.2d) or raster plots of activity, which show changes in fluorescence across space and time (Figure 6.2c).

A112 and G112 animals, both male and female, displayed similar VSDi responses to Schaffer collateral stimulation under basal conditions (Figure 6.3). However, in SR, there was a significant reduction in the peak amplitude of the response in G112 animals regardless of sex (main effect of genotype, $F_{1,19} = 5.26$, $p < 0.05$; Figure 6.3c). While a

trend was observed in the SO peak amplitude in response to Schaffer collateral stimulation in females (Figure 6.3a), this effect was not significant.

3.2 Analysis of DAMGO-mediated response-changes

To determine if the A112G SNP alters hippocampal circuit activity during MOPR stimulation, we first examined responses following application of the highly specific MOPR agonist DAMGO (1 μ M) and normalized these to each animal's basal response. In accordance with previous studies (McQuiston 2007; McQuiston & Saggau 2003) and expectations for agents that inhibit GABAergic release, we found increases in neuronal activation following DAMGO administration in wild-type mice (Figure 6.4a).

In order to compare baseline and DAMGO-mediated responses, we subtracted the raster plot pixel-changes following DAMGO application from the raster plot responses observed under basal conditions in order to highlight the loss of inhibition due to MOPR-stimulated GABA inactivation. Since MOPR stimulation with DAMGO effectively decreases GABA transmission, any increase in excitatory events must have occurred due to this reduction in inhibitory modulation; the subtracted raster plots illustrate this MOPR-mediated loss of inhibition. An advantage of this approach is that it allowed us to more reliably compare drug treatment effects across genotypes and sexes. By subtracting the actual pixel responses between sessions, we eliminated the requirement for excessive numerical transformations and were able to analyze 2D traces quantified directly from the subtracted plot.

Comparing the subtracted raster plots between genotypes and sexes showed that while all groups showed an initial decrease in inhibitory modulation following DAMGO application, the wild-type animals had an elevated and prolonged response compared to the G/G mice (Figure 6.4c). Indeed, these observations were supported by quantification of raster plots for each of the regions within CA1. In order to identify differences between groups, we used a 2D trace of the subtracted pixel-changes over time for each region of CA1 and measured the peak amplitude and duration of the response in addition to the area under the curve (AUC) (Figure 6.5). In the SO, there were significant reductions in the ability of DAMGO to disinhibit excitatory responses both in G/G animals and in females, without an interaction between these effects. The G/G genotype and the females showed reduced disinhibition compared to their respective counterparts for the peak amplitude (main effects of genotype, $F_{1,19} = 7.45$, $p < 0.05$ and sex, $F_{1,19} = 6.30$, $p < 0.05$; Figure 6.5a), duration (main effects of genotype, $F_{1,19} = 22.58$, $p < 0.001$ and sex, $F_{1,19} = 6.05$, $p < 0.05$; Figure 6.5b), and the AUC (main effects of genotype, $F_{1,19} = 20.68$, $p < 0.001$ and sex, $F_{1,19} = 9.94$, $p < 0.01$; Figure 6.5c).

We found a similar pattern in the SR, in which there was a significant reduction in the ability of DAMGO to disinhibit excitatory responses in G/G animals, as demonstrated by decreases in the peak amplitude (main effect of genotype, $F_{1,19} = 13.76$, $p < 0.01$; Figure 6.5d), duration (main effect of genotype, $F_{1,19} = 47.12$, $p < 0.0001$; Figure 6.5e), and the AUC (main effect of genotype, $F_{1,19} = 22.37$, $p < 0.001$; Figure 6.5f). There was also a main effect of sex for the duration of response, in which the females of both genotypes showed reduced disinhibition compared to their male counterparts (main effect

of sex, $F_{1,19} = 10.67$, $p < 0.01$; Figure 6.5e); there was not, however, an interaction between genotype and sex main effects. Another advantage of this analysis was that it allowed us to evaluate differences in SLM, a region that, due to its lower basal responses, we could not otherwise have analyzed. Though the responses for all groups were lower in this region compared to the SR and SO, there was still a significantly reduced disinhibition in the SLM for the G/G animals for the peak (main effect of genotype, $F_{1,19} = 6.30$, $p < 0.05$; Figure 6.5g), duration (main effect of genotype, $F_{1,19} = 8.42$, $p < 0.05$; Figure 6.5h), and AUC (main effect of genotype, $F_{1,19} = 18.76$, $p < 0.001$; Figure 6.5i).

3.3 EEG

MOPRs located on terminals of PV interneurons can strongly modulate oscillatory activity of the hippocampus (Gulyás et al. 2010). Indeed, recent work has demonstrated that PV cells are critical for the generation of gamma oscillations in the hippocampus and neocortex (Fuchs et al. 2007; Lodge et al. 2009). In order to test if CA1-specific A118G differences in MOPR modulation of inhibition examined *in vitro* are reflected in gamma-band brain activity recorded *in vivo*, mice were implanted with low impedance hippocampal depth electrodes to measure EEG activity. Using an auditory stimulus protocol, tone-evoked gamma-band power was evaluated before and after an acute injection of morphine. At baseline (saline condition), total gamma power did not differ between genotypes (A/A vs. G/G; $T_{36,31}=0.9552$, $p = 0.34$). In order to investigate the change in responses following MOPR activation, EEG power following morphine injection and morphine + Naloxone injection were normalized to the baseline data.

Similar to prior work in rats (Zuo et al. 2007), we found that morphine (20 mg/kg, i.p.) reduced auditory-evoked gamma activity in the range of 31 to 51 Hz in all mice. However, this response was significantly reduced in G/G animals (genotype \times condition interaction: $F_{1,38} = 4.49$, $p < 0.05$; Figure 6.6a,b). Co-administration of naloxone (1 mg/kg; i.p.) reversed the effect of morphine similarly in all animals (Figure 6.6c). As such, EEG recordings demonstrate a differential reduction in Gamma activity in after MOPR activation dependent on A112G substitution. This specific reduction in gamma activity after MOPR activation is consistent with the cell-type specific localization of these receptors (Drake & Milner 1999; Drake & Milner 2002), and previous *in vivo* findings (Zuo et al. 2007). The reduced effect of morphine in G/G mice is consistent with the loss-of-function phenotype identified in the hippocampal slice preparation.

4. Discussion:

MOPR stimulation in the hippocampus increases net excitatory activity by decreasing GABAergic inhibition from local interneurons, resulting in the disruption of pyramidal cell firing synchrony and an alteration in hippocampal function (Faulkner et al. 1998). A common SNP in the gene encoding the MOPR has been shown to alter a variety of behaviors and drug responses in clinical populations [for review, (Mague & Blendy 2010)] and in animal models (Barr & Goldman 2006; Mague et al. 2009; Ramchandani et al. 2011; Y. Zhang et al. 2014). Neither the extent of these changes nor the mechanisms mediating the effects are completely understood. We used VSDi techniques to investigate circuit changes in the hippocampus in order to determine if functional alterations resulting from this SNP could better inform results from previous clinical and preclinical studies. Additionally, we utilized *in vivo* EEG recordings to evaluate changes in oscillatory activity in the hippocampus in awake animals that were acutely administered opiates. Overall, we found that the augmentation of excitatory responses elicited by opiate administration in wild-type animals was reduced in animals homozygous for the G112 allele. This reduction was particularly striking in raster plot subtraction analyses in which DAMGO-mediated responses of individual pixels were subtracted from basal responses, revealing the loss of inhibition caused by the MOPR activation. Similar results were found when evaluating hippocampal circuitry *in vivo*: reductions in gamma band activity caused by MOPR activation were decreased in G/G mice. Furthermore, our data suggests that the A112G SNP results in the reduced functionality of the receptor, as it has been shown that MOPR expression levels in the hippocampus are similar between

genotypes and sexes in A112G mice (Mague et al. 2009; Wang et al. 2014; Wang et al. 2012; Y. Zhang et al. 2014).

4.1 Ex Vivo VSDi Recordings Demonstrate that the MOPR A112G SNP Results in a Loss of MOPR Functionality and Altered Hippocampal Circuitry Evoked Responses

While baseline responses were similar between genotypes and sexes, there was a significantly lower peak response in the SR in the G/G animals. This could result from enhanced tonic GABAergic activity, possibly suggesting either a reduction in efficacy of endogenous MOPR modulation of GABA activity or, alternatively, a reduction in endogenous opioidergic tone in G/G animals. However, this effect was not seen for other measures of responses in the SR or SO, suggesting only a subtle consequence of these potential baseline alterations. Similarly, previous behavioral work with these mice did not uncover robust baseline differences, but only reductions in morphine-mediated behaviors (Mague et al. 2009).

Despite similar basal responses, there was a pronounced difference between genotypes following application of DAMGO. Raster plot subtraction analysis revealed robust MOPR deficits in the G/G animals in all CA1 regions tested. Though both genotypes showed an initial peak disinhibitory effect of DAMGO, this response was more intense and prolonged in A/A animals. Since the extent and duration of responses seem to be most affected, these data suggest that there could potentially be alterations in the desensitization or trafficking of the receptor.

In these experiments, we also found significant reductions in the female responses to MOPR activation compared to males, regardless of genotype. This was not surprising given the frequency of reported sex-differences in response to opioid administration (Craft 2008). Opioids have been shown to be more efficacious in males compared to females in both rodent (Kepler et al. 1989) and human (Cepeda & Carr 2003) studies investigating sex-differences in the analgesic properties of opioids. In contrast, female rats respond more robustly to the rewarding properties of opioids (Cicero et al. 2003) and women are more likely to abuse prescription opioid analgesics (Roe et al. 2002). Specifically in the hippocampus, ovarian steroid hormones have been shown to influence levels of opioid peptides (Roman et al. 2006; Williams et al. 2011) and the availability of MOPRs on the surface of PV cells (Torres-Reveron et al. 2009). In contrast to our previous studies, however, we did not demonstrate interactions between genotype and sex. This could suggest that differences in CA1 responses to MOPR activation may not directly underlie the sex-specific reduction in morphine-conditioned place-preference studies (Mague et al. 2009).

Since VSDi responses show net activity of entire circuits, we were unable to isolate responses of specific subpopulations of interneurons and, thus, cannot unequivocally ascribe our findings to MOPR modulation of PV basket cells. However, previous studies have shown that MOPRs are found predominantly on these interneurons (Drake & Milner 1999; Drake & Milner 2002) and that stimulation of these cells disinhibits glutamatergic dendrites (Glickfeld et al. 2008). This is supported by the findings provided by the stimulation protocol utilized in these studies, in which a single

200- μ s pulse was administered, as the PV interneurons have been shown to respond with high reliability to initial, but not repeated, afferent input (Pouille & Scanziani 2004; Spruston 2008). Also, GABA_A receptors located opposite PV cell terminals produce IPSPs that rise and decay very rapidly (Klausberger et al. 2002; Lavoie et al. 1997). Indeed, other studies evaluating MOPR-mediated elevations of CA1 responses to Shaffer collateral stimulation found that paired current pulses, similar to the single pulses utilized in the present studies, were mediated by GABA_A receptors (McQuiston & Saggau 2003), while DAMGO-induced augmentations of CA1 responses following prolonged stimulation were mediated by GABA_B receptors (Mcquiston 2007). These features of PV-containing, fast-spiking interneurons enable them to induce a reliable and brief, yet intense, somatic shunting of postsynaptic conductance (Bartos et al. 2007; Vida et al. 2006). Thus, reduced PV interneuron inhibition is a plausible explanation for the augmentation of CA1 responses following DAMGO administration in these current experiments. The reduced disinhibition demonstrated by the G/G animals following DAMGO administration suggests a disruption in MOPR modulation of these PV interneurons resulting from the A112G SNP.

4.2 In Vivo EEG Electrophysiological Recordings Also Demonstrate that the MOPR A112G SNP Results in Altered Hippocampal Responses

A consequence of the increase in excitatory responses demonstrated in wild-type mice could be a reduction in both neuronal synchrony and the formation of high-frequency oscillatory activity. Indeed, PV interneurons have been shown to be important

in generating gamma-band oscillations in the hippocampus (Bartos et al. 2007; Fuchs et al. 2007). Given the reduced MOPR-mediated augmentation of responses in the G/G animals, we would predict that reductions in gamma-activity resulting from MOPR activation (Sun et al. 2006; Zuo et al. 2007) would be decreased in these animals. Our findings support this prediction. Gamma-band power was decreased in all mice after administration of morphine, though blunted in G/G mice. Naloxone blocked all gamma frequency-related effects of morphine for both genotypes, suggesting that the reductions in gamma were mediated by actions at the MOPR. It should be noted, however, that as we did not measure the effects of naloxone alone, we cannot conclude unequivocally that the reversal in gamma responses results from the blockade of morphine action and not some other mechanism, such as inhibition of endogenous opioids. However, while one study did find significant effects of naloxone alone in monkeys on EEG measures (Ehlers 1989), similar studies have found no effect of naloxone alone *in vitro* (Lynch et al. 1981), in conscious rats (Coltro Campi & Clarke 1995; Tortella et al. 1978), or in children (Nalin et al. 1988), suggesting that naloxone's effects in the EEG studies were most likely due to blockade of the exogenously administered morphine.

Clinical studies, as well as those in rodents and non-human primates, have shown that reductions in evoked gamma power are an intermediate phenotype with broad relevance to neuropsychiatric disorders, pain sensitivity and, in the hippocampus, cognition (Carlson et al. 2011; Uhlhaas & Singer 2011). Thus, these EEG data provide initial evidence those differences in sensitivity shown *in vitro* may act via PV-cells to mediate some of the behavioral phenotypes associated with the A118G allele.

Additionally, because similar EEG studies can be performed in humans, the EEG phenotype provides a framework for translating neurophysiological and behavioral correlates from the A118G mouse model to identifying functional neural substrates underlying the A118G genotype and behavior interaction identified humans.

4.3 Conclusions

We observe an alteration in hippocampal function as a result of the Mu Opioid Receptor SNP, A112G, and the reduced effect of DAMGO and morphine in G/G animals further supports a loss-of-function of the MOPR as a consequence of this SNP. Previous work with this mouse line has provided evidence for reduced MOPR expression and decreased behavioral responses to acute morphine administration; likewise, clinical findings have demonstrated a reduced response to the analgesic properties of opioids (Chou et al. 2006; Sia et al. 2008). In support of these findings, authors often cite *in vitro* studies showing decreases in MOPR expression (Befort et al. 2001; Zhang et al. 2005). However, the present data were derived from evaluation of MOPR function in the hippocampus, which possesses equivalent MOPR expression between genotypes and sexes as demonstrated using RT-PCR (Mague et al. 2009) and quantitative *in vitro* autoradiography (Wang et al. 2014; Wang et al. 2012). From our data, it appears that the strong disinhibition controlled by MOPRs on interneurons of the hippocampus is absent, therefore leading us to conclude that this polymorphism represents a “loss of function” phenotype in the context of hippocampal microcircuitry (Figure 6.1). While others have observed that MOPRs in cultured cells perhaps follow a gain of function phenotype

(Bond et al. 1998; Margas et al. 2007), these models do not possess well-organized circuits and therefore do not accurately reflect complex brain structures. In contrast, our *ex vivo* slices maintain microcircuitry and are representative of a “loss of function” phenotype at the circuitry level, which is closely paralleled by our *in vivo* EEG hippocampal findings following systemic administration of opiates. We posit that the loss of function in our microcircuitry model occurs due to the reduced inhibitory drive onto pyramidal cells (Figure 6.1). However, the mechanism underlying changes in receptor function remains unknown. Attempts to identify changes in agonist binding, protein coupling, downstream signaling, and receptor trafficking have not produced conclusive evidence for the specific deficit [for review, see (Knapman & Connor 2015)]. For instance, in whole-cell patch-clamp studies using a mouse line possessing humanized A/A or G/G alleles, Mahmoud and colleagues found a functional reduction of voltage-gated Ca²⁺ activation following morphine administration in isolated sensory neurons from G/G animals (Mahmoud et al. 2011), consistent with a loss of function of the receptor. In separate experiments using this A112G mouse line, a reduction in GTPγS binding was detected in several brain regions (Wang et al. 2014). In addition, human positron emission topography studies have demonstrated a decreased binding potential of [¹¹C]carfentanil, indicating a reduced MOPR availability, in those with the G allele (Ray et al. 2011; Weerts et al. 2012). Together, these results suggest deficits in the early stages of binding and signal transduction and would be consistent with the immediate changes seen after acute MOPR agonist administration. However, these data do not rule out other changes to protein binding, downstream signaling, internalization, or dimerization. Future

studies specifically aimed at these characteristics will help elucidate the mechanisms whereby this polymorphism disrupts MOPR function. In summary, the modeling of this SNP in mice identified reduced function in the absence of reduced expression and suggests that human SNPs may have more complex consequences on phenotypes than previously appreciated.

Figure Legends:

Figure 6.1 *Schematic highlighting MOPR role in hippocampal circuit. (A, B) Shaffer*

Collateral projections (represented by dotted line) from pyramidal cells in CA3 synapse with dendrites of CA1 pyramidal cells as well as local inhibitory interneurons (shown in blue). A) Thus, stimulating CA3 axons (1) will produce direct activation of CA1 dendrites (2) as well as indirect (i.e., feed-forward) inhibition of these dendrites/cell bodies through GABAergic interneuron activation (3). B) MOPR activation (e.g., with DAMGO or morphine) during CA3 axonal firing (1) will decrease GABA release from the interneuron (3), resulting in a net increase in excitatory influences on CA1 pyramidal cells (2).

Figure 6.2 *VSDi procedure, quantification, and analysis:* (a) A diagram of hippocampus circuitry illustrates the stimulus protocol utilized in this study. A stimulating electrode was placed in the Shaffer collateral axons from CA3 pyramidal cells and a recording electrode was placed in the distal end of SR in CA1. The light gray line represents the pyramidal cell layer and the dotted black line delineates the path of the Shaffer collateral axons. The dark gray box depicts the area visualized in *b*. (b) Horizontal slices containing the hippocampus were visualized under a 10x lens. The black triangles show the stimulating electrode placement and the white triangle shows the placement of the recording electrode. The structures and regions are labeled thusly: SO – stratum oriens, SR – stratum radiatum, SLM – stratum lacunosum moleculare, CTX – cortex, DG – dentate gyrus. The average normalized pixel-changes for the duration indicated following stimulation demonstrates the peak excitatory (b_i) and inhibitory (b_{ii}) responses for a representative wild-type animal. Changes in membrane voltage are illustrated in red (excitation) or blue (inhibition). The black line corresponds to the raster plot shown in *c*. (c) Raster plots corresponding to the pixels along the black line drawn in *figure 6.2b* show the average pixel-changes over time for the SO, SR, and SLM during baseline. Changes in membrane voltage are illustrated in red (excitation) or blue (inhibition). (d) A 2D trace of the SR region from *c*.

Figure 6.3 *Baseline responses:* There were no differences between genotypes or sexes in the SO for amplitude **(a)** or tau **(b)**. In the SR, there was a significant reduction in the peak excitation for G/G mice **(c)** but not for the tau **(d)**. All data are presented as mean \pm SEM, n = 5; * p < 0.05 compared to A/A.

Figure 6.4 Raster plot subtraction analyses: (a) Raster plots corresponding to the pixels along the black line drawn in *figure 6.2b* show the average pixel-changes over time for the SO, SR, and SLM during baseline (a_i) or DAMGO application (a_{ii}). Subtraction of the baseline plots from the DAMGO plots shows the net disinhibition resulting from MOPR activation (c_{iii}). Changes in membrane voltage are illustrated in red (excitation) or blue (inhibition). (b) A 2D trace of the SR region shows the quantification of subtracted raster plots. The *amplitude* was determined by the peak disinhibitory response. The *duration*, shown as the horizontal dashed red line, measured the time (ms) during which disinhibition was elevated above noise. The *area under the curve* (AUC; diagonal red lines) was calculated for a 50-ms window following stimulation. For all 2D plots, the scales of response amplitudes correspond to the numerical axis of the color scales drawn to the left of each trace. (c) Representative subtracted raster plots for A/A male (c_i), A/A female (c_{ii}), G/G male (c_{iii}), and G/G female (c_{iv}) show the loss of inhibition resulting from DAMGO administration.

Figure 6.5 *DAMGO-mediated inhibition is reduced in G/G animals.* **(a)** Analysis of 2D traces from each strata of CA1 reveals alterations in genotype or sex responses to DAMGO administration. In the SO, both the G/G animals and females, each compared to their respective counterparts, showed decreases in the amplitude **(a)**, duration **(b)** and AUC **(c)**. In the SR, G/G animals showed reductions in amplitude **(d)**, duration **(e)**, and AUC **(f)**; additionally, there was a significant reduction in females compared to males for duration only **(e)**. In the SLM, levels of disinhibition were lower compared to the other CA1 regions; however, G/G animals still showed a decreased response to DAMGO administration measured by the amplitude **(g)**, duration **(h)**, and AUC **(i)**. All data are presented as mean \pm SEM, n = 5; * p < 0.05, ** p < 0.01, *** p < 0.001, † p < 0.0001 compared to A/A; + p < 0.05 compared to males.

Figure 6.6 *G/G mice exhibit reduced gamma-related responses to MORP activation.* A)

Total power response for representative A/A (top) and G/G (bottom) mice, for Saline (left), 20 mg/kg Morphine (center), and 20 mg/kg Morphine + 1mg/kg Naloxone (Nal) (right). Note the decrease in high frequency (gamma) activity (box 1). This did not occur at lower frequencies (box 2). B) Group average results for gamma activity (31–51 Hz), * = $p < 0.05$ compared to A/A C) Group Average results for low frequency 6–11 Hz, demonstrate no significant group differences. B and C are presented as mean \pm SEM, n = 8–11.

Figures:

Figure 6. 1

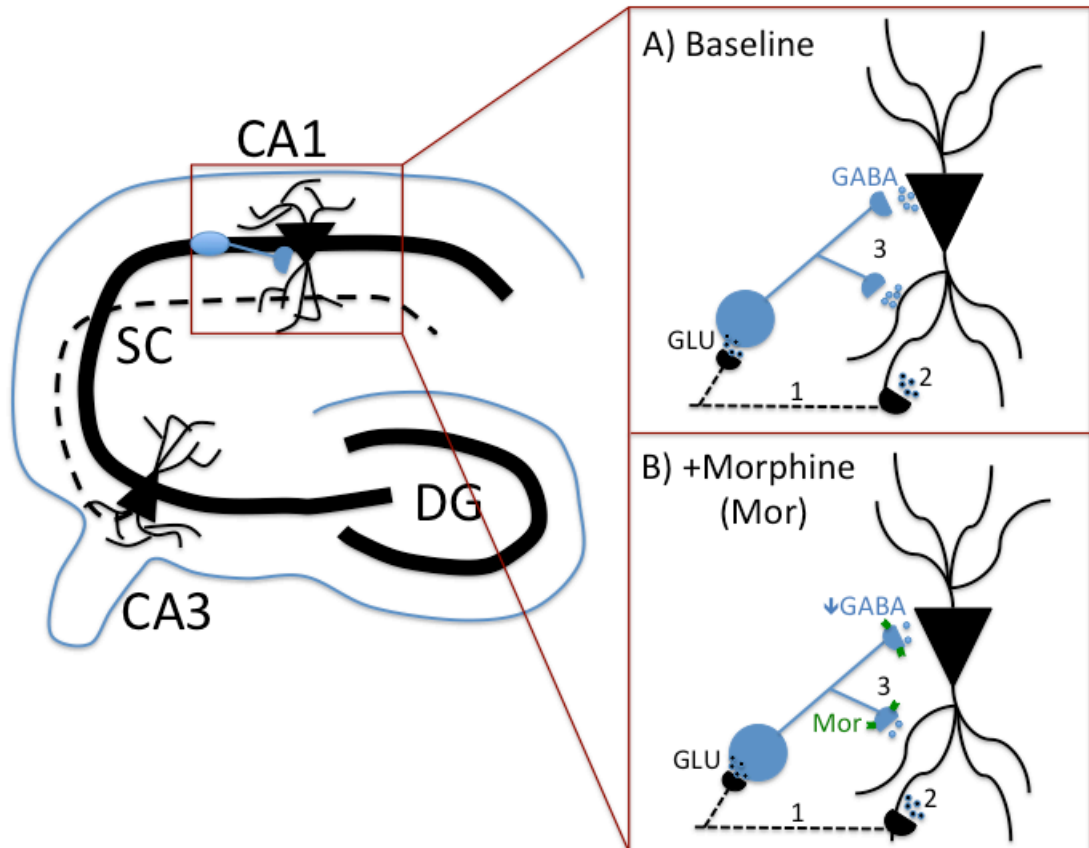


Figure 6. 2

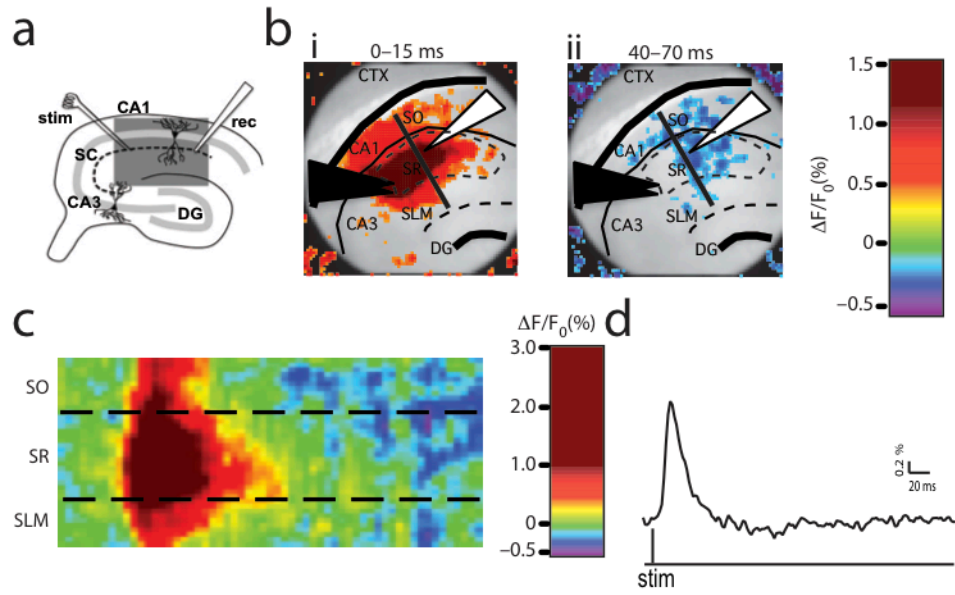


Figure 6.3

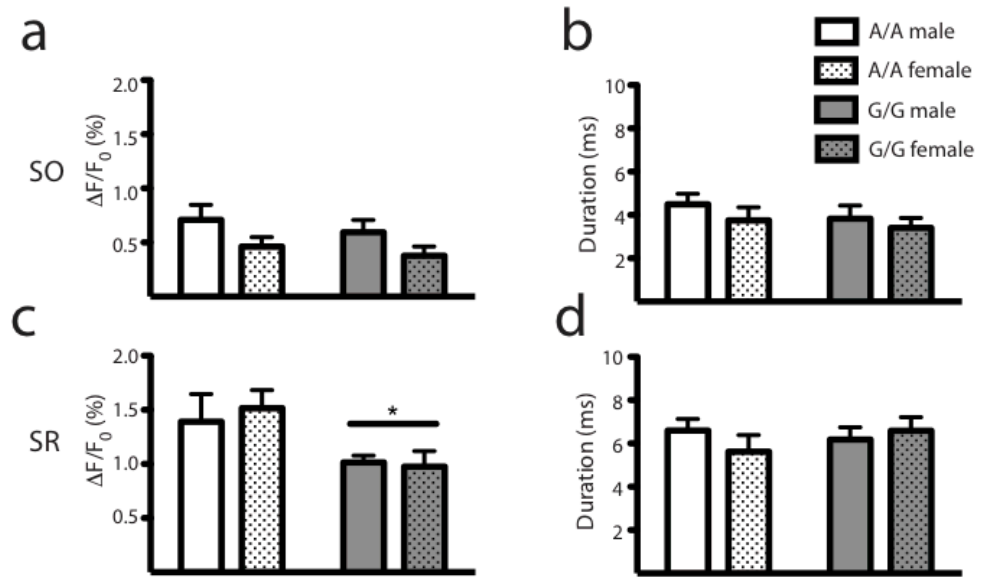


Figure 6. 4

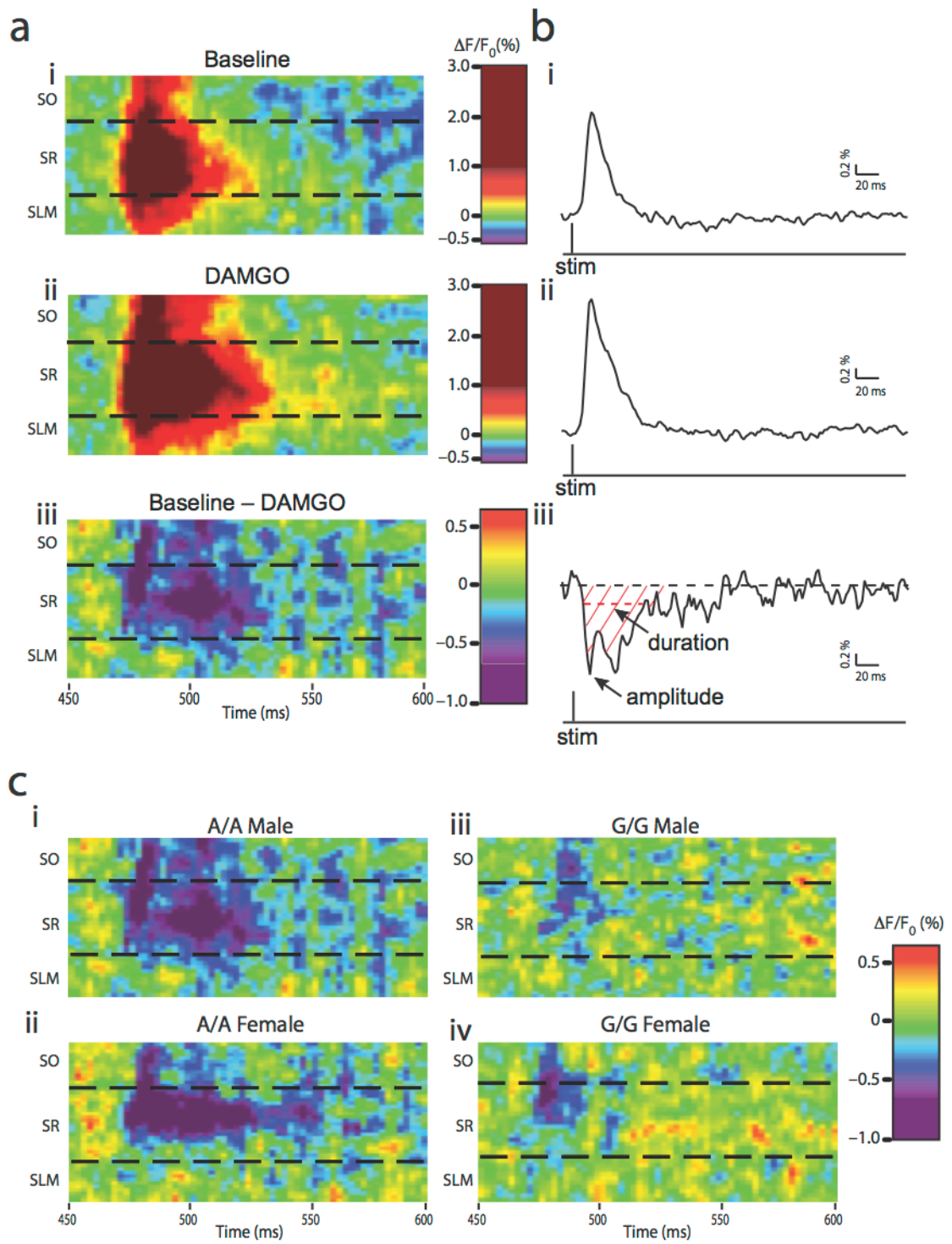


Figure 6. 5

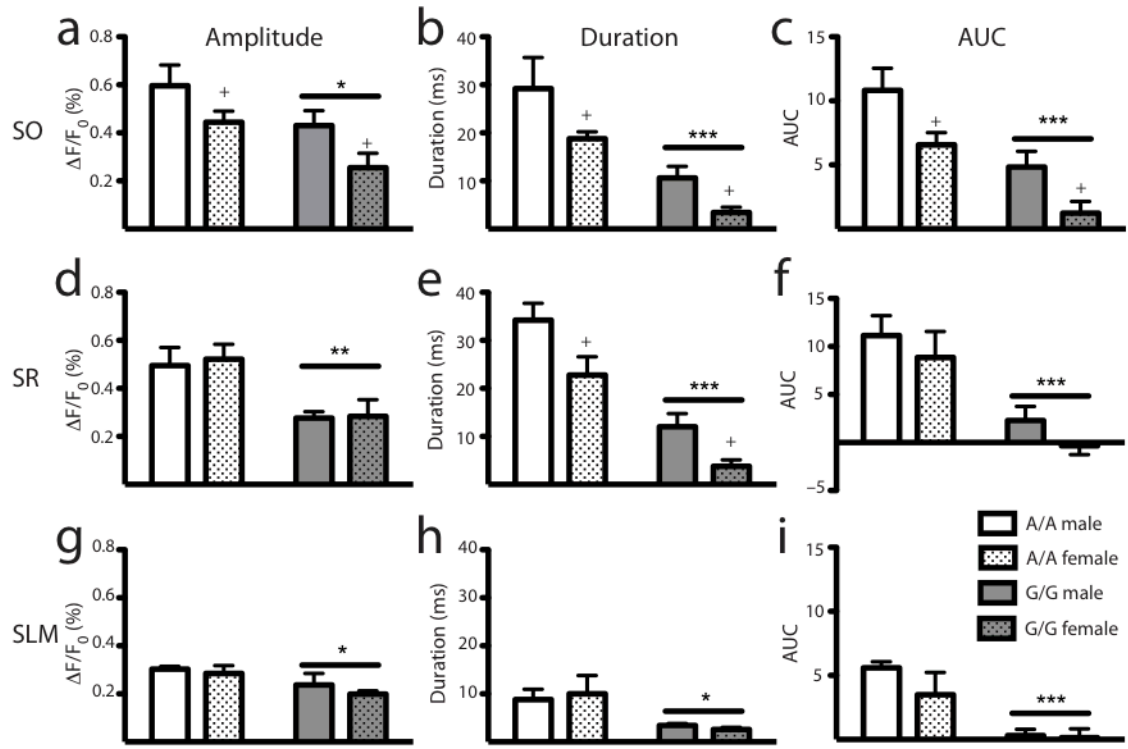
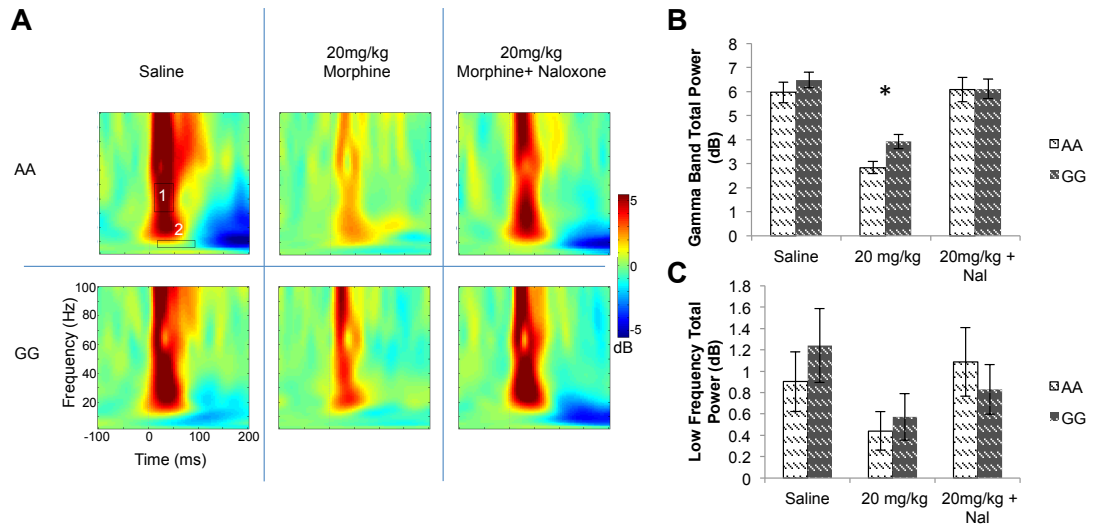


Figure 6. 6



CHAPTER 7

Summary & Conclusion

1. Summary

The purpose of this dissertation was to uncover the underlying neurobiological mechanisms of auditory electrophysiological biomarkers for Autism Spectrum Disorder (ASD), particularly gamma-band oscillatory activity alterations. To do so a multimodal translational approach was undertaken that spanned both preclinical (*in-vitro and in-vivo*) and clinical settings. Moreover, multiple methodologies were implemented within each setting. The auditory electrophysiological biomarkers of interest in this thesis (M100 latency delays and gamma-band perturbations) allows for the direct study of analogous constructs between clinical and preclinical settings. As such, the traditional T1 to T4 translational processes (Szilagyi 2009) has been expanded on, with an iterative process that cycles concepts and hypotheses between preclinical settings and clinical settings. Figure 7.1 demonstrates a methodological benefit to such a translational approach; where spectral decomposition is adapted from the clinical research environment into in-vitro experiment analyses using identical core time-frequency analyses. Without this explicit and concerted effort for translational research such a methodological leap would be unlikely. Furthermore, Figure 7.1 suggests that the gamma-band activity perturbations seen in ASD and their underlying neurobiology may be available for direct in-vitro study. As such, it may be possible to localize ASD-related electrophysiological biomarkers to

within structural laminar or cell types, which is currently impossible for MEG or EEG based studies to resolve.

This dissertation contains the first longitudinal study of auditory magnetoencephalography (MEG) biomarkers for ASD. This study demonstrated the persistence (from childhood into adolescence) of auditory gamma-band activity alterations in individuals with ASD. The auditory phase-locked gamma-band activity in response to simple tones was decreased in ASD individuals versus to typically developing (TD) age-matched controls. Moreover, while non-significant, evoked gamma-band power matured four times slower in ASD. An interesting, though preliminary, additional result from this study was that individuals with ASD who subsequently demonstrated “optimal outcome” (i.e. who did not meet diagnostic criteria at follow-up) had intermediate gamma-band activity responses as compared to TD controls and ASD individuals.

This dissertation also demonstrated that gamma-band activity was coupled to underlying neurochemistry in TD controls in the Superior Temporal Gyrus. Gamma-band inter-trial coherence (ITC) and relative cortical γ -Aminobutyric acid (GABA) concentrations were correlated in TD controls. In addition, gamma-band ITC and relative cortical GABA concentrations were both decreased in individuals with ASD. Additionally there was weaker coupling between these two metrics in our cohort of individuals with ASD. It is not immediately clear if the weaker coupling seen in our cohort of individuals with ASD between gamma-band coherence and relative cortical GABA is due to increased variance from biological variability, or distinct sub-

populations for whom coupling is differentially intact or not. Of note, we propose potential metric of gamma-band activity normalized by relative cortical GABA was suggested and could denote a “functional to neurochemical coupling” or “GABA efficiency” index. Future studies will evaluate whether this metric is able to stratify the ASD population into treatment paths or demonstrate early efficacy of treatment.

Additionally, this dissertation demonstrated that *Pcdh10* heterozygous (*Pcdh10*^{+/-}) mice, who mimic a key range of genetic insult in familial ASD, demonstrate in-vivo gamma-band electrophysiological perturbations. Both stimulus-related and resting-state gamma-band oscillatory activity perturbations were observed in these mice as compared to their wild-type littermates. This was in contrast to the lack of latency perturbations for event related potential (ERP) components. In addition, these *Pcdh10*^{+/-} mice demonstrated increased GABA concentrations, and perturbed coupling of GABA concentrations to gamma-band activity. As such, this study characterized how a key genetic insult of ASD affects electrophysiological activity (both at rest and in response to auditory stimuli), and presented a possible mechanism for such alterations.

Moreover this dissertation demonstrated that the A112G *Oprm1* single nucleotide polymorphism (SNP) caused subtle in-vitro response alteration due to reduced μ opioid functionality in mice. Furthermore such subtle alterations may be the underlying cause of the *increased* gamma-band activity observed in response to simple white-noise clicks seen in these murine SNP (compare to the *decreased* gamma-band activity in *Pcdh10*^{+/-}). This observation coexists with *increased* sociability in mice with A112G *Oprm1* SNPs (Briand et al. 2015). While not conclusive, this suggests that increases in sociability may

occur with increase in gamma-band activity responses, the opposite of what occurs in ASD. Table 7.2 highlights main findings of this dissertation.

2. Conclusion and future directions

In conclusion, this dissertation demonstrated several underlying neurobiological alterations that relate to the auditory electrophysiological perturbations seen in ASD. By utilizing both clinical and preclinical studies observations were made that would have been unlikely in isolation.

This work observed that reduced auditory gamma-band activity is a persistent perturbation from childhood into adolescence in individuals with ASD. Such observations support studies by Rojas and colleagues which demonstrated that auditory gamma-band activity perturbations in adults (Rojas et al. 2008) to similar tones. Syntheses of current and previous observations (Rojas et al. 2008) therefore suggest that gamma-band activity alterations are persistent phenotypes present through the life span of an individual with ASD. Furthermore such gamma-band activity perturbations are observed in first degree relative of individuals with ASD, and so may constitute an endophenotype (Rojas et al. 2008; Rojas et al. 2011). Corresponding alterations to gamma-band activity in adults with ASD have also been demonstrated in the visual system (Grice et al. 2001; Sun et al. 2012) and so suggest that such gamma-band alterations may be a core feature of ASD.

Moreover, this dissertation demonstrated that gamma-band activity alterations may relate to underlying neurochemistry. While there are multiple models for the generation of gamma-band activity, a consistent feature in several schema is the crucial role for GABA (Whittington et al. 2000). Importantly in such systems, the GABA_A receptor's time constant (~25ms) is thought to set the oscillation frequency of the recorded activity (Traub et al. 1996). Indeed, support for such models comes from multiple studies and points towards specific cells, parvalbumin positive basket cells, as the pacemakers (Buzsáki & Wang 2012). Recent clinical studies support such hypotheses with GABAergic pharmaceutical administration in healthy adults altering gamma-band activity (Hall et al. 2010; Muthukumaraswamy et al. 2013; Muthukumaraswamy 2014). Furthermore, correlations between relative cortical GABA concentrations and corresponding gamma-band activity have been observed in neurotypical adults for multiple systems (Muthukumaraswamy et al. 2009; Gaetz et al. 2011; Balz et al. 2015). However, it was unknown if this relationship existed within the auditory system and how ASD impacted to such a correlation. While both decreased relative cortical GABA (Rojas et al. 2014; Gaetz et al. 2014) and gamma-band activity (Wilson et al. 2007; Rojas et al. 2008; Gandal et al. 2010; J Christopher Edgar et al. 2015) in ASD had been repeatedly demonstrated separately, their relationship was unknown. This dissertation demonstrates whereas this coupling does occur in TD controls, it is weakened for our ASD cohort. Further work is needed to determine if the “functional to neurochemical coupling” or “GABA efficiency” index suggested in this study has clinical relevance. This clinical relevance is crucial knowledge because several emerging treatments for ASD focus on

the manipulation of the GABA system, though show only partial efficacy (Erickson et al. 2014; Lemonnier et al. 2012) akin to a subpopulation based differential coupling. Promisingly these compounds have efficacy in murine models for recovering both behavioral (Gandal, Sisti, et al. 2012; Tyzio et al. 2014; Silverman et al. 2015) and neural activity (Gandal, Sisti, et al. 2012; Tyzio et al. 2014) phenotypes with particular relevance to ASD. Moreover, MEG-derived gamma-band activity measures have the potential to be utilized as a proxy measure for relative cortical GABA in the individuals that demonstrate such “functional to neurochemical coupling”, which is of significance because oscillatory activity is simpler to measure than neurochemistry in humans, which is of practical and clinical significance.

In addition, this dissertation’s preclinical research demonstrates that a genetic manipulation mimicking a key genetic insult in familial ASD (*Pcdh10*^{+/-} mice) produced both increased GABA concentrations as well as perturbations to gamma-band activity, but had no effect on ERP component latencies or amplitudes. This is contrary to clinical ASD where both auditory gamma-band activity perturbations (Wilson et al. 2007; Rojas et al. 2008; Gandal et al. 2010; J Christopher Edgar et al. 2015) as well as M100 latency delays (Gage, Siegel & Roberts 2003; Roberts et al. 2010; J Christopher Edgar et al. 2015; Edgar, Lanza, et al. 2014) have been repeatedly observe. As such the findings from this dissertation suggest that gamma-band activity alterations and M100 delays in ASD may not be redundant. Instead they may potentially appear in difference cohorts, or at least may vary independently in the degree of their impairment. Indeed, Gandal and colleagues (2010) demonstrated that only about 15% of the variance in auditory gamma-

band ITC is accounted for by auditory M100 latencies. Additionally, how such alterations to M100 latency or gamma-band activity differentially relate to symptomatology in ASD is unclear.

Gamma-band response alterations were also observed in the A112G *Oprm1* SNP mouse model. These mice demonstrate *increased* gamma-band activity as compared to their wild type littermates, and in addition were previously observed to exhibit *increased* sociability (Briand et al. 2015). Moreover, in-vitro experiments demonstrated that these mice exhibit reduced μ opioid functionality. While not conclusive, this work demonstrates how increases in sociability may be concurrent with increased gamma-band activity, a crucial positive control for the implementation of gamma-band activity as a biomarker for ASD. Williams syndrome (which is marked by increased sociability) also demonstrates increases in gamma-band activity in response to social stimuli (Bernardino et al. 2013), however such findings are confounded by comorbid cognitive disabilities.

Future studies should focus on the dissociation of gamma-band activity alterations and M100 latency delays on clinical symptoms and preclinical behavior. In addition, notably absent from this dissertation, the underlying biological mechanisms of M100 latency delays requires further investigation. Clinical studies suggest that middle response latencies are associated with relevant white matter microstructural properties (Stufflebeam et al. 2008; Roberts et al. 2009; Dockstader et al. 2012; Roberts et al. 2013). Moreover, the relationship of white matter microstructure to evoked electrophysiological responses may be perturbed in ASD (Roberts et al. 2013) Separately, preclinical studies have repeatedly demonstrated delayed middle latency responses in animal models that

recapitulate key aspects of ASD (Gandal et al. 2010; Gandal, Anderson, et al. 2012; Billingslea et al. 2014). Frequently these studies utilized genetically based manipulations to neurotransmitter signaling. While it may be that middle latency response delays are due to signal transduction impairments (i.e. decreased/absent NMDA receptors), the signal transmission (e.g. white matter microstructure) of these mice is still unknown.

This thesis also did not address the effect of current interventions, or biologically targeted novel interventions. For instance a recent study observed that effective behavioral therapy, quantified as improved clinical scores, was concurrent to normalized gamma-band activity (Van Hecke et al. 2013). Subsequently initial rodent studies have demonstrated that behavioral training can recover cortical response latencies (Crystal T. Engineer et al. 2014). It remains unclear what neurobiological changes are occurring with effective behavioral therapies. An outcome of the present study examining the coupling of GABA and gamma-band activity in individuals with ASD suggests that interventions that either increase this coupling, or enhance GABA-related signaling may be of use. Indeed as mentioned above, several GABA-related interventions show efficacy in treating certain ASD symptoms (Berry-Kravis et al. 2012; Lemonnier et al. 2012). To effectively implement such GABA-related treatments in ASD, the source of the increased variance in the GABA to gamma-band activity coupling in ASD needs to be determined (e.g. whether the variance is due to intrinsic heterogeneity of ASD or the existence of 2 (or more) sub-populations within the ASD population). Such future studies would enhance our understanding not only of the biological basis of ASD, but also possible interventions for ASD and related neurodevelopmental disorders.

As such, although there are questions that remain to be answered, this dissertation has characterized key auditory biomarkers for ASD and provided insight into their neurobiological etiology. Moreover, significant progress has been made in extending the traditional sphere of translational research and this work has demonstrated how a cross-species multimodal approach allows for the development of novel techniques and analyses, allowing insight into neurobiological mechanisms of ASD with clinical and therapeutic implications.

Table Legend:

Table 1: *Overview of this dissertation.* Each chapter (1st column), with the system (2nd left), major question (3rd column) and major observation (4th column) for this dissertation. Synthesis of observations are present in last row. MEG = magnetoencephalography; MRS – magnetic resonance spectroscopy; EEG – electroencephalography; HPLC = High Performance Liquid Chromatography; VSDi – Voltage Sensitive Dye Imaging

Figure Legend:

Figure 7.1 *Application of a translational approach to analyses allows for the measurement of similar constructs from clinical to preclinical studies.* (A) A clinical evoked power auditory steady state response (ASSR) to a 40Hz amplitude modulated tone as recorded by magnetoencephalography (MEG) (B) An analogous ASSR as recorded by scalp electroencephalography (EEG; approximately Cz electrode) (C) The corresponding in-vivo murine ASSR in response to a 40Hz white-noise amplitude modulated square wave as recorded by depth EEG (D) An in-vitro steady state response from auditory cortex in response to 40Hz white-matter stimulation as recorded by voltage sensitive dye imaging (VSDi).

Table 7. 1

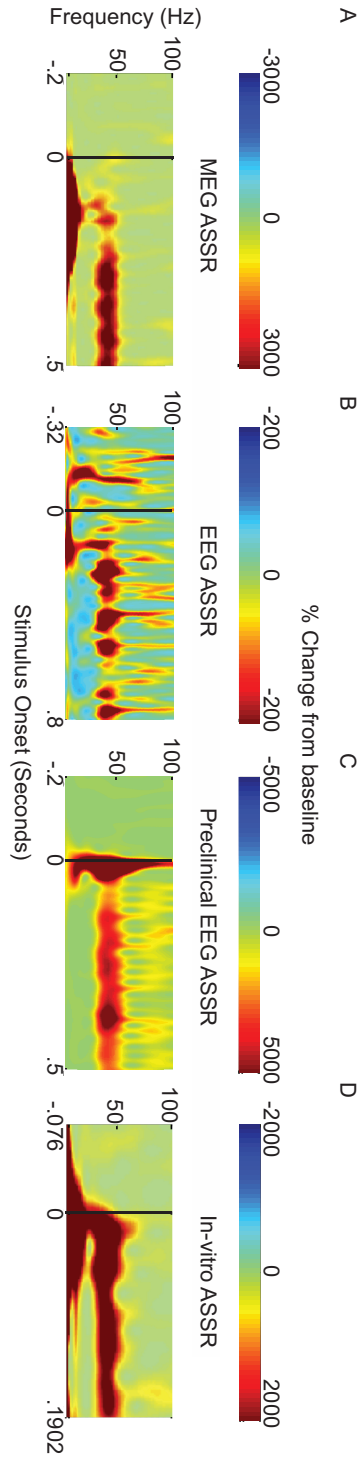
Chapter	System	Major Question	Major Observations
2	<i>In-vivo</i> Human MEG	Are auditory MEG biomarkers persistent in ASD or epiphenomenal effect of age group?	Both M100 latency delays and gamma-band activity deficits are persistent from childhood into adolescence
3	<i>In-vivo</i> Human MEG & <i>in-vivo</i> MRS	Are gamma-band activity deficits observed in Chapter 2 related to GABA decreases?	GABA levels are correlated to gamma-band activity in typically developing individuals. Weaker coupling was observed in ASD, though it is unresolved if the weaker coupling is due to heterogeneity in ASD or separate subpopulations with differential coupling
4	<i>In-vivo</i> Murine EEG & <i>ex-vivo</i> HPLC	Does a murine model that mimics a specific genetic subpopulation of ASD demonstrate weaker coupling (akin to Chapter 3) or conserved/absent coupling?	Alterations to GABA and gamma-band activity, but not N40 latency are observed in <i>Pcdh10^{-/-}</i> mice. These mice, modeling genetic subpopulation of ASD, demonstrate no coupling between GABA and gamma-band activity. Further studies will need to determine if other murine models recapitulate this phenotype or demonstrate coupling
5	<i>In-vivo</i> Murine EEG	Are increases in sociability associated with increase in gamma-band activity (i.e. the reverse of both electrophysiology and behavior in ASD)?	Whereas ASD demonstrates <i>decreased sociability and gamma-band activity</i> this murine model exhibits <i>increases in gamma-band activity and sociability</i>
6	<i>In-vivo</i> VSDI	Can we observe <i>in-vitro</i> functional alterations related to Chapter 5's observation	Subtle alterations to <i>in-vitro</i> electrophysiological are observed in the mice that demonstrate increased sociability and gamma-band activity due to reductions in μ opioid functionality

Synthesis: Gamma-band activity deficits are a persistent perturbation in ASD that may relate to underlying GABAergic tone depending on the specific pathogenic mechanism. Moreover, gamma-band activity may scale (at least partially) independently from M100 deficits, and both biomarkers may account for different impairment domains in ASD.

Tables:

Figures:

Figure 7. 1



BIBLIOGRAPHY

- Achenbach, T.M. & Rescorla, L.A., 2003. *Adult Behavior Checklist*, Burlington, VT: ASEBA.
- Ainsworth, M. et al., 2012. Rates and rhythms: a synergistic view of frequency and temporal coding in neuronal networks. *Neuron*, 75(4), pp.572–83. Available at: <http://www.ncbi.nlm.nih.gov/pubmed/22920250> [Accessed October 21, 2014].
- Ali, E.H. a & Elgoly, A.H.M., 2013. Combined prenatal and postnatal butyl paraben exposure produces autism-like symptoms in offspring: Comparison with valproic acid autistic model. *Pharmacology Biochemistry and Behavior*, 111, pp.102–110. Available at: <http://dx.doi.org/10.1016/j.pbb.2013.08.016>.
- Amann, L.C. et al., 2008. Male and female mice differ for baseline and nicotine-induced event related potentials. *Behavioral neuroscience*, 122(5), pp.982–90. Available at: <http://www.ncbi.nlm.nih.gov/pubmed/18823155>.
- Amann, L.C. et al., 2010. Mouse behavioral endophenotypes for schizophrenia. *Brain research bulletin*, 83(3-4), pp.147–61. Available at: <http://www.ncbi.nlm.nih.gov/pubmed/20433908> [Accessed August 8, 2014].
- American Psychiatric Association ed., 2013. *Diagnostic and Statistical Manual of Mental Disorders, 5th Edition* 5th Editio., Washington, DC: American Psychiatric Publishing, Inc. Available at: <http://dsm.psychiatryonline.org/book.aspx?doi=10.1176/appi.books.9780890425596.893619>.
- Amir, R.E. et al., 1999. Rett syndrome is caused by mutations in X-linked MECP2, encoding methyl-CpG-binding protein 2. *Nature genetics*, 23(2), pp.185–188.
- Anderson, G.M. et al., 1990. The hyperserotonemia of autism. *Annals of the New York Academy of Sciences*, 600(1 The Neurophar), pp.331–40; discussion 341–2. Available at: <http://doi.wiley.com/10.1111/j.1749-6632.1990.tb16893.x> [Accessed November 25, 2014].

- Ang, C.W., Carlson, G.C. & Coulter, D. a, 2006. Massive and specific dysregulation of direct cortical input to the hippocampus in temporal lobe epilepsy. *The Journal of neuroscience : the official journal of the Society for Neuroscience*, 26(46), pp.11850–11856.
- Ang, C.W., Carlson, G.C. & Coulter, D.A., 2005. Hippocampal CA1 circuitry dynamically gates direct cortical inputs preferentially at theta frequencies. *The Journal of neuroscience : the official journal of the Society for Neuroscience*, 25(42), pp.9567–80. Available at: <http://www.pubmedcentral.nih.gov/articlerender.fcgi?artid=2048747&tool=pmcentrez&rendertype=abstract> [Accessed July 11, 2014].
- Anton, R.F. et al., 2008. An evaluation of mu-opioid receptor (OPRM1) as a predictor of naltrexone response in the treatment of alcohol dependence: results from the Combined Pharmacotherapies and Behavioral Interventions for Alcohol Dependence (COMBINE) study. *Archives of general psychiatry*, 65(2), pp.135–44. Available at: <http://www.ncbi.nlm.nih.gov/pubmed/18250251>.
- Arnsten, A.F.T. et al., 1984. Naloxone selective increases information measures processing in humans. *The Journal of Neuroscience*, 4(12), pp.2912–9.
- Balz, J. et al., 2015. GABA concentration in superior temporal sulcus predicts gamma power and perception in the sound-induced flash illusion. *NeuroImage*. Available at: <http://linkinghub.elsevier.com/retrieve/pii/S1053811915010204>.
- Banerjee, A. et al., 2013. Impairment of cortical GABAergic synaptic transmission in an environmental rat model of autism. *The International Journal of Neuropsychopharmacology*, 16(06), pp.1309–1318. Available at: <http://www.pubmedcentral.nih.gov/articlerender.fcgi?artid=3674140&tool=pmcentrez&rendertype=abstract> [Accessed July 22, 2014].
- Barkley, G.L. & Baumgartner, C., 2003. MEG and EEG in epilepsy. *Journal of clinical neurophysiology : official publication of the American Electroencephalographic Society*, 20(3), pp.163–178.
- Barr, C.S. & Goldman, D., 2006. Non-human primate models of inheritance vulnerability to alcohol use disorders. *Addiction*, pp.374–385.
- Bartos, M., Vida, I. & Jonas, P., 2007. Synaptic mechanisms of synchronized gamma

- oscillations in inhibitory interneuron networks. *Nature reviews. Neuroscience*, 8(1), pp.45–56.
- Başar-Eroglu, C. et al., 1996. Gamma-band responses in the brain: A short review of psychophysiological correlates and functional significance. *International Journal of Psychophysiology*, 24(1-2), pp.101–112.
- Basser, P.J., Mattiello, J. & LeBihan, D., 1994. MR diffusion tensor spectroscopy and imaging. *Biophysical Journal*, 66(1), pp.259–267. Available at: <http://linkinghub.elsevier.com/retrieve/pii/S0006349594807751>.
- Befort, K. et al., 2001. A Single Nucleotide Polymorphic Mutation in the Human μ -Opioid Receptor Severely Impairs Receptor Signaling. *Journal of Biological Chemistry*, 276(5), pp.3130–3137.
- Belmonte, M.K. et al., 2004. Autism and abnormal development of brain connectivity. *The Journal of neuroscience : the official journal of the Society for Neuroscience*, 24(42), pp.9228–31. Available at: <http://www.ncbi.nlm.nih.gov/pubmed/15496656> [Accessed August 8, 2014].
- Benasich, A. a et al., 2008. Early cognitive and language skills are linked to resting frontal gamma power across the first 3 years. *Behavioural Brain Research*, 195(2), pp.215–222. Available at: <http://www.pubmedcentral.nih.gov/articlerender.fcgi?artid=2610686&tool=pmcentrez&rendertype=abstract> [Accessed September 17, 2014].
- Berman, J.I. et al., 2015. Alpha-to-gamma phase-amplitude coupling methods and application to autism spectrum disorder. *Brain connectivity*, 5(2), pp.80–90. Available at: <http://www.ncbi.nlm.nih.gov/pubmed/25109843>.
- Berman, J.I. et al., 2012. Variable bandwidth filtering for improved sensitivity of cross-frequency coupling metrics. *Brain connectivity*, 2(3), pp.155–63. Available at: <http://www.pubmedcentral.nih.gov/articlerender.fcgi?artid=3621836&tool=pmcentrez&rendertype=abstract>.
- Bernardino, I. et al., 2013. Neural correlates of visual integration in Williams syndrome: Gamma oscillation patterns in a model of impaired coherence. *Neuropsychologia*, 51(7), pp.1287–1295. Available at: <http://dx.doi.org/10.1016/j.neuropsychologia.2013.03.020>.

- Berry-Kravis, E.M. et al., 2012. Effects of STX209 (Arbaclofen) on Neurobehavioral Function in Children and Adults with Fragile X Syndrome: A Randomized, Controlled, Phase 2 Trial. *Science Translational Medicine*, 4(152), pp.152ra127–152ra127. Available at: <http://www.ncbi.nlm.nih.gov/pubmed/22993294> [Accessed August 8, 2014].
- Billingslea, E.N. et al., 2014. Parvalbumin cell ablation of NMDA-R1 causes increased resting network excitability with associated social and self-care deficits. *Neuropsychopharmacology : official publication of the American College of Neuropsychopharmacology*, 39(7), pp.1603–13. Available at: <http://dx.doi.org/10.1038/npp.2014.7> [Accessed August 8, 2014].
- Bitanhirwe, B.K. et al., 2010. Late Prenatal Immune Activation in Mice Leads to Behavioral and Neurochemical Abnormalities Relevant to the Negative Symptoms of Schizophrenia. *Neuropsychopharmacology*, 35(12), pp.2462–2478. Available at: <http://www.nature.com/doi/10.1038/npp.2010.129>.
- Bond, C. et al., 1998. Single-nucleotide polymorphism in the human mu opioid receptor gene alters beta-endorphin binding and activity: possible implications for opiate addiction. *Proceedings of the National Academy of Sciences of the United States of America*, 95(16), pp.9608–9613.
- Boullin, D.J., Coleman, M. & O'Brien, R.A., 1970. Abnormalities in platelet 5-hydroxytryptamine efflux in patients with infantile autism. *Nature*, 226(5243), pp.371–2. Available at: <http://www.mendeley.com/research/discreteness-conductance-chnge-n-bimolecular-lipid-membrane-presence-certin-antibiotics/> [Accessed August 13, 2014].
- Brenner, C. a et al., 2009. Steady state responses: electrophysiological assessment of sensory function in schizophrenia. *Schizophrenia bulletin*, 35(6), pp.1065–77. Available at: <http://www.pubmedcentral.nih.gov/articlerender.fcgi?artid=2762626&tool=pmcentrez&rendertype=abstract> [Accessed July 31, 2014].
- Briand, L. a. et al., 2015. Mouse Model of OPRM1 (A118G) Polymorphism Increases Sociability and Dominance and Confers Resilience to Social Defeat. *Journal of Neuroscience*, 35(8), pp.3582–3590. Available at: <http://www.jneurosci.org/cgi/doi/10.1523/JNEUROSCI.4685-14.2015>.

- Brown, M.S. et al., 2013. Increased glutamate concentration in the auditory cortex of persons with autism and first-degree relatives: a (1)H-MRS study. *Autism research : official journal of the International Society for Autism Research*, 6(1), pp.1–10. Available at: <http://www.ncbi.nlm.nih.gov/pubmed/23166003> [Accessed August 8, 2014].
- Bucan, M. et al., 2009. Genome-wide analyses of exonic copy number variants in a family-based study point to novel autism susceptibility genes. *PLoS genetics*, 5(6), p.e1000536. Available at: <http://www.pubmedcentral.nih.gov/articlerender.fcgi?artid=2695001&tool=pmcentrez&rendertype=abstract>.
- Buescher, A.V.S. et al., 2014. Costs of Autism Spectrum Disorders in the United Kingdom and the United States. *JAMA pediatrics*, 19104(8), pp.1–8. Available at: <http://www.ncbi.nlm.nih.gov/pubmed/24911948>.
- Buxbaum, J.D. et al., 2002. Association between a GABRB3 polymorphism and autism. *Molecular Psychiatry*, 7(3), pp.311–316.
- Buzsáki, G. & Wang, X.-J., 2012. Mechanisms of Gamma Oscillations. *Annual Review of Neuroscience*, 35(1), pp.203–225. Available at: <http://www.ncbi.nlm.nih.gov/pubmed/22443509> [Accessed July 22, 2014].
- Calfa, G. et al., 2015. Excitation/inhibition imbalance and impaired synaptic inhibition in hippocampal area CA3 of Mecp2 knockout mice. *Hippocampus*, 25(2), pp.159–168. Available at: <http://www.ncbi.nlm.nih.gov/pubmed/25209930> [Accessed November 20, 2014].
- Canolty, R.T. et al., 2006. High gamma power is phase-locked to theta oscillations in human neocortex. *Science (New York, N.Y.)*, 313(5793), pp.1626–8. Available at: <http://www.pubmedcentral.nih.gov/articlerender.fcgi?artid=2628289&tool=pmcentrez&rendertype=abstract> [Accessed August 8, 2014].
- Cardin, J. a et al., 2009. Driving fast-spiking cells induces gamma rhythm and controls sensory responses. *Nature*, 459(7247), pp.663–667. Available at: <http://www.ncbi.nlm.nih.gov/pubmed/19396156> [Accessed July 31, 2014].
- Carlén, M. et al., 2012. A critical role for NMDA receptors in parvalbumin interneurons for gamma rhythm induction and behavior. *Molecular psychiatry*, 17(5), pp.537–48.

Available at:

<http://www.pubmedcentral.nih.gov/articlerender.fcgi?artid=3335079&tool=pmcentrez&rendertype=abstract> [Accessed August 6, 2014].

Carlson, G.C. et al., 2011. Dysbindin-1 mutant mice implicate reduced fast-phasic inhibition as a final common disease mechanism in schizophrenia. *Proceedings of the National Academy of Sciences*, 108(43), pp.E962–E970. Available at: <http://www.pubmedcentral.nih.gov/articlerender.fcgi?artid=3203764&tool=pmcentrez&rendertype=abstract> [Accessed August 8, 2014].

Carlson, G.C. & Coulter, D. a, 2008. In vitro functional imaging in brain slices using fast voltage-sensitive dye imaging combined with whole-cell patch recording. *Nature Protocols*, 3(2), pp.249–255. Available at: <http://www.pubmedcentral.nih.gov/articlerender.fcgi?artid=2483510&tool=pmcentrez&rendertype=abstract> [Accessed August 8, 2014].

Casanova, M.F. et al., 2006. Minicolumnar abnormalities in autism. *Acta neuropathologica*, 112(3), pp.287–303. Available at: <http://www.ncbi.nlm.nih.gov/pubmed/16819561> [Accessed July 22, 2014].

Casanova, M.F. et al., 2002. Minicolumnar pathology in autism. *Neurology*, 58(3), pp.428–32. Available at: <http://www.ncbi.nlm.nih.gov/pubmed/12503647> [Accessed August 8, 2014].

Cellot, G. & Cherubini, E., 2014. Reduced inhibitory gate in the barrel cortex of Neuroligin3R451C knock-in mice, an animal model of autism spectrum disorders. *Physiological Reports*, 2(7), pp.e12077–e12077. Available at: <http://physreports.physiology.org/cgi/doi/10.14814/phy2.12077>.

Cepeda, M.S. & Carr, D.B., 2003. Women experience more pain and require more morphine than men to achieve a similar degree of analgesia. *Anesthesia and Analgesia*, pp.1464–1468. Available at: <http://citeseerx.ist.psu.edu/viewdoc/download?doi=10.1.1.333.6038&rep=rep1&type=pdf>
<http://citeseerx.ist.psu.edu/viewdoc/summary?doi=10.1.1.333.6038>.

Chahrour, M. & Zoghbi, H.Y., 2007. The Story of Rett Syndrome: From Clinic to Neurobiology. *Neuron*, 56(3), pp.422–437.

Chartoff, E.H. et al., 2001. Induction of stereotypy in dopamine-deficient mice requires

- striatal D1 receptor activation. *Proceedings of the National Academy of Sciences of the United States of America*, 98(18), pp.10451–6. Available at: <http://www.pubmedcentral.nih.gov/articlerender.fcgi?artid=56981&tool=pmcentrez&rendertype=abstract>.
- Chou, W.-Y. et al., 2006. Human opioid receptor A118G polymorphism affects intravenous patient-controlled analgesia morphine consumption after total abdominal hysterectomy. *Anesthesiology*, 105(2), pp.334–337. Available at: <http://www.ncbi.nlm.nih.gov/pubmed/16871067>.
- Chugani, D.C. et al., 1999. Developmental changes in brain serotonin synthesis capacity in autistic and nonautistic children. *Annals of neurology*, 45(3), pp.287–95. Available at: <http://www.ncbi.nlm.nih.gov/pubmed/10072042>.
- Chugani, D.C., 2012. Neuroimaging and neurochemistry of autism. *Pediatric clinics of North America*, 59(1), pp.63–73, x. Available at: <http://www.ncbi.nlm.nih.gov/pubmed/22284793> [Accessed September 8, 2014].
- Cicero, T.J., Aylward, S.C. & Meyer, E.R., 2003. Gender differences in the intravenous self-administration of mu opiate agonists. *Pharmacology Biochemistry and Behavior*, 74(3), pp.541–549. Available at: <http://www.ncbi.nlm.nih.gov/pubmed/12543217>.
- Cieślińska, A. et al., 2015. Influence of candidate polymorphisms on the dipeptidyl peptidase IV and μ -opioid receptor genes expression in aspect of the β -casomorphin-7 modulation functions in autism. *Peptides*, 65, pp.6–11. Available at: <http://linkinghub.elsevier.com/retrieve/pii/S0196978115000108>.
- Coltro Campi, C. & Clarke, G.D., 1995. Effects of highly selective kappa-opioid agonists on EEG power spectra and behavioural correlates in conscious rats. *Pharmacology, biochemistry, and behavior*, 51(4), pp.611–6. Available at: <http://www.ncbi.nlm.nih.gov/pubmed/7675832>.
- Connolly, P.M. et al., 2003. Inhibition of auditory evoked potentials and prepulse inhibition of startle in DBA/2J and DBA/2Hsd inbred mouse substrains. *Brain research*, 992(1), pp.85–95. Available at: <http://www.ncbi.nlm.nih.gov/pubmed/14604776>.
- Constantino, J. & Gruber, C.P., 2012. *Social Responsiveness Scale 2nd Editio.*, Los

Angeles, CA: Western Psychological Services.

- Constantino, J.N. et al., 2003. Validation of a brief quantitative measure of autistic traits: Comparison of the social responsiveness scale with the Autism Diagnostic Interview-Revised. *Journal of Autism and Developmental Disorders*, 33(4), pp.427–433.
- Contreras, D. & Llinas, R., 2001. Voltage-sensitive dye imaging of neocortical spatiotemporal dynamics to afferent activation frequency. *The Journal of neuroscience : the official journal of the Society for Neuroscience*, 21(23), pp.9403–13. Available at: <http://www.ncbi.nlm.nih.gov/pubmed/11717373> [Accessed August 8, 2014].
- Cornew, L. et al., 2012. Resting-State Oscillatory Activity in Autism Spectrum Disorders. *Journal of Autism and Developmental Disorders*, 42(9), pp.1884–1894. Available at: <http://www.ncbi.nlm.nih.gov/pubmed/22207057> [Accessed August 8, 2014].
- Cousijn, H. et al., 2014. Resting GABA and glutamate concentrations do not predict visual gamma frequency or amplitude. *Proceedings of the National Academy of Sciences of the United States of America*, 111(25), pp.9301–6. Available at: <http://www.pubmedcentral.nih.gov/articlerender.fcgi?artid=4078853&tool=pmcentrez&rendertype=abstract> [Accessed July 10, 2014].
- Craft, R.M., 2008. Sex differences in analgesic, reinforcing, discriminative, and motoric effects of opioids. *Experimental and Clinical Psychopharmacology*, 16(5), pp.376–385. Available at: <http://www.ncbi.nlm.nih.gov/pubmed/18837634>.
- Crawley, J.N., 2007. *What's Wrong With My Mouse?*, Hoboken, NJ, USA: John Wiley & Sons, Inc. Available at: <http://doi.wiley.com/10.1002/0470119055>.
- Csicsvari, J. et al., 2003. Mechanisms of gamma oscillations in the hippocampus of the behaving rat. *Neuron*, 37(2), pp.311–22. Available at: <http://www.ncbi.nlm.nih.gov/pubmed/12546825> [Accessed August 8, 2014].
- Danielsson, S. et al., 2005. Epilepsy in young adults with autism: A prospective population-based follow-up study of 120 individuals diagnosed in childhood. *Epilepsia*, 46(6), pp.918–923.

- Dawson, G. et al., 2000. Case Study of the Development of an Infant with Autism from Birth to Two Years of Age. *Journal of Applied Developmental Psychology*, 21(3), pp.299–313. Available at: <http://linkinghub.elsevier.com/retrieve/pii/S0193397399000428>.
- Dawson, G. et al., 2012. Early Behavioral Intervention Is Associated With Normalized Brain Activity in Young Children With Autism. *Journal of the American Academy of Child & Adolescent Psychiatry*, 51(11), pp.1150–1159. Available at: <http://www.pubmedcentral.nih.gov/articlerender.fcgi?artid=3607427&tool=pmcentrez&rendertype=abstract> [Accessed August 20, 2014].
- Dawson, G. et al., 2010. Randomized, controlled trial of an intervention for toddlers with autism: the Early Start Denver Model. *Pediatrics*, 125(1), pp.e17–23. Available at: <http://www.ncbi.nlm.nih.gov/pubmed/19948568> [Accessed July 15, 2014].
- Definitions, B. & Group, W., 2001. Biomarkers and surrogate endpoints: Preferred definitions and conceptual framework. *Clinical Pharmacology & Therapeutics*, 69(3), pp.89–95. Available at: <http://doi.wiley.com/10.1067/mcp.2001.113989>.
- Delorme, A. & Makeig, S., 2004. EEGLAB: An open source toolbox for analysis of single-trial EEG dynamics including independent component analysis. *Journal of Neuroscience Methods*, 134(1), pp.9–21.
- Deutsch, S.I. et al., 2010. Cholinergic Abnormalities in Autism. *Clinical Neuropharmacology*, 33(3), pp.114–120. Available at: <http://www.ncbi.nlm.nih.gov/pubmed/20190638> [Accessed August 8, 2014].
- Developmental Disabilities Monitoring Network Surveillance Year 2010 Principal Investigators & Centers for Disease Control and Prevention (CDC), 2014. Prevalence of autism spectrum disorder among children aged 8 years - autism and developmental disabilities monitoring network, 11 sites, United States, 2010. *Morbidity and mortality weekly report. Surveillance summaries (Washington, D.C. : 2002)*, 63(2), pp.1–21. Available at: <http://www.ncbi.nlm.nih.gov/pubmed/24670961> [Accessed September 13, 2014].
- Dockstader, C. et al., 2012. White matter maturation in visual and motor areas predicts the latency of visual activation in children. *Human brain mapping*, 33(1), pp.179–91. Available at: <http://www.ncbi.nlm.nih.gov/pubmed/21432944> [Accessed December 22, 2014].

- Drake, C.T. & Milner, T. a., 2002. Mu opioid receptors are in discrete hippocampal interneuron subpopulations. *Hippocampus*, 12, pp.119–136.
- Drake, C.T. & Milner, T. a., 1999. Mu opioid receptors are in somatodendritic and axonal compartments of GABAergic neurons in rat hippocampal formation. *Brain Research*, 849, pp.203–215.
- Drakenberg, K. et al., 2006. Mu opioid receptor A118G polymorphism in association with striatal opioid neuropeptide gene expression in heroin abusers. *Proceedings of the National Academy of Sciences of the United States of America*, 103(20), pp.7883–7888.
- Dunn, L.M. & Dunn, D., 2007. *Peabody Picture Vocabulary Test* 4th Editio., San Antonio, TX: NCS Pearson.
- Ecker, C. et al., 2010. Describing the Brain in Autism in Five Dimensions--Magnetic Resonance Imaging-Assisted Diagnosis of Autism Spectrum Disorder Using a Multiparameter Classification Approach. *Journal of Neuroscience*, 30(32), pp.10612–10623. Available at: <http://www.jneurosci.org/cgi/doi/10.1523/JNEUROSCI.5413-09.2010>.
- Ecker, C. et al., 2010. Investigating the predictive value of whole-brain structural MR scans in autism: A pattern classification approach. *NeuroImage*, 49(1), pp.44–56. Available at: <http://linkinghub.elsevier.com/retrieve/pii/S1053811909009045>.
- Edgar, J.C. et al., 2015. Auditory encoding abnormalities in children with autism spectrum disorder suggest delayed development of auditory cortex. *Molecular autism*, 6(69). Available at: <http://www.molecularautism.com/content/6/1/69>.
- Edgar, J.C., Chen, Y.-H., et al., 2014. Cortical thickness as a contributor to abnormal oscillations in schizophrenia? *NeuroImage: Clinical*, 4, pp.122–129. Available at: <http://dx.doi.org/10.1016/j.nicl.2013.11.004>.
- Edgar, J.C., Lanza, M.R., et al., 2014. Missing and delayed auditory responses in young and older children with autism spectrum disorders. *Frontiers in human neuroscience*, 8(June), p.417. Available at: <http://www.pubmedcentral.nih.gov/articlerender.fcgi?artid=4047517&tool=pmcentrez&rendertype=abstract> [Accessed September 30, 2014].

- Edgar, J.C. et al., 2015. Neuromagnetic oscillations predict evoked-response latency delays and core language deficits in autism spectrum disorders. *Journal of autism and developmental disorders*, 45(2), pp.395–405. Available at: <http://www.ncbi.nlm.nih.gov/pubmed/23963591> [Accessed August 8, 2014].
- Edgar, J.C. et al., 2016. Translating Adult Electrophysiology Findings to Younger Patient Populations: Difficulty Measuring 40-Hz Auditory Steady-State Responses in Typically Developing Children and Children with Autism Spectrum Disorder. *Developmental neuroscience*. Available at: <http://www.ncbi.nlm.nih.gov/pubmed/26730806>.
- Ehlers, C.L., 1989. EEG and ERP responses to naloxone and ethanol in monkeys. *Progress in neuro-psychopharmacology & biological psychiatry*, 13(David 1980), pp.217–228.
- Elsabbagh, M. et al., 2009. Neural correlates of eye gaze processing in the infant broader autism phenotype. *Biological psychiatry*, 65(1), pp.31–8. Available at: <http://www.ncbi.nlm.nih.gov/pubmed/19064038> [Accessed September 13, 2014].
- Engineer, C.T. et al., 2014. Degraded auditory processing in a rat model of autism limits the speech representation in non-primary auditory cortex. *Developmental neurobiology*, 74(10), pp.972–86. Available at: <http://www.ncbi.nlm.nih.gov/pubmed/24639033> [Accessed November 24, 2014].
- Engineer, C.T. et al., 2015. Degraded neural and behavioral processing of speech sounds in a rat model of Rett syndrome. *Neurobiology of Disease*, 83, pp.26–34. Available at: <http://dx.doi.org/10.1016/j.nbd.2015.08.019>.
- Engineer, C.T. et al., 2014. Speech sound discrimination training improves auditory cortex responses in a rat model of autism. *Frontiers in Systems Neuroscience*, 8(August), pp.1–10. Available at: http://www.frontiersin.org/Systems_Neuroscience/10.3389/fnsys.2014.00137/abstract [Accessed August 8, 2014].
- Erickson, C. a et al., 2014. STX209 (arbaclofen) for autism spectrum disorders: an 8-week open-label study. *Journal of autism and developmental disorders*, 44(4), pp.958–64. Available at: <http://www.ncbi.nlm.nih.gov/pubmed/24272415> [Accessed August 8, 2014].

- Fatemi, S.H. et al., 2014. Downregulation of GABAA receptor protein subunits $\alpha 6$, $\beta 2$, δ , ϵ , $\gamma 2$, θ , and $\rho 2$ in superior frontal cortex of subjects with autism. *Journal of autism and developmental disorders*, 44(8), pp.1833–45. Available at: <http://www.ncbi.nlm.nih.gov/pubmed/24668190> [Accessed July 23, 2014].
- Fatemi, S.H., Folsom, T.D., et al., 2009. Expression of GABA(B) receptors is altered in brains of subjects with autism. *Cerebellum (London, England)*, 8(1), pp.64–9. Available at: <http://www.pubmedcentral.nih.gov/articlerender.fcgi?artid=2732344&tool=pmcentrez&rendertype=abstract> [Accessed August 8, 2014].
- Fatemi, S.H., Reutiman, T.J., et al., 2009. GABA(A) receptor downregulation in brains of subjects with autism. *Journal of autism and developmental disorders*, 39(2), pp.223–30. Available at: <http://www.pubmedcentral.nih.gov/articlerender.fcgi?artid=2697059&tool=pmcentrez&rendertype=abstract> [Accessed August 8, 2014].
- Fatemi, S.H. et al., 2002. Glutamic acid decarboxylase 65 and 67 kDa proteins are reduced in autistic parietal and cerebellar cortices. *Biological psychiatry*, 52(8), pp.805–10. Available at: <http://www.ncbi.nlm.nih.gov/pubmed/12372652> [Accessed August 8, 2014].
- Fatemi, S.H. et al., 2008. Maternal infection leads to abnormal gene regulation and brain atrophy in mouse offspring: Implications for genesis of neurodevelopmental disorders. *Schizophrenia Research*, 99(1-3), pp.56–70. Available at: <http://linkinghub.elsevier.com/retrieve/pii/S0920996407005191>.
- Faulkner, H.J., Traub, R.D. & Whittington, M. a, 1998. Disruption of synchronous gamma oscillations in the rat hippocampal slice: a common mechanism of anaesthetic drug action. *British journal of pharmacology*, 125(3), pp.483–92. Available at: <http://www.pubmedcentral.nih.gov/articlerender.fcgi?artid=1565655&tool=pmcentrez&rendertype=abstract> [Accessed August 8, 2014].
- Ferguson, J.N. et al., 2000. Social amnesia in mice lacking the oxytocin gene. *Nature genetics*, 25(3), pp.284–288.
- FieldtripWiki, 2015a. Use independent component analysis (ICA) to remove ECG artifacts. Available at:

[http://www.fieldtriptoolbox.org/example/use_independent_component_analysis_ica_to_remove_ecg_artifacts?s\[\]=artifact&s\[\]=removal](http://www.fieldtriptoolbox.org/example/use_independent_component_analysis_ica_to_remove_ecg_artifacts?s[]=artifact&s[]=removal) [Accessed January 1, 2015].

FieldtripWiki, 2015b. Use independent component analysis (ICA) to remove EOG artifacts. Available at:
[http://www.fieldtriptoolbox.org/example/use_independent_component_analysis_ica_to_remove_eog_artifacts?s\[\]=artifact&s\[\]=removal](http://www.fieldtriptoolbox.org/example/use_independent_component_analysis_ica_to_remove_eog_artifacts?s[]=artifact&s[]=removal) [Accessed January 1, 2015].

Fonov, V. et al., 2011. Unbiased average age-appropriate atlases for pediatric studies. *NeuroImage*, 54(1), pp.313–327. Available at:
<http://dx.doi.org/10.1016/j.neuroimage.2010.07.033>.

Fuchs, E.C. et al., 2007. Recruitment of parvalbumin-positive interneurons determines hippocampal function and associated behavior. *Neuron*, 53(4), pp.591–604. Available at: <http://www.sciencedirect.com/science/article/pii/S0896627307000724>.

Gaetz, W. et al., 2012. Functional and structural correlates of the aging brain: relating visual cortex (V1) gamma band responses to age-related structural change. *Human brain mapping*, 33(9), pp.2035–46. Available at:
<http://www.pubmedcentral.nih.gov/articlerender.fcgi?artid=3197906&tool=pmcentrez&rendertype=abstract> [Accessed September 17, 2014].

Gaetz, W. et al., 2014. GABA estimation in the brains of children on the autism spectrum: measurement precision and regional cortical variation. *NeuroImage*, 86, pp.1–9. Available at: <http://www.ncbi.nlm.nih.gov/pubmed/23707581> [Accessed August 8, 2014].

Gaetz, W. et al., 2011. Relating MEG measured motor cortical oscillations to resting γ -aminobutyric acid (GABA) concentration. *NeuroImage*, 55(2), pp.616–21. Available at: <http://www.ncbi.nlm.nih.gov/pubmed/21215806> [Accessed August 8, 2014].

Gage, N.M., Siegel, B., Callen, M., et al., 2003. Cortical sound processing in children with autism disorder: an MEG investigation. *Neuroreport*, 14(16), pp.2047–51.

Gage, N.M., Siegel, B. & Roberts, T.P., 2003. Cortical auditory system maturational abnormalities in children with autism disorder: an MEG investigation. *Developmental Brain Research*, 144(2), pp.201–209. Available at:
<http://www.ncbi.nlm.nih.gov/pubmed/12935917> [Accessed August 8, 2014].

- Gandal, M.J., Sisti, J., et al., 2012. GABAB-mediated rescue of altered excitatory-inhibitory balance, gamma synchrony and behavioral deficits following constitutive NMDAR-hypofunction. *Translational psychiatry*, 2(7), p.e142. Available at: <http://www.pubmedcentral.nih.gov/articlerender.fcgi?artid=3410621&tool=pmcentrez&rendertype=abstract> [Accessed August 8, 2014].
- Gandal, M.J., Anderson, R.L., et al., 2012. Mice with reduced NMDA receptor expression: more consistent with autism than schizophrenia? *Genes, brain, and behavior*, 11(6), pp.740–50. Available at: <http://www.ncbi.nlm.nih.gov/pubmed/22726567> [Accessed August 8, 2014].
- Gandal, M.J. et al., 2010. Validating γ oscillations and delayed auditory responses as translational biomarkers of autism. *Biological psychiatry*, 68(12), pp.1100–6. Available at: <http://www.ncbi.nlm.nih.gov/pubmed/21130222> [Accessed August 8, 2014].
- Gevens, a et al., 1995. Mapping cognitive brain function with modern high-resolution electroencephalography. *Trends in neurosciences*, 18(10), pp.429–436.
- Glickfeld, L.L., Atallah, B. V & Scanziani, M., 2008. Complementary modulation of somatic inhibition by opioids and cannabinoids. *The Journal of neuroscience : the official journal of the Society for Neuroscience*, 28(8), pp.1824–32. Available at: <http://www.pubmedcentral.nih.gov/articlerender.fcgi?artid=3505026&tool=pmcentrez&rendertype=abstract>.
- Goffin, D. et al., 2012. Rett syndrome mutation MeCP2 T158A disrupts DNA binding, protein stability and ERP responses. *Nature neuroscience*, 15(2), pp.274–83. Available at: <http://www.pubmedcentral.nih.gov/articlerender.fcgi?artid=3267879&tool=pmcentrez&rendertype=abstract> [Accessed July 30, 2014].
- Gogolla, N. et al., 2009. Common circuit defect of excitatory-inhibitory balance in mouse models of autism. *Journal of ...*, 1(2), pp.172–81. Available at: <http://www.pubmedcentral.nih.gov/articlerender.fcgi?artid=2906812&tool=pmcentrez&rendertype=abstract> [Accessed February 4, 2013].
- Gogolla, N. et al., 2014. Sensory Integration in Mouse Insular Cortex Reflects GABA Circuit Maturation. *Neuron*, 83(4), pp.894–905. Available at: <http://dx.doi.org/10.1016/j.neuron.2014.06.033> [Accessed August 1, 2014].

- Gonzalez-Burgos, G. & Lewis, D. a, 2008. GABA neurons and the mechanisms of network oscillations: implications for understanding cortical dysfunction in schizophrenia. *Schizophrenia bulletin*, 34(5), pp.944–61. Available at: <http://www.pubmedcentral.nih.gov/articlerender.fcgi?artid=2518635&tool=pmcentrez&rendertype=abstract> [Accessed July 10, 2014].
- Gordon, I. et al., 2013. Oxytocin enhances brain function in children with autism. *Proceedings of the National Academy of Sciences of the United States of America*, 110(52), pp.20953–8. Available at: <http://www.pubmedcentral.nih.gov/articlerender.fcgi?artid=3876263&tool=pmcentrez&rendertype=abstract> [Accessed July 10, 2014].
- Gotham, K., Pickles, A. & Lord, C., 2009. Standardizing ADOS Scores for a Measure of Severity in Autism Spectrum Disorders. *Journal of Autism and Developmental Disorders*, 39(5), pp.693–705. Available at: <http://link.springer.com/10.1007/s10803-008-0674-3>.
- Gou, Z., Choudhury, N. & Benasich, A. a, 2011. Resting frontal gamma power at 16, 24 and 36 months predicts individual differences in language and cognition at 4 and 5 years. *Behavioural brain research*, 220(2), pp.263–70. Available at: <http://www.pubmedcentral.nih.gov/articlerender.fcgi?artid=3107993&tool=pmcentrez&rendertype=abstract> [Accessed September 30, 2014].
- Granpeesheh, D. et al., 2009. Retrospective analysis of clinical records in 38 cases of recovery from autism. *Annals of clinical psychiatry : official journal of the American Academy of Clinical Psychiatrists*, 21(4), pp.195–204.
- Gray, C.M. et al., 1989. Oscillatory responses in cat visual cortex exhibit inter-columnar synchronization which reflects global stimulus properties. *Nature*, 338(6213), pp.334–7. Available at: <http://www.ncbi.nlm.nih.gov/pubmed/?term=2922061> [Accessed August 8, 2014].
- Green, L. et al., 2001. Oxytocin and autistic disorder: Alterations in peptide forms. *Biological Psychiatry*, 50(8), pp.609–613.
- Grice, S.J. et al., 2001. Disordered visual processing and oscillatory brain activity in autism and Williams syndrome. *Neuroreport*, 12(12), pp.2697–700. Available at: <http://www.ncbi.nlm.nih.gov/pubmed/11522950> [Accessed September 30, 2014].

- Groves, N.J. et al., 2013. Adult vitamin D deficiency leads to behavioural and brain neurochemical alterations in C57BL/6J and BALB/c mice. *Behavioural Brain Research*, 241(1), pp.120–131. Available at: <http://dx.doi.org/10.1016/j.bbr.2012.12.001>.
- Gruss, M. & Braun, K., 2004. Age- and region-specific imbalances of basal amino acids and monoamine metabolism in limbic regions of female Fmr1 knock-out mice. *Neurochemistry international*, 45(1), pp.81–8. Available at: <http://www.ncbi.nlm.nih.gov/pubmed/15082225>.
- Gruss, M. & Braun, K., 2001. Alterations of amino acids and monoamine metabolism in male Fmr1 knockout mice: a putative animal model of the human fragile X mental retardation syndrome. *Neural plasticity*, 8(4), pp.285–98. Available at: <http://www.pubmedcentral.nih.gov/articlerender.fcgi?artid=2565378&tool=pmcentrez&rendertype=abstract> [Accessed August 8, 2014].
- Gulyás, A.I. et al., 2010. Parvalbumin-containing fast-spiking basket cells generate the field potential oscillations induced by cholinergic receptor activation in the hippocampus. *The Journal of neuroscience : the official journal of the Society for Neuroscience*, 30(45), pp.15134–45. Available at: <http://www.pubmedcentral.nih.gov/articlerender.fcgi?artid=3044880&tool=pmcentrez&rendertype=abstract>.
- Hall, S.D. et al., 2010. Neuronal network pharmacodynamics of GABAergic modulation in the human cortex determined using pharmaco-magnetoencephalography. *Human brain mapping*, 31(4), pp.581–94. Available at: <http://www.pubmedcentral.nih.gov/articlerender.fcgi?artid=3179593&tool=pmcentrez&rendertype=abstract> [Accessed August 8, 2014].
- Hämäläinen, M.S. et al., 1993. Magnetoencephalography - theory, instrumentation, and applications to noninvasive studies of the working human brain. *Reviews of modern physics*, 65(2), pp.413–505.
- Han, S. et al., 2012. Autistic-like behaviour in Scn1a^{+/-} mice and rescue by enhanced GABA-mediated neurotransmission. *Nature*, 489(7416), pp.385–90. Available at: <http://dx.doi.org/10.1038/nature11356> [Accessed July 10, 2014].
- Harada, M. et al., 2011. Non-invasive evaluation of the GABAergic/glutamatergic system in autistic patients observed by MEGA-editing proton MR spectroscopy using a

- clinical 3 tesla instrument. *Journal of autism and developmental disorders*, 41(4), pp.447–54. Available at: <http://www.ncbi.nlm.nih.gov/pubmed/20652388> [Accessed August 8, 2014].
- Hari, R. et al., 1980. Auditory evoked transient and sustained magnetic fields of the human brain. Localization of neural generators. *Experimental brain research*, 40(2), pp.237–40. Available at: <http://www.scopus.com/inward/record.url?eid=2-s2.0-0018825765&partnerID=tZOtx3y1>.
- Van Hecke, A.V. et al., 2013. Measuring the Plasticity of Social Approach: A Randomized Controlled Trial of the Effects of the PEERS Intervention on EEG Asymmetry in Adolescents with Autism Spectrum Disorders. *Journal of autism and developmental disorders*. Available at: <http://www.ncbi.nlm.nih.gov/pubmed/23812665> [Accessed September 29, 2014].
- Helt, M. et al., 2008. Can children with autism recover? If so, how? *Neuropsychology Review*, 18(4), pp.339–366.
- Herbert, M.R. et al., 2004. Localization of white matter volume increase in autism and developmental language disorder. *Annals of Neurology*, 55(4), pp.530–540. Available at: <http://doi.wiley.com/10.1002/ana.20032>.
- Herdman, A.T. et al., 2003. Determination of activation areas in the human auditory cortex by means of synthetic aperture magnetometry. *NeuroImage*, 20(2), pp.995–1005.
- Herrmann, C.S. & Demiralp, T., 2005. Human EEG gamma oscillations in neuropsychiatric disorders. *Clinical neurophysiology : official journal of the International Federation of Clinical Neurophysiology*, 116(12), pp.2719–33. Available at: <http://www.ncbi.nlm.nih.gov/pubmed/16253555> [Accessed August 8, 2014].
- Herrmann, C.S., Fründ, I. & Lenz, D., 2010. Human gamma-band activity: a review on cognitive and behavioral correlates and network models. *Neuroscience and biobehavioral reviews*, 34(7), pp.981–92. Available at: <http://www.ncbi.nlm.nih.gov/pubmed/19744515> [Accessed August 8, 2014].
- Hertz, L., 2013. The Glutamate-Glutamine (GABA) Cycle: Importance of Late Postnatal Development and Potential Reciprocal Interactions between Biosynthesis and

- Degradation. *Frontiers in endocrinology*, 4(May), p.59. Available at: <http://www.pubmedcentral.nih.gov/articlerender.fcgi?artid=3664331&tool=pmcentrez&rendertype=abstract>.
- Huang, P. et al., 2012. A common single nucleotide polymorphism A118G of the μ opioid receptor alters its N-glycosylation and protein stability. *Biochemical Journal*, 441(1), pp.379–386. Available at: <http://www.biochemj.org/bj/441/bj4410379.htm>.
- Hurley, R.S.E. et al., 2007. The broad autism phenotype questionnaire. *Journal of autism and developmental disorders*, 37(9), pp.1679–90. Available at: <http://www.ncbi.nlm.nih.gov/pubmed/17146701>.
- Hus, V. & Lord, C., 2014. The Autism Diagnostic Observation Schedule, Module 4: Revised Algorithm and Standardized Severity Scores. *Journal of Autism and Developmental Disorders*, 44(8), pp.1996–2012. Available at: <http://link.springer.com/10.1007/s10803-014-2080-3>.
- Ide, S., Itoh, M. & Goto, Y.I., 2005. Defect in normal developmental increase of the brain biogenic amine concentrations in the mecp2-null mouse. *Neuroscience Letters*, 386, pp.14–17.
- Ingalhalikar, M. et al., 2014. Creating multimodal predictors using missing data: Classifying and subtyping autism spectrum disorder. *Journal of neuroscience methods*, 235, pp.1–9. Available at: <http://www.ncbi.nlm.nih.gov/pubmed/24983132> [Accessed September 30, 2014].
- Jamain, S. et al., 2002. Linkage and association of the glutamate receptor 6 gene with autism. *Molecular psychiatry*, 7(3), pp.302–10. Available at: <http://www.pubmedcentral.nih.gov/articlerender.fcgi?artid=2547854&tool=pmcentrez&rendertype=abstract> [Accessed August 8, 2014].
- Jenkins, J. et al., 2014. Auditory Evoked M100 Response Latency Is Delayed in Children with 16p11.2 Deletion but not 16p11.2 Duplication. *Cerebral Cortex*, in press.
- Jou, R.J. et al., 2011. Structural neural phenotype of autism: preliminary evidence from a diffusion tensor imaging study using tract-based spatial statistics. *AJNR. American journal of neuroradiology*, 32(9), pp.1607–13. Available at: <http://www.ncbi.nlm.nih.gov/pubmed/21799040> [Accessed August 7, 2014].

- Karvat, G. & Kimchi, T., 2014. Acetylcholine elevation relieves cognitive rigidity and social deficiency in a mouse model of autism. *Neuropsychopharmacology : official publication of the American College of Neuropsychopharmacology*, 39(4), pp.831–40. Available at: <http://www.ncbi.nlm.nih.gov/pubmed/24096295> [Accessed September 18, 2014].
- Kelley, E. et al., 2006. Residual language deficits in optimal outcome children with a history of autism. *Journal of Autism and Developmental Disorders*, 36(6), pp.807–828.
- Kepler, K.L. et al., 1989. Roles of gender, gonadectomy and estrous phase in the analgesic effects of intracerebroventricular morphine in rats. *Pharmacology, biochemistry, and behavior*, 34(1), pp.119–27. Available at: <http://www.ncbi.nlm.nih.gov/pubmed/2626443>.
- Khan, S. et al., 2013. Local and long-range functional connectivity is reduced in concert in autism spectrum disorders. *Proceedings of the National Academy of Sciences of the United States of America*, 110(8), pp.3107–12. Available at: <http://www.pnas.org/cgi/content/long/110/8/3107> [Accessed August 8, 2014].
- Kim, S.-Y. et al., 2011. Non-clustered protocadherin. *Cell Adhesion & Migration*, 5(2), pp.97–105. Available at: <http://www.tandfonline.com/doi/abs/10.4161/cam.5.2.14374>.
- Klausberger, T., Roberts, J.D. & Somogyi, P., 2002. Cell Type- and Input-Specific Differences in the Number and Subtypes of Synaptic GABAA Receptors in the Hippocampus. *Journal of Neuroscience*, 22(7), pp.2513–2521. Available at: <http://www.jneurosci.org/cgi/content/abstract/22/7/2513>.
- Knapman, A. & Connor, M., 2015. Cellular signalling of non-synonymous single-nucleotide polymorphisms of the human μ -opioid receptor (OPRM1). *British Journal of Pharmacology*, 172(2), pp.349–363. Available at: <http://www.pubmedcentral.nih.gov/articlerender.fcgi?artid=4292952&tool=pmcentrez&rendertype=abstract> \n<http://doi.wiley.com/10.1111/bph.12644>.
- Knapman, A., Santiago, M. & Connor, M., 2014. Buprenorphine signalling is compromised at the N40D polymorphism of the human μ opioid receptor in vitro. *British journal of pharmacology*, 171(18), pp.4273–88. Available at: <http://www.ncbi.nlm.nih.gov/pubmed/24846673>.

- Kohl, M.M. & Paulsen, O., 2010. The roles of GABAB receptors in cortical network activity. *Advances in pharmacology (San Diego, Calif.)*, 58(10), pp.205–29. Available at: [http://dx.doi.org/10.1016/S1054-3589\(10\)58009-8](http://dx.doi.org/10.1016/S1054-3589(10)58009-8) [Accessed August 8, 2014].
- Krishnan, G.P. et al., 2009. Steady state and induced auditory gamma deficits in schizophrenia. *NeuroImage*, 47(4), pp.1711–1719. Available at: <http://dx.doi.org/10.1016/j.neuroimage.2009.03.085>.
- Kujala, J. et al., 2015. Gamma oscillations in V1 are correlated with GABAA receptor density: A multi-modal MEG and Flumazenil-PET study. *Scientific Reports*, 5(October), p.16347. Available at: <http://www.nature.com/articles/srep16347>.
- Kwon, J.S. et al., 1999. Gamma frequency-range abnormalities to auditory stimulation in schizophrenia. *Archives of general psychiatry*, 56(11), pp.1001–5. Available at: <http://www.pubmedcentral.nih.gov/articlerender.fcgi?artid=2863027&tool=pmcentrez&rendertype=abstract>.
- de Lacy, N. & King, B.H., 2013. Revisiting the Relationship Between Autism and Schizophrenia: Toward an Integrated Neurobiology. *Annual Review of Clinical Psychology*, 9(1), pp.555–587. Available at: <http://www.ncbi.nlm.nih.gov/pubmed/23537488>.
- Lally, N. et al., 2014. Glutamatergic correlates of gamma-band oscillatory activity during cognition: a concurrent ER-MRS and EEG study. *NeuroImage*, 85 Pt 2, pp.823–33. Available at: <http://www.ncbi.nlm.nih.gov/pubmed/23891885> [Accessed August 25, 2014].
- Lang, M. et al., 2014. Rescue of behavioral and EEG deficits in male and female Mecp2-deficient mice by delayed Mecp2 gene reactivation. *Human Molecular Genetics*, 23(2), pp.303–318. Available at: <http://www.hmg.oxfordjournals.org/cgi/doi/10.1093/hmg/ddt421>.
- Lange, N. et al., 2010. Atypical diffusion tensor hemispheric asymmetry in autism. *Autism research : official journal of the International Society for Autism Research*, 3(6), pp.350–8. Available at: <http://www.pubmedcentral.nih.gov/articlerender.fcgi?artid=3215255&tool=pmcentrez&rendertype=abstract> [Accessed November 25, 2014].

- Lavoie, A.M. et al., 1997. Activation and deactivation rates of recombinant GABA(A) receptor channels are dependent on alpha-subunit isoform. *Biophysical journal*, 73(5), pp.2518–2526. Available at: [http://dx.doi.org/10.1016/S0006-3495\(97\)78280-8](http://dx.doi.org/10.1016/S0006-3495(97)78280-8).
- Lawrence, Y. a et al., 2010. Parvalbumin-, calbindin-, and calretinin-immunoreactive hippocampal interneuron density in autism. *Acta neurologica Scandinavica*, 121(2), pp.99–108. Available at: <http://www.ncbi.nlm.nih.gov/pubmed/19719810> [Accessed August 8, 2014].
- Leahy, R.M. et al., 1998. A study of dipole localization accuracy for MEG and EEG using a human skull phantom. *Electroencephalography and clinical neurophysiology*, 107(2), pp.159–73. Available at: <http://www.ncbi.nlm.nih.gov/pubmed/9751287> [Accessed October 28, 2014].
- Leicht, G. et al., 2010. Reduced early auditory evoked gamma-band response in patients with schizophrenia. *Biological psychiatry*, 67(3), pp.224–31. Available at: <http://www.ncbi.nlm.nih.gov/pubmed/19765689> [Accessed August 8, 2014].
- Lemonnier, E. et al., 2012. A randomised controlled trial of bumetanide in the treatment of autism in children. *Translational psychiatry*, 2(12), p.e202. Available at: <http://www.ncbi.nlm.nih.gov/pubmed/23233021> [Accessed August 8, 2014].
- Lerman, C. et al., 2004. The functional mu opioid receptor (OPRM1) Asn40Asp variant predicts short-term response to nicotine replacement therapy in a clinical trial. *The pharmacogenomics journal*, 4(3), pp.184–192.
- Liao, W. et al., 2012. MeCP2^{+/-} mouse model of RTT reproduces auditory phenotypes associated with Rett syndrome and replicate select EEG endophenotypes of autism spectrum disorder. *Neurobiology of disease*, 46(1), pp.88–92. Available at: <http://www.ncbi.nlm.nih.gov/pubmed/22249109> [Accessed August 8, 2014].
- Lieberwirth, C. & Wang, Z., 2014. Social bonding: regulation by neuropeptides. *Frontiers in neuroscience*, 8(June), p.171. Available at: <http://www.pubmedcentral.nih.gov/articlerender.fcgi?artid=4067905&tool=pmcentrez&rendertype=abstract>.
- Lin, H.-C. et al., 2013. The amygdala excitatory/inhibitory balance in a valproate-induced rat autism model. *PloS one*, 8(1), p.e55248. Available at:

<http://www.pubmedcentral.nih.gov/articlerender.fcgi?artid=3558482&tool=pmcentrez&rendertype=abstract> [Accessed August 8, 2014].

- Lodge, D.J., Behrens, M.M. & Grace, A. a, 2009. A loss of parvalbumin-containing interneurons is associated with diminished oscillatory activity in an animal model of schizophrenia. *The Journal of neuroscience : the official journal of the Society for Neuroscience*, 29(8), pp.2344–2354.
- Lord, C. et al., 2000. The Autism Diagnostic Observation Schedule-Generic: A standard measure of social and communication deficits associated with the spectrum of autism. *Journal of Autism and Developmental Disorders*, 30(3), pp.205–223.
- Loyd, D.R., Wang, X. & Murphy, A.Z., 2008. Sex differences in micro-opioid receptor expression in the rat midbrain periaqueductal gray are essential for eliciting sex differences in morphine analgesia. *The Journal of neuroscience : the official journal of the Society for Neuroscience*, 28(52), pp.14007–14017.
- Lynch, G.S. et al., 1981. Effects of enkephalin, morphine, and naloxone on the electrical activity of the in vitro hippocampal slice preparation. *Experimental neurology*, 71, pp.527–540.
- Macdonald, K.D. et al., 1998. Focal stimulation of the thalamic reticular nucleus induces focal gamma waves in cortex. *Journal of neurophysiology*, 79(1), pp.474–7. Available at: <http://www.ncbi.nlm.nih.gov/pubmed/9425216>.
- Mague, S.D. et al., 2015. Mouse model of OPRM1 (A118G) polymorphism has altered hippocampal function. *Neuropharmacology*, 1(May), pp.1–10. Available at: <http://linkinghub.elsevier.com/retrieve/pii/S0028390815001616>.
- Mague, S.D. et al., 2009. Mouse model of OPRM1 (A118G) polymorphism has sex-specific effects on drug-mediated behavior. *Proceedings of the National Academy of Sciences of the United States of America*, 106(26), pp.10847–10852.
- Mague, S.D. & Blendy, J. a., 2010. OPRM1 SNP (A118G): Involvement in disease development, treatment response, and animal models. *Drug and Alcohol Dependence*, 108(3), pp.172–182. Available at: <http://dx.doi.org/10.1016/j.drugalcdep.2009.12.016>.

- Maharajh, K. et al., 2007. Auditory steady state and transient gamma band activity in bipolar disorder. *International Congress Series*, 1300, pp.707–710. Available at: <http://linkinghub.elsevier.com/retrieve/pii/S0531513107000258> [Accessed September 19, 2014].
- Mahmoud, S.M.B. et al., 2011. Pharmacological Consequence of the A118G [mu] Opioid Receptor Polymorphism on Morphine- and Fentanyl-mediated Modulation of Ca²⁺ Channels in Humanized Mouse Sensory Neurons. *Anesthesiology*, 115(5), pp.1054–1062.
- Mann, E.O. & Mody, I., 2010. Control of hippocampal gamma oscillation frequency by tonic inhibition and excitation of interneurons. *Nature neuroscience*, 13(2), pp.205–12. Available at: <http://www.pubmedcentral.nih.gov/articlerender.fcgi?artid=2843436&tool=pmcentrez&rendertype=abstract> [Accessed August 8, 2014].
- Margas, W. et al., 2007. Modulation of Ca. *Journal of Neurophysiology*, (Ikeda 1991), pp.1058 –1067.
- Martin, D.L. & Rimvall, K., 1993. Regulation of gamma-aminobutyric acid synthesis in the brain. *Journal of neurochemistry*, 60(2), pp.395–407.
- Maxwell, C.R., Villalobos, M.E., et al., 2013. Atypical Laterality of Resting Gamma Oscillations in Autism Spectrum Disorders. *Journal of autism and developmental disorders*, p.[Epub ahead of print]. Available at: <http://www.ncbi.nlm.nih.gov/pubmed/23624928> [Accessed August 8, 2014].
- Maxwell, C.R., Parish-Morris, J., et al., 2013. The broad autism phenotype predicts child functioning in autism spectrum disorders. *Journal of neurodevelopmental disorders*, 5(1), p.25. Available at: <http://www.pubmedcentral.nih.gov/articlerender.fcgi?artid=3848833&tool=pmcentrez&rendertype=abstract> [Accessed October 28, 2014].
- McDougle, C.J. et al., 1996. Effects of tryptophan depletion in drug-free adults with autistic disorder. *Archives of general psychiatry*, 53(11), pp.993–1000. Available at: <http://www.ncbi.nlm.nih.gov/pubmed/8911222> [Accessed September 19, 2014].
- McFadden, K.L. et al., 2012. Abnormalities in gamma-band responses to language stimuli in first-degree relatives of children with autism spectrum disorder: an MEG

study. *BMC psychiatry*, 12(1), p.213. Available at:
<http://www.pubmedcentral.nih.gov/articlerender.fcgi?artid=3557147&tool=pmcentrez&rendertype=abstract> [Accessed August 8, 2014].

McNamara, I.M. et al., 2008. Further studies in the developmental hyperserotonemia model (DHS) of autism: social, behavioral and peptide changes. *Brain research*, 1189, pp.203–14. Available at: <http://www.ncbi.nlm.nih.gov/pubmed/18062943> [Accessed September 18, 2014].

McQuiston, a R. & Saggau, P., 2003. Mu-opioid receptors facilitate the propagation of excitatory activity in rat hippocampal area CA1 by disinhibition of all anatomical layers. *Journal of neurophysiology*, 90(3), pp.1936–1948.

McQuiston, A.R., 2007. Effects of μ -Opioid Receptor Modulation on GABA B Receptor Synaptic Function in Hippocampal CA1. *Journal of neurophysiology*, 97, pp.2301–2311.

Meguro-Horike, M. et al., 2011. Neuron-specific impairment of inter-chromosomal pairing and transcription in a novel model of human 15q-duplication syndrome. *Human molecular genetics*, 20(19), pp.3798–810. Available at:
<http://www.pubmedcentral.nih.gov/articlerender.fcgi?artid=3168289&tool=pmcentrez&rendertype=abstract> [Accessed August 6, 2014].

Mescher, M. et al., 1998. Simultaneous in vivo spectral editing and water suppression. *NMR in biomedicine*, 11(6), pp.266–72. Available at:
<http://www.ncbi.nlm.nih.gov/pubmed/9802468> [Accessed August 8, 2014].

Modahl, C. et al., 1998. Plasma oxytocin levels in autistic children. *Biological psychiatry*, 43(4), pp.270–7. Available at: <http://www.ncbi.nlm.nih.gov/pubmed/9513736> [Accessed August 8, 2014].

Montgomery, S.M., Betancur, M.I. & Buzsáki, G., 2009. Behavior-dependent coordination of multiple theta dipoles in the hippocampus. *The Journal of neuroscience : the official journal of the Society for Neuroscience*, 29(5), pp.1381–94. Available at: <http://www.ncbi.nlm.nih.gov/pubmed/19193885>.

Montgomery, S.M. & Buzsáki, G., 2007. Gamma oscillations dynamically couple hippocampal CA3 and CA1 regions during memory task performance. *Proceedings of the National Academy of Sciences of the United States of America*, 104(36),

pp.14495–14500.

- Mori, S. & Barker, P.B., 1999. Diffusion magnetic resonance imaging: its principle and applications. *Anatomical Record*, 257(3), pp.102–109. Available at: <http://www.ncbi.nlm.nih.gov/pubmed/10397783> \n[http://onlinelibrary.wiley.com/doi/10.1002/\(SICI\)1097-0185\(19990615\)257:3<102::AID-AR7>3.0.CO;2-6/asset/7_ftp.pdf?v=1&t=hlio1sf8&s=69fb7ab382453f66fcfd0b7fa5f11eb06f7bef7b](http://onlinelibrary.wiley.com/doi/10.1002/(SICI)1097-0185(19990615)257:3<102::AID-AR7>3.0.CO;2-6/asset/7_ftp.pdf?v=1&t=hlio1sf8&s=69fb7ab382453f66fcfd0b7fa5f11eb06f7bef7b) \n<http://onlinelibrary.wiley.com/stor>.
- Morrow, E.M. et al., 2008. Identifying autism loci and genes by tracing recent shared ancestry. *Science (New York, N.Y.)*, 321(5886), pp.218–23. Available at: <http://www.ncbi.nlm.nih.gov/pubmed/18621663>.
- Mukaddes, N.M. et al., 2014. Characteristics of Children Who Lost the Diagnosis of Autism: A Sample from Istanbul, Turkey. *Autism Research and Treatment*, 2014(doi.10.1155/2014/472120), pp.1–10. Available at: <http://www.pubmedcentral.nih.gov/articlerender.fcgi?artid=4022169&tool=pmcentrez&rendertype=abstract>.
- Muthukumaraswamy, S.D. et al., 2013. Elevating endogenous GABA levels with GAT-1 blockade modulates evoked but not induced responses in human visual cortex. *Neuropsychopharmacology : official publication of the American College of Neuropsychopharmacology*, 38(6), pp.1105–12. Available at: <http://dx.doi.org/10.1038/npp.2013.9> [Accessed August 8, 2014].
- Muthukumaraswamy, S.D. et al., 2009. Resting GABA concentration predicts peak gamma frequency and fMRI amplitude in response to visual stimulation in humans. *Proceedings of the National Academy of Sciences of the United States of America*, 106(20), pp.8356–61. Available at: <http://www.pubmedcentral.nih.gov/articlerender.fcgi?artid=2688873&tool=pmcentrez&rendertype=abstract> [Accessed August 8, 2014].
- Muthukumaraswamy, S.D., 2014. The use of magnetoencephalography in the study of psychopharmacology (pharmaco-MEG). *Journal of psychopharmacology (Oxford, England)*, 28(9), pp.815–29. Available at: <http://www.ncbi.nlm.nih.gov/pubmed/24920134> [Accessed November 20, 2014].
- Nagode, D. a et al., 2014. Optogenetic identification of an intrinsic cholinergically driven inhibitory oscillator sensitive to cannabinoids and opioids in hippocampal CA1. *The*

Journal of physiology, 592, pp.103–23. Available at:
<http://www.ncbi.nlm.nih.gov/pubmed/24190932>.

Nakamura, T. et al., 2015. Relationships among Parvalbumin-Immunoreactive Neuron Density, Phase-Locked Gamma Oscillations, and Autistic/Schizophrenic Symptoms in PDGFR- β Knock-Out and Control Mice. *Plos One*, 10(3), p.e0119258. Available at: <http://dx.plos.org/10.1371/journal.pone.0119258>.

Nakao, S. et al., 2008. Contact-dependent promotion of cell migration by the OL-protocadherin-Nap1 interaction. *Journal of Cell Biology*, 182(2), pp.395–410.

Nalin, A. et al., 1988. Lack of clinical-EEG effects of naloxone injection on infantile spasms. *Child's Nervous System*, 4, pp.365–366. Available at:
<http://www.ncbi.nlm.nih.gov/pubmed/15237199>.

Neumaier, J.F., Mailheau, S. & Chavkin, C., 1988. Opioid receptor-mediated responses in the dentate gyrus and CA1 region of the rat hippocampus. *The Journal of pharmacology and experimental therapeutics*, 244(2), pp.564–70. Available at:
<http://www.ncbi.nlm.nih.gov/pubmed/2894454>.

Nguyen, M. et al., 2014. Decoding the contribution of dopaminergic genes and pathways to autism spectrum disorder (ASD). *Neurochemistry international*, 66, pp.15–26. Available at: <http://www.ncbi.nlm.nih.gov/pubmed/24412511> [Accessed September 19, 2014].

Nutt, D. et al., 2015. Differences between magnetoencephalographic (MEG) spectral profiles of drugs acting on GABA at synaptic and extrasynaptic sites: A study in healthy volunteers. *Neuropharmacology*, 88, pp.155–163. Available at:
<http://linkinghub.elsevier.com/retrieve/pii/S0028390814003001>.

O'Donnell, W.T. & Warren, S.T., 2002. A decade of molecular studies of fragile X syndrome. *Annual review of neuroscience*, 25(1), pp.315–38. Available at:
<http://www.annualreviews.org/doi/abs/10.1146/annurev.neuro.25.112701.142909>.

O'Roak, B.J. et al., 2012. Sporadic autism exomes reveal a highly interconnected protein network of de novo mutations. *Nature*, 485(7397), pp.246–250. Available at:
<http://dx.doi.org/10.1038/nature10989>.

- Oostenveld, R. et al., 2011. FieldTrip: Open Source Software for Advanced Analysis of MEG, EEG, and Invasive Electrophysiological Data. *Computational Intelligence and Neuroscience*, 2011, pp.1–9. Available at: <http://www.pubmedcentral.nih.gov/articlerender.fcgi?artid=3021840&tool=pmcentrez&rendertype=abstract> [Accessed July 26, 2014].
- Oram Cardy, J.E. et al., 2008. Auditory evoked fields predict language ability and impairment in children. *International journal of psychophysiology : official journal of the International Organization of Psychophysiology*, 68(2), pp.170–5. Available at: <http://www.ncbi.nlm.nih.gov/pubmed/18304666> [Accessed September 30, 2014].
- Oram Cardy, J.E. et al., 2004. Prominence of M50 auditory evoked response over M100 in childhood and autism. *Neuroreport*, 15(12), pp.1867–70. Available at: <http://www.ncbi.nlm.nih.gov/pubmed/15305126> [Accessed September 30, 2014].
- Orekhova, E. V et al., 2007. Excess of High Frequency Electroencephalogram Oscillations in Boys with Autism. *Biological Psychiatry*, 62(9), pp.1022–1029. Available at: <http://www.ncbi.nlm.nih.gov/pubmed/17543897> [Accessed August 8, 2014].
- Orinstein, A.J. et al., 2015. Social Function and Communication in Optimal Outcome Children and Adolescents with an Autism History on Structured Test Measures. *Journal of Autism and Developmental Disorders*. Available at: <http://link.springer.com/10.1007/s10803-015-2409-6>.
- Owen, J.P. et al., 2014. Aberrant white matter microstructure in children with 16p11.2 deletions. *The Journal of neuroscience : the official journal of the Society for Neuroscience*, 34(18), pp.6214–23. Available at: <http://www.ncbi.nlm.nih.gov/pubmed/24790192> [Accessed July 11, 2014].
- Owen, S.F. et al., 2013. Oxytocin enhances hippocampal spike transmission by modulating fast-spiking interneurons. *Nature*, 500(7463), pp.458–62. Available at: <http://www.ncbi.nlm.nih.gov/pubmed/23913275> [Accessed August 8, 2014].
- Paetau, R. et al., 1995. Auditory evoked magnetic fields to tones and pseudowords in healthy children and adults. *Journal of clinical neurophysiology : official publication of the American Electroencephalographic Society*, 12(2), pp.177–185.
- Pérez Velázquez, J.L. & Galán, R.F., 2013. Information gain in the brain's resting state:

- A new perspective on autism. *Frontiers in Neuroinformatics*, 7(December), p.37.
Available at:
<http://www.pubmedcentral.nih.gov/articlerender.fcgi?artid=3870924&tool=pmcentrez&rendertype=abstract>.
- Pilpel, Y. & Segal, M., 2005. Rapid WAVE dynamics in dendritic spines of cultured hippocampal neurons is mediated by actin polymerization. *J Neurochem*, 95(5), pp.1401–1410. Available at:
http://www.ncbi.nlm.nih.gov/entrez/query.fcgi?cmd=Retrieve&db=PubMed&dopt=Citation&list_uids=16190876.
- Piven, J., Palmer, P., Jacobi, D., et al., 1997. Broader autism phenotype: Evidence from a family history study of multiple-incidence autism families. *American Journal of Psychiatry*, 154(2), pp.185–190.
- Piven, J., Palmer, P., Landa, R., et al., 1997. Personality and language characteristics in parents from multiple-incidence autism families. *American Journal of Medical Genetics*, 74(4), pp.398–411. Available at:
[http://doi.wiley.com/10.1002/\(SICI\)1096-8628\(19970725\)74:4<398::AID-AJMG11>3.0.CO;2-D](http://doi.wiley.com/10.1002/(SICI)1096-8628(19970725)74:4<398::AID-AJMG11>3.0.CO;2-D).
- Port, R.G. et al., 2014. Convergence of circuit dysfunction in ASD: a common bridge between diverse genetic and environmental risk factors and common clinical electrophysiology. *Frontiers in Cellular Neuroscience*, 8(December), pp.1–14.
Available at:
http://www.frontiersin.org/Cellular_Neuroscience/10.3389/fncel.2014.00414/abstract [Accessed December 22, 2014].
- Port, R.G. et al., 2015. Prospective MEG biomarkers in ASD: pre-clinical evidence and clinical promise of electrophysiological signatures. *The Yale journal of biology and medicine*, 88(1), pp.25–36. Available at:
<http://www.ncbi.nlm.nih.gov/pubmed/25745372>.
- Pouille, F. & Scanziani, M., 2004. Routing of spike series by dynamic circuits in the hippocampus. *Nature*, 429(6993), pp.717–723.
- Purcell, a E. et al., 2001. Postmortem brain abnormalities of the glutamate neurotransmitter system in autism. *Neurology*, 57(9), pp.1618–28. Available at:
<http://www.ncbi.nlm.nih.gov/pubmed/11706102> [Accessed August 8, 2014].

- Ramchandani, V. a et al., 2011. A genetic determinant of the striatal dopamine response to alcohol in men. *Molecular psychiatry*, 16(8), pp.809–817. Available at: <http://dx.doi.org/10.1038/mp.2010.56>.
- Ray, L. a & Hutchison, K.E., 2004. A polymorphism of the mu-opioid receptor gene (OPRM1) and sensitivity to the effects of alcohol in humans. *Alcoholism, clinical and experimental research*, 28(12), pp.1789–1795.
- Ray, L. a & Hutchison, K.E., 2007. Effects of naltrexone on alcohol sensitivity and genetic moderators of medication response: a double-blind placebo-controlled study. *Archives of general psychiatry*, 64(9), pp.1069–1077.
- Ray, R. et al., 2011. Human Mu Opioid Receptor (OPRM1 A118G) polymorphism is associated with brain mu-opioid receptor binding potential in smokers. *Proceedings of the National Academy of Sciences of the United States of America*, 108(22), pp.9268–73. Available at: <http://www.pubmedcentral.nih.gov/articlerender.fcgi?artid=3107291&tool=pmcentrez&rendertype=abstract>.
- Rezayof, A. et al., 2007. GABA A receptors of hippocampal CA1 regions are involved in the acquisition and expression of morphine-induced place preference. , pp.24–31.
- Rice, K. et al., 2012. Parsing heterogeneity in autism spectrum disorders: visual scanning of dynamic social scenes in school-aged children. *Journal of the American Academy of Child and Adolescent Psychiatry*, 51(3), pp.238–48. Available at: <http://www.sciencedirect.com/science/article/pii/S0890856711011798> [Accessed October 16, 2014].
- Roberts, T.P. et al., 2000. Latency of the auditory evoked neuromagnetic field components: stimulus dependence and insights toward perception. *Journal of clinical neurophysiology : official publication of the American Electroencephalographic Society*, 17(2), pp.114–29. Available at: <http://www.ncbi.nlm.nih.gov/pubmed/10831104> [Accessed December 22, 2014].
- Roberts, T.P. & Poeppel, D., 1996. Latency of auditory evoked M100 as a function of tone frequency. *Neuroreport*, 7(6), pp.1138–40. Available at: <http://www.ncbi.nlm.nih.gov/pubmed/8817518> [Accessed December 22, 2014].
- Roberts, T.P.L. et al., 2012. Delayed magnetic mismatch negativity field, but not auditory

- M100 response, in specific language impairment. *Neuroreport*, 23(8), pp.463–8. Available at: <http://www.pubmedcentral.nih.gov/articlerender.fcgi?artid=3345126&tool=pmcentrez&rendertype=abstract> [Accessed August 8, 2014].
- Roberts, T.P.L. et al., 2009. Developmental correlation of diffusion anisotropy with auditory-evoked response. *Neuroreport*, 20(18), pp.1586–91. Available at: <http://www.ncbi.nlm.nih.gov/pubmed/19898261> [Accessed August 8, 2014].
- Roberts, T.P.L. et al., 2013. Maturation differences in thalamocortical white matter microstructure and auditory evoked response latencies in autism spectrum disorders. *Brain research*, 1537, pp.79–85. Available at: <http://www.pubmedcentral.nih.gov/articlerender.fcgi?artid=3970268&tool=pmcentrez&rendertype=abstract> [Accessed August 8, 2014].
- Roberts, T.P.L. et al., 2010. MEG detection of delayed auditory evoked responses in autism spectrum disorders: towards an imaging biomarker for autism. *Autism research : official journal of the International Society for Autism Research*, 3(1), pp.8–18. Available at: <http://www.pubmedcentral.nih.gov/articlerender.fcgi?artid=3099241&tool=pmcentrez&rendertype=abstract> [Accessed August 8, 2014].
- Roe, C.M., McNamara, A.M. & Motheral, B.R., 2002. Gender- and age-related prescription drug use patterns. *The Annals of pharmacotherapy*, 36(1), pp.30–39.
- Rojas, D.C. et al., 2014. Decreased left perisylvian GABA concentration in children with autism and unaffected siblings. *NeuroImage*, 86, pp.28–34. Available at: <http://www.ncbi.nlm.nih.gov/pubmed/23370056> [Accessed August 8, 2014].
- Rojas, D.C. et al., 2006. Development of the 40Hz steady state auditory evoked magnetic field from ages 5 to 52. *Clinical neurophysiology : official journal of the International Federation of Clinical Neurophysiology*, 117(1), pp.110–7. Available at: <http://www.ncbi.nlm.nih.gov/pubmed/16316780> [Accessed August 8, 2014].
- Rojas, D.C. et al., 2007. Neuromagnetic evidence of broader auditory cortical tuning in schizophrenia. *Schizophrenia research*, 97(1-3), pp.206–14. Available at: <http://www.pubmedcentral.nih.gov/articlerender.fcgi?artid=2219386&tool=pmcentrez&rendertype=abstract>.

- Rojas, D.C. et al., 2008. Reduced neural synchronization of gamma-band MEG oscillations in first-degree relatives of children with autism. *BMC Psychiatry*, 8(1), p.66. Available at: <http://www.pubmedcentral.nih.gov/articlerender.fcgi?artid=2518921&tool=pmcentrez&rendertype=abstract> [Accessed August 8, 2014].
- Rojas, D.C. et al., 2011. Transient and steady-state auditory gamma-band responses in first-degree relatives of people with autism spectrum disorder. *Molecular autism*, 2(1), p.11. Available at: <http://www.molecularautism.com/content/2/1/11> [Accessed August 8, 2014].
- Rojas, D.C., Becker, K.M. & Wilson, L.B., 2015. Magnetic Resonance Spectroscopy Studies of Glutamate and GABA in Autism: Implications for Excitation-Inhibition Imbalance Theory. *Current Developmental Disorders Reports*, 2(1), pp.46–57. Available at: <http://link.springer.com/10.1007/s40474-014-0032-4>.
- Rojas, D.C. & Wilson, L.B., 2014. γ -band abnormalities as markers of autism spectrum disorders. *Biomarkers in medicine*, 8(3), pp.353–68. Available at: <http://www.futuremedicine.com/doi/abs/10.2217/bmm.14.15> [Accessed November 26, 2014].
- Roman, E. et al., 2006. Variations in opioid peptide levels during the estrous cycle in Sprague-Dawley rats. *Neuropeptides*, 40(3), pp.195–206.
- Rubenstein, J.L.R. & Merzenich, M.M., 2003. Model of autism: increased ratio of excitation/inhibition in key neural systems. *Genes, brain, and behavior*, 2(5), pp.255–67. Available at: <http://www.ncbi.nlm.nih.gov/pubmed/14606691> [Accessed August 5, 2014].
- Russo, N.M. et al., 2010. Biological changes in auditory function following training in children with autism spectrum disorders. *Behavioral and brain functions : BBF*, 6, p.60. Available at: <http://www.pubmedcentral.nih.gov/articlerender.fcgi?artid=2965126&tool=pmcentrez&rendertype=abstract>.
- Rutter, M., Bailey, A. & Lloyd, C., 2003. *SCQ: Social Communication Questionnaire*, Los Angeles, CA: Western Psychological Services.
- Santangelo, S.L. & Tsatsanis, K., 2005. What is known about autism: genes, brain, and

behavior. *American journal of pharmacogenomics : genomics-related research in drug development and clinical practice*, 5(2), pp.71–92. Available at: <http://link.springer.com/10.2165/00129785-200505020-00001> [Accessed August 8, 2014].

Saunders, J. a et al., 2013. Knockout of NMDA receptors in parvalbumin interneurons recreates autism-like phenotypes. *Autism research : official journal of the International Society for Autism Research*, 6(2), pp.69–77. Available at: <http://www.ncbi.nlm.nih.gov/pubmed/23441094> [Accessed August 8, 2014].

Saunders, J.A., Gandal, M.J., Roberts, T.P., et al., 2012. NMDA antagonist MK801 recreates auditory electrophysiology disruption present in autism and other neurodevelopmental disorders. *Behavioural brain research*, 234(2), pp.233–7. Available at: <http://www.ncbi.nlm.nih.gov/pubmed/22771812> [Accessed August 8, 2014].

Saunders, J.A., Gandal, M.J. & Siegel, S.J., 2012. NMDA antagonists recreate signal-to-noise ratio and timing perturbations present in schizophrenia. *Neurobiology of disease*, 46(1), pp.93–100. Available at: <http://dx.doi.org/10.1016/j.nbd.2011.12.049> [Accessed August 8, 2014].

Semel, E.M. & Wiig, E.H., 2003. *Clinical evaluation of language fundamentals (CELF-4)*, San Antonio, TX: The Psychological Corporation.

Šerý, O. et al., 2010. A118G polymorphism of OPRM1 gene is associated with schizophrenia. *Journal of Molecular Neuroscience*, 41(1), pp.219–222.

Sheikhani, A. et al., 2012. Detection of abnormalities for diagnosing of children with autism disorders using of quantitative electroencephalography analysis. *Journal of medical systems*, 36(2), pp.957–63. Available at: <http://www.ncbi.nlm.nih.gov/pubmed/20711644> [Accessed August 8, 2014].

Shimmura, C. et al., 2013. Enzymes in the glutamate-glutamine cycle in the anterior cingulate cortex in postmortem brain of subjects with autism. *Molecular autism*, 4(1), p.6. Available at: <http://www.pubmedcentral.nih.gov/articlerender.fcgi?artid=3621600&tool=pmcentrez&rendertype=abstract>.

Shuang, M. et al., 2004. Family-based association study between autism and glutamate

- receptor 6 gene in Chinese Han trios. *American journal of medical genetics. Part B, Neuropsychiatric genetics : the official publication of the International Society of Psychiatric Genetics*, 131B(1), pp.48–50. Available at: <http://www.ncbi.nlm.nih.gov/pubmed/15389769> [Accessed August 8, 2014].
- Sia, A.T. et al., 2008. A118G single nucleotide polymorphism of human mu-opioid receptor gene influences pain perception and patient-controlled intravenous morphine consumption after intrathecal morphine for postcesarean analgesia. *Anesthesiology*, 109(3), pp.520–526.
- Siegel, S.J. et al., 2003. Effects of strain, novelty, and NMDA blockade on auditory-evoked potentials in mice. *Neuropsychopharmacology : official publication of the American College of Neuropsychopharmacology*, 28(4), pp.675–682.
- Silverman, J.L. et al., 2010. Behavioural phenotyping assays for mouse models of autism. *Nature reviews. Neuroscience*, 11(7), pp.490–502. Available at: [10.1038/nrn2851](https://doi.org/10.1038/nrn2851) [Accessed August 8, 2014].
- Silverman, J.L. et al., 2015. GABAB Receptor Agonist R-Baclofen Reverses Social Deficits and Reduces Repetitive Behavior in Two Mouse Models of Autism. *Neuropsychopharmacology*, (July 2014), pp.1–30. Available at: <http://www.nature.com/doi/10.1038/npp.2015.66>.
- Soghomonian, J.J. & Martin, D.L., 1998. Two isoforms of glutamate decarboxylase: why? *Trends in Pharmacological Sciences*, 19(12), pp.500–5. Available at: <http://www.ncbi.nlm.nih.gov/pubmed/9871412>.
- Sohal, V.S. et al., 2009. Parvalbumin neurons and gamma rhythms enhance cortical circuit performance. *Nature*, 459(7247), pp.698–702. Available at: <http://www.pubmedcentral.nih.gov/articlerender.fcgi?artid=2752642&tool=pmcentrez&rendertype=abstract> [Accessed July 31, 2014].
- Spruston, N., 2008. Pyramidal neurons: dendritic structure and synaptic integration. *Nature reviews. Neuroscience*, 9(3), pp.206–221.
- Staal, W.G., 2014. Autism, DRD3 and repetitive and stereotyped behavior, an overview of the current knowledge. *European neuropsychopharmacology : the journal of the European College of Neuropsychopharmacology*, pp.1–6. Available at: <http://www.ncbi.nlm.nih.gov/pubmed/25224105> [Accessed September 18, 2014].

- Strutz-Seebohm, N. et al., 2006. Functional significance of the kainate receptor GluR6(M836I) mutation that is linked to autism. *Cellular physiology and biochemistry : international journal of experimental cellular physiology, biochemistry, and pharmacology*, 18(4-5), pp.287–94. Available at: <http://www.ncbi.nlm.nih.gov/pubmed/17167233> [Accessed August 8, 2014].
- Stufflebeam, S.M. et al., 2008. A non-invasive method to relate the timing of neural activity to white matter microstructural integrity. *NeuroImage*, 42(2), pp.710–6. Available at: <http://www.pubmedcentral.nih.gov/articlerender.fcgi?artid=2610633&tool=pmcentrez&rendertype=abstract> [Accessed December 8, 2014].
- Stufflebeam, S.M. et al., 1998. Peri-threshold encoding of stimulus frequency and intensity in the M100 latency. *Neuroreport*, 9(1), pp.91–4. Available at: <http://www.ncbi.nlm.nih.gov/pubmed/9592054> [Accessed December 22, 2014].
- Sun, L. et al., 2012. Impaired gamma-band activity during perceptual organization in adults with autism spectrum disorders: evidence for dysfunctional network activity in frontal-posterior cortices. *The Journal of neuroscience : the official journal of the Society for Neuroscience*, 32(28), pp.9563–73. Available at: <http://www.ncbi.nlm.nih.gov/pubmed/22787042> [Accessed August 8, 2014].
- Sun, N. et al., 2006. Dynamic changes in orbitofrontal neuronal activity in rats during opiate administration and withdrawal. *Neuroscience*, 138(1), pp.77–82. Available at: <http://www.ncbi.nlm.nih.gov/pubmed/16377092>.
- Sun, Y. et al., 2011. γ oscillations in schizophrenia: mechanisms and clinical significance. *Brain research*, 1413, pp.98–114. Available at: <http://www.ncbi.nlm.nih.gov/pubmed/21840506> [Accessed August 8, 2014].
- Szilagyi, P.G., 2009. Translational research and pediatrics. *Academic pediatrics*, 9(2), pp.71–80. Available at: <http://www.sciencedirect.com/science/article/pii/S1876285908002623>.
- Tallon-Baudry, C. & Bertrand, O., 1999. Oscillatory gamma activity in humans and its role in object representation. *Trends in cognitive sciences*, 3(4), pp.151–162. Available at: <http://www.ncbi.nlm.nih.gov/pubmed/11102663> [Accessed August 1, 2014].

- Tansey, K.E. et al., 2010. Oxytocin receptor (OXTR) does not play a major role in the aetiology of autism: Genetic and molecular studies. *Neuroscience Letters*, 474(3), pp.163–167. Available at: <http://dx.doi.org/10.1016/j.neulet.2010.03.035>.
- Tatard-Leitman, V.M. et al., 2014. Pyramidal Cell Selective Ablation of N-Methyl-D-Aspartate Receptor 1 Causes Increase in Cellular and Network Excitability. *Biological psychiatry*, pp.1–12. Available at: <http://www.ncbi.nlm.nih.gov/pubmed/25156700> [Accessed October 28, 2014].
- Tecchio, F. et al., 2003. Auditory sensory processing in autism: a magnetoencephalographic study. *Biological psychiatry*, 54(6), pp.647–54. Available at: <http://linkinghub.elsevier.com/retrieve/pii/S0006322303002956> [Accessed September 30, 2014].
- Thomases, D.R., Cass, D.K. & Tseng, K.Y., 2013. Periadolescent exposure to the NMDA receptor antagonist MK-801 impairs the functional maturation of local GABAergic circuits in the adult prefrontal cortex. *The Journal of neuroscience : the official journal of the Society for Neuroscience*, 33(1), pp.26–34. Available at: <http://www.pubmedcentral.nih.gov/articlerender.fcgi?artid=3544161&tool=pmcentrez&rendertype=abstract> [Accessed July 26, 2014].
- Tierney, A.L. et al., 2012. Developmental trajectories of resting EEG power: an endophenotype of autism spectrum disorder. *PloS one*, 7(6), p.e39127. Available at: <http://www.pubmedcentral.nih.gov/articlerender.fcgi?artid=3380047&tool=pmcentrez&rendertype=abstract> [Accessed August 8, 2014].
- Tiesinga, P. & Sejnowski, T.J., 2009. Cortical Enlightenment: Are Attentional Gamma Oscillations Driven by ING or PING? *Neuron*, 63(6), pp.727–732. Available at: <http://dx.doi.org/10.1016/j.neuron.2009.09.009>.
- Tordjman, S. et al., 2014. Gene X environment Interactions in Autism Spectrum Disorders: Role of Epigenetic Mechanisms. *Frontiers in Psychiatry*, 5(August), p.53. Available at: <http://www.pubmedcentral.nih.gov/articlerender.fcgi?artid=4120683&tool=pmcentrez&rendertype=abstract>.
- Torres-Reveron, A. et al., 2009. Ovarian steroids alter mu opioid receptor trafficking in hippocampal parvalbumin GABAergic interneurons. *Experimental Neurology*, 219(1), pp.319–327. Available at:

<http://dx.doi.org/10.1016/j.expneurol.2009.06.001>.

- Tort, A.B.L. et al., 2010. Measuring phase-amplitude coupling between neuronal oscillations of different frequencies. *Journal of neurophysiology*, 104(2), pp.1195–1210.
- Tortella, F.C., Moreton, J.E. & Khazan, N., 1978. Electroencephalographic and behavioral effects of D-ala2-methionine-enkephalinamide and morphine in the rat. *The Journal of pharmacology and experimental therapeutics*, 206, pp.636–643.
- Traub, R.D. et al., 1996. Analysis of gamma rhythms in the rat hippocampus in vitro and in vivo. *The Journal of physiology*, 493 (Pt 2(1996), pp.471–84. Available at: <http://www.pubmedcentral.nih.gov/articlerender.fcgi?artid=1158931&tool=pmcentrez&rendertype=abstract> [Accessed August 8, 2014].
- Troisi, A. et al., 2012. Variation in the -opioid receptor gene (OPRM1) moderates the influence of early maternal care on fearful attachment. *Social Cognitive and Affective Neuroscience*, 7(5), pp.542–547. Available at: <http://scan.oxfordjournals.org/lookup/doi/10.1093/scan/nsr037>.
- Tsai, N. et al., 2012. Multiple Autism-Linked Genes Mediate Synapse Elimination via Proteasomal Degradation of a Synaptic Scaffold PSD-95. *Cell*, 151(7), pp.1581–1594. Available at: <http://linkinghub.elsevier.com/retrieve/pii/S0092867412014250>.
- Turetsky, B.I. et al., 2007. Neurophysiological endophenotypes of schizophrenia: the viability of selected candidate measures. *Schizophrenia bulletin*, 33(1), pp.69–94. Available at: <http://www.pubmedcentral.nih.gov/articlerender.fcgi?artid=2632291&tool=pmcentrez&rendertype=abstract> [Accessed August 8, 2014].
- Tyzio, R. et al., 2014. Oxytocin-mediated GABA inhibition during delivery attenuates autism pathogenesis in rodent offspring. *Science (New York, N.Y.)*, 343(6171), pp.675–9. Available at: <http://www.ncbi.nlm.nih.gov/pubmed/24503856> [Accessed July 9, 2014].
- Uhlhaas, P.J. & Singer, W., 2010. Abnormal neural oscillations and synchrony in schizophrenia. *Nature Reviews Neuroscience*, 11(2), pp.100–113. Available at: <http://www.nature.com/doi/10.1038/nrn2774>.

- Uhlhaas, P.J. & Singer, W., 2011. The Development of Neural Synchrony and Large-Scale Cortical Networks During Adolescence: Relevance for the Pathophysiology of Schizophrenia and Neurodevelopmental Hypothesis. *Schizophrenia Bulletin*, 37(3), pp.514–523. Available at: <http://schizophreniabulletin.oxfordjournals.org/cgi/doi/10.1093/schbul/sbr034>.
- Vida, I., Bartos, M. & Jonas, P., 2006. Shunting Inhibition Improves Robustness of Gamma Oscillations in Hippocampal Interneuron Networks by Homogenizing Firing Rates. *Neuron*, 49(1), pp.107–117. Available at: <http://linkinghub.elsevier.com/retrieve/pii/S0896627305010627>.
- Wang, G.Y., Kydd, R.R. & Russell, B.R., 2015. Quantitative EEG and Low-Resolution Electromagnetic Tomography (LORETA) Imaging of Patients Undergoing Methadone Treatment for Opiate Addiction. *Clinical EEG and Neuroscience*. Available at: <http://eeg.sagepub.com/lookup/doi/10.1177/1550059415586705>.
- Wang, Y.-J. et al., 2014. Brain region- and sex-specific alterations in DAMGO-stimulated [(35) S]GTP γ S binding in mice with Oprm1 A112G. *Addiction biology*, 19(3), pp.354–61. Available at: <http://www.ncbi.nlm.nih.gov/pubmed/22862850>.
- Wang, Y.J. et al., 2012. Reduced expression of the mu opioid receptor in some, but not all, brain regions in mice with OPRM1 A112G. *Neuroscience*, 205, pp.178–184. Available at: <http://dx.doi.org/10.1016/j.neuroscience.2011.12.033>.
- Way, B.M. et al., 2010. Dispositional mindfulness and depressive symptomatology: correlations with limbic and self-referential neural activity during rest. *Emotion*, 10(1), pp.12–24.
- Way, B.M., Taylor, S.E. & Eisenberger, N.I., 2009. Variation in the mu-opioid receptor gene (OPRM1) is associated with dispositional and neural sensitivity to social rejection. *Proceedings of the National Academy of Sciences of the United States of America*, 106(35), pp.15079–15084.
- Wechsler, D., 2011. *Wechsler Abbreviated Scale of Intelligence* 2nd Editio., San Antonio, TX: NCS Pearson.
- Wechsler, D., 2003. *Wechsler Intelligence Scale for children* 3rd ed., San Antonio, TX: The Psychological Corporation.

- Weerts, E.M. et al., 2012. Influence of OPRM1 Asn40Asp variant (A118G) on [11C]carfentanil binding potential: preliminary findings in human subjects. *The International Journal of Neuropsychopharmacology*, pp.1–7.
- Whitaker-Azmitia, P.M., 2001. Serotonin and brain development: role in human developmental diseases. *Brain research bulletin*, 56(5), pp.479–85. Available at: <http://www.ncbi.nlm.nih.gov/pubmed/11750793>.
- Whittington, M. a et al., 1998. Morphine disrupts long-range synchrony of gamma oscillations in hippocampal slices. *Proceedings of the National Academy of Sciences of the United States of America*, 95(10), pp.5807–11. Available at: <http://www.pubmedcentral.nih.gov/articlerender.fcgi?artid=20461&tool=pmcentrez&rendertype=abstract> [Accessed August 8, 2014].
- Whittington, M.A. et al., 2000. Inhibition-based rhythms: experimental and mathematical observations on network dynamics. *International journal of psychophysiology : official journal of the International Organization of Psychophysiology*, 38(3), pp.315–36. Available at: <http://www.sciencedirect.com/science/article/pii/S0167876000001732> [Accessed August 8, 2014].
- Whittington, M.A. & Traub, R.D., 2003. Interneuron Diversity series: Inhibitory interneurons and network oscillations in vitro. *Trends in Neurosciences*, 26(12), pp.676–682. Available at: <http://linkinghub.elsevier.com/retrieve/pii/S0166223603003369>.
- van den Wildenberg, E. et al., 2007. A functional polymorphism of the mu-opioid receptor gene (OPRM1) influences cue-induced craving for alcohol in male heavy drinkers. *Alcoholism, clinical and experimental research*, 31(1), pp.1–10. Available at: <http://www.ncbi.nlm.nih.gov/pubmed/17207095>.
- Williams, K.T., 2007. *Expressive Vocabulary Test* 2nd Editio., Circle Pines, MN: AGS Publishing.
- Williams, T.J. et al., 2011. Age- and hormone-regulation of opioid peptides and synaptic proteins in the rat dorsal hippocampal formation. *Brain Research*, 1379, pp.71–85. Available at: <http://dx.doi.org/10.1016/j.brainres.2010.08.103>.
- Wilson, T.W. et al., 2007. Children and adolescents with autism exhibit reduced MEG

- steady-state gamma responses. *Biological psychiatry*, 62(3), pp.192–7. Available at: <http://www.pubmedcentral.nih.gov/articlerender.fcgi?artid=2692734&tool=pmcentrez&rendertype=abstract> [Accessed August 8, 2014].
- Wöhr, M. et al., 2015. Lack of parvalbumin in mice leads to behavioral deficits relevant to all human autism core symptoms and related neural morphofunctional abnormalities. *Translational Psychiatry*, 5(3), p.e525. Available at: <http://www.nature.com/doifinder/10.1038/tp.2015.19>.
- Wu, S. et al., 2005. Positive Association of the Oxytocin Receptor Gene (OXTR) with Autism in the Chinese Han Population. *Biological Psychiatry*, 58(1), pp.74–77. Available at: <http://linkinghub.elsevier.com/retrieve/pii/S0006322305003100>.
- Yamamoto, T. et al., 1988. Magnetic localization of neuronal activity in the human brain. *Proc Natl Acad Sci U S A*, 85(22), pp.8732–8736.
- Yamawaki, N. et al., 2008. Pharmacologically induced and stimulus evoked rhythmic neuronal oscillatory activity in the primary motor cortex in vitro. *Neuroscience*, 151(2), pp.386–95. Available at: <http://www.ncbi.nlm.nih.gov/pubmed/18063484> [Accessed July 30, 2014].
- Yang, Y. & Pan, C., 2013. Role of metabotropic glutamate receptor 7 in autism spectrum disorders: a pilot study. *Life sciences*, 92(2), pp.149–53. Available at: <http://www.ncbi.nlm.nih.gov/pubmed/23201551>.
- Yerys, B.E. & Pennington, B.F., 2011. How do we establish a biological marker for a behaviorally defined disorder? Autism as a test case. *Autism Research*, 4(4), pp.239–241.
- Yizhar, O. et al., 2011. Neocortical excitation/inhibition balance in information processing and social dysfunction. *Nature*, 477(7363), pp.171–178. Available at: <http://www.ncbi.nlm.nih.gov/pubmed/21796121> [Accessed July 18, 2014].
- Zablotsky, B. et al., 2015. *Estimated prevalence of autism and other developmental disabilities following questionnaire changes in the 2014 National Health Interview Survey*,
- Zappella, M., 2002. Early-onset Tourette syndrome with reversible autistic behaviour: a

dysmaturational disorder. *European child & adolescent psychiatry*, 11(1), pp.18–23. Available at: <http://link.springer.com/10.1007/s007870200003>.

Zhang, K. et al., 2014. Loss of glutamic acid decarboxylase (Gad67) in Gpr88-expressing neurons induces learning and social behavior deficits in mice. *Neuroscience*, 275, pp.238–247. Available at: <http://dx.doi.org/10.1016/j.neuroscience.2014.06.020> [Accessed July 20, 2014].

Zhang, Y. et al., 2005. Allelic expression imbalance of human mu opioid receptor (OPRM1) caused by variant A118G. *Journal of Biological Chemistry*, 280(38), pp.32618–32624.

Zhang, Y. et al., 2014. Mouse Model of the OPRM1 (A118G) Polymorphism: Differential Heroin Self-Administration Behavior Compared with Wild-Type Mice. *Neuropsychopharmacology*, 1(August), pp.1–38. Available at: <http://www.nature.com/doi/10.1038/npp.2014.286> \n <http://www.ncbi.nlm.nih.gov/pubmed/25336208>.

Zhong, J. et al., 2009. BC1 Regulation of Metabotropic Glutamate Receptor-Mediated Neuronal Excitability. *Journal of Neuroscience*, 29(32), pp.9977–9986. Available at: <http://www.jneurosci.org/cgi/doi/10.1523/JNEUROSCI.3893-08.2009>.

Zikopoulos, B. & Barbas, H., 2013. Altered neural connectivity in excitatory and inhibitory cortical circuits in autism. *Frontiers in Human Neuroscience*, 7(September), p.609. Available at: <http://www.pubmedcentral.nih.gov/articlerender.fcgi?artid=3784686&tool=pmcentrez&rendertype=abstract> [Accessed July 17, 2014].

Zuo, Y.-F. et al., 2007. A comparison between spontaneous electroencephalographic activities induced by morphine and morphine-related environment in rats. *Brain research*, 1136(1), pp.88–101. Available at: <http://www.ncbi.nlm.nih.gov/pubmed/17234161>.